2012

Optimal Design of an Air-Cooled Condenser for Flue Gas from a Power Plant

Michael John Kessen
Lehigh University

Optimal Design of an Air-Cooled Condenser for Flue Gas from a Power Plant

by

Michael John Kessen

Presented to the Graduate and Research Committee

of Lehigh University

in Candidacy for the Degree of

Doctor of Philosophy

in

Mechanical Engineering

Lehigh University

January 2012

Signature Sheet

Approved and recommended for acceptance as a dissertation in partial fulfillment of the requirements for the degree of Doctor of Philosophy.

_____

Date

_____

Dissertation Advisor, Dr. Edward Levy

_____

Accepted Date

Committee Members:

_____

Committee Chair: Dr. Edward Levy

_____

Dr. Harun Bilirgen

_____

Dr. Hugo Caram

_____

Dr. Sudhakar Neti

_____

Dr. Charles Smith

Acknowledgements

I would like to thank Dr. Edward Levy and the Energy Research Center for all the support and help during my graduate studies. Dr. Levy has been an excellent advisor and I am forever grateful for all the discussions we had. I look forward to continuing to work with Dr. Levy on future publications. I am grateful for the Energy Research Center and all its resources I used while completing my studies.

I would like to thank Dr. Harun Bilirgen of the Energy Research Center for his guidance and mentoring. I would like the thank Dr. Carlos Romero, Mr. Zheng Yao, and Dr. Kwangkook Jeong for their help and support. I would also like to thank Jodie Johnson and Ursla Levy of the Energy Research Center for their never-ending commitment to make the Energy Research Center a productive place to work.

I would like the thank Kent Hayhurst, Richard Eime, Greg Fegley, Fred Bechtoldt, and Lain Hardcastle, the engineers at the Lehigh University Boiler House, for their unlimited help, support, and guidance with constructing the heat exchanger experimental apparatus. I would also like to thank Dick Towne of the mechanical engineering machine shop for his help with fabricating prototypes.

I would also like to thank my family and friends for their unconditional support.

List of Figures

List of Tables

Nomenclature

A	*Area [ft^2]*
Cp	*Specific Heat [BTU/lbm-F]*
d_h	*Hydraulic Diameter [ft]*
D	*Mass Diffusion [ft^2/sec]*
Eu	*Euler Number*
f	*friction factor*
F_L	*Fin Length*
F_P	*Fin Pitch*
F_T	*Fin Thickness*
g	*gravity [ft^2/sec]*
G	*Mass Velocity*
h	*Convective Heat Transfer Coefficient [BTU/hr-ft^2-^oF]*
ID	*Inner Diameter [ft]*
k	*Mass Transfer Coefficient [lbm/hr-ft^2-difference p_v]*
p	*Pressure [psia]*
L	*Tube Length [ft]*
$\dot{m}$	*Mass Flowrate [lbm/hr]*
M	*Molar Mass [lbm/lbmol]*
N	*Number of Fins*
Nu	*Nusselt Number*
OD	*Outer Diameter [ft]*
Pr	*Prandtl Number*
Q	*Heat Transfer [BTU/hr]*
Re	*Reynolds Number*
S_D	*Diagonal Tube Pitch [ft]*
S_L	*Longitudinal Tube Pitch [ft]*
S_T	*Transverse Tube Pitch [ft]*
T	*Temperature [degree F]*
u	*velocity [ft/sec]*
X	*Quality of Condensible Vapor*
z	*Number of Rows*

α	*void fraction, Thermal Diffusivity [ft^2/sec]*
λ	*Thermal Conductivity [BTU/hr-ft-F]*
η	*Overall Surface Efficiency*
η_f	*Fin Efficiency*
ρ	*Density [lbm/ft^3]*
Φ	*Two Phase Multiplier*

SUBSCRIPTS

a	*air*
amb	*ambient*
D	*tube diameter*
Fr	*frictional*
F	*fin*
dg	*dry gas*
g	*flue gas*
i	*inner, interfacial*
l	*liquid*
lm	*log mean difference*
lo	*liquid only*
nc	*noncondensible gases*
s	*surface*
T	*Total*
t	*total*
v	*vapor*
vo	*vapor only*

Abstract

It is becoming increasingly more important for some power plants to reduce water consumption rates. By 2030, the demand for water consumption in certain regions of the United States will increase by as much as 119% over 2005 usage rates. Engineers continue to improve the efficiencies of power plants to reduce water consumption rates. But this dissertation presents a new way in which power plants can reduce water consumption rates.

One way to reduce a power plant's water consumption is to recover water vapor from the boiler flue gas. In the present study, an air-cooled condenser was developed which cools flue gas and condenses water vapor from the flue gas. The heat exchanger, modeled after typical air-cooled condensers used for condensing steam in power plant cycles, is a cross-flow finned-tube arrangement with the flue gas flowing through the tubes and the cooling air flowing around the tubes. At the exit of the heat exchanger, the condensed moisture from the flue gas would be collected and treated and then used in the plant to reduce the amount of water usually taken from rivers, lakes, or municipal systems.

The present study focused on developing a heat and mass transfer simulation which predicted heat transfer rates, water condensation rates, and associated costs of building and operating the system. To validate the simulation, a prototype heat exchanger was fabricated and processed flue gas from an industrial boiler. The performance of the prototype was compared with the predictions of the simulation. The cost of the system was estimated using capital cost correlations for air-cooled condensers and calculating the operating costs and savings of the system using the performance results from the simulation.

Four specific applications of the condenser were investigated, two in which ambient air was used as the heat sink and two in which boiler combustion air was used as the heat sink. The case studies showed that the ACC system could provide fuel savings up to 5,400 tons per year or up to 500 gpm of water.

Introduction

The purpose of this research was to design an air-cooled condenser (ACC) for boiler flue gas in a coal-fired power plant. Currently, such plants emit flue gas at temperatures above 300^{o}F to avoid ductwork corrosion caused by condensing sulfuric acid. Flue gas can have SO_3 concentrations of up to 35 ppm and, depending on the moisture content, sulfuric acid starts condensing at temperatures ranging from 225^{o}F to 310^{o}F. By emitting flue gas at an elevated temperature, large amounts of water and energy are wasted. The proposed ACC will recover water and low grade heat from flue gas.

A typical flue gas flow rate in a power plant is 6,000,000 lbm/hr. Depending on the coal, water moisture concentrations can range from 6 to 15 vol %, or 216,000 to 540,000 lbm/hr respectively. If recovered, the water can be used to supply approximately 10 to 29 % (depending on fuel) of the makeup water used in an evaporative cooling tower [20].

Thermoelectric plants withdraw and consume substantial amounts of water for cooling. In 2005, U.S. coal-fired plants equipped with evaporative cooling towers consumed 2.4 billion gallons of water per day (BGD). By 2030, it is estimated that the consumption rate will increase by 17 to 29%, depending on the technology employed. This increase is a national average, but on a regional level the consumption will be lower in some areas and higher in others. One study predicts coal-fired power plants in Florida and New York will increase their water consumption rates by 119 and 67% respectively [1].

Another factor affecting water usage in thermoelectric plants is CO_2 mitigation. Retrofitting equipment to reduce carbon dioxide emissions will reduce the plant's efficiency and increase the plant's cooling needs. Estimations by the National Energy Technology Laboratory predict that if all the new and existing pulverized coal plants with scrubbers and IGCC (gasification and combined cycle) were to deploy carbon capture technologies by 2030, the thermoelectric industry's water consumption rate would increase an additional 27 to 52%, depending on the configuration [1].

In contrast to typical power plant applications, the proposed air-cooled condenser will be used to condense moisture in flue gas rather than condensing pure steam in a steam condenser. The differences between flue gas moisture and steam required special design considerations which are addressed in the present work.

The first objective of the present study was to develop a model which simulated the heat and mass transfer processes in condensing flue gas. Whereas steam is a single-component, condensible fluid, flue gas is a mixture of condensible and noncondensible gases. Therefore, the simultaneous sensible and latent heat transfers were modeled. The model was then validated with experimental measurements and used to design and optimize a system for a power plant.

Chapter 1 begins with a literature review of the current state-of-the-art. Chapter 1 also discusses the differences between modeling a single component condensible gas and a mixture of condensible and noncondensible gases. Chapter 1 also describes the pressure drop correlations and heat transfer correlations in the heat and mass transfer simulation, the major components of the economic model used to define the cost of the ACC, and the optimization technique.

Chapter 2 discusses the heat and mass transfer simulation developed in the present work. The details of the numerical procedure are described along with the algorithm to solve the governing equations. Also discussed is how the optimization procedure was implemented.

Chapter 3 describes the experimental investigation performed in the present research. The experimental apparatus is discussed and detailed drawings are shown. Also described in Chapter 3 are results of the experimental measurements. The chapter is concluded by showing evidence that the heat and mass transfer simulation discussed in Chapter 2 is accurate.

Chapter 4 is a discussion of design choices which are most important to meet design objectives. The experimental results and results from the heat and mass transfer simulation are used to support arguments.

Chapter 5 discusses the details of the calculation procedure to determine the size and cost of the ACC. Parametric simulations are presented to show how each design choice affects the

size and cost of the ACC. The final two sections of Chapter 5 discuss two applications for the ACC: with and without a wet flue gas desulphurization (FGD) system. The geometry and process conditions of the ACC were optimal for each application.

The final chapter of the present study, Chapter 6, discusses the application of the ACC to pre-heat combustion air. The calculation procedure is discussed, followed by the optimal geometry and process conditions. The chapter concludes by providing an estimate for the fuel savings due to pre-heating combustion air.

Appendix A of the present study lists details of the experimental results not presented in Chapter 3. Appendix B lists additional results from the optimization simulations discussed in Chapters 5 and 6. Appendix C details the assumptions for the fuel savings calculations in Chapter 6.

1 Literature Review

1.1 The State-of-the-Art in Flue Gas Condensers

The Condensing Heat Exchanger Corporation (CHX) in partnership with Foster Wheeler Corporation and The Babcock and Wilcox Company developed a flue gas condensing heat exchanger with Teflon covered tubes [2-8]. The purpose of the Teflon covering on the tubes is to minimize potential failure due to corrosion; however its drawbacks are decreased thermal conductivity and increased manufacturing costs. The Teflon covering on the tubes is 0.015 inches thick and the Teflon covering on the shell walls of the heat exchanger is 0.06 inches thick. There are 110 documented installations of the CHX designed condensers but no heat and mass transfer performance tests are documented.

The CHX heat exchanger is a shell-and-tube design. Water flows on the tube-side and flue gas flows on the shell-side. The tubes are approximately one inch in diameter, three feet long, and arranged in a staggered matrix. The full-scale heat exchanger is assembled with a modular design and the desired surface area is obtained by stacking modules. A demonstration test was carried out by Consolidated Edison at its 74^{th} Street station in New York City. This heat exchanger processed 320,000 lbm/hr of flue gas. At the time of publication in 1992, the economizer was expected to stay in service for 20 years. The last published update in Butcher et al. in 1996 [6] states continued service with a heat rate improvement of 800 BTU/kWh

To enhance the Teflon covered heat exchanger, the Integrated Flue Gas Treatment (IFGT) system was developed. This system has four sections: In the first section, the flue gas flows downwards over a bank of tubes where sensible heat transfer occurs. The second region is a U-bend which redirects the flow upwards and the third region is a condenser where the flue gas flows around another bank of chilled tubes. Water condenses from the flue gas and falls into a collection basin. In this third region a reagent can be injected to further enhance condensation and also neutralize acid emissions. The fourth region employs a mist eliminator to recover the entrained liquid from the flue gas.

A demonstration project of the IFGT system determined particulate capture efficiencies, SO_2 removal efficiencies, mercury reduction, and tube wear. The IFGT system processed 25,000 lbm/hr flue gas from an oil-fired unit. Sulfur dioxide removal efficiency was 98%, sulfur trioxide removal efficiency was over 65%, and mercury removal efficiency was 50%. Results from other tests can be found in Butcher et al. [6] where conditions were changed to observe the effects of fuels, loading conditions, and spray reagents.

A long term test to determine the durability of the Teflon tubes was performed in 1996 [7]. This long term test subjected the tubes to 750 SCFM at 300^{o}F continuously for 260 days, and there was a 20 minute tube wash every 8 hours. Measured results showed no significant degradation of the Teflon coating. Microscopic degradation was measured on some tubes and the authors reported it was negligible and should cause no problems in extended operations. The life of the tubes was expected to be greater than 10 years. The IFGT system was patented in 1996 by the Babcock and Wilcox Company [8] and continues to be sold by it.

North Atlantic Technologies [9-10] developed a flue gas condensing heat exchanger for an industrial boiler. The heat exchanger was a plate-type configuration like what is shown in Figure 1.1. The plates were coated with a porcelain enamel to resist corrosion. While this application may work for an industrial boiler, which produces approximately 20,000 lbm/hr of flue gas, porcelain enameled plates are impractical for a heat exchanger that has to process approximately 6,000,000 lbm/hr of flue gas.

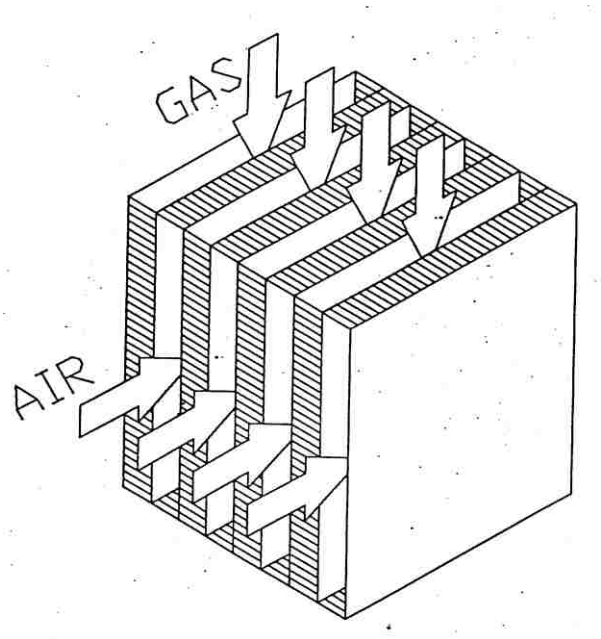

Figure 1.1 - Plate-type heat exchanger.

CON-X [12] developed a direct contact heat exchanger where water is sprayed directly onto the hot flue gas to saturate and cool the flue gas, and then collect condensed water. The largest application of this design was on a flue gas stream of 35,000 lbm/hr. Svedberg [11] also proposed a direct cooler for recovering waste heat from flue gas. His approach injects a hygroscopic fluid to absorb the water vapors from the flue gas. No pilot scale systems have been developed. In the CON-X design, the amount of water recovered from the flue gas depends on the exit temperature of the flue gas, and to have an exiting flue gas moisture concentration of four percent would require the exiting flue gas temperature be 84^{o}F. For Svedburg's design, the effectiveness of the hygroscopic fluid could improve water recovery efficiency.

The Energy Research Center investigated water-cooled shell-and-tube type heat exchangers for condensing moisture from flue gas [13,14,20]. The study involved testing pilot scale bare tube and fin tube heat exchangers on flue gas streams from fuel oil, natural gas, and coal. The experiments were used to validate an analytical model developed to simulate the shell-and-tube heat exchangers. The agreement between the simulation and experiments was good, and the investigation of a full-scale design is in progress.

Investigations were done to integrate the heat recovery system into the plant [20]. The heat exchanger system was analyzed for a power plant with a cold side ESP, but without an FGD. Cooling water availability is limited to the boiler feed-water taken from the discharge of the main steam condenser, which presents a limitation. In a typical power plant, the ratio of the mass flow rates of flue gas to cooling water is 2:1. It was found that when using water-cooled heat exchangers, only a small part of the captured latent heat can be utilized for preheating feed water. Additional heat sinks are needed for maximum water recovery from the flue gas.

1.2 Comparison between Dry Steam Condensers and Dry Flue Gas Condensers

In power plant applications, air-cooled heat exchangers are typically used as condensers. A schematic of a dry direct steam condenser system is shown in Figure 1.2. This condenser design has an A-frame construction with forced air cooling. The largest example of a dry direct air-cooled steam condenser is the Matimba Plant, in the Republic of South Africa [15]. The power plant has six units at 665 MW, and each unit has 384 heat exchanger tube bundles for cooling. Each bundle is almost 10 feet wide and roughly 32 feet long with two rows of galvanized plate fin elliptical tubes. In total the plant has 2304 tube bundles. The tube bundles are arranged in an A-frame configuration, similar to that shown in Figure 1.2.

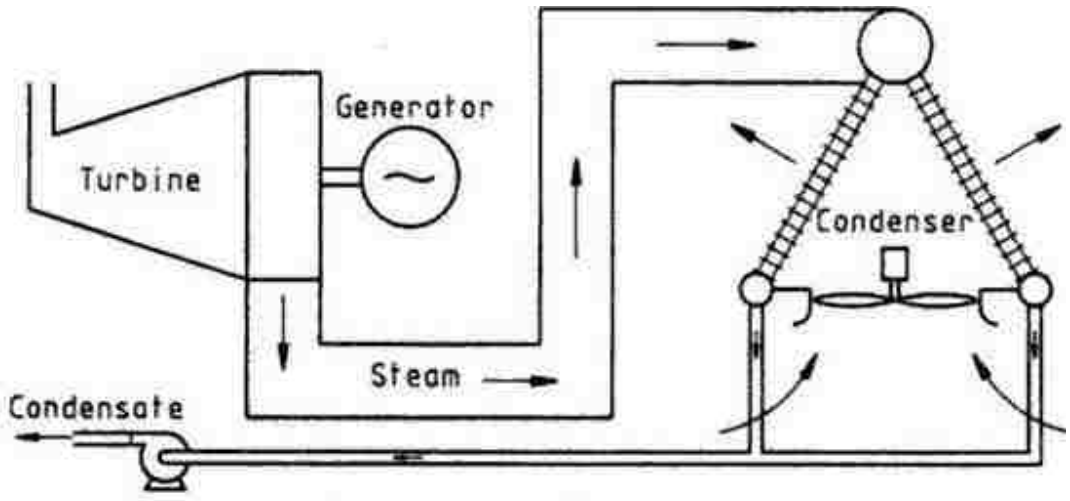

Figure 1.2 – Dry direct steam air-cooled condenser system.

The size of a dry, direct air-cooled steam condenser for a 600 MW power plant was calculated using a heat exchanger handbook [21-22]. For condensing steam at 93^{o}F with cooling air entering at 75^{o}F, the necessary surface area of the condenser is approximately 1,600,000 ft^{2}. As shown in Chapter 5 and 6 the flue gas air-cooled condenser for the same power plant would have approximately 60,000 to 200,000 of surface area. The flue gas condenser is approximately 1/8th the size.

A dry, direct air-cooled steam condenser performs total condensation of the steam and purges trapped noncondensible gases that enter the flow upstream due to leakage. The presence of noncondensible gases creates a resistance to latent heat transfer which adversely affects the performance of the steam condenser. A study by Stewart et al. [19] showed how noncondensible gases can greatly affect the heat transfer performance. Noncondensible gases exist because of leakage in steam condensers and therefore it is difficult to quantify their presence in the flow, so noncondensibles are typically ignored during engineering calculations. However, in a flue gas condenser, where noncondensible gases would make up approximately 90% of the gas, the effects must be simulated.

Figure 1.3 shows the case of a flue gas condenser where the flow is a mixture of condensible and noncondensible gases. The figure shows that in order for condensation to occur the vapor must diffuse from the bulk flow through the noncondensible gases, towards the condensate interface. Simulating this phenomenon is the main challenge with designing an air-cooled condenser (ACC) for flue gas because heat transfer handbooks [22-24] provide methods for rating and sizing pure substance condensers, but they do not provide methods to rate flue gas condensers.

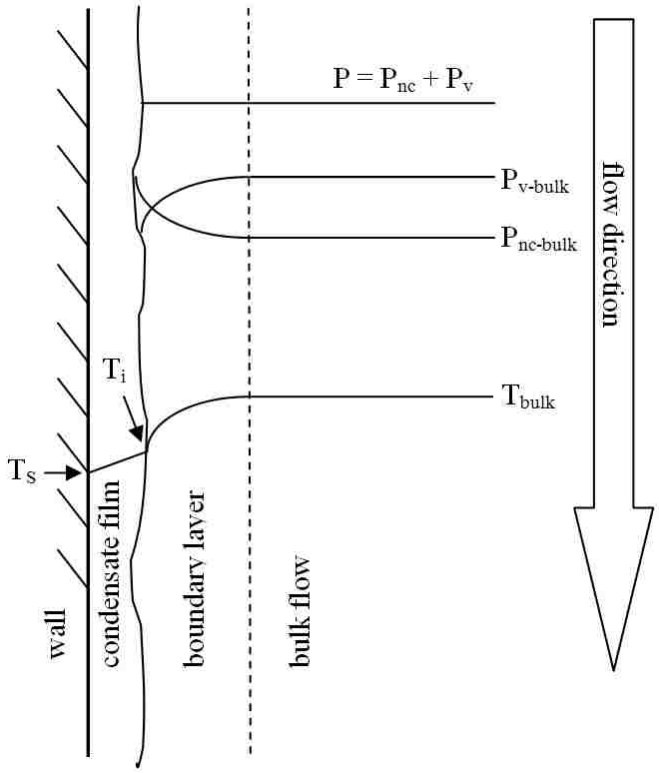

Figure 1.3 - Condensation in the presence of noncondensible gases

The earliest attempt to quantify the effect of noncondensible gases was by Colburn et al. and Chilton et al. [16-18,45], and they developed a heat and mass transfer analogy for condensing vapors in the presence of noncondensible gases. They also developed an analytical expression that must be satisfied at each point in a condenser. Webb and Wanniarachi [25] developed an iterative solution technique to solve the expression. Analytical modeling was performed by Jeong et al. [13-14] using this iterative procedure and Jeong et al. conducted experiments to validate the analytical model for external flow. In the present study an internal flow was investigated.

1.3 Heat and Mass Transfer Analogy

The methodology to calculate the condensation rate of a condensible vapor from a mixture of condensible and noncondensible gases was developed for steady diffusion of a single vapor through a non-diffusing gas. A relationship exists between mass transfer and heat transfer, and

the mass transfer coefficient can be calculated based on the heat transfer coefficient. The mass transfer coefficient k_g is Equation 1.1 [25].

$$k_g = \frac{h_g M_{H_2O}}{C_{p,g} M_g Le^{2/3} P_{lm}} \tag{1.1}$$

$$P_{lm} = \frac{p_{nc,bulk} - p_{nc,i}}{ln\left(\frac{p_{nc,bulk}}{p_{nc,wall}}\right)} \tag{1.2}$$

$$Le = \frac{\alpha_g}{D_g} \tag{1.3}$$

An approximation used in this calculation is that the diffusion coefficient of water vapor through flue gas D_g behaves like water vapor through air. This approximation was used by Osakabe [26] and Jeong et al. [13-14].

The driving potential for mass transfer was the gradient of the vapor partial pressure between the bulk flow and the tube wall (or condensate interface). The condensation rate (Equation 1.4) was calculated using this gradient, and then the latent heat (Equation 1.5) was calculated based on the condensation rate.

$$\dot{m}_{cd} = k_g A_g \left(p_{v,bulk} - p_{v,i}\right) \tag{1.4}$$

$$Q_{lat} = \dot{m}_{cd} h_{fg} \tag{1.5}$$

The relationship developed by Colburn and Hougen that must be satisfied everywhere in the condenser quantified conservation of energy for both sensible and latent heat. Shown as Equation 1.6, it states that the sensible and latent energy transferred from the flue gas must be the same as the sensible energy absorbed by the coolant. To apply Equation 1.6 to a heat exchanger required a stepwise calculation procedure because the quantity $\left(p_{v,bulk} - p_{v,i}\right)$ was not constant in the regions of the heat exchanger where condensation occurred.

$$h_g A_g \left(T_g - T_s\right) + h_{fg} k_g A_g \left(p_{v,bulk} - p_{v,i}\right) = h_a A_a (T_s - T_a) \tag{1.6}$$

The property values of the flue gas were determined using the law of mixtures for the molecular weight and specific heat, density using the ideal gas law, and diffusion properties from the method developed by Wilke [59-60] and Bird et al. [48]. The method of Wilke and Bird et al., is shown in Equation 1.7, it was developed for multi-component mixtures of polyatomic non-polar molecules. Equation 1.7 is theoretically for mixtures of non-polar molecules, and flue gas is a mixture of non-polar and polar molecules, but it was used in this study because comparisons performed by Wilke showed the average deviation between the calculations and experimental measurements to be approximately 4 percent for mixtures containing non-polar polyatomic gases.

$$\mu = \sum_{i=1}^{n} \frac{\mu_i}{1 + \frac{1}{x_i}\sum_{j=1, j\neq i}^{j=n} x_j \phi_{ij}}$$
$$\phi_{ij} = \frac{1}{\sqrt{8}}\left(1 + \frac{M_i}{M_j}\right)^{-1/2}\left[1 + \left(\frac{\mu_i}{\mu_j}\right)^{1/2}\left(\frac{M_j}{M_i}\right)^{1/4}\right]^2 \quad (1.7)$$

The Nusselt number for the gas side, h_g was taken from Gnielinski [27] for internal, fully-developed turbulent flow.

$$Nu_{D'} = \frac{(f/8)(Re_D - 1000)Pr}{1 + 12.7(f/8)^{1/2}(Pr^{2/3} - 1)}$$
$$0.5 \leq \text{Pr} \leq 2000 \quad (1.8)$$
$$2300 \leq Re_D \leq 5 \times 10^6$$

An empirical correlation (Equation 1.9) to account for entrance effects was developed by by Al-Arabi [28] for a sharp-edged inlet and turbulent flow. For long tubes, the entrance effects become negligible.

$$Nu_D = Nu_{D'}\left(1 + \frac{1.683}{(L/ID)^{0.577}}\right) \tag{1.9}$$

The friction factor (Equation 1.10) for turbulent flow in smooth tubes was taken from Munson [29].

$$f = 0.79(lnRe - 1.64)^{-2} \tag{1.10}$$

The gas side heat transfer coefficient was calculated using Equation 1.11.

$$h_g = \frac{Nu_D \times \lambda_g}{ID} \tag{1.11}$$

The heat transfer coefficient for the air side was calculated using bare tube bundle correlations and accounting for fins by calculating a fin efficiency. The Nusselt number for flow in a staggered bare tube bundle was found in Incropera [39]. Constants for the correlation are listed in Table 1.2. Row correction factors to account for the rows prior to the fully developed region are listed in Table 1.1.

$$\begin{gathered} Nu_{D'} = C * {Re_D}^m Pr^{0.36}\left(Pr/Pr_{surface}\right)^{0.25} \\ Nu_D = Nu_{D'} \times Correction \\ 0.7 \leq Pr \leq 500 \\ 1000 \leq Re_D \leq 2 \times 10^6 \end{gathered} \tag{1.12}$$

Table 1.1 - Row correction factors for air-side heat transfer coefficient.

Row #	1	2	3	4	5	6	7	8	9
Aligned Tubes	0.7	0.8	0.86	0.9	0.92	0.95	0.97	0.98	0.99
Staggered Tubes	0.64	0.76	0.84	0.89	0.92	0.95	0.97	0.98	0.99

Table 1.2 - Constants for Equation 1.12.

Configuration	$Re_{E,max}$	C	m
Aligned $(S_t/S_l > 0.7)^*$	10^3-2*10^5	0.27	0.63
Staggered $(S_t/S_l < 2)$	10^3-2*10^5	$0.35(S_t/S_l)^{1/5}$	0.6
Staggered $(S_t/S_l) > 2$	10^3-2*10^5	0.40	0.60

* for $(S_t/S_l < 0.7)$ heat transfer is inefficient and aligned tubes should not be used.

The heat transfer coefficient for the bare tube bundle was calculated with Equation 1.13.

$$h_{air} = \frac{Nu_D \times \lambda_a}{OD} \tag{1.13}$$

The fin efficiency was defined as the ratio of the actual heat transfer rate to the heat transfer rate if the entire fin were at the base temperature T_s. The base temperature T_s is the temperature at the location where the fin is attached to the tube. The theoretical fin efficiency for annular fins is Equation 1.14, taken from Incropera [39].

$$\eta_F = \frac{2r_1}{m(r_{2c}^2 - r_1^2)} \frac{K_1(mr_1)I_1(mr_{2c}) - I_1(mr_1)K_1(mr_{2c})}{I_0(mr_1)K_1(mr_{2c}) - K_0(mr_1)I_1(mr_{2c})}$$
$$m = (2h_a/\lambda_F F_T)^{0.5} \tag{1.14}$$

where I_0 and K_0 are modified, zero-order Bessel functions of the first and second kind, and I_1 and K_1 are modified, first-order Bessel functions of the first and second kind, $r_1$refers to the inner radius of the fin and r_{2c} refers to the summation of the outer radius of the fin and half the fin thickness. An overall surface efficiency η_o was calculated using Equation 1.15 to account for the number of fins on the tube and the spacing between them.

$$\eta_o = 1 - \frac{NA_F}{A_t}(1 - \eta_F) \tag{1.15}$$

where N is the total number of fins, A_F is the surface area of one fin, A_t is the total exterior surface area of the tube including the fins. Newton's law of cooling applied to the air side (Equation 1.16) has the term η_o to account for the overall surface efficiency.

$$Q = h_a \eta_o A_t (T_a - T_s) \tag{1.16}$$

Another approach to predicting the heat transfer coefficient is to use empirical data. Experimental bare tube data and finned tube data can be found in Zhukauskas and Ulinskas [46] and Stasiulevicius and Skrinska [34]. Correlated data from Mirkovic [30] and Ganguli [31] can be used employing the row correction function from Gionollio and Cuti [32]. If the air-side Reynolds number is below 18000, the correlations for finned-tubes developed by Briggs and Young [33] apply.

1.4 Fluid Pressure Losses in the Heat Exchanger

The pressure drop associated with air flowing around staggered finned tube bundles was investigated by Stasiulevicius and Skrinska [34]. They measured pressure losses for 24 finned tube bundles and correlated the data for the Euler number. All measured values were within 20% of the equation and the empirical correlations are Equations 1.17 and 1.18.

$$10^3 < Re_D < 10^5 \qquad Eu = \frac{\Delta p}{\rho {u_a}^2} = \frac{6.55\left(1 - {F_P}/{_{OD}}\right)^{1.8} Re^{-0.25}}{\left({S_T}/{_{OD}}\right)^{0.55}\left({S_L}/{_{OD}}\right)^{0.5}\left(1 - {F_H}/{_{OD}}\right)^{1.4}} z \tag{1.17}$$

$$10^5 < Re_D < 10^6 \qquad Eu = \frac{\Delta p}{\rho {u_a}^2} = \frac{0.37\left(1 - {F_P}/{_{OD}}\right)^{1.8}}{\left({S_T}/{_{OD}}\right)^{0.55}\left({S_L}/{_{OD}}\right)^{0.5}\left(1 - {F_H}/{_{OD}}\right)^{1.4}} z \tag{1.18}$$

The range of geometries of the tube bundles used in Stasiulevicius and Skrinska's experiments are listed in [34].

Table 1.3 - Range of design parameters for the fin tube bundles used in the experiments of Stasiulevicius and Skrinska's.

Dimensionless Variable	Minimum Experimental Value	Maximum Experimental Value
St/OD	2.2	4.1
Sl/OD	1.3	2.1
F_L/OD	0.125	0.5
F_p/OD	0.125	0.28

To determine the pressure loss of the flue gas in an ACC, the flow must be defined as single-phase or two-phase. For a single-phase flow inside a circular pipe, the integral momentum balance written over the cross-sectional area of a pipe like the element in Figure 1.4 is Equation 1.19 [61].

$$\int_A \left[p - \left(p + \frac{dp}{dz}\delta z\right)\right] dA = \int_S \tau_o \delta z dS + \int_A \frac{d}{dz}(Gu)\,\delta z dA + \int_A \rho g \sin\theta\, \delta z dA \qquad (1.19)$$

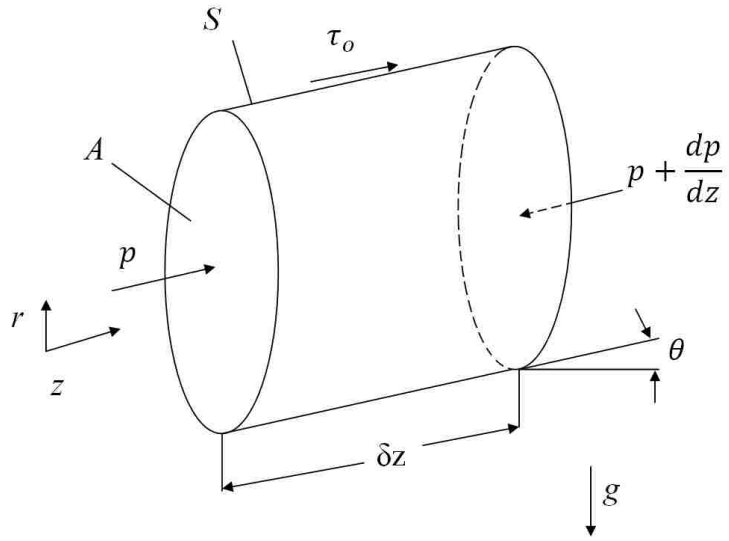

Figure 1.4 - Differential element for Equation 1.19.

where p is the pressure at a given point in the cross-section at axial position z, τ_o is the wall shear stress at a point around the periphery surface S, and G, u, and ρ are the local mass flux, velocity and density of the fluid respectively. θ is the angle of inclination of the channel from the horizontal and A is the channel cross-sectional area. For a circular tube, uniform density and uniform velocity across the cross-section, it follows that:

$$-\frac{dp}{dz} = \frac{S}{A}\tau_o + G\frac{du}{dz} + \rho g \sin\theta \tag{1.20}$$

The three right-hand-side terms in Equation 1.20 represent the pressure drop associated with friction, acceleration, and gravity respectively. Assuming constant flow velocity in the axial direction and neglecting gravity, the pressure drop due to the wall shear stress can be determined using Equation 1.21, and the friction factor using Equation 1.22. [61].

$$\frac{dp}{dz} = \Delta P_{tube} = f\frac{L}{ID}\frac{\rho V^2}{2} \tag{1.21}$$

$$(0.79\ln(\mathrm{Re}) - 1.64)^{-2} \tag{1.22}$$

Treating the gas as a two-phase fluid, the integral momentum balance written over the differential element in Figure 1.4 is Equation 1.23.

$$\int_A \left[p - \left(p + \frac{dp}{dz}\delta z\right)\right] dA = \int_S \tau_o \delta z dS + \int_A \frac{d}{dz}\left(G_L u_L + G_g u_g\right)\delta z dA + \int_A \rho g \sin\theta\, \delta z dA \tag{1.23}$$

where the subscripts L and g denote the liquid and gas phases. The right-hand side terms correspond to shear stress, acceleration, and gravitational effects respectively. Evaluating Equation 1.23 for a circular tube with uniform density and velocity across the cross section, and employing the two-phase multiplier Φ_{lo}^2 on the shear stress term, results in Equation 1.24.

$$-\left(\frac{dP}{dz}\right) = \Phi_{\mathrm{lo}}^2 \frac{2f_{lo}G^2}{\rho_l d_h} + [(1-\alpha)\rho_l + \alpha\rho_v]g\ sin(\theta) + \frac{d}{dz}\left[\frac{G^2x^2}{\rho_v\alpha} + \frac{G^2(1-x)^2}{\rho_l(1-\alpha)}\right] \quad (1.24)$$

The two-phase multiplier Φ_{lo}^2 method was proposed by Lockhart and Martinelli [37] as a way of determining the friction pressure loss of a two-phase flow using empirical data. The method utilizes a generalized correlation which covers all combinations of laminar and turbulent regimes for both the liquid and gas phases. The method covers all flow regimes and two-phase flow patterns, but the method does not apply when the flow pattern changes along the tube length. For example, this method does not apply to a slug flow because a slug flow is alternating sections of liquid and large pockets of vapor. But it is applicable to a whispy flow or annular flow, in which the flow pattern is the same at all cross sections [37]. The two phase multiplier is a ratio of the frictional pressure loss to the frictional pressure loss if the fluid were single-phase.

$$\Phi_{\mathrm{lo}}^2 = \left[\frac{(\mathrm{dP/dz})_{\mathrm{fr}}}{(\mathrm{dP/dz})_{\mathrm{lo}}}\right] \quad (1.25)$$

In Equation 1.25, $(dP/dz)_{fr}$ is the actual pressure gradient in the tube and $(dP/dz)_{lo}$ is the fictitious single-phase pressure gradient if the flow were just liquid. $(dP/dz)_{lo}$ can be evaluated using Equation 1.21, or by using the Blasius correlation (Equations 1.26 and 1.27) for turbulent, single-phase flow in round tubes.

$$-\left(\frac{dP}{dz}\right)_{lo} = \frac{2f_{lo}G^2}{\rho_l d_h} \quad (1.26)$$

$$f_{lo} = 0.079Re_{lo}^{-0.25} \quad (1.27)$$

Kroger, Carey, and Kolev [15,36,38] all recommend using the same correlation for calculating the two-phase multiplier Φ_{lo}^2, Equation 1.28. The equation correlates 25,000 experimental data points within 30-40%. It is valid for vertical and horizontal, single-component, and two-component two-phase flows.

$$\Phi_{\mathrm{lo}}^2 = C_{F1} + \frac{3.24 C_{F2}}{Fr^{0.045} We^{0.035}}$$

$$CF1 = (1-x)^2 + x^2 \left(\frac{\rho_l}{\rho_v}\right)\left(\frac{f_{vo}}{f_{lo}}\right) \tag{1.28}$$

$$CF2 = x^{0.78}(1-x)^{0.24}\left(\frac{\rho_l}{\rho_v}\right)^{0.91}\left(\frac{\mu_v}{\mu_l}\right)^{0.19}\left(1-\frac{\mu_v}{\mu_l}\right)^{0.7}$$

$$Fr = \frac{G^2}{g d_h \rho^2} \tag{1.29}$$

$$We = \frac{G^2 d_h}{\rho \sigma} \tag{1.30}$$

$$f_{vo} = 0.079 Re_{vo}^{-0.25} \tag{1.31}$$

There is an additional pressure loss of the flue gas associated with the gas entering and exiting the tubes. Assuming that the tubes are connected to manifolds where the tubes have sharp-edged inlets and exits and the flow in the manifolds flows horizontal (see Figure 2.1) the inlet and exit pressure losses are Equation 1.32 and 1.33 [43].

Inlet $$\Delta P_{inlet} = 0.56 \frac{\rho V^2}{2} \tag{1.32}$$

Exit $$\Delta P_{exit} = 0.8 \frac{\rho V^2}{2} \tag{1.33}$$

1.5 Economic model for air-cooled heat exchanger

The economic model has two applications in this research. The model was used to estimate how much the heat exchanger would cost, and it was used for a functional relationship to compare heat exchanger size and performance. It was used to optimize the heat exchanger design. One important aspect of this research was utilizing a cost function to optimize the geometry of the heat exchanger and the economic model developed here made that possible. The

second important contribution of the economic model was to estimate what the cost of the ACC would be. The economic model is a combination of capital cost, operating costs, and operating savings. This section discusses each component.

The final function developed in this economic model is a combination of capital cost, operating costs, and operating savings. Minimizing the function leads to minimizing capital cost, minimizing operating costs and maximizing operating savings. This is the most important aspect of the economic model, having a function to minimize which leads to an ACC with desirable performance.

The economic model predicts the absolute cost of the system. One must keep in mind that the correlations used to estimate the capital costs were derived from data on actual costs of ACCs. However, the authors [62-64] state the correlations are order of magnitude estimates and should be used as preliminary estimates. These estimates are the first step in determining the cost of a large heat exchanger, and the next step is to hire a company which specializes in providing quotes for large heat exchangers. Even with the uncertainty in the cost estimates, the economic model provides a good estimate of the cost as well as establishes the relationship between heat transfer, pressure loss, and surface area necessary to optimize the overall design. To further improve this technique, one could use the same methodology established here with their own capital cost function.

The capital cost of the heat exchanger was calculated in the present study using an order of magnitude estimate based on surface area. Smith [62] provides an estimate for fob (‘fob’ implies free-on-board which means the manufacturer pays for loading charges, but not shipping and installation). Clerk [63] provides a “field-erect” cost for air-cooled heat exchangers also based on the interior surface area of the tubes. In addition, Clerk showed the uninstalled costs to be separated into five major components and these are listed in Table 1.4.

Table 1.4 - Cost fractions of a typical un-installed air cooler [63].

Bundle	**45%**
Heaters	12%
Fans and Motors	19 %
Louvers	12 %
Steel structures, stairways, ladders etc…	12 %
Total	100 %

Clerk then estimated the erection costs to be an additional 20% of the fob cost. Guthrie [64] provides an estimate for capital cost based on interior surface area of the tubes which includes:

- Tube bundle
- Fan and motor
- Casing, structure
- Stairways etc…
- Field erection
- Subcontractor indirect costs

These three sources have in common that the cost was estimated with a power-law function based on the interior surface area of the tubes, like Equation 1.34. In Equation 1.34 and the estimates by Clerk, Smith, and Guthrie, there are factors f_i that account for changes from the nominal design (e.g. different materials, operating pressures, tube lengths etc…).

$$\$ = A(surface\ area)^n * \left(\sum_{i=1}^{m} f_i\right) \tag{1.34}$$

In Equation 1.34, *A* is a constant, *n* is the size exponential factor 0.8, and *f* is the factor accounting for different tube materials, tube lengths, operating pressures, etc…

When optimizing heat exchanger designs, order of magnitude estimates for cost are frequently used. Such estimates are typically power-law relationships based on surface area,

because they lend themselves to being optimized. Simply, to minimize Equation 1.34, one must minimize the surface area. There are many studies that investigate optimizing heat exchangers [50-58]. These studies all used a power-law relationship that estimated cost based on surface area. [50,51,54-58] investigated shell-and-tube exchangers, [52] investigated a plate-type heat exchanger, and [53] used the correlation by Smith [62] to estimate the cost of an ACC.

The power-law relationships for capital cost were published in years passed, therefore to calculate the present value of the cost, indexes were taken out of *Chemical Engineering*. Equation 1.35 shows how the index values were applied.

The capital cost was calculated on an annual basis to compare with annual operating costs. Equation 1.36 was used to calculate an annualized cost over *n* years at a fixed interest rate of *i*.

$$Capital\ Cost\ (year\ A) = \ Capital\ Cost\ (year\ B)\frac{CE\ Index\ (year\ A)}{CE\ Index\ (year\ B)} \tag{1.35}$$

$$Annualized\ Captial\ Cost = \ Capital\ Cost * \frac{i(1+i)^n}{(1+i)^n - 1} \tag{1.36}$$

The operating costs of the heat exchanger were assumed to be the cost of operating the cooling air fans and the additional load on the flue gas fan. The power supplied to the fans was calculated using the isentropic relationship shown in Equation 1.37, taken from the Babcock and Wilcox handbook [65].

$$Power = k\frac{\Delta P_{air\ or\ flue\ gas}\dot{V}}{\eta_f} \tag{1.37}$$

$$k = \frac{\frac{\gamma}{\gamma - 1}\left[\left(\frac{P_2}{P_1}\right)^{\frac{\gamma-1}{\gamma}} - 1\right]}{\frac{P_2}{P_1} - 1}$$

where k is the compressibility factor, V is the volumetric flow rate, η_f is the fan efficiency (0.875 in the present study), and γ is 1.4 for air. The operating cost was determined assuming the plant operated 7000 hours per year and the cost of electricity for the plant was five cents per kilowatt-hour.

$$Annual\ Fan\ Operating\ Cost = Power * 0.05\frac{\$}{kW - hr} * 7000\frac{hrs}{yr} \tag{1.38}$$

An additional operating cost not addressed in this present study was the cost associated with treatment of the water recovered from the flue gas. Before the water can be used in other equipments, it must be treated. These costs were yet to be determined.

The operating savings of the air-cooled heat exchanger was the reduction in water consumption of the plant. The value of the water would be determined by what the power plant pays for water. Assuming the plant operates for 7000 hours per year, the annual operating savings would be determined using Equation 1.39. For the simulations, water was estimated to cost $1.50 per 1000 gallons.

$$Operating\ Savings = \dot{m}_{condensate} * 7000\frac{hrs}{yr} * \frac{\$_{H_2O}}{lbm} \tag{1.39}$$

Another opportunity to reduce plant operating costs is to use the recovered energy to pre-heat combustion air. The operating savings in this case would include fuel savings. This is further discussed in Chapter 6.

The net annual cost of the ACC was calculated using Equation 1.40. This equation was used to optimize the design of the ACC. The net annual cost relates the heat and mass transfer

performance, pressure drop performance, and size of the ACC. The optimization seeks to minimize this function.

$$Annual\ Cost = Annualized\ Capital\ Cost + Operating\ Costs - Operating\ Savings \tag{1.40}$$

1.6 Optimization Techniques for Heat Exchangers

Two types of optimization procedures were reviewed in detail for this application, genetic algorithms and the Nelder-Mead method. Ultimately the Nelder-Mead method was chosen for its more methodical approach and explicit algorithm.

The Nelder-Mead optimization is an algorithm which minimizes a real-valued function. It minimizes a function of *n* real variables using only the function values, no derivative information. It directly searches for a minimum using a simplex, which is a geometric figure consisting of vertexes that number one more than the number of dimensions. For example, a simplex in a one-dimensional space is shown in Figure 1.5. There is one function variable *x* shown on the abscissa, the ordinate is the function value at *x*. It is a one-dimensional function and therefore the simplex is a line with two vertexes. Likewise, a two-dimensional simplex can be visualized as a triangle on top of a landscape. For each iteration of the optimization the function value of each vertex is compared and the vertex having the largest function value is replaced by a new vertex having a lower function value. The algorithm stops when a minimum is converged upon.

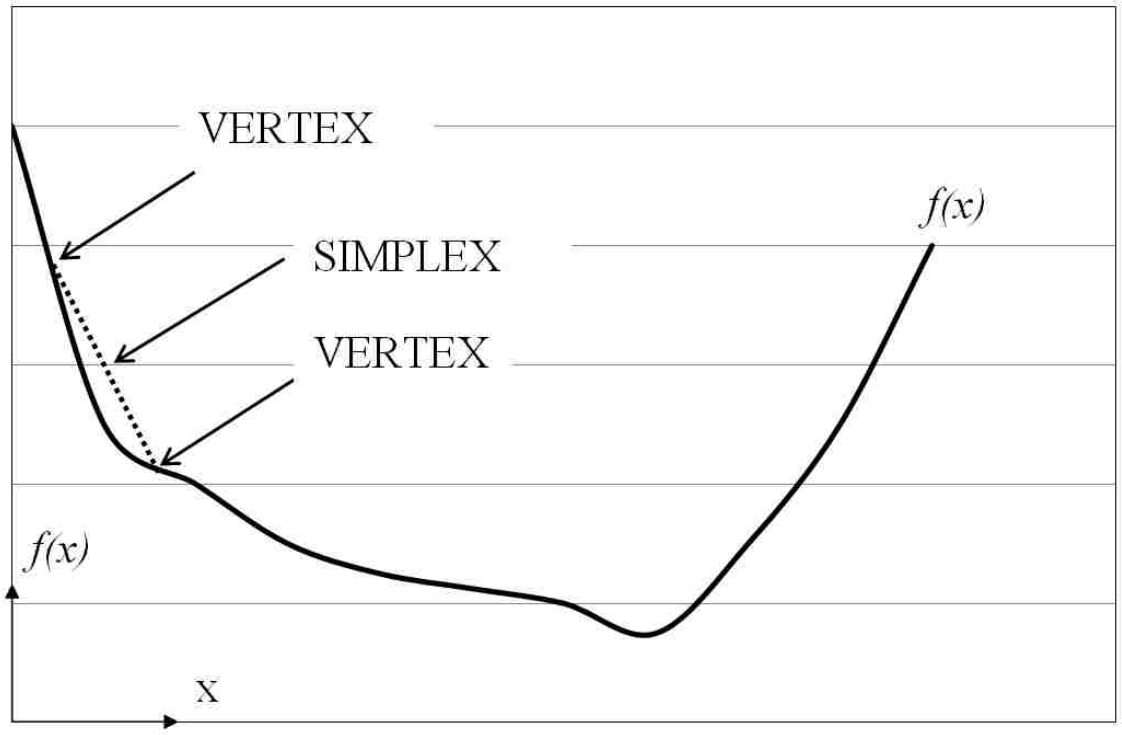

Figure 1.5 - Example of a general 1-Dimensional simplex on a function *f*.

For example, consider in Figure 1.6 the two-dimensional landscape in which the minimum of the function is at the origin of the space. The concentric circles in the figure are paths of constant function values, with larger circles having larger function values. The simplex has been arbitrarily placed away from the minimum. Evaluating the function at each vertex using the x and y coordinates of the three vertices, V1, V2, and V3, indicates that V2 has the highest function value. To replace V2 with a more optimal value, the Nelder-Mead algorithm calls for a reflection of the simplex. The reflection is performed using the known x and y values of V1, V2, and V3. The result of the reflection is shown in Figure 1.7.

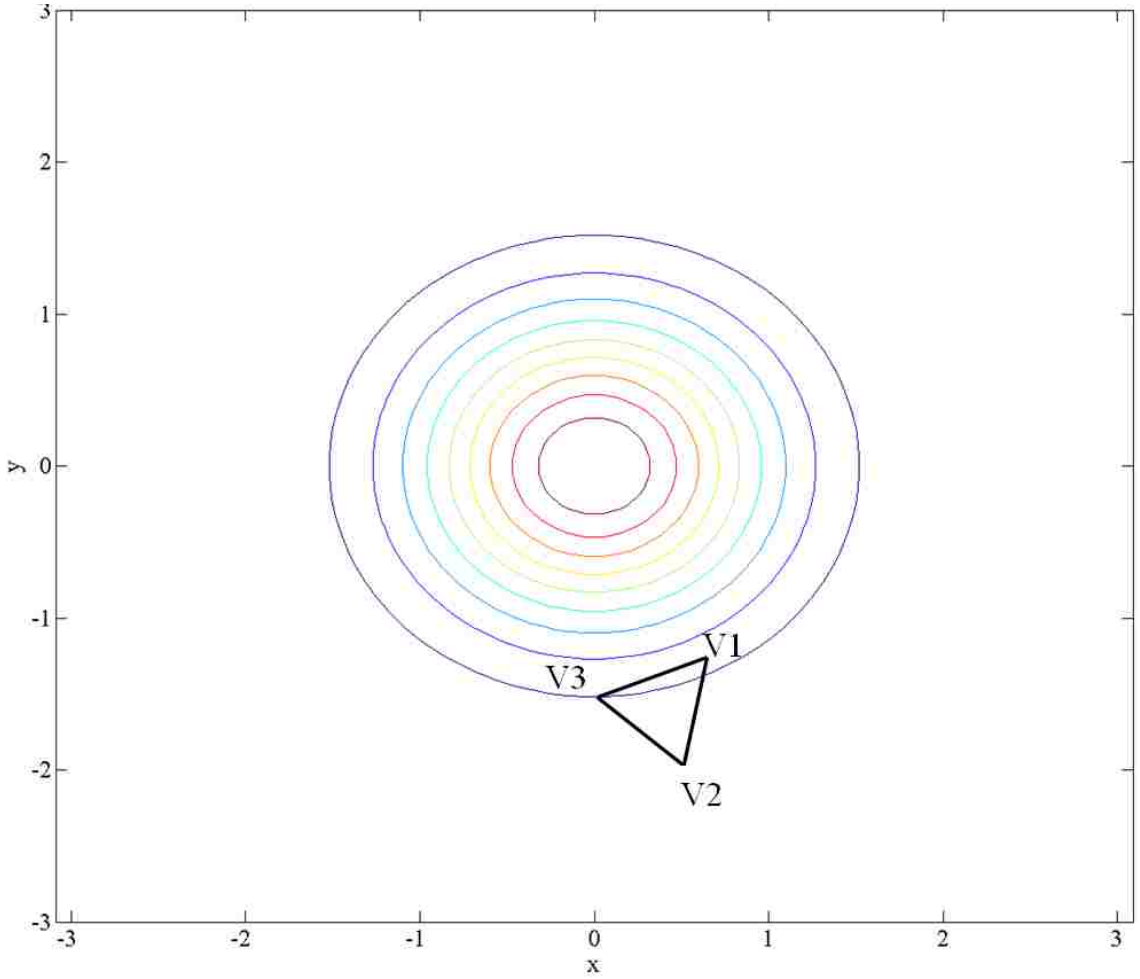

Figure 1.6 – Initial simplex for a 2-dimensional landscape. Concentric circles denote paths of constant function values..

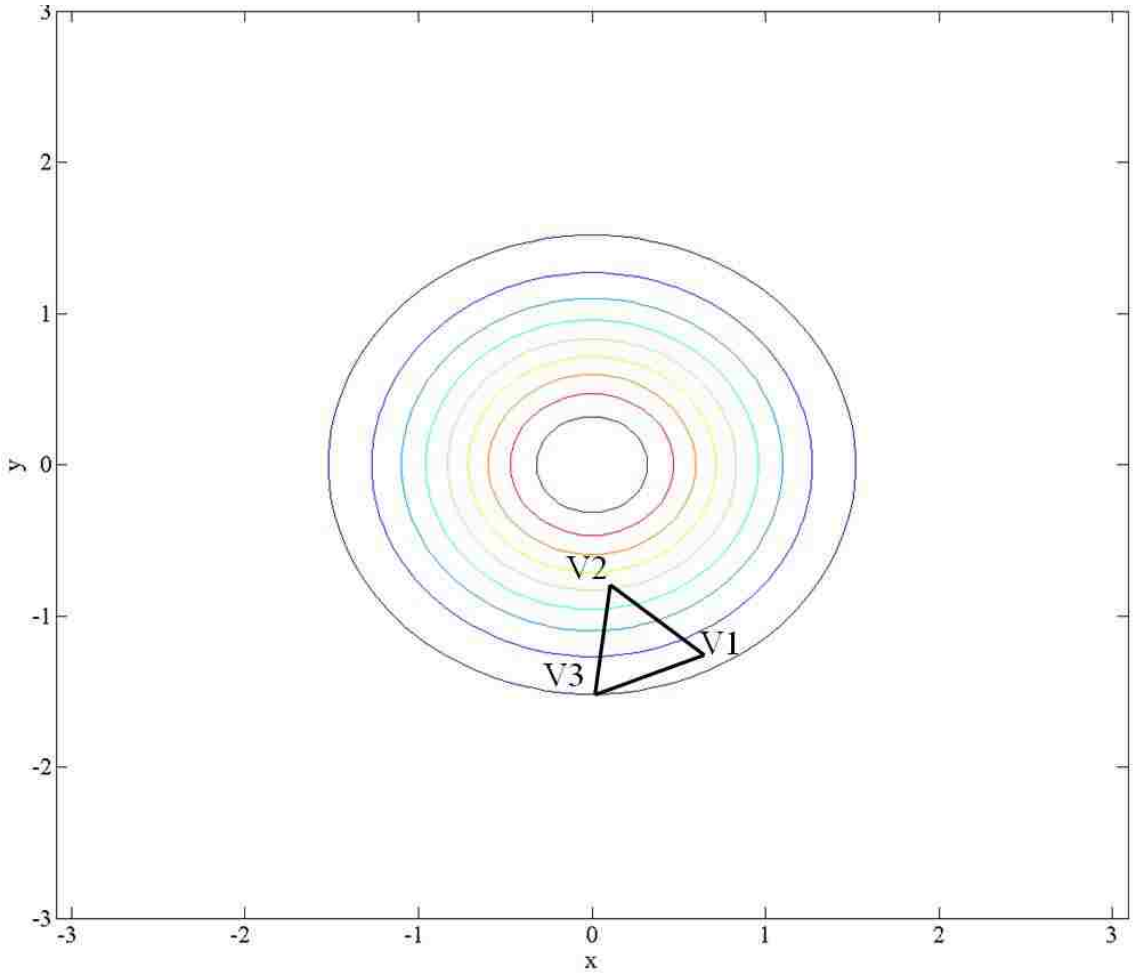

Figure 1.7 – Reflected simplex for a 2-dimensional landscape. Concentric circles denote paths of constant function values..

After reflecting the V2 vertex, evaluation reveals that V2 is a new minimum. Therefore in an effort to converge on the minimum quickly, this reflection is expanded and the simplex becomes a different size, shown in Figure 1.8. With each iteration, the simplex "walks" in the direction towards the minimum until a criterion is satisfied.

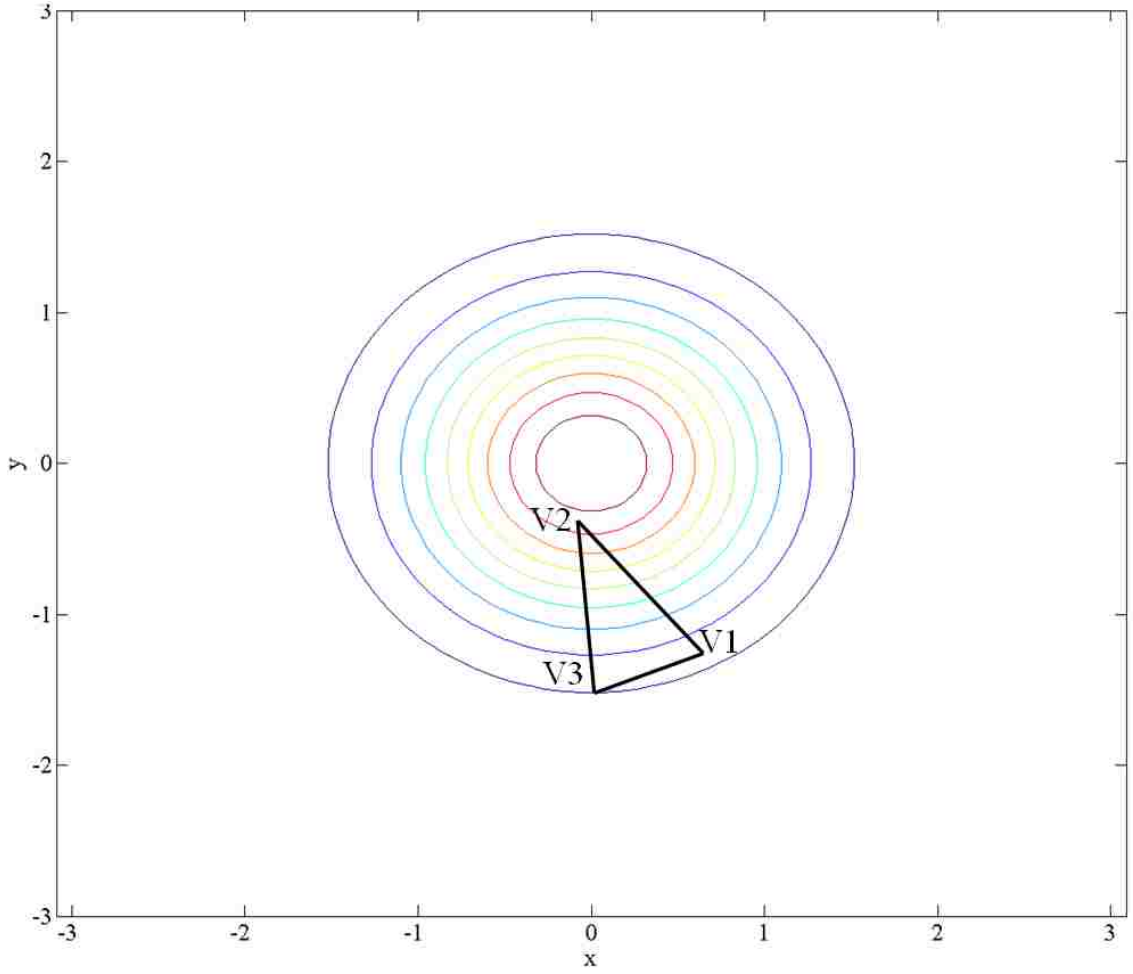

Figure 1.8 - Expanded simplex for a 2-Dimensional landscape. Concentric circles denote paths of constant function values.

In total, there are four different operations for the simplex: reflection, expansion, contraction, and shrinkage, and there are four scalar parameters that characterize these operations. The standard choice of the parameters was taken from Lagarias [41] as:

- $\rho = 1$ (reflection coefficient)
- $\chi = 2$ (expansion coefficient)
- $\gamma = ½$ (contraction coefficient)
- $\sigma = ½$ (shrinkage coefficient)

The following page discusses one iteration of the algorithm.

1. Order the n+1 vertices to satisfy $f(x_1) \leq f(x_2) \leq \cdots \leq f(x_{n+1})$

2. Reflection: Compute the reflection point x_r using Equation 1.41

$$x_r = (1 + \rho)\bar{x} - \rho x_{n+1} \tag{1.41}$$

where $\bar{x} = \sum_{i=1}^{n} {}^{x_i}/_{n}$ is the centroid of the n best points (all vertices except for x_{n+1}.

Evaluate the function $f_r = f(x_r)$

if $f_1 \leq f_r \leq f_n$ accept the reflected point and terminate the iteration.

3. Expand: If $f_r < f_1$, calculate the expansion point x_e according to Equation 1.42

$$x_e = (1 + \rho\chi)\bar{x} - \rho\chi x_{n+1} \tag{1.42}$$

evaluate the function $f_e = f(x_e)$

if $f_e < f_r$ accept x_e and terminate the iteration, otherwise accept x_r and terminate the iteration.

4. Contraction: If $f_r \geq f_n$ perform a contraction between $\bar{x}$ and the better of x_{n+1} and x_r.

4a. If $f_n \leq f_r < f_{n+1}$ perform an outside contraction according to Equation 1.43

$$x_{oc} = (1 + \rho\gamma)\bar{x} - \rho\gamma x_{n+1} \tag{1.43}$$

evaluate $f_{oc} = f(x_{oc})$. If $f_{oc} \leq f_r$ accept x_{oc} and terminate the iteration, otherwise go to step 5 and perform a shrink.

4b. If $f_r \geq f_{n+1}$ perform an inside contraction according to Equation 1.44.

$$x_{ic} = (1 - \gamma)\bar{x} + \gamma x_{n+1} \tag{1.44}$$

evaluate $f_{ic} = f(x_{ic})$. If $f_{ic} < f_{n+1}$ accept x_{ic} and terminate the iteration, otherwise go to step 5 and perform a shrink.

5. Shrink: Evaluate *f* at the *n* points according to Equation 1.45

$$v_i = x_1 + \sigma(x_i - x_1) \tag{1.45}$$

where $i = 2, \dots, n+1$. The vertices of the simplex for the next iteration consist of $x_1, v_2, \dots, v_{n+1}$.

To start the iteration, an initial simplex was defined. Walters [42] discusses multiple methods for determining the initial simplex, and the tilted initial simplex method was used for the simulations in this research.

2 Simulation

A major component of this dissertation was to develop a simulation to predict the performance of the air-cooled condenser (ACC). The condenser geometry was discretized and, using MATLAB, governing equations for heat transfer, mass transfer, and pressure loss were solved. The simulations modeled different diameter tubes, different fin pitch, length, and thickness, and various transverse tube spacing. It also modeled different inlet flue gas temperatures, inlet cooling air temperatures, inlet moisture concentrations, and flue gas and cooling air flow rates.

The simulation was validated using the experimental measurements which are described in Chapter 3. Following the validation, the simulation was used to size a full-scale air-cooled condenser for a power plant. The cost model and optimization technique described in the Literature Review were used to design the full-scale ACC.

This chapter discusses the structure of the simulation, first describing the discretization of the geometry and the algorithm for the heat and mass transfer calculations. Then important assumptions are discussed. The chapter ends with a description of how the Nelder-Mead optimization method was incorporated into the simulation.

2.1 Numerical Procedure for the Simulation

The first step for the simulation was choosing the domain. The air-cooled condenser is shown in Figure 2.1 and Figure 2.2. Figure 2.1 shows a 3-Dimensional view of what an ACC could look like. It is an A-frame construction with a forced-draft fan configuration. The flue gas is distributed to the tube bundles with a manifold which acts as the top support of the tube bundles. Collection manifolds at the exits of the tubes separates the water and flue gas, and in between these collection basins is the cooling air fan. Figure 2.2 shows an end view of an ACC with one row of tubes. The simulation was developed for the general case which can simulate any number of tube rows.

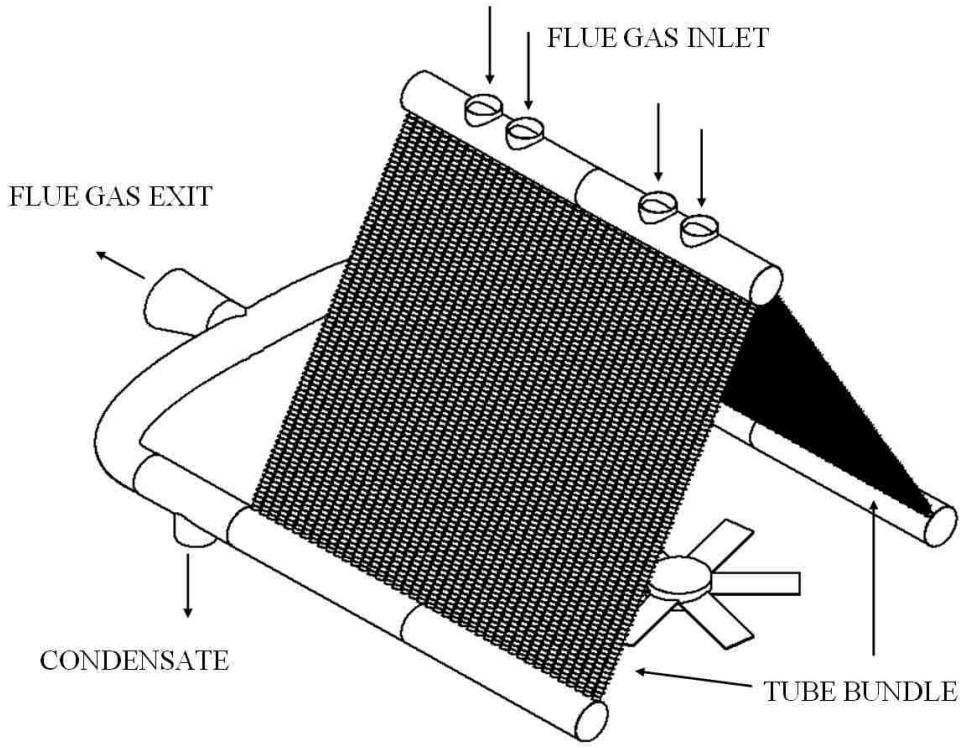

Figure 2.1 - Schematic of full-scale air-cooled with multiple tube bundles each having one row of tubes.

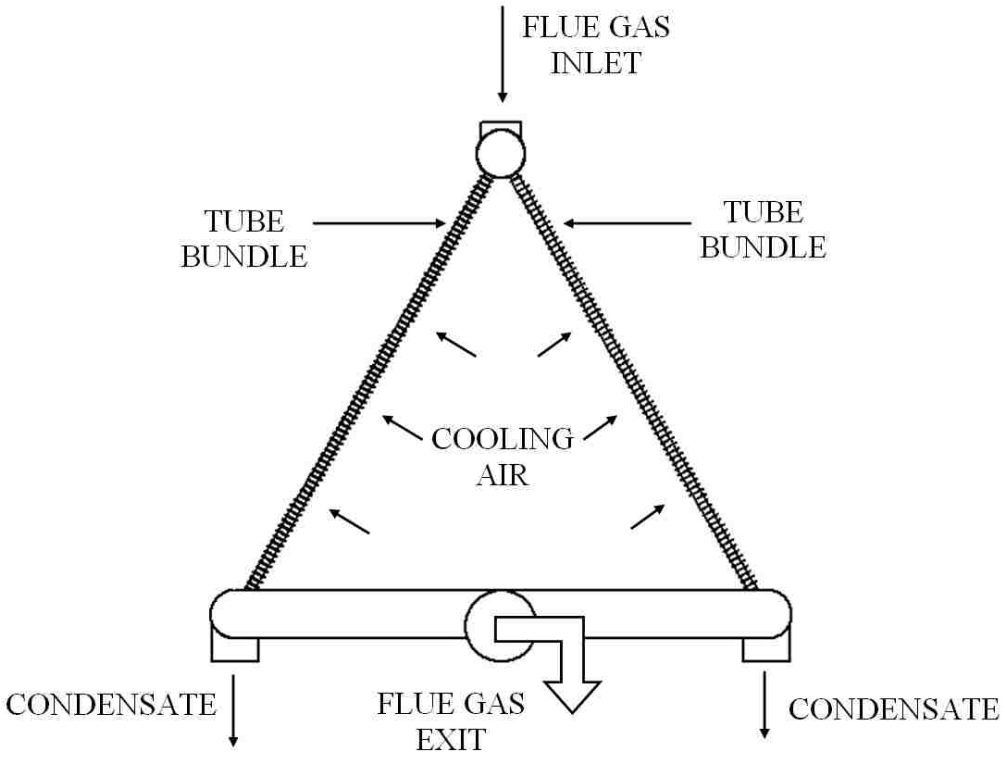

Figure 2.2 - End view of air-cooled condenser with a tube bundle having 1 row of tubes.

In the simulation every tube in the tube bundles was not simulated. Due to the symmetry of the system, only one column of tubes was simulated. A general configuration of one tube bundle of the system is shown in Figure 2.3. It was assumed a tube bundle will have many columns and the end-effects of the cooling air flowing around the outer columns were negligible. Figure 2.4 shows the column of tubes that was modeled in the simulation.

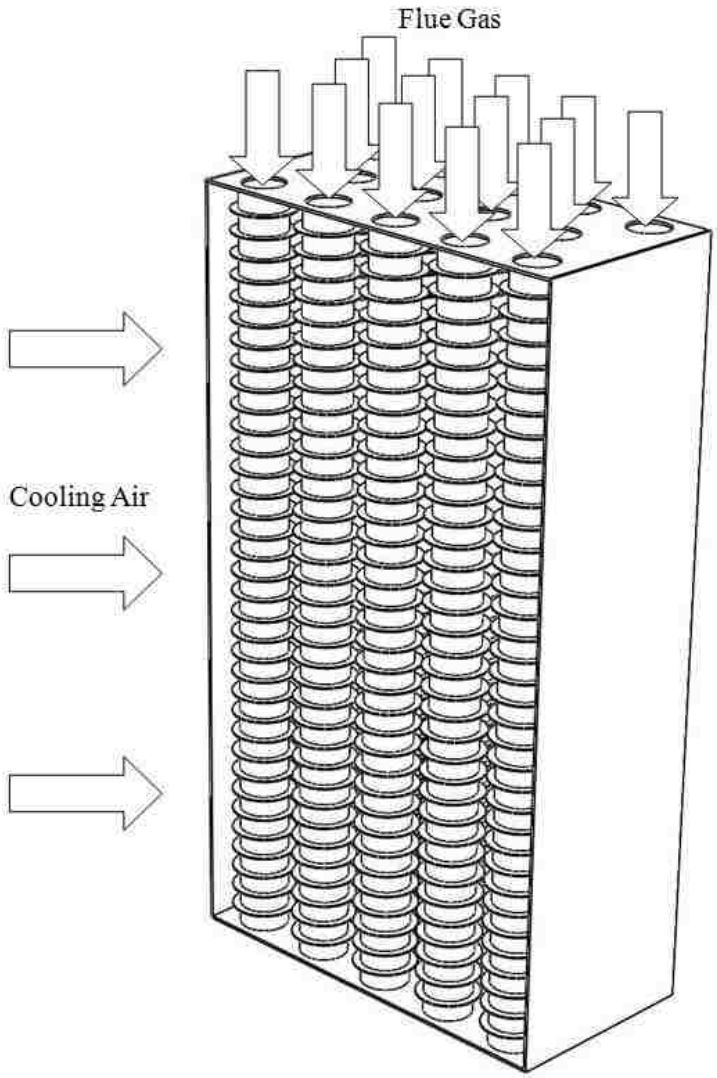

Figure 2.3 - General configuration of one tube bundle having three rows.

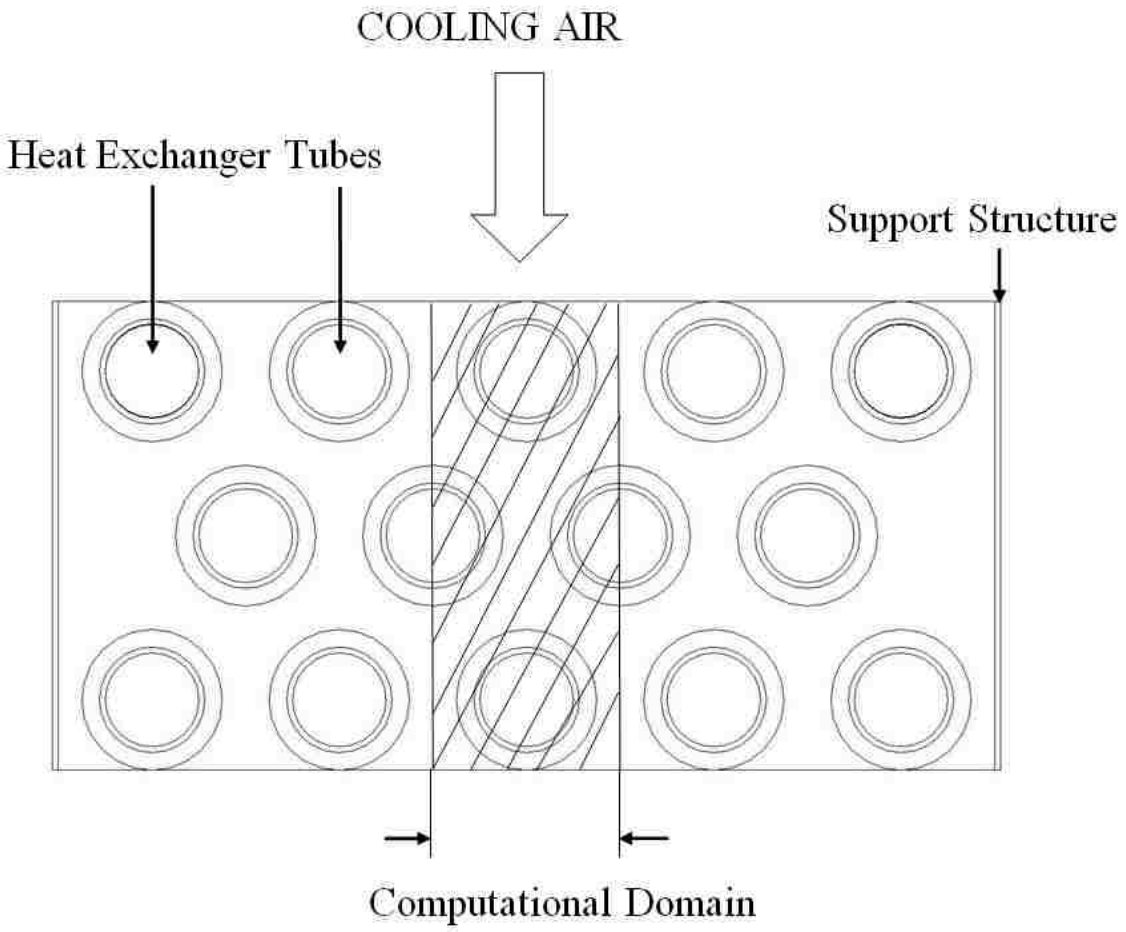

Figure 2.4 - Top view of tube bundle showing the column of tubes that was modeled in the simulation.

The simulation employed 1-Dimensional analytical computations to calculate the axial temperature distributions of the flue gas, cooling air, and tube wall surface. In addition, the flue gas moisture concentration distribution was solved for by calculating the water vapor condensation rate. These four distributions were calculated along the axial direction of the tubes using Equations 2.1 through 2.3.

The initial conditions were the inlet flue gas temperature, inlet cooling air temperature, inlet flue gas moisture concentration and inlet flue gas and cooling air flow rates. Figure 2.5 shows the tubes from the hashed region in Figure 2.4 with the initial conditions, which are summarized in Table 2.1. Table 2.2 shows the four variables in the simulation.

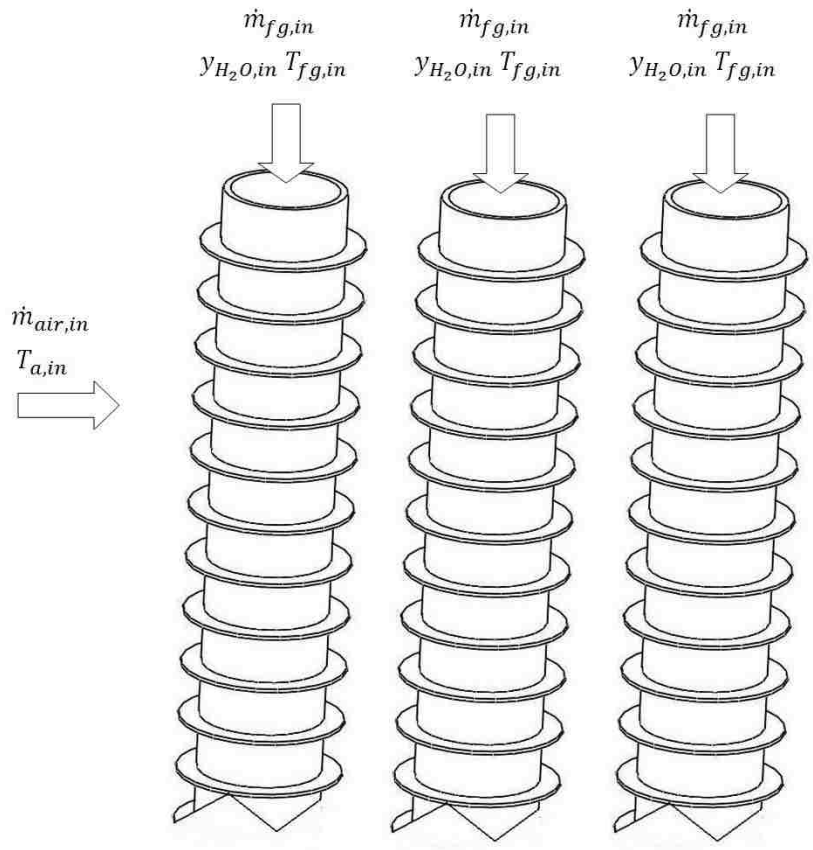

Figure 2.5 – Tubes simulated by the heat and mass transfer simulation.

Table 2.1 - Initial conditions for heat and mass transfer simulation.

Initial Condition	
Inlet Flue Gas Temperature	T_{fg}
Inlet Flue Gas Moisture Concentration	y_{H2O}
Inlet Cooling Air Temperature	T_a
Flue Gas Flow Rate	m_{fg}
Cooling Air Flow Rate	m_{air}

Table 2.2 - Unknowns for heat and mass transfer simulation.

Variables in Heat and Mass Transfer Simulation	
Flue Gas Temperature	T_{fg}
Cooling Air Temperature	T_a
Tube Wall Surface Temperature	T_s
Flue Gas Moisture Concentration	y_{H2O}

If there was no condensation of water vapor, there would have been only 3 variables to solve for, $T_{fg,}$ T_a, and T_s, and it would have been a trivial problem. But because of condensation there was one more variable than governing equations and an iterative procedure was used to find the solution. The governing equations used to model the ACC are Equations 2.1 through 2.3.

$$h_g A_g\left(T_g - T_s\right) + h_{fg} k_g A_g\left(p_{v,bulk} - p_{v,i}\right) = h_a A_a (T_s - T_a) \tag{2.1}$$

$$\dot{m}_a Cp_a\left(T_{a,exit} - T_{a,inlet}\right) = h_a A_a (T_s - T_a) \tag{2.2}$$

$$\dot{m}_g Cp_g\left(T_{g,exit} - T_{g,inlet}\right) = h_g A_g\left(T_s - T_g\right) \tag{2.3}$$

Equation 2.1 was described in the Literature Review (Equation 1.6), which was derived by Colburn et al. [16-18] to be the expression that must be satisfied everywhere in a heat exchanger where condensation occurred in the presence of noncondensible gases. Equations 2.2 and 2.3 are conservation of sensible energy for the flue gas and cooling air, and were derived by reducing the Energy Equation (Equation 2.4) applied to the control volumes shown in Figure 2.6. The eliminated terms in Equation 2.4 were due to the system being steady, neglecting velocity effects and gravitational effects, and no external work $\dot{W}_s$ being done to the system.

$$\dot{Q} + \dot{m}_{inlet}\left(h_{inlet} + \frac{V^2}{2g_c} + \frac{gz}{g_c}\right) = \dot{W}_s + \dot{m}_{exit}\left(h_{exit} + \frac{V^2}{2g_c} + \frac{gz}{g_c}\right) + \left(\frac{dE}{dt}\right)_{c.v.} \tag{2.4}$$

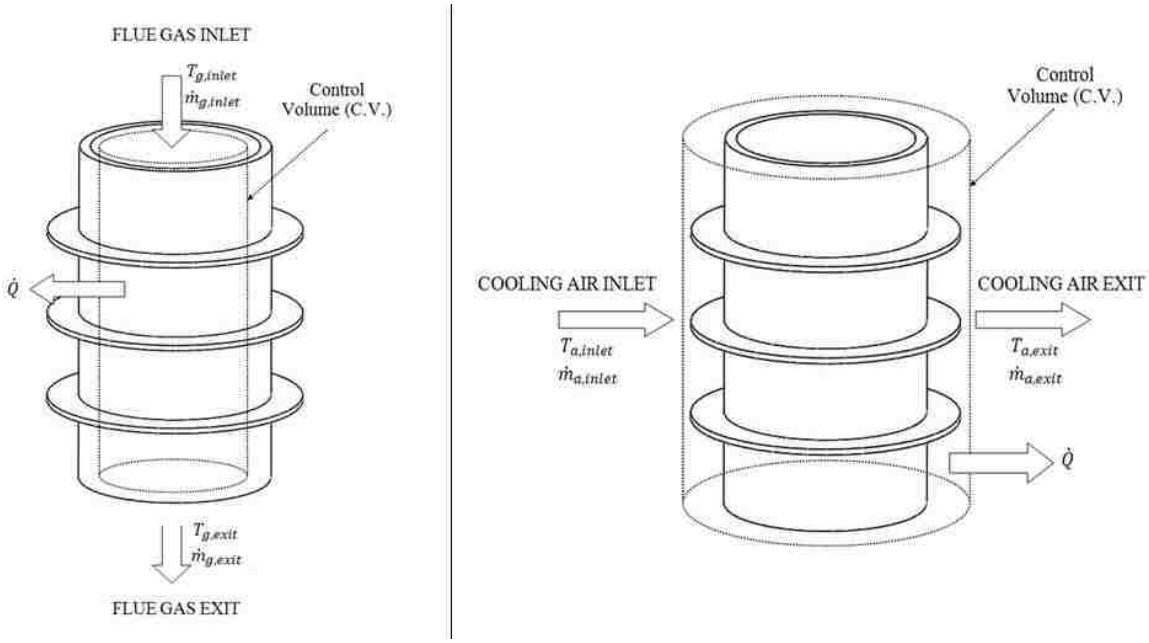

Figure 2.6 - Control volumes for flue gas (Equation 2.2) and cooling air (Equation 2.3) for the energy equation.

Because of condensation, heat exchanger analysis methods such as LMTD and ε-NTU were not applicable. A stepwise calculation procedure was necessary because in Equation 2.1 the driving potential for condensation $(p_{v,bulk} - p_{v,i})$ changed as condensation occured. Discretization and stepwise calculations were recommended by Webb et al. [25] and shown by Jeong et al. [13-14] to accurately model condensation of water vapor from flue gas. The computational domain for the air-cooled condenser developed in this study is depicted by the two-dimensional matrix in Figure 2.7 along with the physical representation of one matrix element.

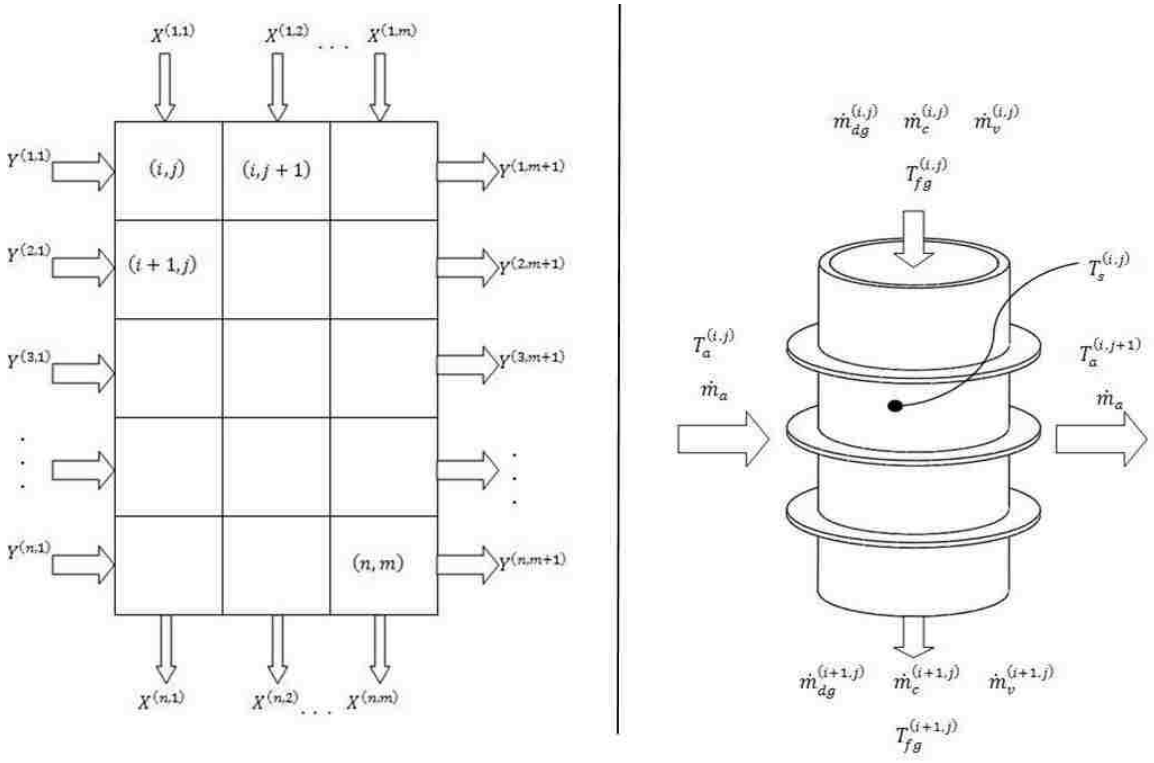

Figure 2.7 - 2-D matrix representation of discretized heat exchanger tubes and physical representation of one matrix element.

The algorithm of the heat and mass transfer code developed for this research is shown in Figure 2.8. The simulation began with the user inputting the initial conditions, and assuming a tube wall surface temperature, T_s distribution for each tube (A uniform distribution was used that was equal to the dew point temperature of the flue gas.). Then the heat exchanger was discretized into an *n* x *m* matrix to look like Figure 2.7. The simulation started the stepwise calculation with element (1,1). The fluid properties, heat and mass transfer coefficients, and flow parameters were calculated using the assumed value of T_s and the initial conditions. These property values and heat and mass transfer coefficients were then used to recalculate a value of T_s using the Colburn Hougen Equation (Equation 2.1). Then Equations 2.2 and 2.3 were used to calculate the temperatures $T_{fg}^{(2,1)}$ and $T_a^{(1,2)}$. The pressure drops of the flue gas and cooling air were also calculated for cell (1,1).

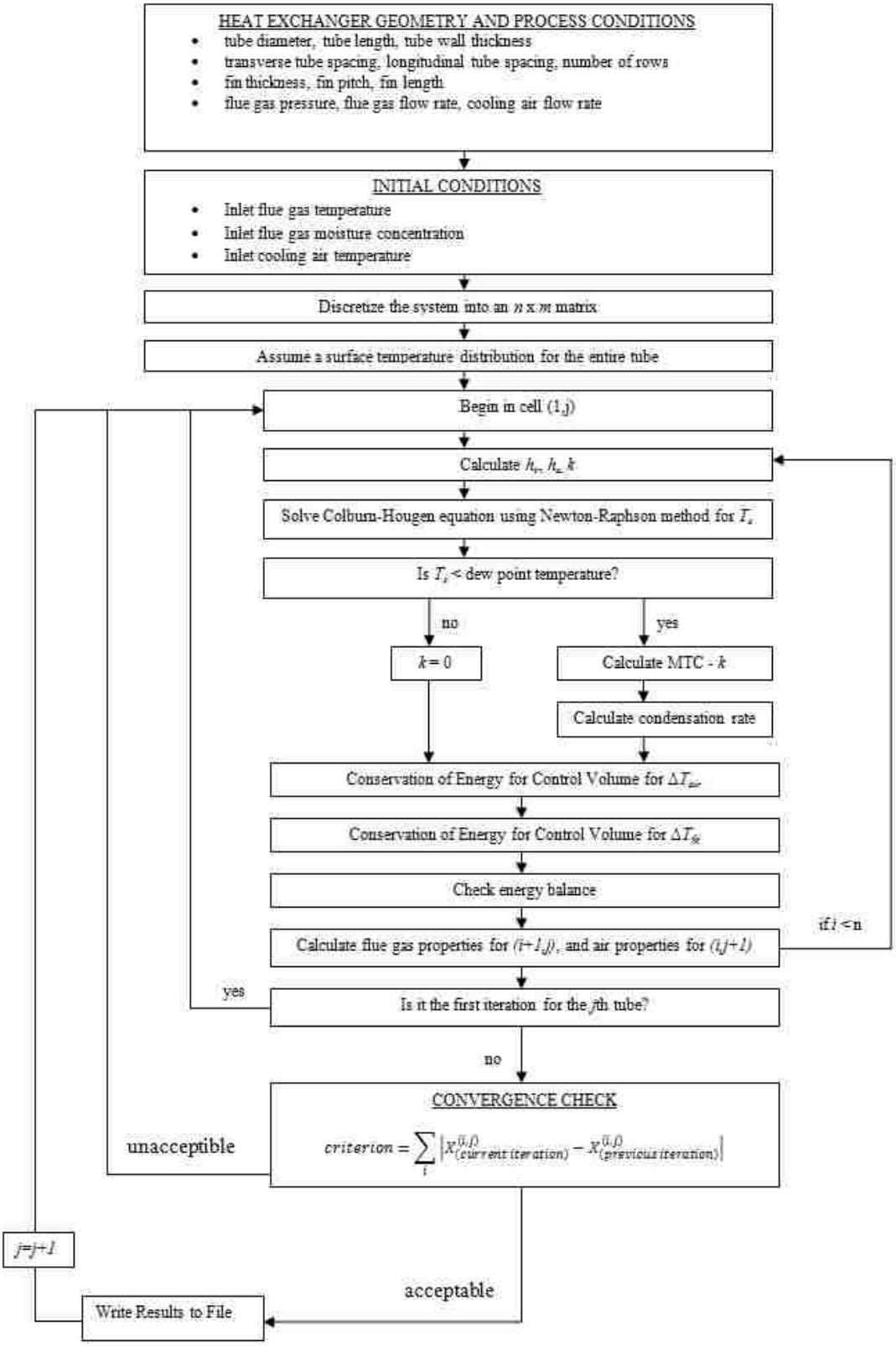

Figure 2.8 - Algorithm of heat and mass transfer simulation.

This completed the first element, and the procedure was repeated for elements (2,1), (3,1),…(n,1). That completed the first iteration of the first tube, and these are the first estimates of the distributions T_g, T_{air}, T_s, and moisture concentration y_{H_2O}. The second iteration used the calculated T_s values from the first iteration to recalculate the distributions of T_{fg}, T_{air}, T_s, and y_{H_2O}. The third iteration used T_s values from the second iteration, etc. To determine when the solution was found, the distributions of T_s and T_g for subsequent iterations were compared using the convergence criterion in Equation 2.5.

$$0.01 * n < \sum_{i=1}^{n} \left| {}^{z}X^{(i,j)} - {}^{z}X^{(i,j)} \right| \tag{2.5}$$

where z is the iteration variable, X is the flue gas temperature or tube surface temperature, (i, j) is the element, and n is the total number of elements for 1 tube. Equation 2.5 states that, the average temperature change of each element experiences a change in subsequent iterations of less than 0.01 ^{o}F.

The solution for each downstream tube is calculated in the same way, with the incoming cooling air temperature distribution for each tube was taken as the exiting values from the upstream tube.

The appropriate size of the elements in Figure 2.7 was determined using a sensitivity analysis. The step size was decreased in subsequent simulations and the results compared. Table 2.3 lists the conditions for the simulations for the sensitivity tests and Figure 2.9 and Figure 2.10 show the results which indicate that a step size equivalent to an order of magnitude less than the inner tube diameter was appropriate. This ensured accurate results while not compromising computing time.

Table 2.3 - Process conditions for one set of simulations to determine appropriate length of a control volume.

Process Condition	Value
Tube Inner Diameter [in]	3
Tube Outer Diameter [in]	0.625
Tube Length [ft]	10
Fin Thickness [in]	0.03125
Fin Pitch [in]	0.25
Fin Length [in]	0.5
Flue Gas Velocity [ft/sec]	28
Inlet Flue Gas Temperature [F]	150
Cooling Air Velocity [ft/sec]	25
Inlet Cooling Air Temperature [F]	70
Inlet Flue Gas Moisture Concentration [% wet]	10.7

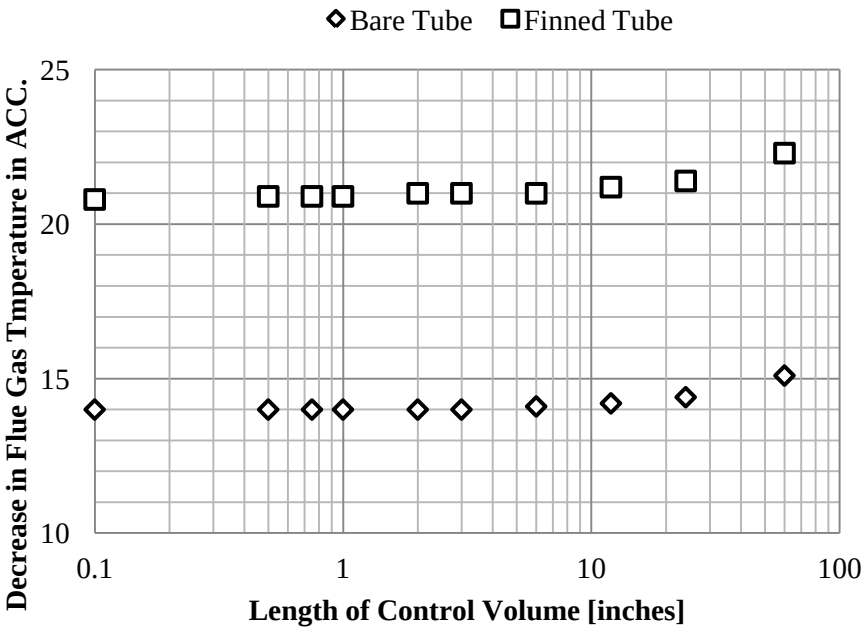

Figure 2.9 - Effect of control volume size on heat and mass transfer solution for decrease in flue gas temperature through tubes with and without fins.

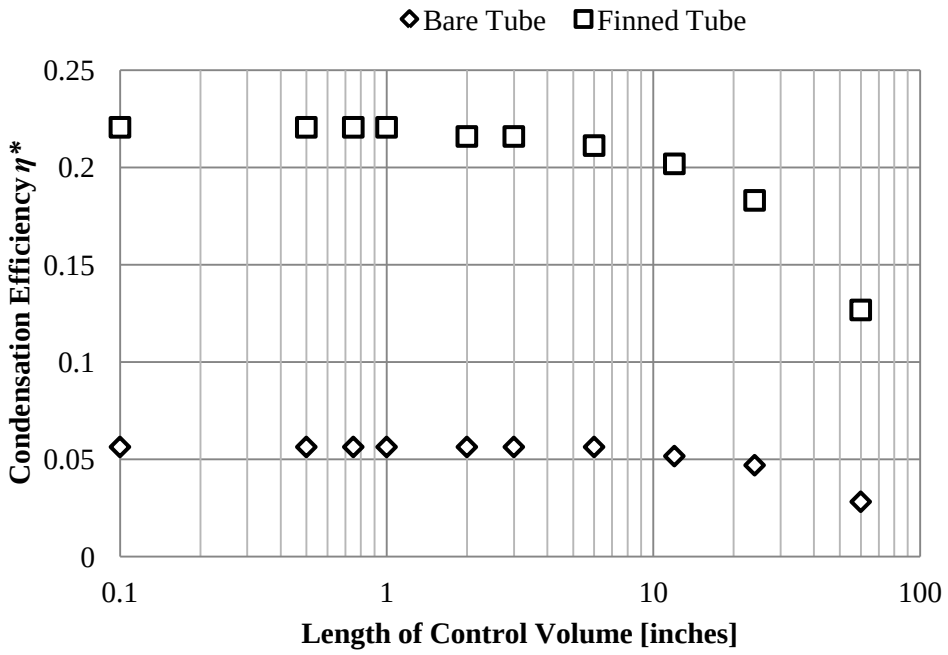

Figure 2.10 - Effect of control volume size on heat and mass transfer solution for condensation efficiency of heat exchangers with and without fins.

*Condensation Efficiency is defined as the ratio of the amount of vapor condensed in the heat exchanger to the amount of vapor entering the heat exchanger, Equation 2.6.

$$\eta = \frac{\dot{m}_{v,in} - \dot{m}_{v,exit}}{\dot{m}_{v,in}} \tag{2.6}$$

2.2 Heat and Mass Transfer Model Assumptions

2.2.1 Neglecting the Heat Transfer Resistance of the Tube Wall

The heat and mass transfer simulation assumed the resistance to heat transfer of conduction through the wall was much less than the resistances due to convection, and therefore the tube wall could be neglected. The equations to calculate resistances for convection and conduction through a circular tube wall are Equation 2.7 and 2.8, and Figure 2.11 shows the resistances to the flue gas and cooling air. Table 2.4 lists the calculated values of resistances for two cases, one with high flue gas and cooling air velocity and one case with low velocities. This shows the range of probable resistances. Table 2.5 tabulates the process conditions for the

calculations. The heat transfer resistance of the tube wall was much less than the contribution from convection, and the tube wall was neglected in the simulation.

$$R_{convection} = \frac{1}{hA} \tag{2.7}$$

$$R_{conduction\ of\ cylindrical\ tube} = \frac{ln(r_o/r_i)}{2\pi kL} \tag{2.8}$$

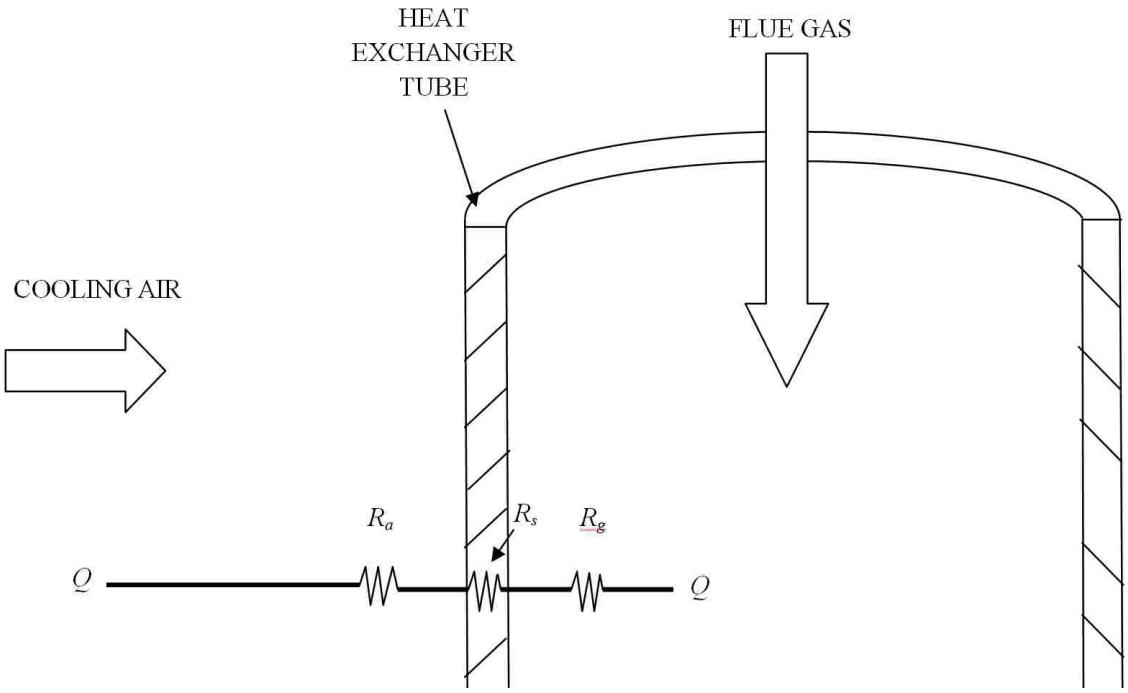

Figure 2.11 - Heat transfer resistances between flue gas and cooling air.

Table 2.4 - Resistances to heat transfer between flue gas and cooling air.

	Resistance to Heat Transfer [hr-F/BTU]		
	Cooling Air R_a	**Tube Wall R_s**	**Flue Gas R_g**
Resistance to Heat Transfer Case I	3.77E-02	6.42E-04	8.18E-01
Resistance to Heat Transfer Case II	1.64E-02	6.42E-04	1.12E-01

Table 2.5 - Case studies for calculating heat transfer resistances.

Case I		Case II	
Flue Gas Velocity [ft/sec]	10	**Flue Gas Velocity [ft/sec]**	60
Cooling Air Velocity [ft/sec]	7.5	**Cooling Air Velocity [ft/sec]**	30
Flue Gas Temperature [^{o}F]	135	**Flue Gas Temperature [^{o}F]**	135
Cooling Air Temperature [^{o}F]	75	**Cooling Air Temperature [^{o}F]**	75
Outside Tube Diameter [in]	1.25	**Outside Tube Diameter [in]**	1.25
Inside Tube Diameter [in]	1.125	**Inside Tube Diameter [in]**	1.125
Tube Length [in]	36	**Tube Length [in]**	36

2.2.2 Neglecting the Presence of the Liquid-Film

It was assumed that a continuous liquid film did not exist on the interior walls of the air-cooled condenser (ACC). Rather, a rivulet type of flow existed and had negligible effects on the thermodynamics and hydrodynamics of the system. The flue gas entered the ACC as a single-phase fluid and condensation began at the point where the tube wall surface temperature was less than the flue gas dew point temperature. At this location condensation occurred on the tube walls. However, these few droplets of condensation were not enough to form a liquid film. The droplets coalesced to form streams which flowed down the tube walls. After a critical flow rate, the streams then formed a continuous film. It was assumed that this critical flow rate would never exist in the ACC and as a result, it was assumed that a continuous film would never exist.

Experiments were performed to support the assumption that a liquid film did not form. The objective was to quantify liquid and gas flow rates that sustained a continuous liquid film.

These results were used to determine if the full-scale ACC would have a continuous liquid film on the interior walls of the tubes. The experimental apparatus built for this experiment is shown in Figure 2.12 and Figure 2.13 and consists of two acrylic tubes connected with a plenum. A compressed air-line supplied a gas flow through the tubes and the plenum was filled with liquid that was injected onto the interior walls of the acrylic tube. The gas and liquid flow rates were measured when a continuous liquid film was observed.

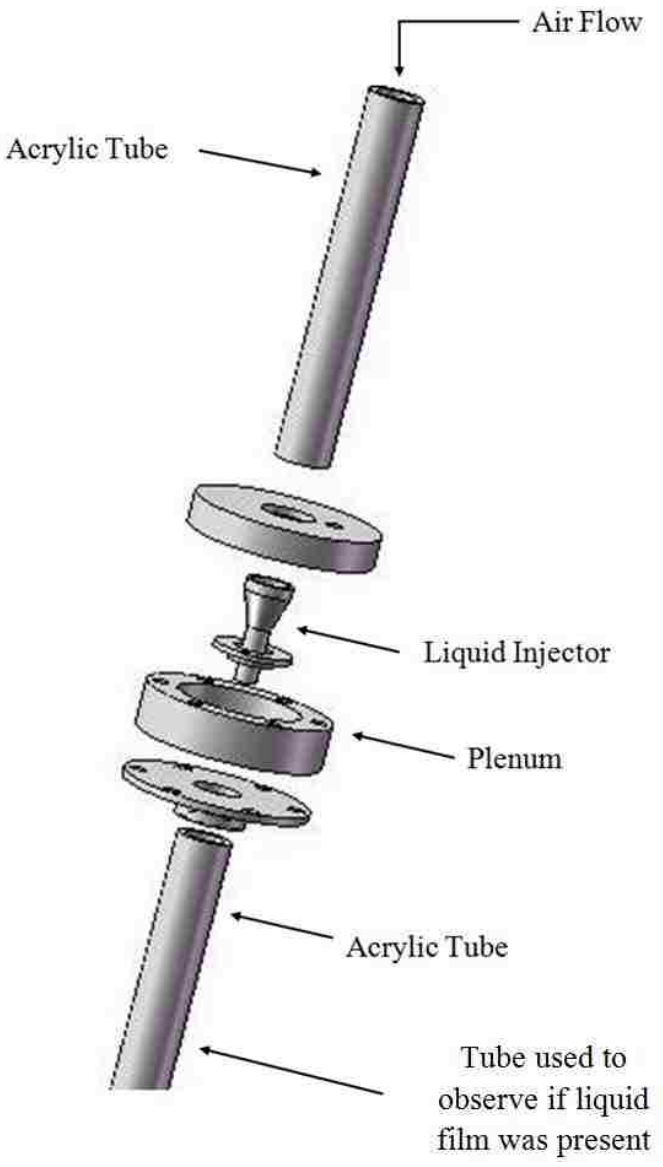

Figure 2.12 – Expanded view of experimental apparatus used to observe liquid film behavior.

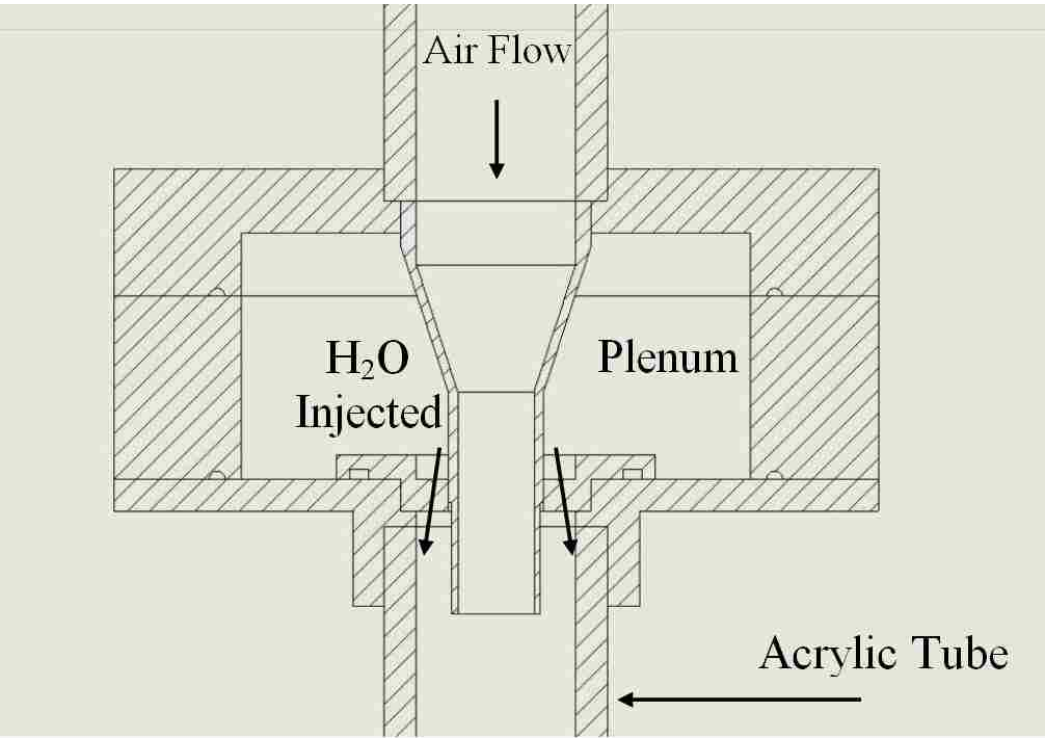

Figure 2.13 - Detailed design of experimental apparatus to observe liquid film behavior.

Figure 2.14 shows the gas Reynolds numbers (Equation 2.9) and the liquid film Reynolds numbers (Equation 2.10) that sustained a continuous liquid film. The results showed there was a strong dependence between the two. A larger gas flow rate through the tube required a smaller liquid film flow rate, and when the gas flow rate was reduced more liquid was necessary to sustain a continuous film.

$$Re = \frac{\rho V_g A}{\mu} \tag{2.9}$$

$$Re_{film} = \frac{4\dot{m}_{liquid}}{ID * \mu} \tag{2.10}$$

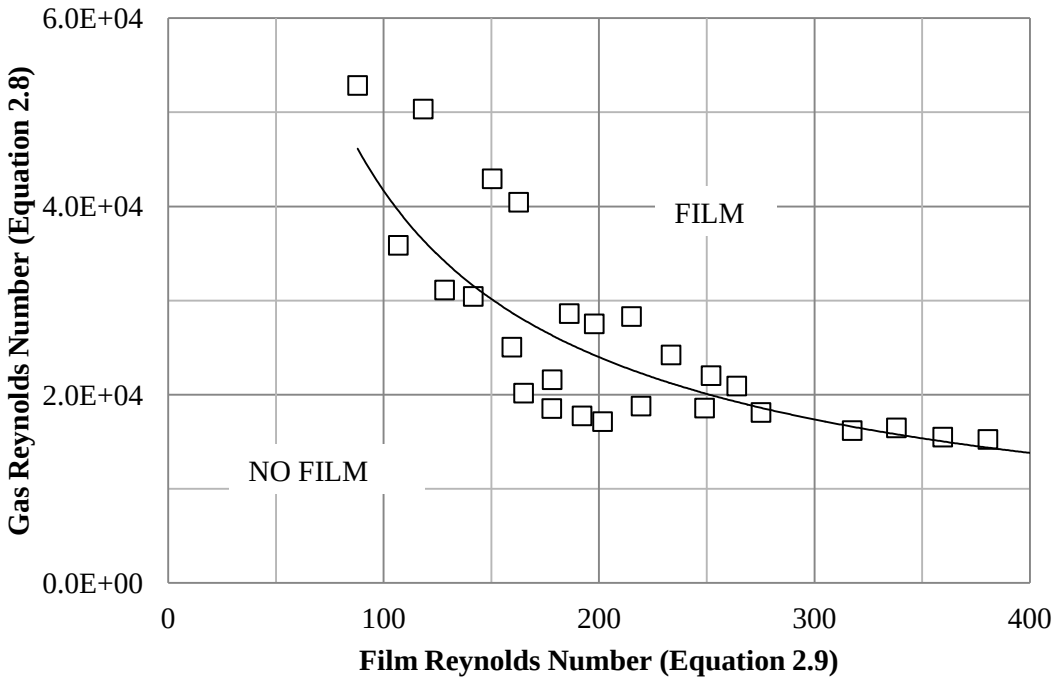

Figure 2.14 - Minimal conditions to sustain a continuous liquid film on the interior wall of a tube.

To show that the flue gas Reynolds number and liquid film Reynolds number in the ACC were less than the required values to form a liquid film, data from the ACC experiments and full-scale simulations were compared to Figure 2.14. In Figure 2.15, data from the full-scale simulation in the present study is plotted along with data from the experimental investigation described in Chapter 3. These results indicate that it is likely the flow conditions in the ACC would not sustain a continuous liquid film on the interior walls of the heat exchanger tubes and because of these results the simulation in the present study does not account for a liquid film.

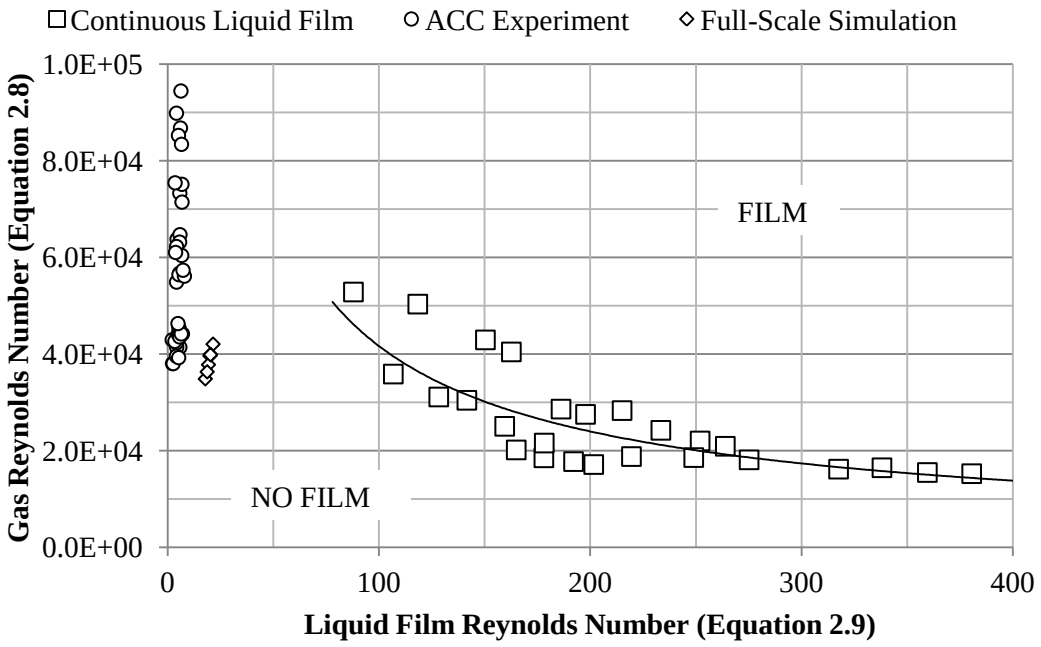

Figure 2.15 – Liquid film Reynolds numbers for the full scale ACC and laboratory scale ACC which show that a continuous film will not exist in the ACC.

Figure 2.16 shows the partial pressure and temperature distributions of the flue gas for the cases with and without a liquid film. In the case with a liquid film, the heat and mass transfer model would have an additional temperature to solve for, the temperature of the interface between the condensate film and the flue gas, T_i. In addition, including the condensate film would require simulating the heat transfer resistance of the condensate film.

Also shown in Figure 2.16 are the partial pressure distributions of the noncondensible gases P_{nc} and vapor P_v. Depending on which model is used, the partial pressure of vapor where condensation occurs would be dependent on the temperature of the condensate interface or tube wall, T_i and T_s respectively.

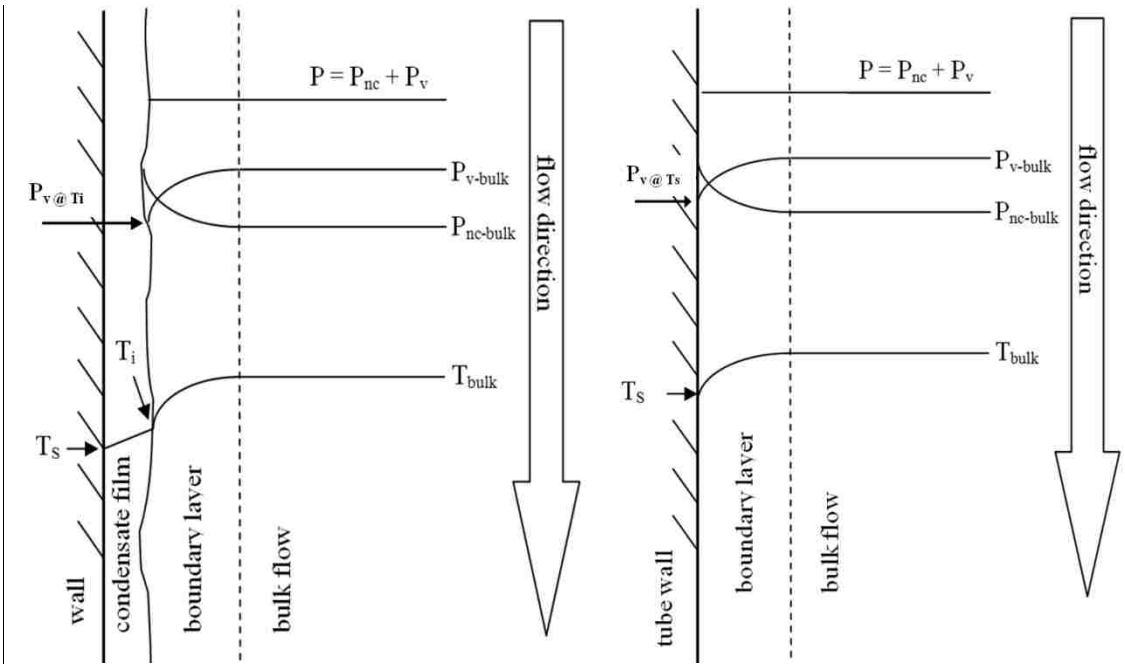

Figure 2.16 - Distributions of partial pressures and temperature of flue gas inside the heat exchanger tubes for the cases with and without a liquid film.

It was shown that the resistance to heat transfer of the tube wall was negligible compared to the resistances due to convection, thus the temperature of the tube wall on the interior is the same as the exterior. And it was also shown in Figure 2.15 that it can not be proven that a liquid film exists on the interior tube walls. Therefore, the overall temperature distribution across a heat exchanger tube in the present study was assumed to be as depicted in Figure 2.17.

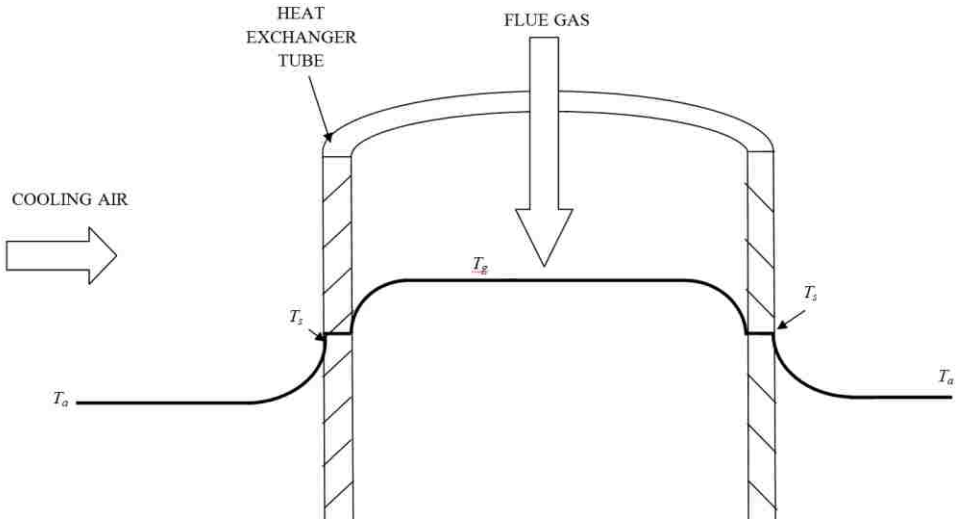

Figure 2.17 - Overall temperature distribution across the heat exchanger tube in the ACC.

The simulation used the single-phase flow model to estimate the pressure losses of the flue gas. Calculations were done to compare the pressure losses calculated with the single-phase and two-phase models discussed in the Literature Review. Figure 2.18 shows the results. The process conditions for these comparisons are listed in Table 2.6. The two-phase model predicted on averaged a 63 percent greater pressure loss. However, there was not enough evidence to suggest that the two-phase model was more appropriate, considering that the flue gas entered the ACC as a single phase fluid and at the exit of the heat exchanger the volume percent of the flue gas was 99.9 percent gas when 50 percent of the water vapor condensed. A conservative estimate could be that the actual pressure loss was somewhere between the single-phase and two-phase flow pressure loss estimates.

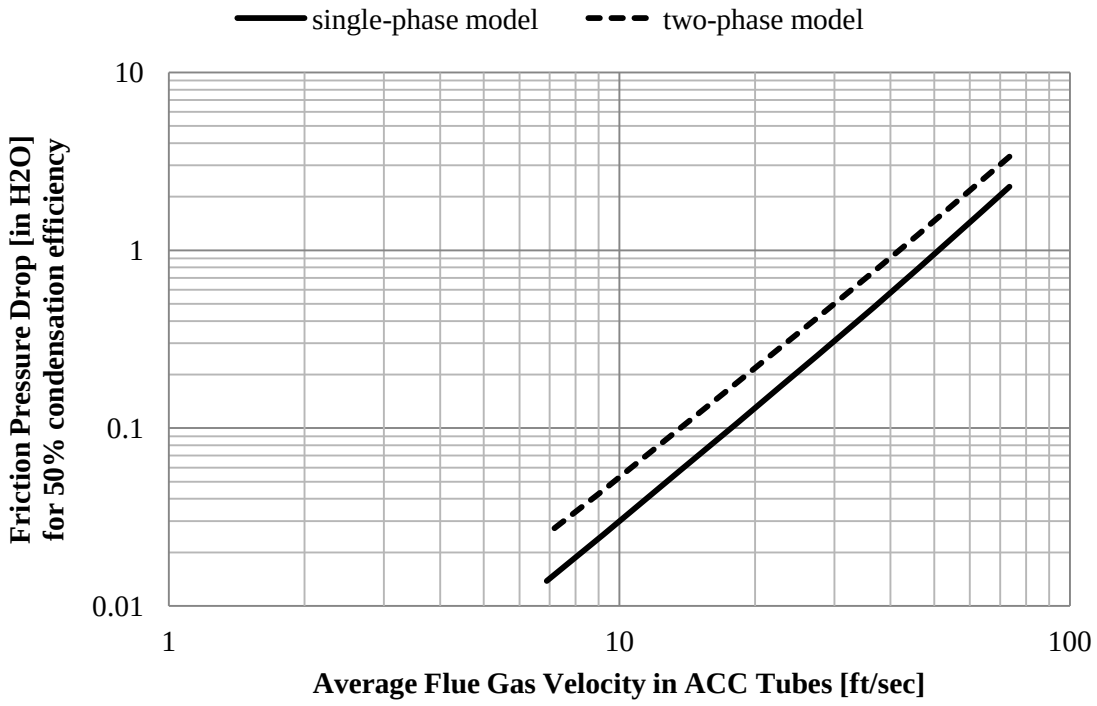

Figure 2.18 - Comparison between single-phase and two-phase pressure loss models for the flue gas flow.

Table 2.6 - Process conditions and tube geometry for simulations that compared the single-phase and two-phase pressure loss models.

Inlet Flue Gas Temp [^{o}F[	135
Inlet Moisture Concentration [% wet-basis]	11%
Tube Diameter [in]	4
Tube Length [ft]	40

2.3 Comparing the Results of the Simulation with Data from the Literature

Prior to simulating the experimental apparatus and designing the full-scale ACC, data from the literature was used to validate as much of the simulation as possible. In the literature there was experimental data about heat transfer for air-cooled, finned-tube heat exchangers. In addition, results from a computational fluid dynamics study were available.

The relevant experimental data was found in Stasiulevicius and Skrinska [34]. They experimentally determined the mean Nusselt Number between the tube wall and the cooling air in rows 1 and 5 of a tube bundle by installing calorimeters. The experiments were conducted while keeping the tube wall temperature constant. In the present study, the simulation modeled the tube geometries of Stasiulevicius and Skrinska's experiments with the same process conditions as their experiments, including constant tube wall temperature. The mean Nusselt numbers determined in the simulation were compared with the experimental measurements and the results are shown in Figure 2.19 and Figure 2.20. In all but two tests for row 1, the experimental measurements of Stasiulevicius and Skrinska agreed with the calculated average heat transfer coefficients of the simulation.

These results indicated that the heat transfer simulation of the present study predicted the experimentally measured heat transfer coefficients between the tube wall and air to within 20 percent.

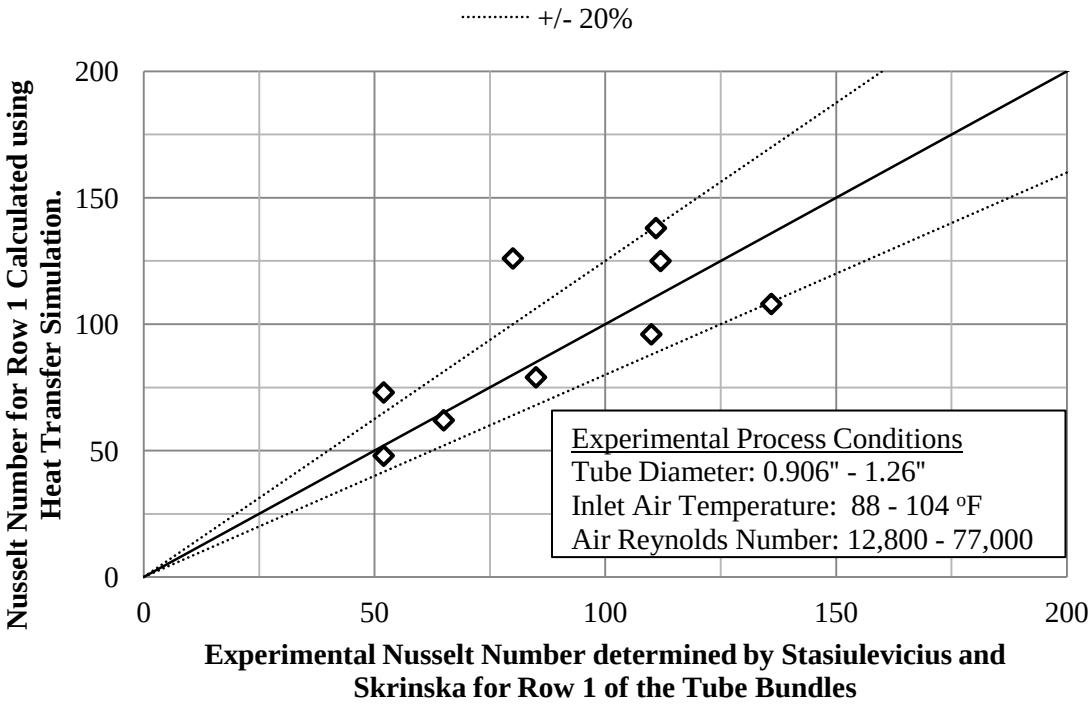

Figure 2.19 - Comparison of heat transfer simulation with published experimental data.

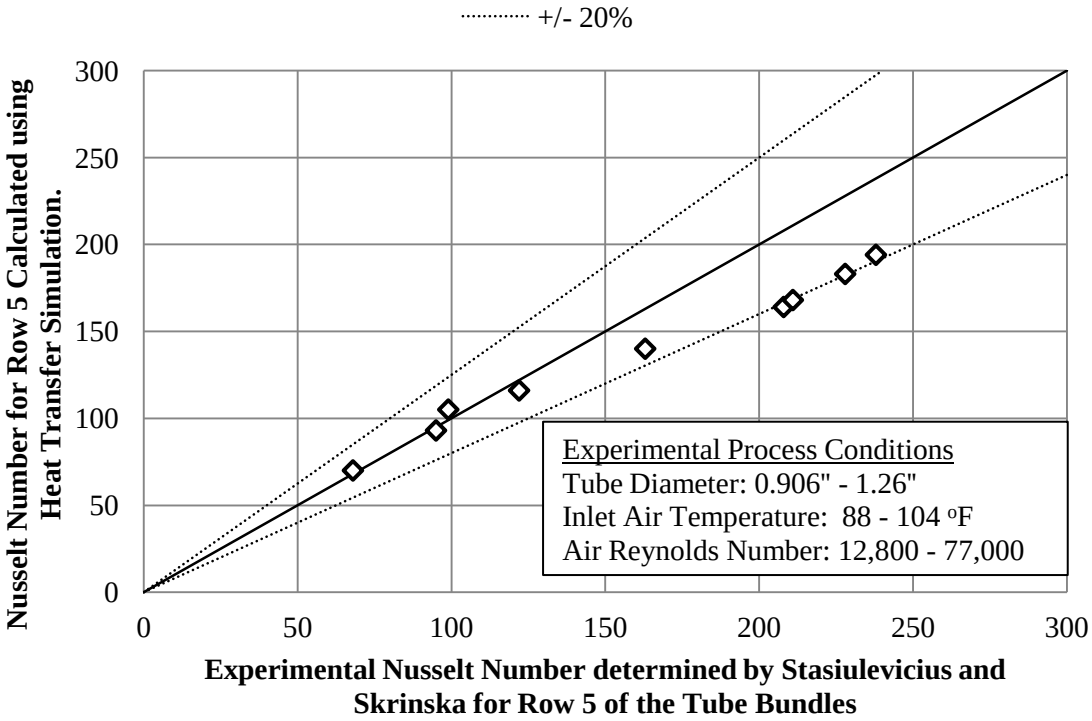

Figure 2.20 - Comparison of heat transfer simulation with published experimental data.

Computational Fluid Dynamic (CFD) software was used by Dunbar [66] to investigate the heat transfer and pressure loss associated with finned tubes. The CFD simulations were for air flowing around 1 steel finned tube. The base of the tube was at a constant temperature, and the simulation calculated the conductive heat transfer through the fin and the convective heat transfer from the tube and fin to the air. The simulation also calculated the pressure drop of the air flowing around the finned tube.

For the comparison, the heat transfer simulation in the present study modeled the tube geometry and process conditions of the CFD simulations. This comparison neglected the condensation aspect of the simulation and focused on the air-side. This was done using a constant tube wall surface temperature. The purpose was to show the heat transfer correlations and pressure drop correlations used in the present study were valid. Figure 2.21 shows the heat transfer per unit length of tube from both the CFD simulation and the heat transfer simulations. The average difference between the CFD results and heat transfer simulation was approximately 4%.

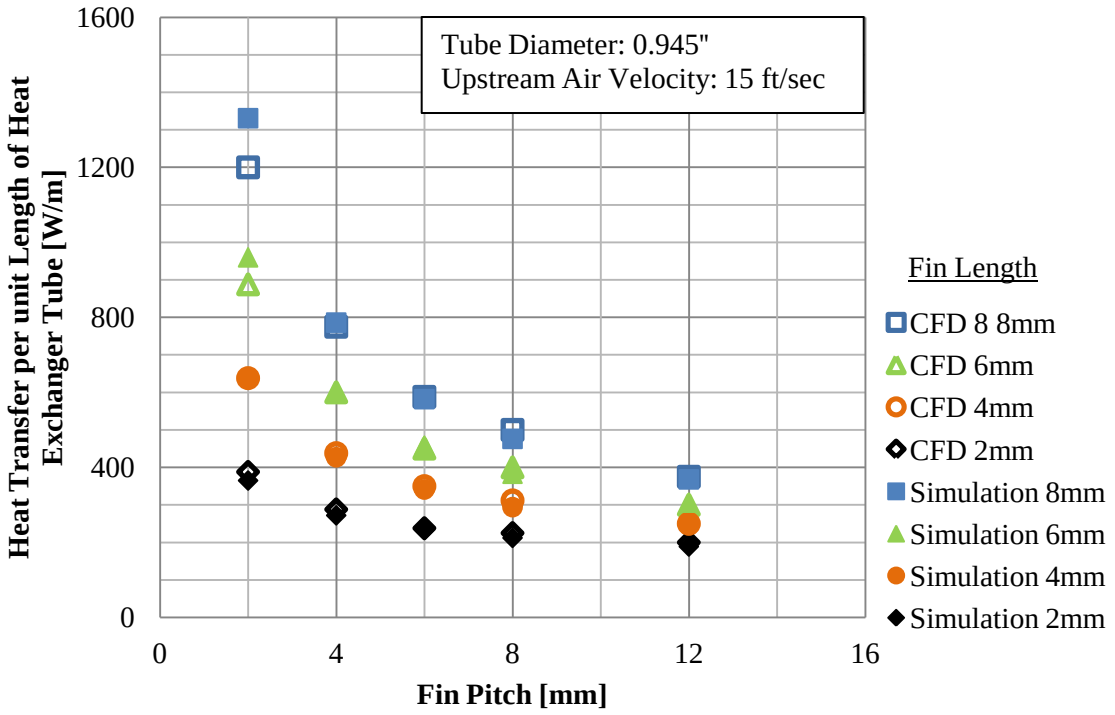

Figure 2.21 - Comparison of CFD results with heat transfer simulation.

The pressure loss of the air flowing around the finned tube is compared in Figure 2.22, which indicates agreement within 22 %. From these comparisons of the experimental data and CFD simulations it was concluded that the heat transfer simulation is using reliable correlations to determine heat transfer between the tube wall and cooling air and the pressure loss of the cooling air. The validation of the gas-side heat transfer and mass transfer is discussed Chapter 3.

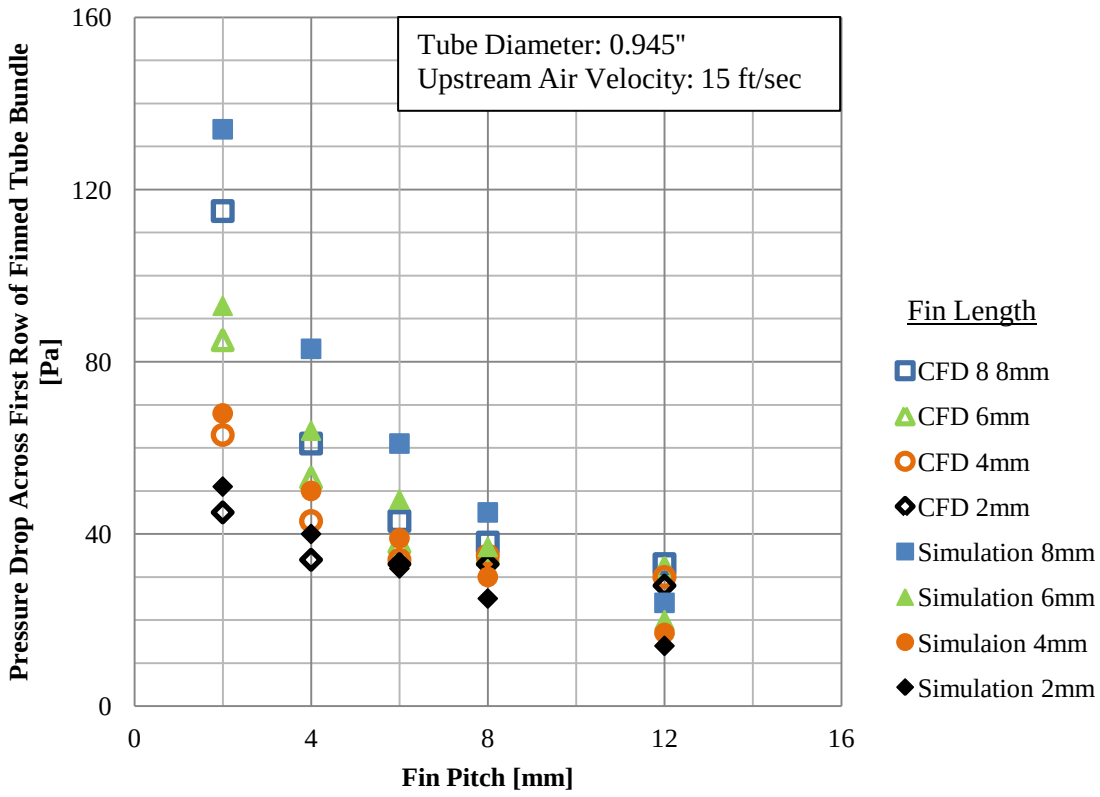

Figure 2.22 - Comparison of CFD results with heat and mass transfer simulation.

2.4 Incorporating the Nelder-Mead Optimization into the Simulation

Recall from Section 1.6 that the Nelder-Mead method is a simplex method where the simplex has vertices that number one more than the number of variables in the objective function. Book-keeping for the optimization was done using a matrix where columns represented function variables and rows represented vertices, like what is shown in Figure 2.23. The example in Figure 2.23 shows the ACC being optimized for two variables, fin pitch and fin length, and therefore there are three vertices, labeled V_1, V_2, and V_3. To plot the simplex, each row of the matrix represents a vertex. The final column of each row was the function value, net annualized cost. The net annualized cost was found by inputting the fin pitch and fin length values into the simulation.

	F_p	F_L	Net Annualized Cost
V_1	MATRIX(1,1)	MATRIX(1,2)	MATRIX (1,3)
V_2	MATRIX(2,1)	MATRIX(2,2)	MATRIX(2,3)
V_3	MATRIX(3,1)	MATRIX(3,2)	MATRIX(3,3)

Figure 2.23 - Matrix representation of simplex used in the optimization.

To show the process of optimizing the ACC, an example is discussed where two design variables were optimized, fin pitch and fin length. This example was for the lab-scale air-cooled condenser described in Chapter 3 and the process conditions and tube geometry are listed in Table 2.7. The initial simplex's matrix representation is in Figure 2.24 and is graphically shown in Figure 2.25. The domain for this optimization was:

- Fin Pitch: 0.2 – 1.0 inch
- Fin Length: 0.25 – 1.0 inch

Table 2.7 - Process conditions for example optimization.

Upstream Air Velocity [ft/sec]	**18**
Pressure [ATM]	**1**
Gas Temp [^{o}F]	**135**
Gas Velocity [ft/sec]	**40**
Gas Moisture Concentration [wet %]	**10**
Heat Exchanger Tube Diameter [inches]	**1.25**
Tube Wall Thickness [inches]	**0.0625**
Tube Length [ft]	**3**
Heat Exchanger Tubes	**3**
Tube Rows	**1**
Fin Thickness [inch]	**0.125**

	Fin Length	Fin Pitch	Net Annual Cost
V_1	0.25	0.2	$144.27
V_2	0.35	0.2	$143.16
V_3	0.30	1.0	$146.49

Figure 2.24 - Matrix representation of initial simplex for example optimization.

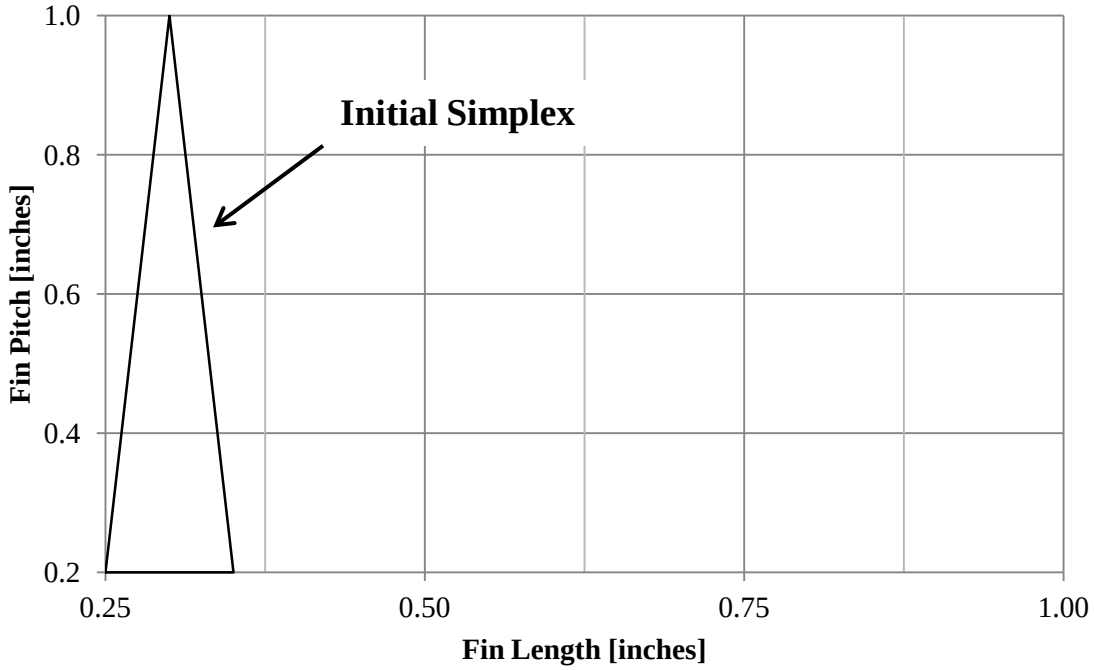

Figure 2.25 - Initial simplex for example optimization.

Comparing the net annualized costs of the three vertexes in Figure 2.24 and Figure 2.25, indicates V_3 was the most expensive. Therefore V_3 was replaced according to the Nelder-Mead algorithm, and the the simplex matrix is shown in Figure 2.26 and shown graphically in Figure 2.27.

	Fin Length	Fin Pitch	Net Annual Cost
V_1	0.25	0.20	$144.27
V_2	0.35	0.20	$143.16
V_3	0.30	0.60	$145.96

Figure 2.26 - Matrix representation of second simplex for example optimization.

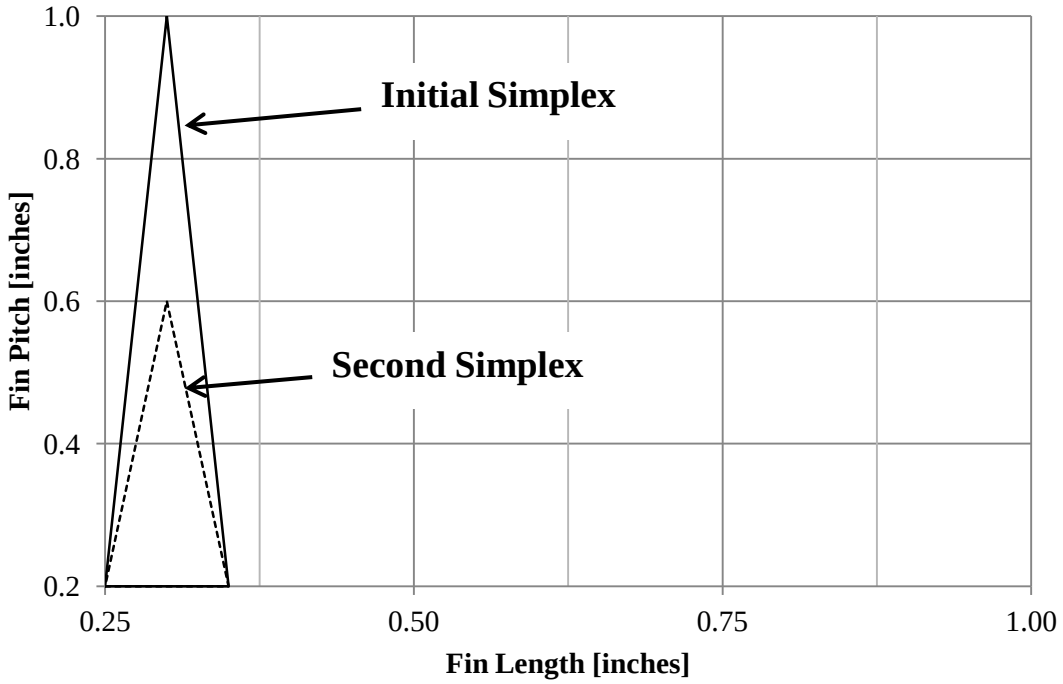

Figure 2.27 - Second simplex for example optimization.

The algorithm was repeated until the minimum was found. Figure 2.28 shows the final simplex matrix, which has the optimal fin pitch and fin length values. The net annualized cost was approximately $139, compared with the initial $143 to $146. This optimization was completed in 36 iterations, and Figure 2.29 shows the path that the simplex traversed to reach the minimum. In this example, the optimal design was one with a small fin pitch and large fin length.

	Fin Length	**Fin Pitch**	**Net Annual Cost**
$\boldsymbol{V_1}$	0.998689	0.202635	139.11
$\boldsymbol{V_2}$	0.995036	0.202305	139.12
$\boldsymbol{V_3}$	0.994994	0.201086	139.10

Figure 2.28 - Matrix representation of the final simplex for the example optimization.

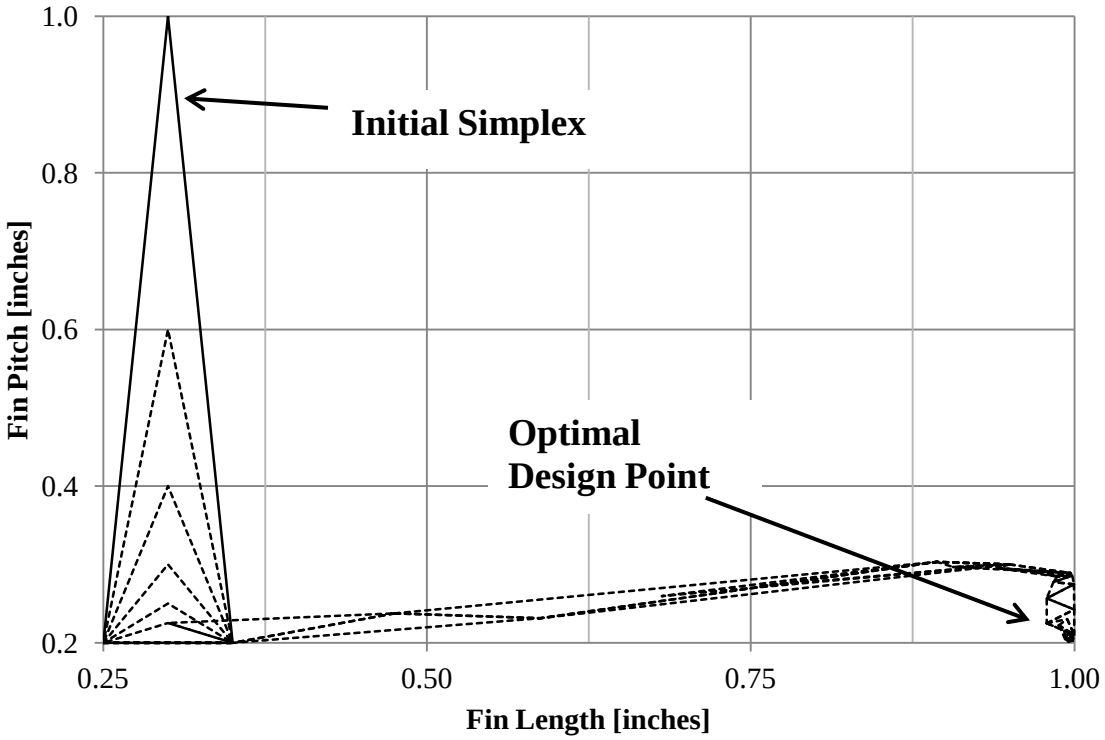

Figure 2.29 - The 36 simplexes calculated to determine the optimal fin pitch and fin length.

Figure 2.30 shows the fin length and fin pitch domain with contours for the net annualized cost. The lines in the graph represent constant net annualized cost. It is seen that the minimum cost was on the lower right side of the graph, with a fin length of 1 inch and fin pitch of 0.2 inches, and the net annualized cost increased as fin length decreased and fin pitch increased.

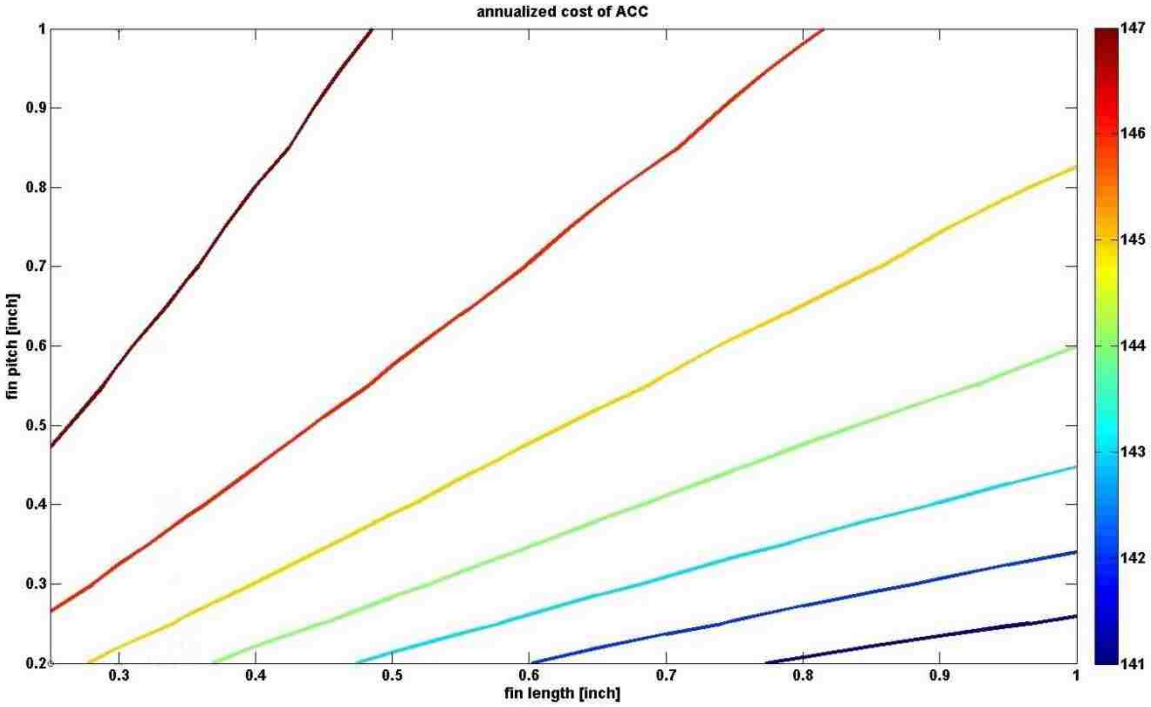

Figure 2.30 - Cost contours of the fin pitch and fin length domain.

When optimizing the full-scale heat exchanger, the variables did not have the same units because the optimizations included geometry variables and velocity variables. Therefore the simplexes were built using normalized values of the variables, which ranged from 0 to 1. The normalized values were based on the domain of each variable. For example, when the flue gas domain for the optimization was between 7.5 ft/sec and 70 ft/sec, the velocity was normalized with respect to 62.5 ft/sec.

3 Experimental Investigation

3.1 Overview of Experimental Apparatus

A lab-scale air-cooled condenser (ACC) was fabricated and installed in Lehigh University's heating, ventilation, and cooling powerhouse, and processed a slip stream of flue gas from an industrial boiler. The boiler was a Babcock and Wilcox design which burned natural gas, and had a 40,000 lbm/hr steam capacity. The slip stream was extracted from the boiler downstream of the economizer, and then flowed through two water-cooled heat exchangers to lower its temperature to the desired value (between 100 and 150^{o}F) before entering the ACC. The water-cooled heat exchangers and ACC comprise the main components of the experimental apparatus (Figure 3.1).

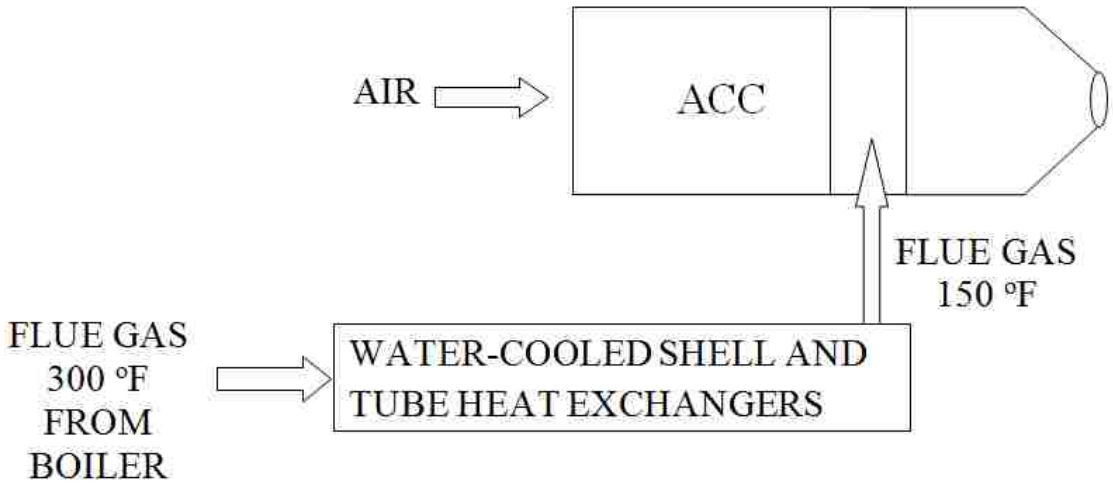

Figure 3.1 - Schematic of Experimental Apparatus

The design of the air-cooled condenser (ACC) is shown in Figure 3.2 and Figure 3.3. The respective drawings show the side-view and top-view. In Figure 3.2, the air flowed left to right through the rectangular duct, and the flue gas entered from the top and flowed vertically downward through small diameter tubes. At the flue gas exit, there was additional ductwork to separate the condensate from the flue gas.

The air duct was designed to minimize pressure loss. The inlet region had a curved leading edge with a radius of 2 inches, which reduced the dynamic pressure loss coefficient from 0.5 to approximately 0.05. The exit diffuser had a vertical contraction of approximately 5^{o} and a horizontal expansion of approximately 10^{o}. Designing the inlet and exit regions in such a way allowed for greater air velocities through the tube bundle. The ID fan was placed downstream of the tube bundle at the diffuser exit because an induced draft design creates a more organized flow structure in the duct compared to a forced draft design.

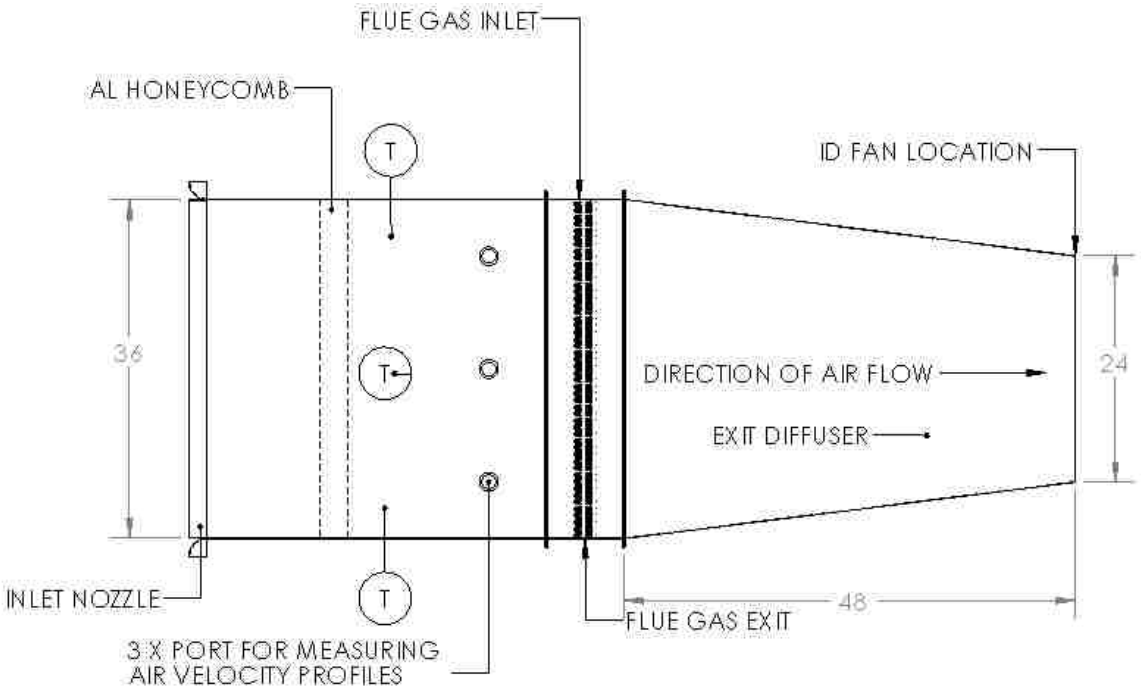

Figure 3.2 – Side view of ACC

Seen also in Figure 3.2 and Figure 3.3 are the ¼ inch aluminum honeycomb, the temperature measurement locations (denoted by T), the ports for measuring air velocity profiles, and the tube bundle.

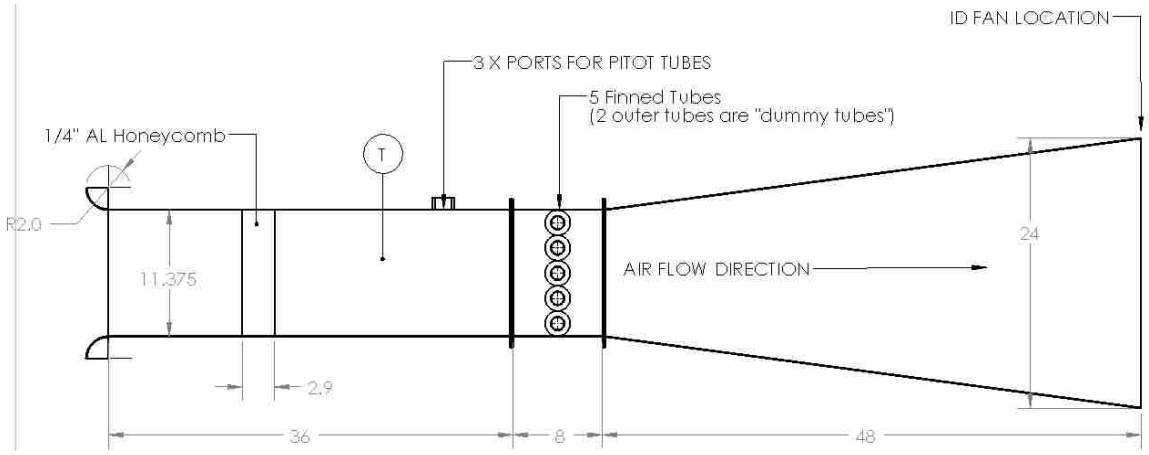

Figure 3.3 - Top view of ACC

The dimensions of the air-cooled condenser are listed in Table 3.1 and shown in Figure 3.4. The finned tubes were fabricated from stainless steel and the fin attachment method used was a brazing method. Five finned tubes were installed in the ACC but the two outer tubes did not process flue gas. The purpose of the two outer tubes was to maintain the appropriate air flow structure around the tubes that processed flue gas. Figure 3.5 shows a schematic of the entire apparatus and photographs of the apparatus are shown in Figure 3.6 through Figure 3.9.

Table 3.1 - Geometric Characteristics of ACC.

TUBE DIMENSION		FIN DIMENSION		SURFACE DIMENSION	
Tube ID	1.125 in	**Fin Spacing**	0.2 in	**Gas-Side Surface Area**	2.64 ft^2
Tube OD	1.25 in	**Fin Length**	1/2 in	**Air-Side Surface Area**	23.8ft^2
Tube Length	3 feet	**Fin Thickness**	0.0625 in		
Wall Thickness	0.065 in				
Number of Tubes	3				
Transverse Tube Spacing	2.25 in				
Diagonal Tube Spacing	2.25 in				
Duct Width	11.375 in				

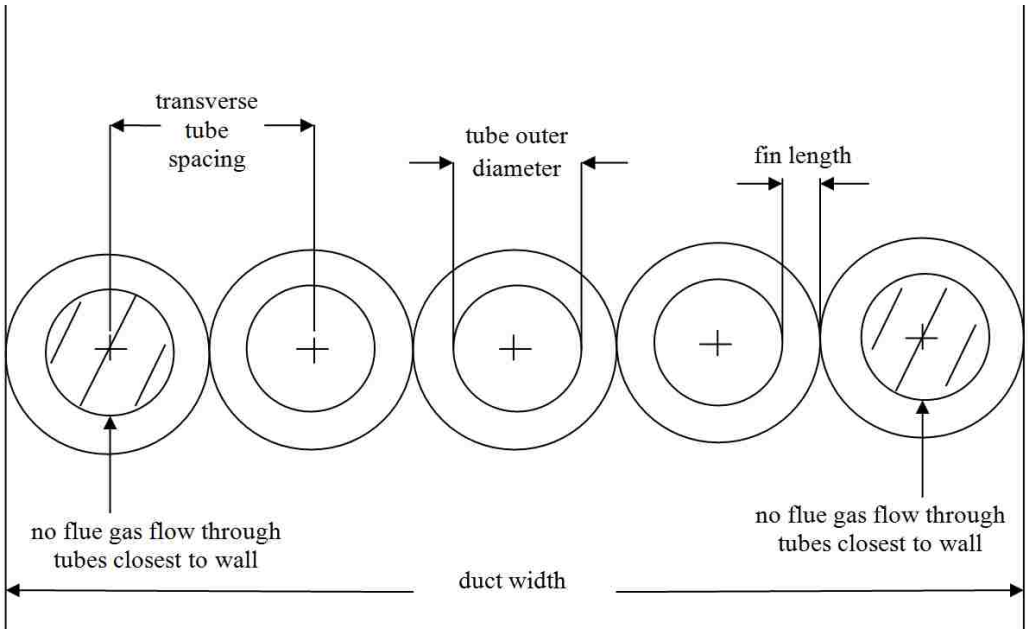

Figure 3.4 - Schematic of tube bundle dimensions.

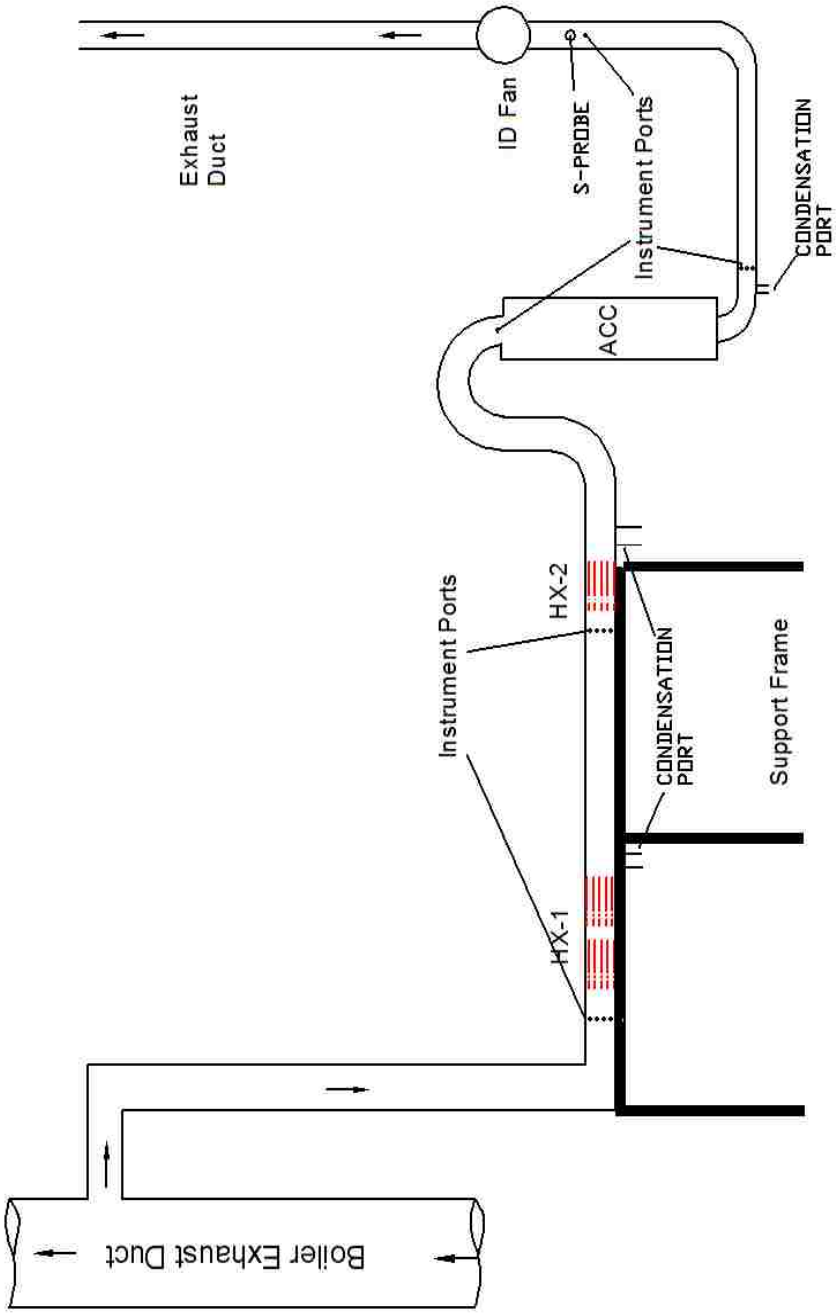

Figure 3.5 - Schematic of experimental setup including water-cooled and air-cooled heat exchangers

Figure 3.6 - Photograph of experimental apparatus in Lehigh University laboratory

Figure 3.7 - Inlet region of the ACC showing the inlet nozzle and aluminum honeycomb.

Figure 3.8 - Finned tube bundle in the main test section, along with the three pitot tubes used to measure the air-flow rate across the duct cross-section.

Figure 3.9 - Cooling air fan at the exit of the duct.

The instrumentation is described in Table 3.2. The apparatus was instrumented to collect data that was used to calculate an energy balance for each heat exchanger. The instruments selected measured temperatures, flow rates, and condensation rates for each heat exchanger over a recorded period of time. Data acquisition software tabulated the temperature values of the thermocouples, and the flow rates were recorded periodically throughout the experiments. The condensation rate was determined following each experiment.

Table 3.2 - Instrumentation for Lab-scale Air-Cooled Condenser Experiment

MEASURED VARIABLE	METHOD	INSTRUMENTS
Flue gas temperature	Single-point bulk flow measurement	Thermocouple
Air temperature	3-point profile	Thermocouple
Water temperature	Single-point measurement	Thermocouple
Tube wall temperature	Single point measurement Stagnation Point	Cement-on surface thermocouple
Flue gas velocity	Single-point measurement (at center of circular 3-inch diameter tube)	S-probe
Air velocity	12-point profile across 11.25'' rectangular duct	Pitot-tube
Water flow rate	Two flow meters placed in series	Rotameter
Water vapor condensation rate	Collection basin	Scale
Flue gas moisture content	Wet-bulb/controlled condensation method	Thermocouple/EPA Method 8.

The experiments were conducted when the heat exchangers reached steady thermal operating conditions. The range of process conditions for the air-cooled condenser (ACC) is listed in Table 3.3, and details of each test date and test process condition are tabulated in the Appendix.

Table 3.3 - Range of Process Conditions for ACC Experiments

PROCESS CONDITION	RANGE		UNIT
	MIN	MAX	
Inlet Flue Gas Temperature	105	152	^{o}F
Flue Gas Velocity	26	72	ft/sec
Flue Gas Reynolds Number	13000	35000	
Inlet Air Temperature	55	68	^{o}F
Air Velocity between Tubes	19	37	ft/sec
Air Reynolds Number	16000	24000	

3.2 Experimental Results

A total of 35 experiments was carried out to observe the effects of varying the process conditions listed in Table 3.3. This section presents parametric tests that show how those process conditions affected the performance of the air-cooled condenser (ACC). Additional test results and those described in this chapter are tabulated in the Appendix.

3.2.1 Water-Cooled and Air-Cooled Heat Exchanger System

In the test shown in Figure 3.10, the abscissa is cumulative heat transfer surface area and the ordinate axis is temperature. The first heat exchanger, which was water-cooled, had 17.5 ft^2 of tube surface area, the second water-cooled heat exchanger had 12.5 ft^2 of tube surface area, and the air-cooled heat exchanger had 2.6 ft^2 of surface area (23.8 ft^2 including the fins). This graph shows the temperature measurements of the working fluids and tube wall surfaces for each heat exchanger.

The flue gas entered the first water-cooled heat exchanger at 330^oF and exited the second water-cooled heat exchanger at 132^oF before entering the ACC. In the ACC, the flue gas was cooled to 112^oF. Cooling water entered the counter-flow, water-cooled heat exchangers at 104^oF and exited at 122^oF. Cooling air entered the ACC at 63^oF and exited at 66^oF. The temperatures of the tube walls are also shown in the figure. The results indicate that the temperature of the tubes in the water-cooled heat exchangers were much the same as the cooling water inside the tubes. This was because the heat transfer coefficient on the water-side was much larger than on the gas-side. The main resistance to heat transfer in the water-cooled heat exchangers was due to the characteristics of the flue gas flow. In the ACC, the tube wall temperature was close to the mean temperature of the flue-gas and cooling air temperatures.

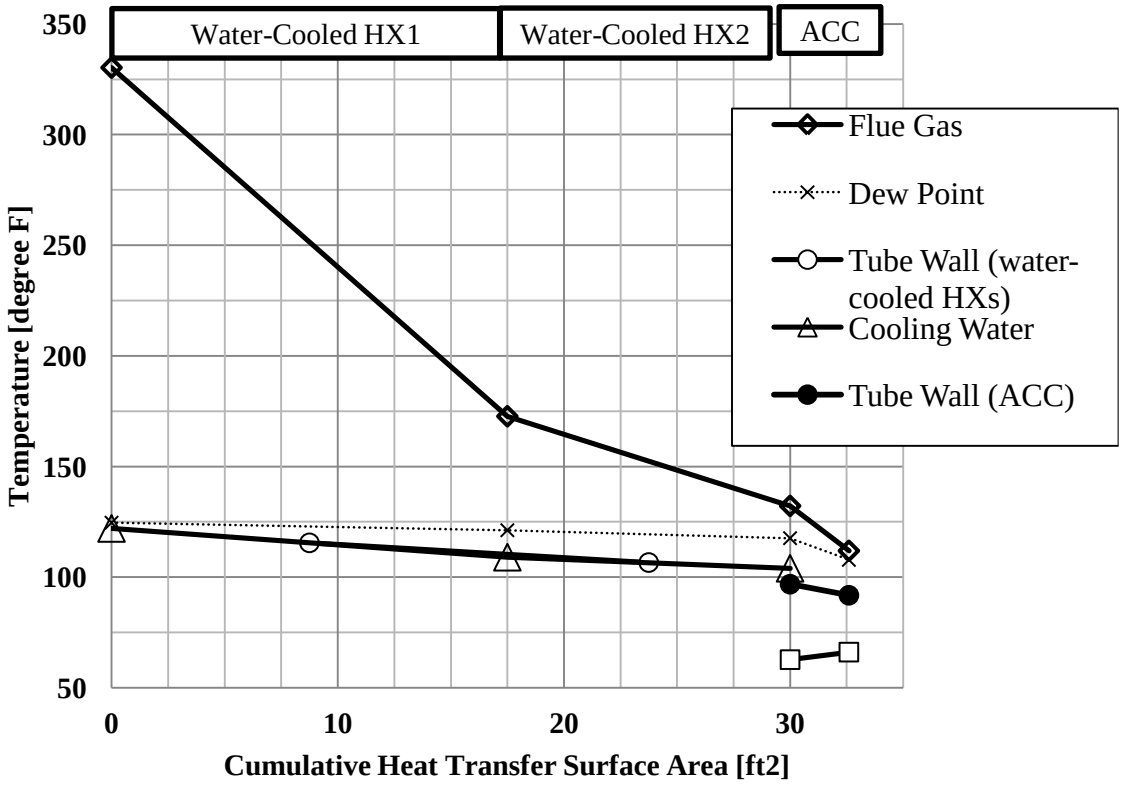

Figure 3.10 - Temperature distribution for water-cooled and air-cooled heat exchangers. Symbols denote measurement locations.

It is well known that when the temperature of the heat exchanger tubes is less than the water vapor dew point of the flue gas, water vapor will condense onto the tubes. The dew point temperature of the flue gas is also shown in Figure 3.10, and Figure 3.11 shows that water condensed from the flue gas in the heat exchangers where the tube wall temperature was below the dew point. In this test, this was the case for all three heat exchangers.

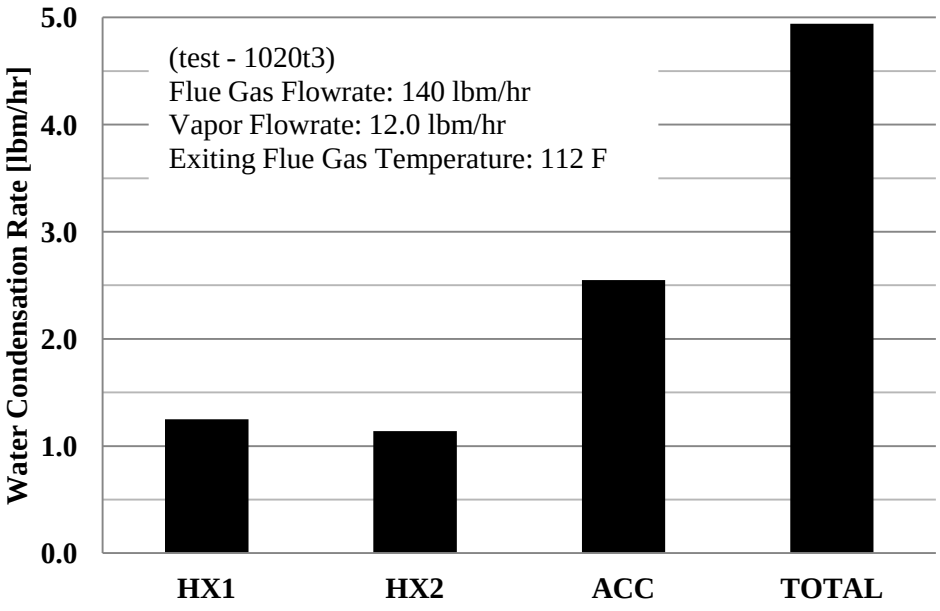

Figure 3.11 - Condensation rate of water vapor in each heat exchanger.

Figure 3.12 shows a curve fit of experimental data of the water vapor concentration of the flue gas as it flowed through the heat exchanger system. The flue gas moisture concentration at the exit of the system was determined by measuring the wet bulb and dry bulb temperatures downstream of the ACC and determining the specific humidity from an ASHRAE handbook. Then, the flue gas moisture concentration at the inlet of each heat exchanger was determined by adding the amount of water condensed and collected in each heat exchanger to the water vapor flow rate in the flue gas. The equations are 3.1 through 3.4. In this test, the moisture concentration was 13.3 percent at the inlet and 8.3 percent at the exit. The water capture efficiency/condensation efficiency η of this test, defined in Equation 3.5 was 41.2%.

$$\dot{m}_{v,ACC\ exit} = \phi \dot{m}_{dg} \tag{3.1}$$

$$\dot{m}_{v,ACC\ inlet} = \dot{m}_{v,ACC\ exit} + \dot{m}_{cd,ACC} \tag{3.2}$$

$$\dot{m}_{v,HX2\ inlet} = \dot{m}_{v,ACC\ inlet} + \dot{m}_{cd,HX2} \tag{3.3}$$

$$\dot{m}_{v,HX1\ inlet} = \dot{m}_{v,HX2\ inlet} + \dot{m}_{cd,HX1} \tag{3.4}$$

$$\eta = \frac{\dot{m}_{condensate}}{\dot{m}_{vapor\ at\ inlet}} \tag{3.5}$$

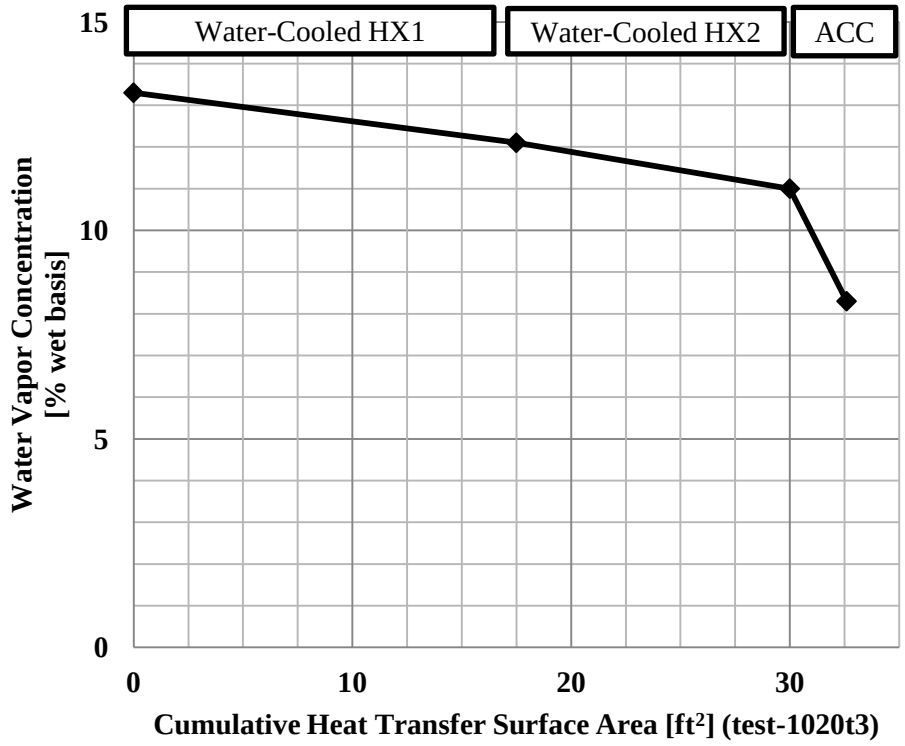

Figure 3.12 – Experimental measurements and curve fit of moisture concentration of the flue gas.

The flue gas exited at 112°F with a water vapor concentration of 8.3 percent. At this temperature and moisture concentration there is potential to cool the flue gas to a lower temperature and recover additional quantities of water to improve the water capture efficiency. This would require additional surface area.

The energy balances of the heat exchangers from this test are shown in Table 3.4. These quantities were calculated using Equation 3.6 through 3.10 and the measured temperatures. Q_{air} is inferred from $Q_{gas(latent)}$ and $Q_{gas(sensible)}$ because the temperature of the air exiting the ACC was not measured.

Table 3.4 - Energy Transfer Rates for test-1020t3.

[BTU/hr] (test1020t3)	Heat Exchanger 1	Heat Exchanger 2	ACC
Q gas (sensible)	**6469**	**1267**	**751**
Q gas (latent)	**1283**	**1181**	**2656**
Q air	**-**	**-**	**3407 (est.)**
Q water	**5147**	**2045**	**-**
$Q_{difference}$	**-2605**	**-402**	**N/A**

$$Q_{gas\ (sensible)} = \dot{m}_{gas} C_{p\ gas} \left(T_{gas\ in} - T_{gas\ out}\right) \tag{3.6}$$

$$Q_{gas\ (latent)} = \dot{m}_{condensate} h_{fg} \tag{3.7}$$

$$Q_{air} = Q_{gas\ (sensible)} + Q_{gas\ (latent)} \tag{3.8}$$

$$Q_{water} = \dot{m}_{water} C_{p\ water} (T_{water\ out} - T_{water\ in}) \tag{3.9}$$

$$Q_{difference} = Q_{water} - Q_{gas\ (sensible)} - Q_{gas\ (latent)} \tag{3.10}$$

For more information on parametric tests of the water cooled heat exchangers, see Jeong et al. [13-14]. Additional data can also be found in the Appendix. The remainder of this chapter will focus on the performance of the air-cooled condenser.

A note on measuring temperature during the experiments. Of the measured temperature values shown in Figure 3.10, three were estimated using heat transfer calculations because of uncertainty in their measurements. These were tube wall temperatures in the water-cooled heat exchangers and the exit air temperature of the ACC. The measurements of the tube wall temperatures in the water-cooled heat exchangers could not be made because the ½ inch diameter tubes had too much curvature and would not permit cement-on-surface thermocouples to adhere to the tubes. Concerning the exit air temperature of the ACC, the purpose of the measurement was to calculate an energy balance for the ACC, which required that a temperature difference be measured. However the thermocouples used for the temperature measurements had an uncertainty of 2^{o}F, which translated to a 2.8^{o}F uncertainty in the temperature difference. This uncertainty was calculated using Equation 3.11 and Equation 3.12. Since the expected temperature increase of the air in the ACC was roughly 3 to 4 degrees, the measurement would be meaningless.

$$\Delta T = T_{a,in} - T_{a,exit} \tag{3.11}$$

$$d(\Delta T) = \sqrt{\left(\frac{\partial(\Delta T)}{\partial T_{a,in}} dT_{a,in}\right)^2 + \left(\frac{\partial(\Delta T)}{\partial T_{a,exit}} dT_{a,exit}\right)^2} \tag{3.12}$$

$$dT_{a,in} = 2^o F$$

$$dT_{a,exit} = 2^o F$$

$$d(\Delta T) = \sqrt{(1 * 2^o F)^2 + (-1 * 2^o F)^2} = 2.8^o F$$

3.2.2 Experimental Parametric Tests of the Air-Cooled Condenser

Tests were carried out in which the temperature of the flue gas entering the air-cooled condenser was varied. In one particular set of tests the inlet flue gas temperature ranged from 105°F to 140°F, which affected the moisture concentration because some water vapor condensed out in the water-cooled heat exchangers and this amount varied based on the temperature. The flue gas temperatures and moisture concentrations entering the ACC during this test are listed in Table 3.5, along with the measured change of flue gas temperature, change of inlet air temperature, flue gas velocity, air velocity, and water condensation rate.

Table 3.5 - Process conditions for a parametric test of inlet flue gas temperature.

Test Name	1108t3	1015t3	1020t3	1013t1
Inlet Flue Gas Temperature [°F]	104.3	119.3	132.2	138.5
Inlet Flue Gas Moisture [% wet-basis]	6	10	11	12.7
Water Condensation rate in the ACC [lbm/hr]	1.42	2.6	2.55	3.5
Decrease in Flue Gas Temperature in the ACC [°F]	15.8	13.1	20.3	22.8
Inlet Cooling Air Temperature to the ACC [°F]	55.1	59.5	62.7	55.8
Cooling Air Velocity in the ACC [ft/sec]	24.6	23	22.5	25.9
Flue Gas Velocity in the ACC [ft/sec]	24.1	27.5	28.4	27.9
Heat Transfer Rate in the ACC (sensible + latent) [BTU/hr]	2006	3213	3407	4483

From this set of tests it was observed that changing the temperature of the flue gas entering the ACC had a significant impact on heat transfer rates. This was due to variations in the mean temperature difference between the cooling air and flue gas and as well as the moisture concentration of the flue gas. Figure 3.13 shows the increase in heat transfer rate. Figure 3.14 shows the condensation efficiency, and it was relatively constant. Figure 3.15 shows the condensation rate and it was greater in tests with higher inlet flue gas moisture concentrations.

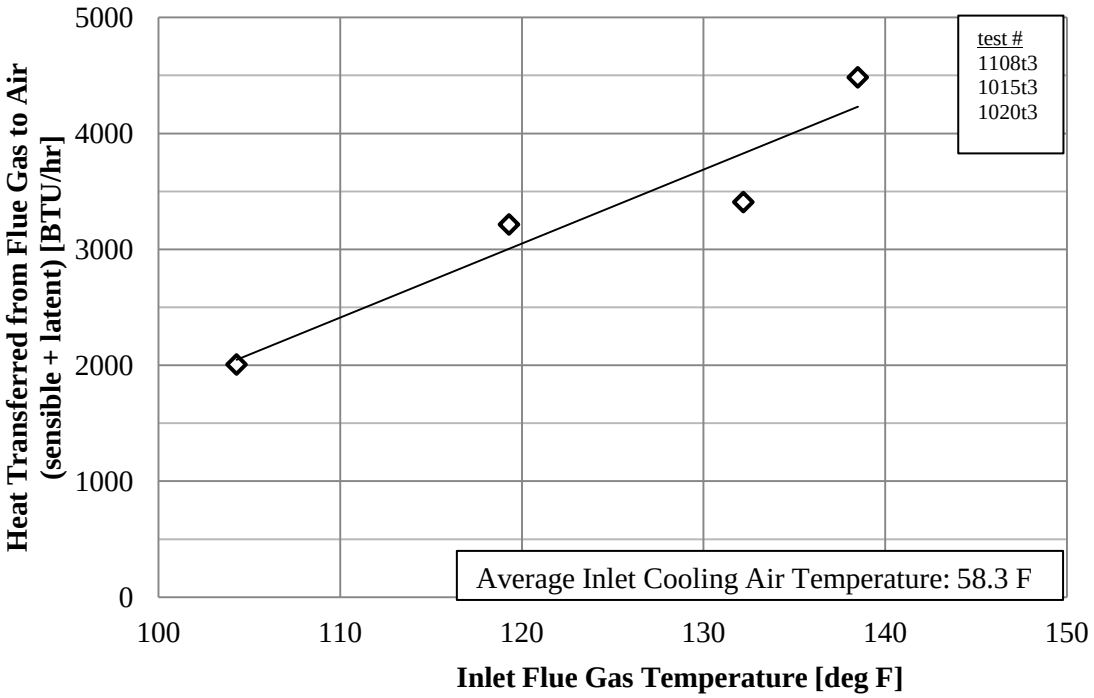

Figure 3.13 - Heat transfer rate versus inlet flue gas temperature (experimental data and curve fit).

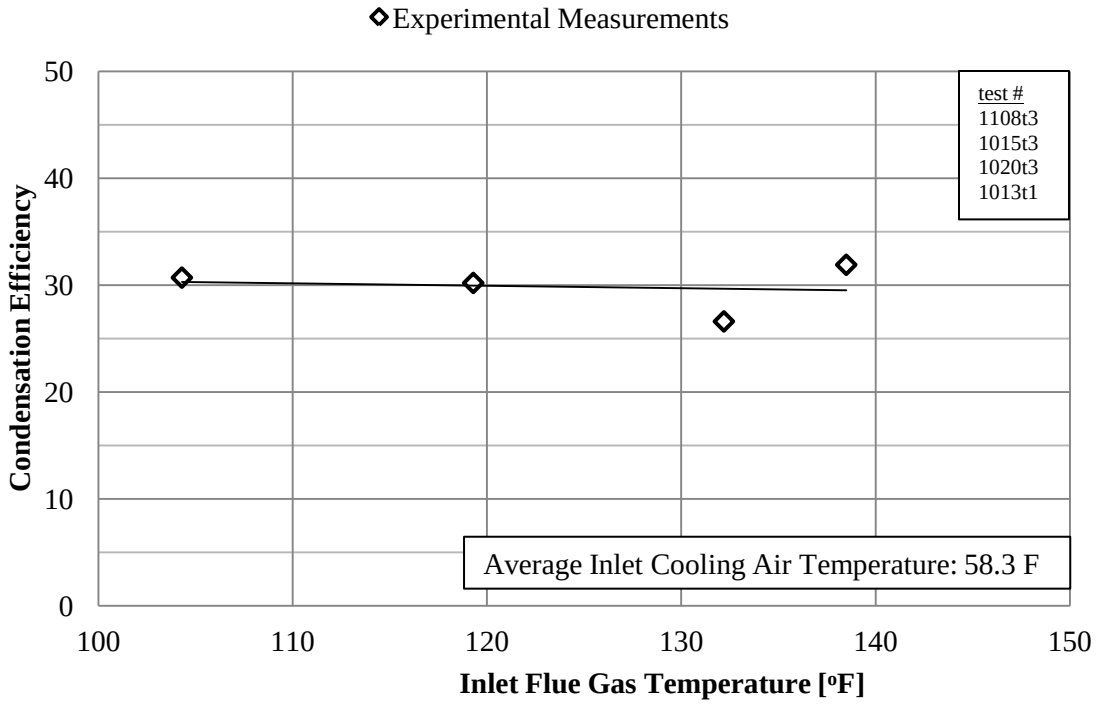

Figure 3.14 - Condensation efficiency versus inlet flue gas temperature (experimental data and curve fit).

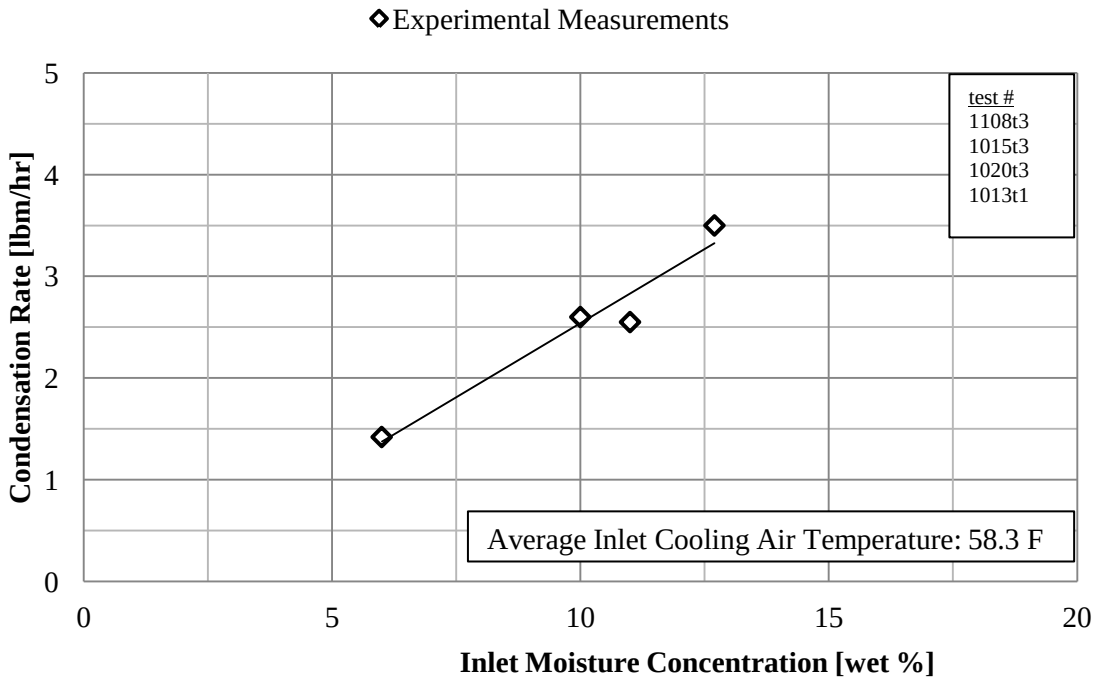

Figure 3.15 - Condensation rate versus inlet flue gas moisture concentration (experimental data and curve fit).

Additional parametric tests to study the effects of inlet flue gas temperature showed similar trends. In Figure 3.16 and Figure 3.17, it is seen that with increasing inlet flue gas temperature and inlet moisture concentration, the ACC condensed larger quantities of water and there was a larger decrease in flue gas temperature. Further details of these experiments can be found in the Appendix.

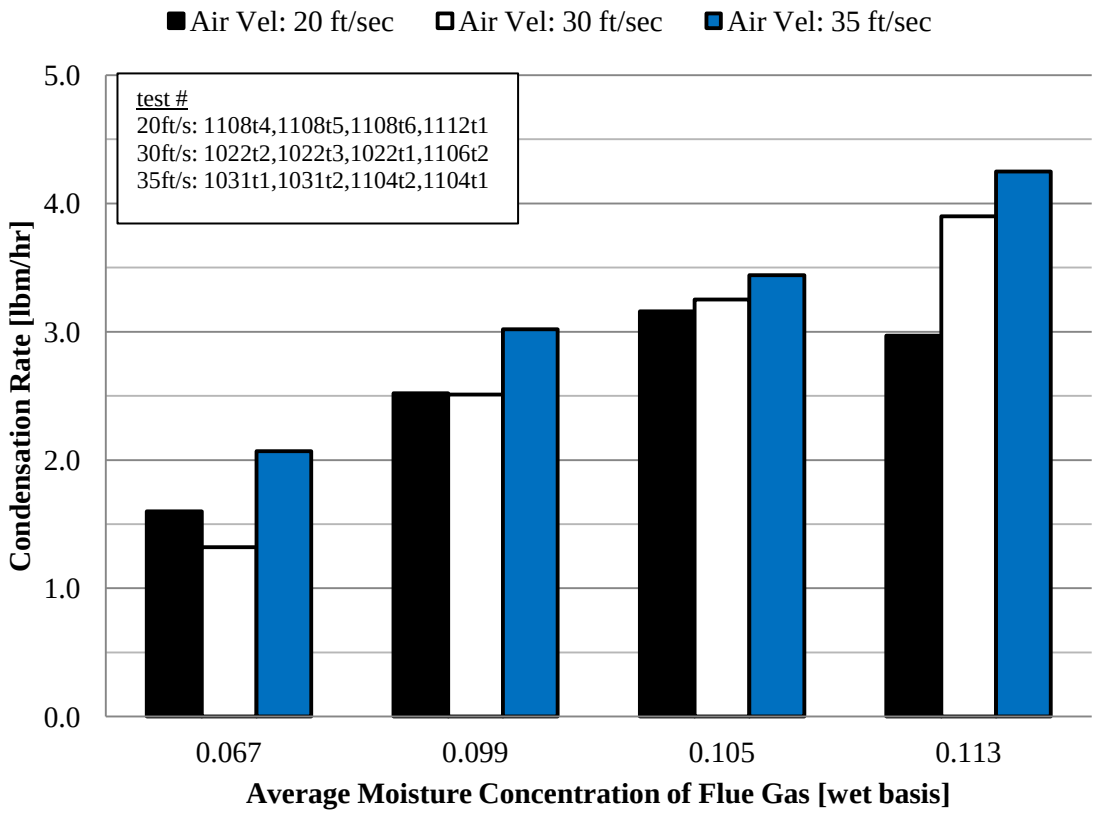

Figure 3.16 - Measured condensation rate for various inlet flue gas temperatures and moisture concentrations.

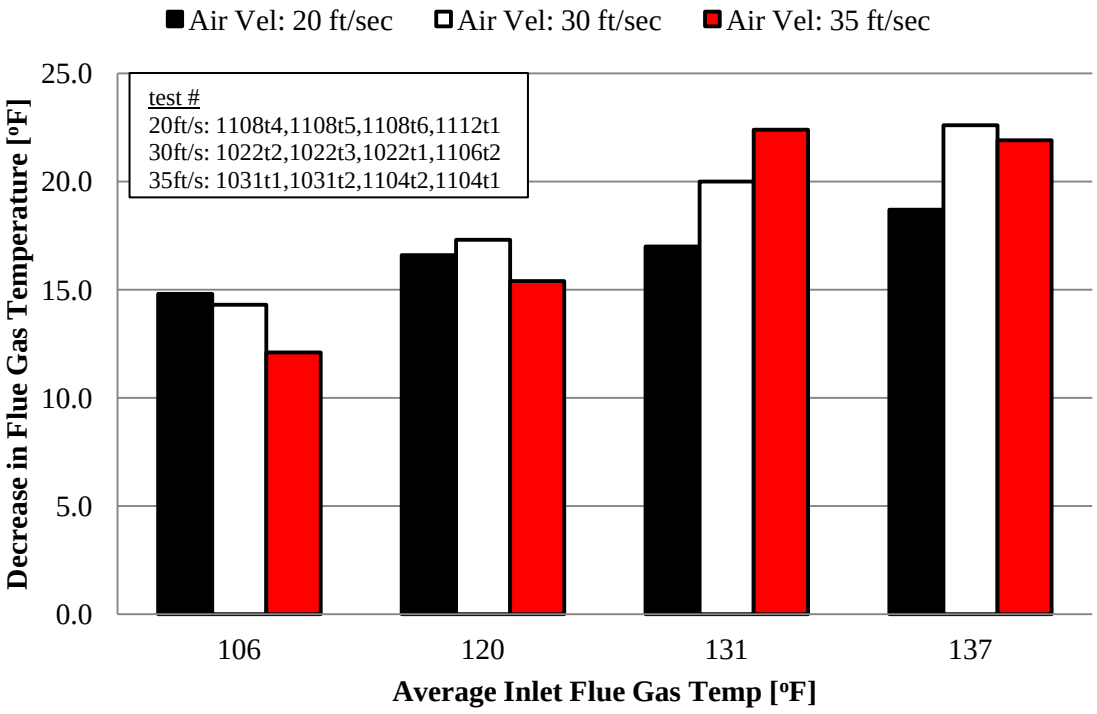

Figure 3.17 - Change in temperature for various inlet flue gas temperatures and moisture concentrations.

It was expected that a lower tube wall temperature would strengthen the mechanisms for condensation. This was tested in experiment by increasing the velocity of the cooling air and Table 3.6 shows process conditions and experimental measurements for tests conducted to study the effects of cooling air velocity.

Table 3.6 - Parametric test for cooling air velocity.

Test Name	1112t1	1013t1	1106t2	1104t1
Inlet Flue Gas Temperature to the ACC [°F]	136.4	138.5	138.2	136.2
Maximum Cooling Air Velocity Around the Tubes in the ACC [ft/sec]	23.9	25.9	31.1	34.7
Inlet Flue Gas Moisture Concentration in the ACC (y_{H_2O}) [% wet-basis]	12.7	12.7	13.3	13.5
Water Condensation Rate in the ACC [lbm/hr]	2.97	3.5	3.9	4.24
Average Tube Wall Surface Temperature of the Thermocouples shows in Figure 3.15. [°F]	98.5	95.2	95	91.1

The tube wall temperature was measured at two locations along the length of the tubes. The cement-on-surface thermocouples were placed on the ACC tubes at locations shown in Figure 3.18 and Figure 3.19. The heat exchanger tubes were 36 inches long and one thermocouple was placed 12 inches from the top of the tube and another thermocouple was placed 24 inches from the top of the tube. The average of the measured values is what is listed in Table 3.6. Figure 3.20 shows measurements of the tube wall temperature for increased cooling air velocities. As was expected, the increased cooling air velocity decreased the tube wall temperature. Figure 3.21 shows the increase in condensation efficiency.

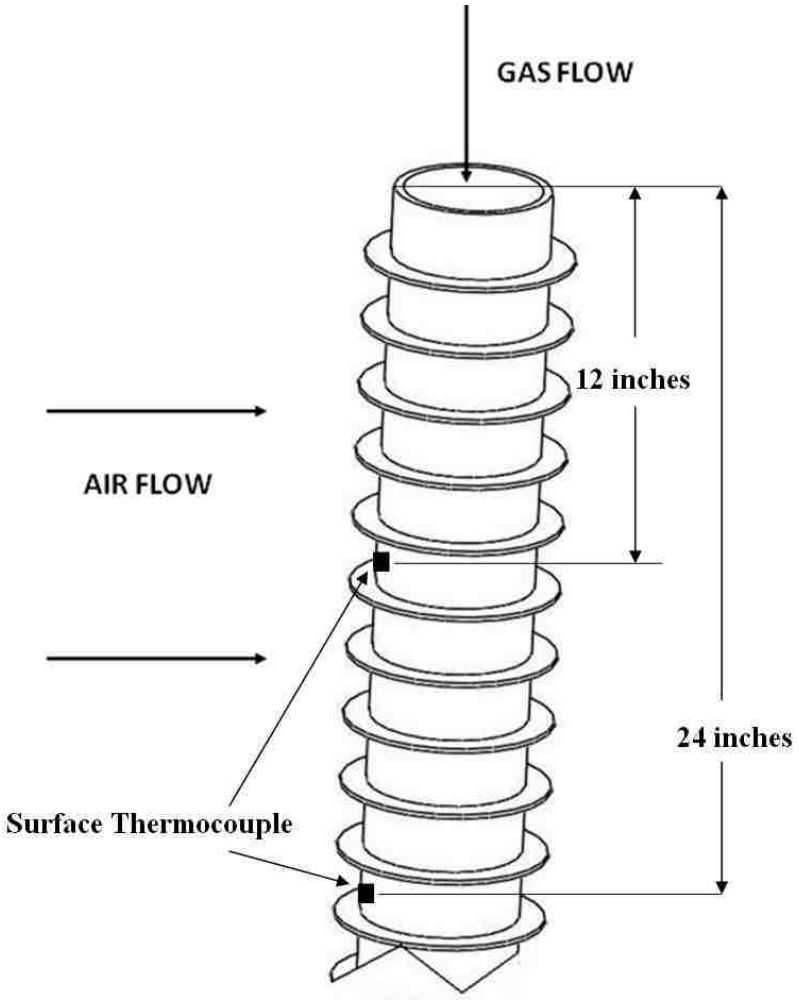

Figure 3.18 – Axial location of thermocouples that measured temperature of the tube wall surface.

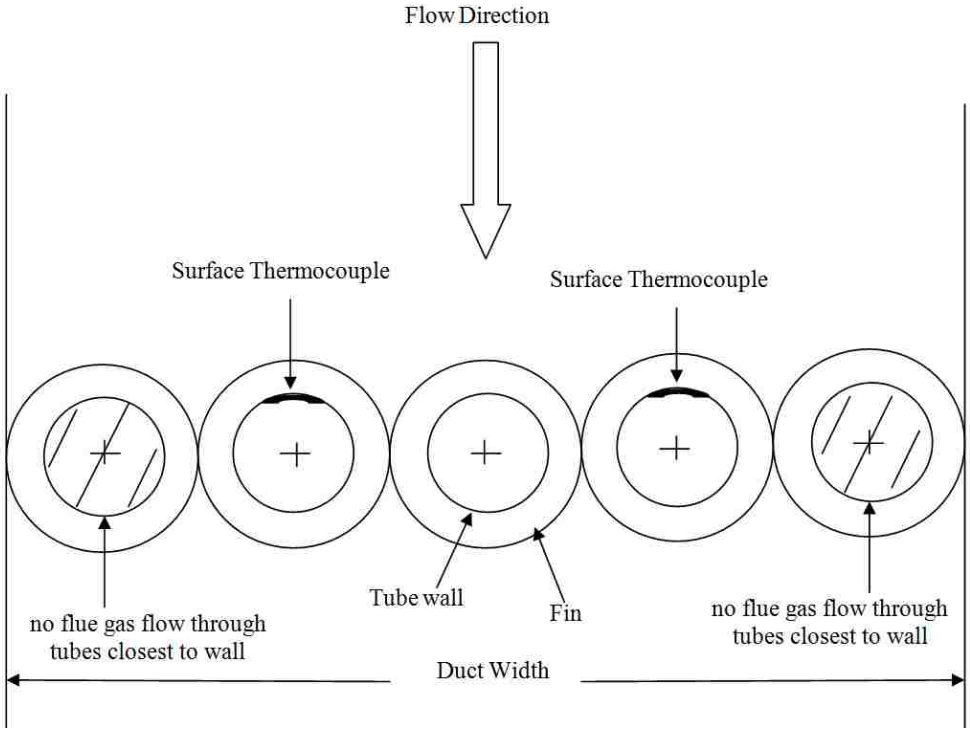

Figure 3.19 - Schematic of which tubes in the bundle measured temperature of the tube wall surface.

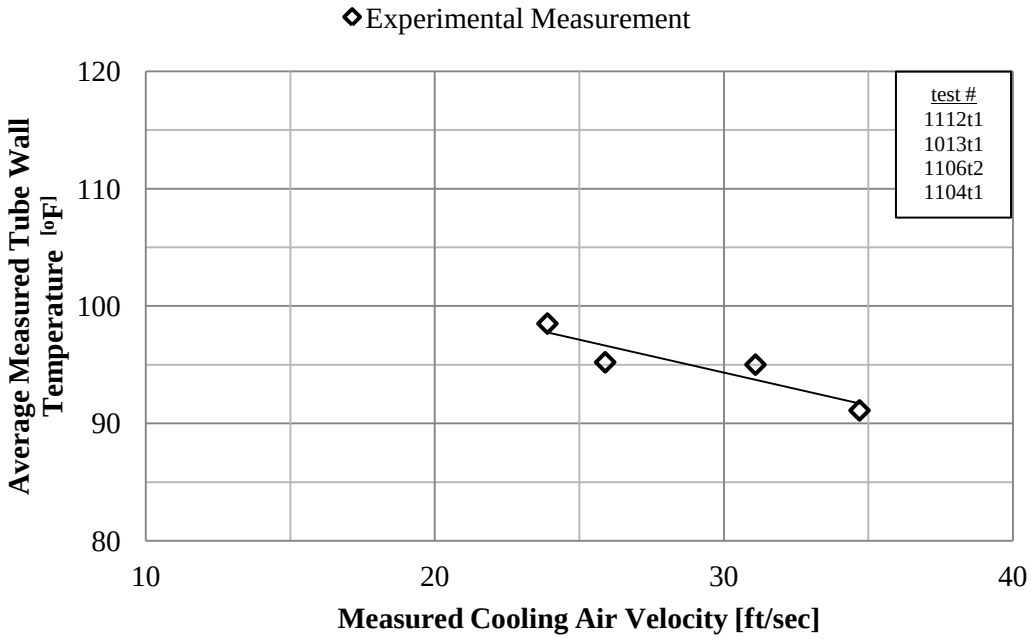

Figure 3.20 - Tube wall temperature versus cooling air velocity (experimental data and curve fit).

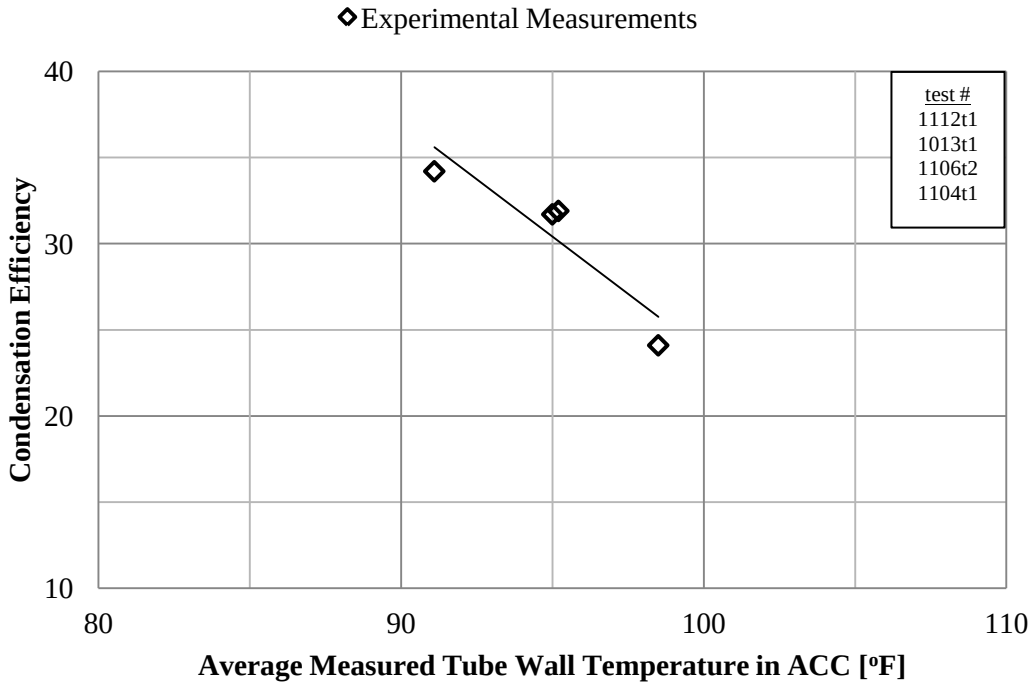

Figure 3.21 - Condensation efficiency for various tube wall temperatures (experimental data and curve fit).

Another process condition that affected heat exchanger performance was flue gas velocity. Increasing the flue gas velocity increased the heat transfer coefficient on the flue gas side, and also the mass transfer coefficient. Due to the complex coupling of heat and mass transfer, it was difficult to predict what effects would be observed. Parametric tests were carried out with flue gas velocities ranging from 29 feet per second to 72 feet per second. The process conditions were:

- Inlet flue gas temperature: 141^{o}F (standard deviation of 0.8^{o}F)
- Inlet flue gas moisture concentration: 11.8 % (standard deviation of 0.3%)
- Inlet cooling air temperature: 60.3^{o}F (standard deviation of 3.4^{o}F)
- Air velocities of 24 ft/sec, 30 ft/sec, and 35 ft/sec.

The effect shown in Figure 3.22 is a decrease in condensation efficiencies, and Figure 3.23 and Figure 3.24 show a relatively constant water condensation rate and overall heat transfer rates respectively.

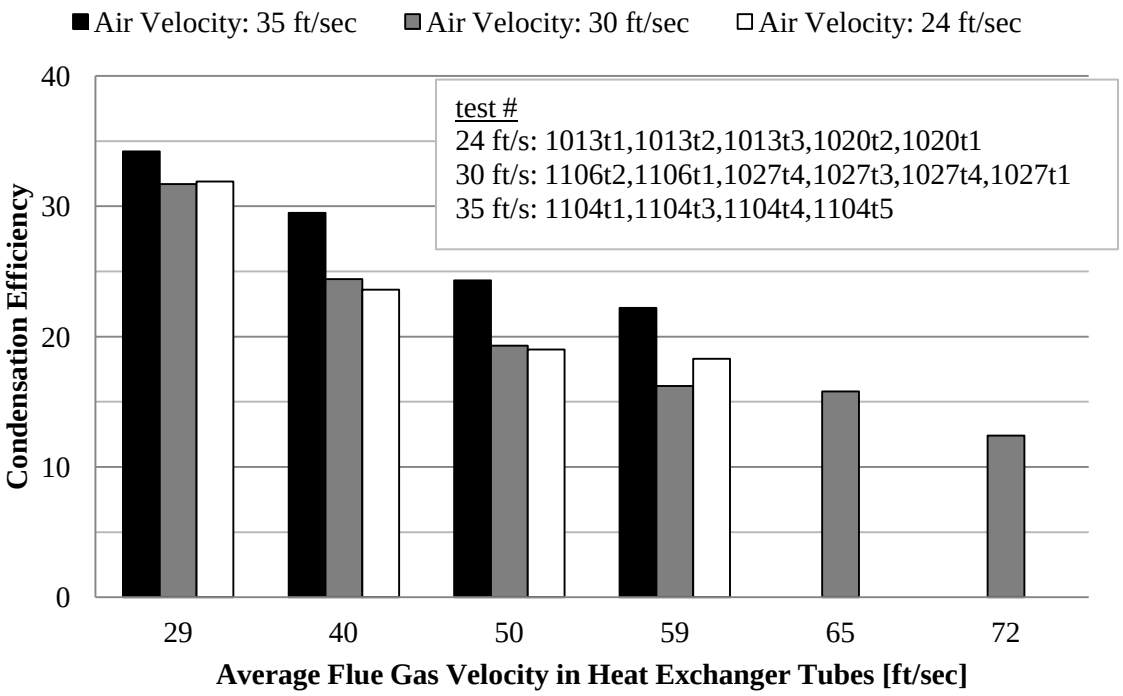

Figure 3.22 - Experimental measurements of condensation efficiency versus flue gas velocity.

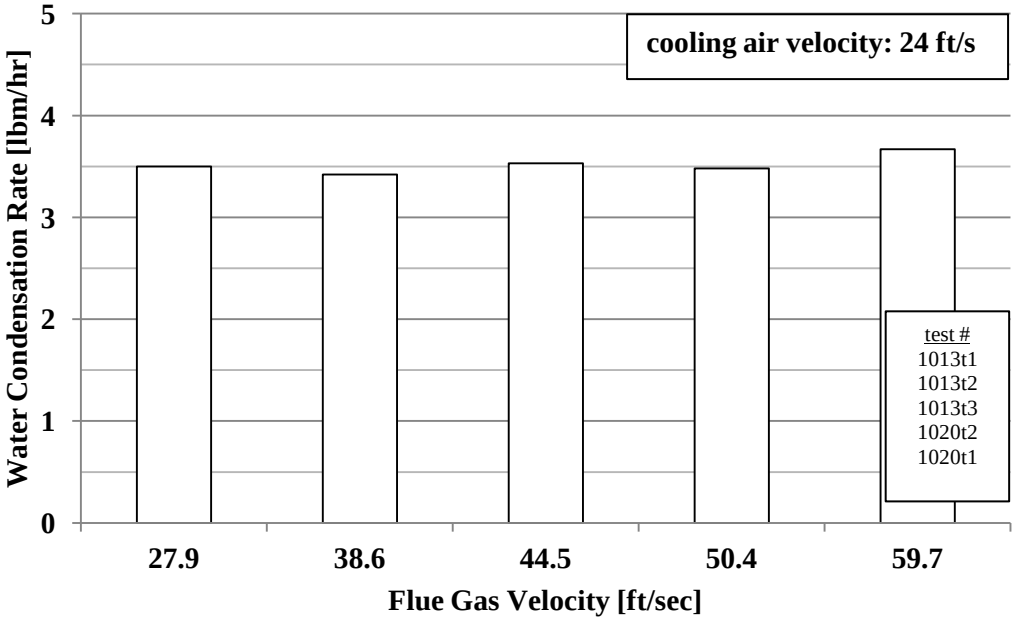

Figure 3.23 - Experimental measurements of condensation rate versus flue gas velocity.

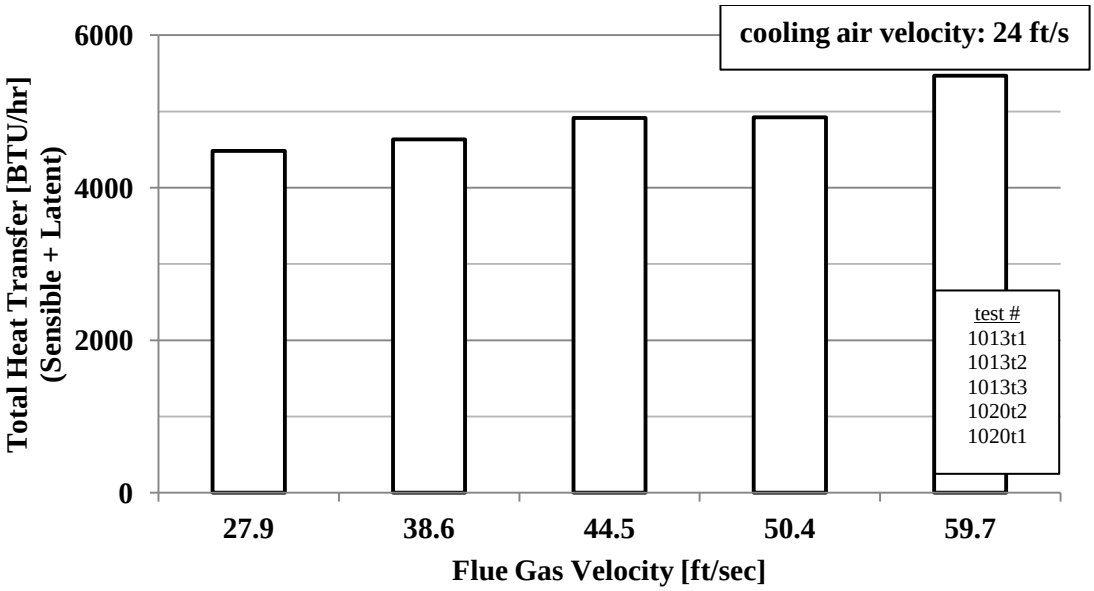

Figure 3.24 - Heat transfer rate calculated from experimental measurements versus flue gas velocity.

Since increasing only the flue gas velocity resulted in decreased condensation efficiencies, it was suspected that increasing the cooling air velocity while increasing the flue gas velocity would curb any decrease in condensation efficiency. Therefore, additional tests were conducted in which both the flue gas and cooling air velocities were increased simultaneously. Table 3.7 lists the process conditions and condensation rates for the tests. The condensation efficiencies and condensation rates are plotted in Figure 3.25 and Figure 3.26. The condensation rate increased and the condensation efficiency remained relatively constant. Figure 3.27 shows the overall increase in heat transfer rates due to increasing both the air-side and gas-side velocities simultaneously.

Table 3.7 - Parametric test for flue gas velocity and cooling air velocity.

Test Name	1112t1	1013t2	1106t1	1104t4
Inlet Gas Temperature [^{o}F]	136.4	139.6	141.7	141.7
Flue Gas Velocity [ft/sec]	30.9	38.6	41	48.1
Cooling Air Velocity [ft/sec]	23.9	25.9	31.0	35.0
Water Condensation Rate [lbm/hr]	2.97	3.42	4.03	4.11
Condensation Efficiency [%]	24.1	23.6	24.4	24.3

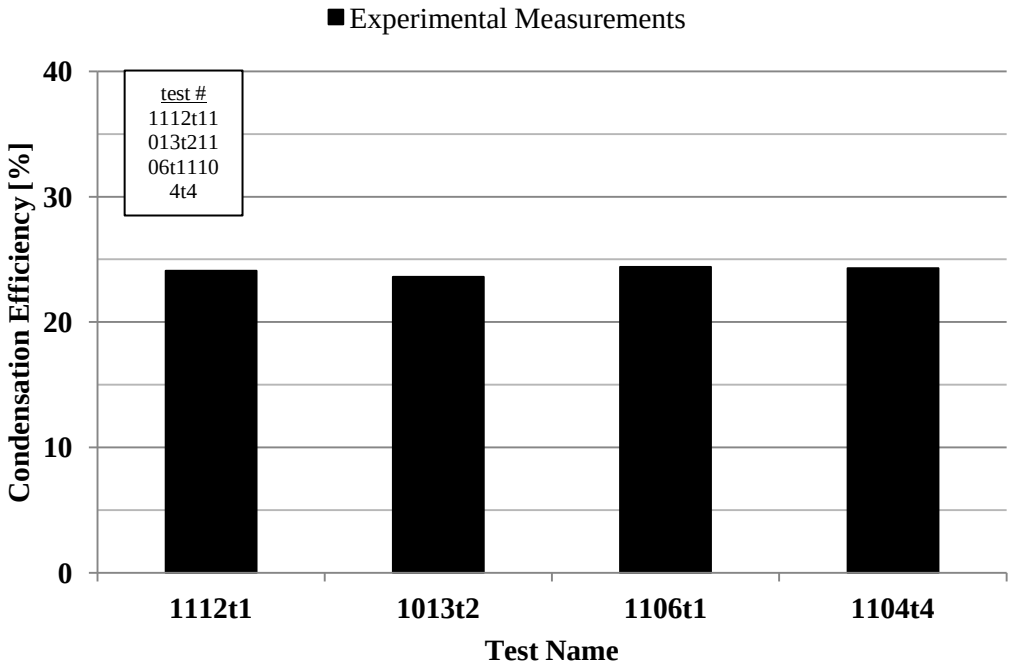

Figure 3.25 - Condensation efficiency for increasing cooling air and flue gas velocities.

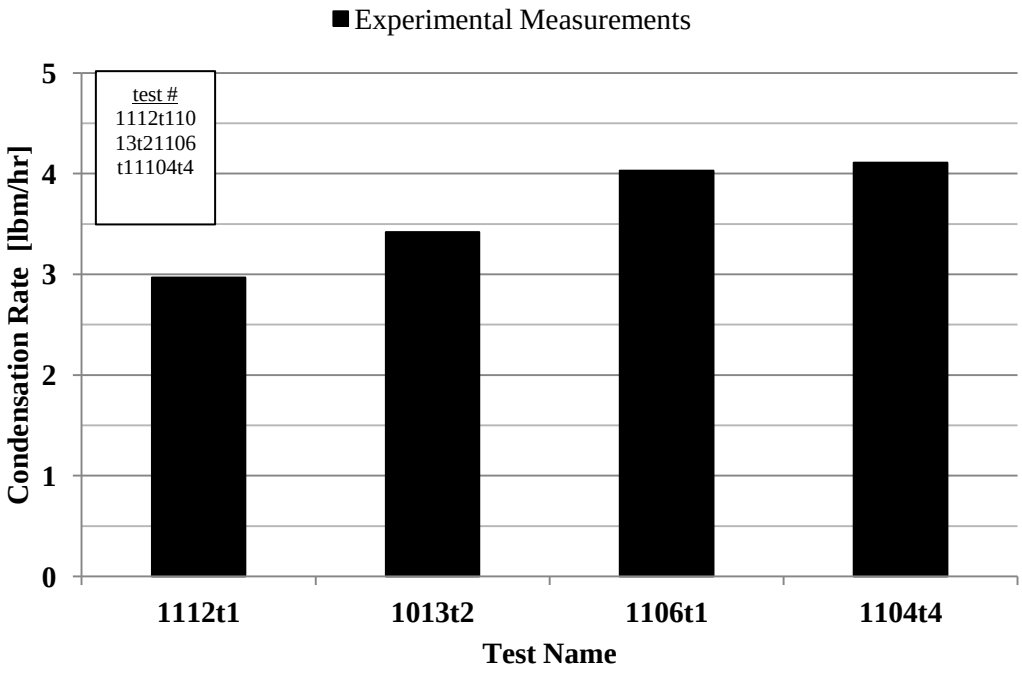

-

Figure 3.26 - Condensation rate for increasing cooling air and flue gas velocities.

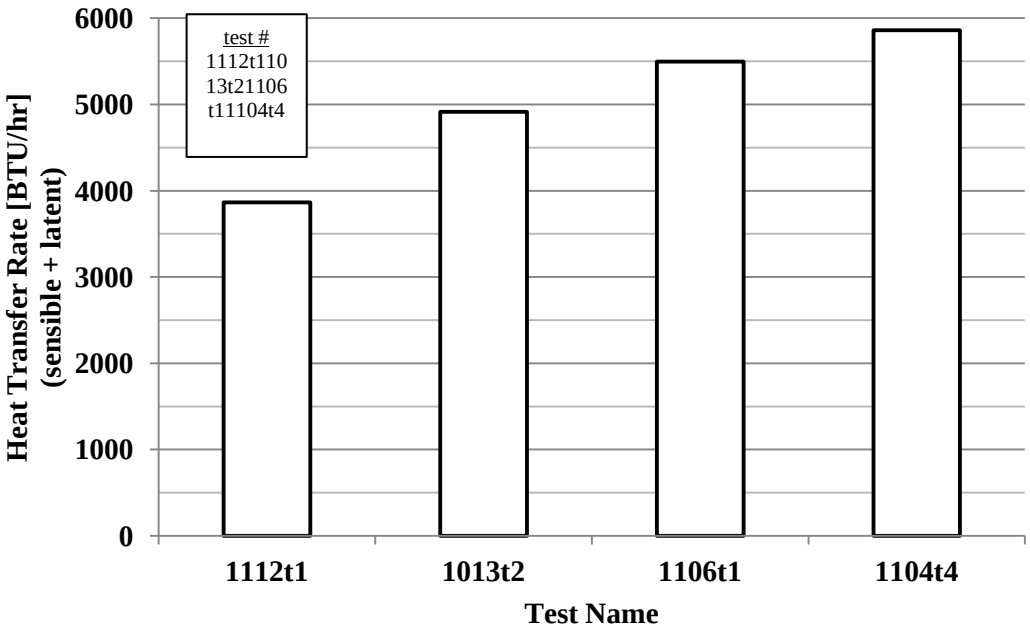

Figure 3.27 - Heat transfer rate for increasing cooling air and flue gas velocities.

3.3 Agreement of Experimental Results and Theory

One objective of the experimental research was to provide data to validate the accuracy of the heat and mass transfer simulation. The heat and mass transfer model described in Chapter 2 was applied to the experimental apparatus and its predictions were compared to the experimental measurements. The process conditions of the experiment (e.g. inlet flue gas temperature, flue gas velocity, inlet air temperature, air velocity) were inputs to the model, and the outputs were condensation rate, increase in air temperature, and decrease in flue gas temperature. This section discusses the agreement between the measured values from experiment and calculated values from simulation and verifies that the heat and mass transfer model accurately predicts the ACC's performance.

The heat and mass transfer model solves governing equations for temperature distributions. These temperature distributions (e.g. flue gas, cooling air, and tube surface) are then used to calculate heat and mass transfer rates. Therefore to properly validate the model, its

calculated temperature distributions are compared to experimentally measured temperatures. Further validation is completed by comparing condensation rates and heat transfer rates.

Beginning with the temperature distribution comparisons, Table 3.8 shows the process conditions for a test with a relatively low flue gas velocity of 28.4 ft/sec and Figure 3.28 shows the temperature distributions for one of the tubes in the heat exchanger during the test. Also in the figure is the tube orientation corresponding to the abscissa in the graph (in the heat exchanger the tubes are oriented vertically). There are four lines on the graph in Figure 3.28 corresponding to the flue gas temperature, tube wall surface temperature, and inlet and exit air temperature. The lines show theoretical calculations and the markers symbolize experimental measurements. During experiment the inlet cooling air temperature was not always uniform across the cross-section and that is why in Figure 3.28 the air temperature was 59^{o}F at the top of the cross-section and 66^{o}F at the bottom.

Table 3.8 also compares the values for the decrease in flue gas temperature determined in experiment and the simulation. The simulation predicted an 18.5^{o}F decrease, and the experimental measurement was a 20.2^{o}F decrease in flue gas temperature. Given that the experimental uncertainty in the measurement of the temperature difference of the flue gas was 2.8^{o}F (discussed in the section on page 71), the simulation accurately predicted the temperature decrease of the flue gas. The measured rate of condensation during the experiment was 2.55 lbm/hr, while the simulation predicted 2.75 lbm/hr. The difference being 0.2 lbm/hr, or 7.8%.

Table 3.8 - Process conditions and performance results for test 1020t3

Test Name	1020t3	
	Experimental	Simulation
Flue Gas Velocity in Tubes [ft/sec]	28.4	
Cooling Air Velocity between Tubes [ft/sec]	22.5	
Average Inlet Cooling Air Temperature [^{o}F]	62.5	
Average Exit Cooling Air Temperature [^{o}F]	-	66.1
Inlet Moisture Concentration [% wet basis]	11.0%	11.0%
Gas-side Surface Area [ft^2]	2.64	
Air-side Surface Area [ft^2]	23.8	
Condensation Rate [lbm/hr]	2.55	2.75
Decrease in Flue Gas Temperature [^{o}F]	20.2	18.5

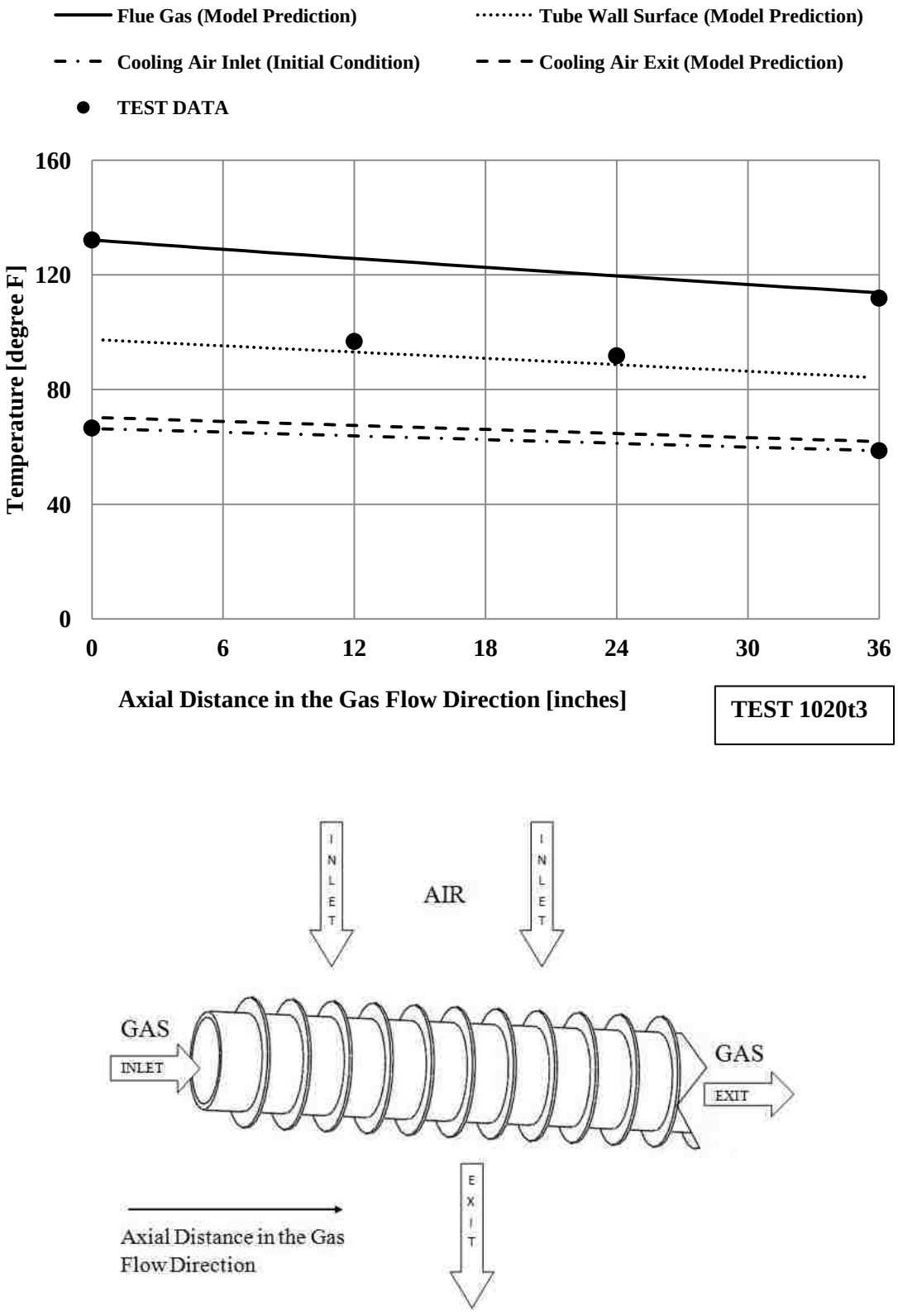

Figure 3.28 - Temperature distributions for one tube of the ACC during test 1020t3.

In another test the flue gas velocity was 50 ft/sec. Table 3.9 shows the process conditions and performance results, and Figure 3.29 displays the temperature distributions for one of the tubes in the ACC. The simulation predicted a 16.5°F decrease, and the experimental measurement was 19.1°F, an under prediction of 13.6%. The measured condensation rate and predicted condensation rate differed by 17%. The surface temperature measurements agree with the predicted values from the model, as shown in Figure 3.29.

Table 3.9 – Process conditions and performance results for test 1020t2.

Test Name	**1020t2**	
	Experimental	**Simulation**
Flue Gas Velocity in Tubes [ft/sec]	**50.4**	
Cooling Air Velocity between Tubes [ft/sec]	**22.5**	
Average Inlet Cooling Air Temperature [°F]	**58.7**	
Average Exit Cooling Air Temperature [°F]	**-**	**63.8**
Inlet Moisture Concentration [% wet basis]	**12.00%**	**12.00%**
Gas-side Surface Area [ft^2]	**2.64**	
Air-side Surface Area [ft^2]	**23.8**	
Condensation Rate [lbm/hr]	**3.48**	**4.06**
Decrease in Flue Gas Temperature [°F]	**19.1**	**16.5**

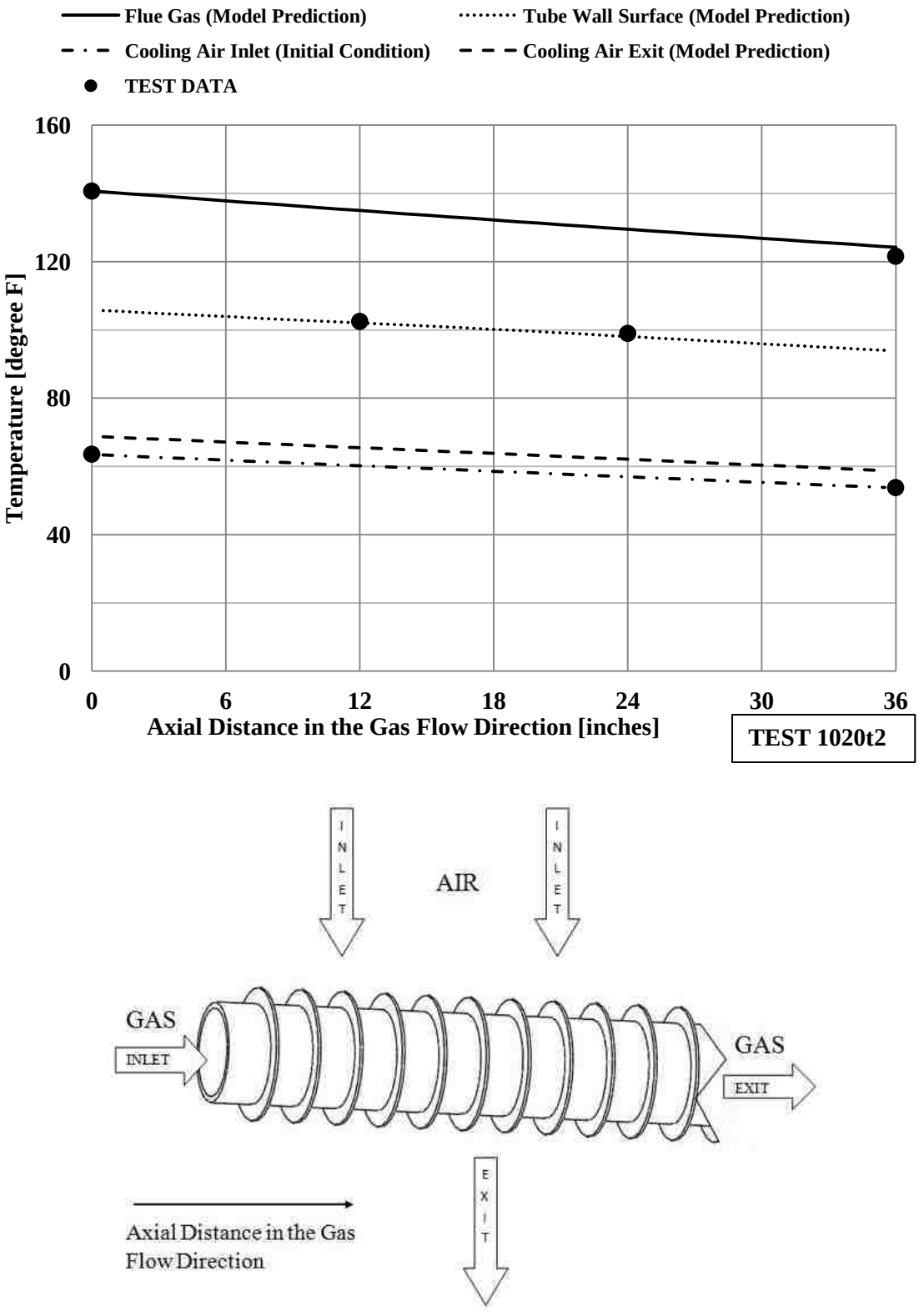

Figure 3.29 - Temperature distributions for one tube of the ACC during test 1020t2.

It was observed that as the flue gas velocity was further increased, the model was less accurate at predicting the heat and mass transfer performance of the heat exchanger. Around 70 ft/sec, the model over predicted latent heat transfer and under predicted sensible heat transfer. Table 3.10 shows a test with a flue gas velocity of 72 feet per second and the differences between the model's predictions and the experimental measurements were 41% for latent heat transfer and 25% for sensible heat transfer. It was expected that uncertainty in the mass transfer coefficient caused the discrepancy and this is discussed in the following paragraph.

Table 3.10 - Process conditions and performance results for test 1027t1.

Test Name	**1027t1**	
	Experimental	**Simulation**
Flue Gas Velocity in Tubes [ft/sec]	**72**	
Cooling Air Velocity between Tubes [ft/sec]	**29.2**	
Average Inlet Cooling Air Temperature [^{o}F]	**65.8**	
Average Exit Cooling Air Temperature [^{o}F]	**-**	**70**
Inlet Moisture Concentration [% wet basis]	**11.70%**	**11.70%**
Gas-side Surface Area [ft^2]	**2.64**	
Air-side Surface Area [ft^2]	**23.8**	
Condensation Rate [lbm/hr]	**3.13**	**4.06**
Decrease in Flue Gas Temperature [^{o}F]	**18.9**	**14.2**

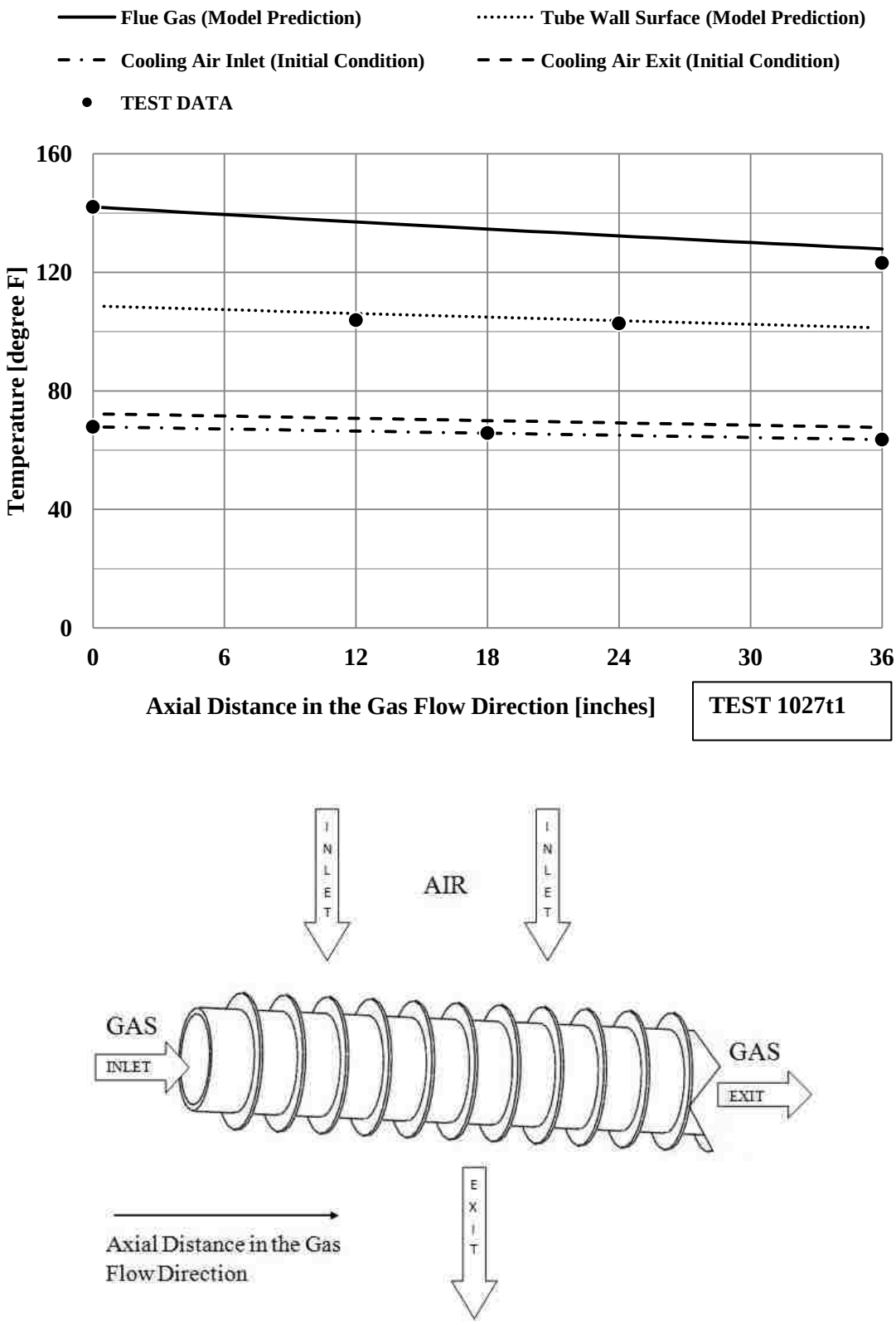

Figure 3.30 - Temperature distributions for one tube of the ACC during test 1027t1.

In the examples in this section where flue gas velocity was 50 and 72 ft/sec, it was seen that as the flue gas velocity was increased, the simulation became less precise at predicting the heat and mass transfer measurements. The suspicion was that the mass transfer coefficient was less accurate as the flue gas velocity was increased. As described in Chapter 2, which discusses the simulation, the diffusion coefficient used in the calculation for water vapor through flue gas was approximated assuming it behaves like water vapor through air. To test the sensitivity of the mass transfer coefficient it was reduced by 20 percent, 30 percent, 40 percent, and 50 percent and then calculating the heat and mass transfer rates.

Table 3.11 lists simulations for the case in Figure 3.29, which the flue gas velocity was approximately 50 feet per second. The first column shows the measured decrease in flue gas temperature and the measured condensation rate. The second column named 'Simulation' is the calculated mass transfer coefficient k_g and calculated heat and mass transfer performance ΔT and $\dot{m}_{cd}$. The remaining columns show calculations for the cases where the mass transfer coefficient was decreased by 20 percent, 30 percent, 40 percent, and 50 percent, respectively. The simulation originally predicted temperature decreases and condensation rates to within 14 percent and 17 percent respectively, and by lowering the mass transfer coefficient by 30 percent, the agreement for the temperature decrease and condensation rate becomes 5% and 0.8% respectively.

Table 3.11 - Effects of decreasing the mass transfer coefficient for flue gas velocity of 50 ft/sec (Test1020T2).

	Experiment	**Simulation**	$k_g = k_g * 0.8$	$k_g = k_g * 0.7$	$k_g = k_g * 0.6$	$k_g = k_g * 0.5$
k_g	-	2.47	1.96	1.71	1.46	1.22
ΔT-gas [°F]	19	16.5	17.5	18.1	18.8	19.6
$\dot{m}_{cd}$ **[lbm/hr]**	3.48	4.05	3.69	3.45	3.18	2.85

The same analysis was performed for the case when the flue gas velocity was 72 feet per second, and the results shown in Table 3.12 indicate that when the mass transfer coefficient was decreased by 40 percent the decrease in flue gas temperature and condensation rate agreed with the experimental measurements by 16 percent and 5 percent, respectively. This is in comparison to the original simulations in which the agreement was 25 percent for the temperature decrease and 41 percent for the condensation rate.

Table 3.12 - Effects of decreasing the mass transfer coefficient for flue gas velocity of 72 ft/sec (Test1020T2).

	Experiment	**Simulation**	$k_g = k_g * 0.8$	$k_g = k_g * 0.7$	$k_g = k_g * 0.6$	$k_g = k_g * 0.5$
k_g	-	3.3	2.62	2.28	1.95	1.62
ΔT-gas [°F]	18.9	14.1	14.8	15.2	15.8	16.4
$\dot{m}_{cd}$ [lbm/hr]	3.13	4.11	3.78	3.57	3.3	3

The following three figures compare measurements from all 35 experiments. Figure 3.31 shows the decrease in flue gas temperature across the air-cooled condenser. The abscissa is the measured flue gas temperature drop and the ordinate is the calculated decrease in flue gas temperature. A straight line with a slope of 1 indicates perfect agreement between the calculations and the experiment. The figure shows that the simulation predicted the temperature decrease within 20 percent.

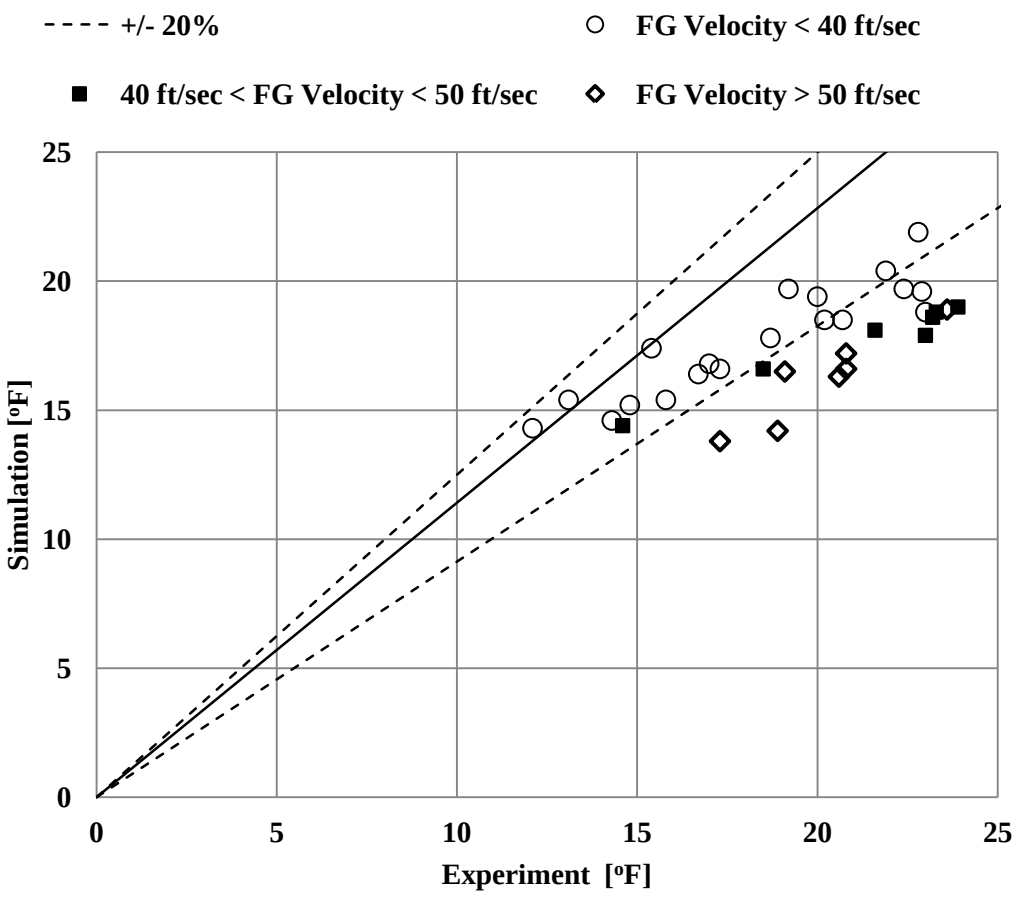

Figure 3.31 - Accuracy of simulation for calculating decrease in flue gas temperature in the ACC.

Figure 3.32 compares tube wall surface temperature measurements to the calculated values. The calculated values were within 5°F of the measurements. To put 5°F into perspective, the log mean temperature difference between the gas and air was on average 61°F, and the uncertainty in the thermocouples was +/- 2°F.

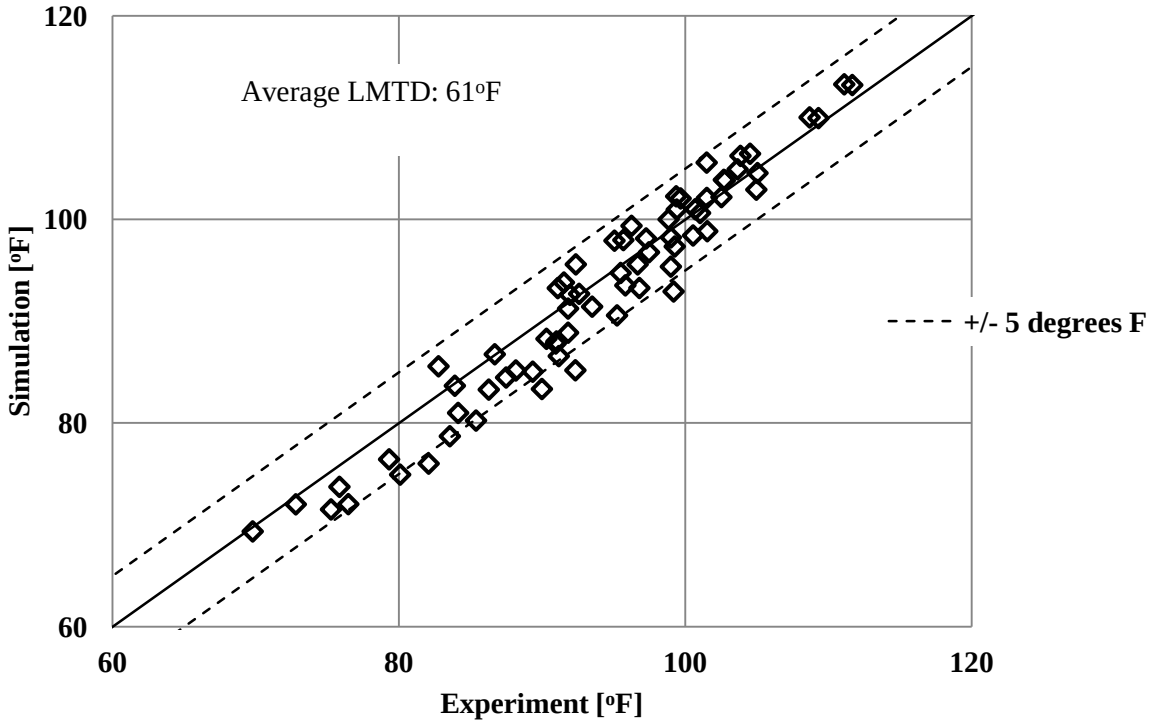

Figure 3.32 - Accuracy of simulation for predicting tube wall temperature of the ACC.

Figure 3.33 shows the condensation rates for the 35 experiments. Aside from one outlier, the measured values and calculated values differ by less than 15 percent of each other. The results presented in this chapter show that the model accurately predicted the heat and mass transfer performance of the ACC with process conditions that ranges those listed in Table 3.3. Additional comparisons between the experimental measurements and calculated predictions are tabulated in the Appendix A.

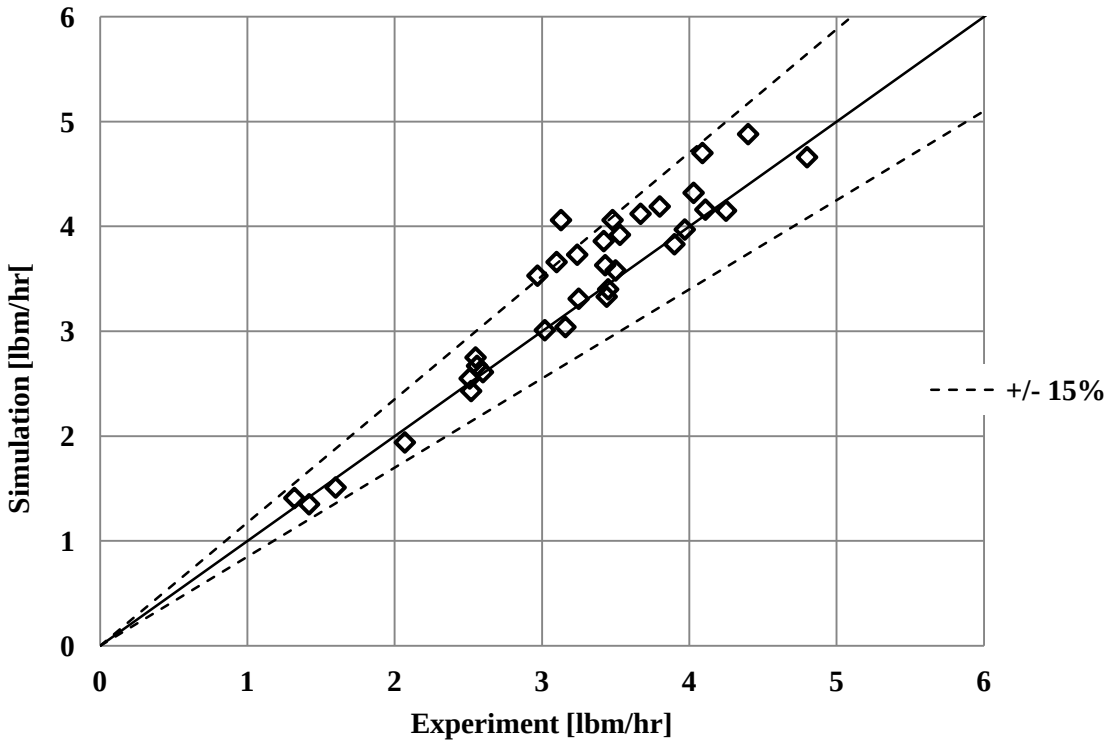

Figure 3.33 - Accuracy of simulation for predicting condensation rate of water vapor in the ACC.

3.4 A note on measuring the moisture concentration of the flue gas

For natural gas, the flue gas moisture concentration is typically in the vicinity of 10 to 11 percent, on a wet-gas basis. For the experiments in this study, assuming that natural gas was comprised of only methane, and using a measured excess oxygen level of 8.8 percent, the theoretical value for the moisture concentration of the flue gas was 10.1 percent. For the 35 tests conducted, the average moisture concentration of the flue gas was determined to be 14.5% using a wet bulb and dry bulb thermometer. This concentration exceeds what is typical of natural gas fired boilers and led to an investigation of the experimental technique used to determine moisture concentration.

The moisture concentration was initially determined by placing a wet and dry bulb thermometer at the exit of the ACC where the flue gas temperature was between 80°F and 120°F. To determine the moisture concentration upstream of the heat exchangers, the volume of water collected from each condensing heat exchanger was added to the volume of moisture in the flue gas. An example of the values measured in experiment and used to calculate the moisture concentrations are provided in Table 3.13.

Table 3.13 - Values used to calculate the moisture concentration of the flue gas.

		0208t1	0208t2
Measured	Wet Bulb Temp [degree Fahrenheit]	115.3	113.4
Measured	Dry Bulb Temp [degree Fahrenheit]	119.6	119.6
Calculated	Specific Humidity [lbm H2O / lbm dry gas]	0.069	0.064
	Molar Mass of Flue Gas	30	30
	Molar Mass of Water	18	18
Calculated	Moisture Concentration at Exit [% molar dry basis]	11.5	10.7
Measured	Flue Gas Flow rate [lbm/hr]	184	188
Calculated	Vapor Flow rate at Exit [lbm/hr]	12.7	12.0
Measured	Condensation Rate in ACC [lbm/hr]	3.12	3.16
Measured	Condensation Rate in HX2 [lbm/hr]	4.55	6.16
Measured	Condensation Rate in HX1 [lbm/hr]	0	0
Calculated	Vapor Flow rate at Inlet [lbm/hr]	20.4	21.4
Calculated	Moisture Concentration at Inlet [% molar wet basis]	16.6	17.0

While this method is reliable, the unusually high moisture concentrations it estimated were cause for concern. To check these results a controlled condensation method was used to determine the moisture concentration of the flue gas. The method used was modeled after EPA Method 8, and a schematic is shown in Figure 3.34. The method was to bubble a known amount of flue gas through impingers that were filled with water and then the moisture in the flue gas condensed into the water filled impingers. The weight of the impingers was measured before and after the test and the difference was the amount of moisture in the flue gas.

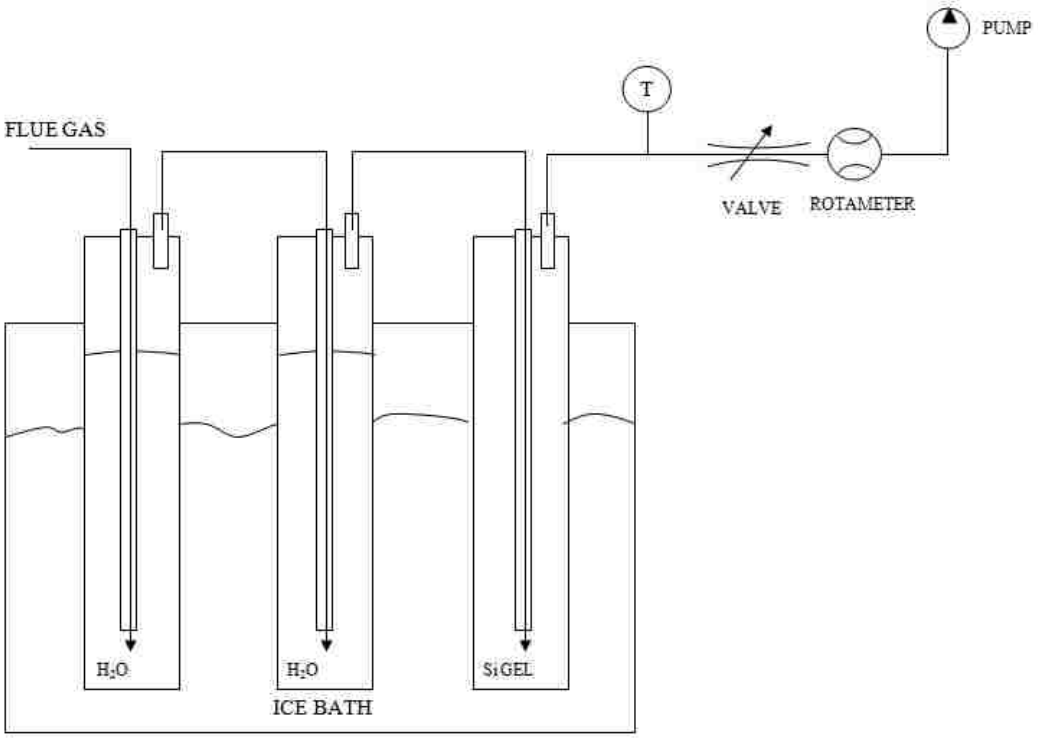

Figure 3.34 - Controlled condensation method used to determine the moisture concentration of the flue gas.

The controlled condensation method was used in the two tests shown in Table 3.13, and the results are provided in Table 3.14. The results indicate that the moisture concentration of the flue gas was higher than what is theoretically calculated, and is accurately predicted using the wet bulb and dry bulb thermometer. Investigations were performed to confirm that the water-cooled

heat exchangers were not leaking. It was suspected that a steam leak near the port for the flue gas stream caused the excessive moisture concentrations.

Table 3.14 - Controlled condensation method to determine flue gas moisture concentration.

		0208t1	0208t2
Measured	Impinger 1 Before Test [grams]	660.6	860.3
Measured	Impinger 2 Before Test [grams]	735	735.9
Measured	Impinger 3 Before Test [grams]	639.8	643.6
Measured	Impinger 1 After Test [grams]	707.9	863.2
Measured	Impinger 2 After Test [grams]	735.7	779.2
Measured	Impinger 3 After Test [grams]	643.6	645.2
Measured	Moisture Captured [grams]	51.8	47.8
Measured	Flue Gas Flow rate through CCM [scfh]	6.03	6.52
Measured	Test Duration [minutes]	145	120
Measured	Gas Temperature exiting CCM [degree F]	65.7	68.2
Calculated	Moisture Concentration Assuming Gas is Saturated at Gas Temperature exiting CCM	18.7	19.5
Calculated	Moisture Concentration Assuming Gas is Dry when Exiting CCM.	16.5	17.1

4 Choosing Process Conditions to Meet Performance Objectives

The purpose of a flue gas condenser can be to recover water and/or recover low-grade heat. This chapter discusses the process conditions which promote greater rates of water recovery and greater rates of heat transfer. Presented are experimental data, computer simulations, and heat and mass transfer theory to aid the discussion about the effects of the process conditions.

4.1 Effects of Inlet Flue Gas Temperature and Inlet Moisture Concentration

It was shown in Figure 3.15 that increasing the inlet flue gas temperature and inlet moisture concentration increased the water condensation rate. Equations 4.1 through 4.4 are the theoretical mass transfer equations to calculate condensation rate. In Equation 4.1 the driving potential for condensation is the difference in vapor partial pressures between the bulk flow and tube wall (or condensate interface if there is a liquid film). These equations indicate that a higher moisture concentration y_{H_2O} will yield increased rates of condensation, which was observed in experiments.

$$\dot{m}_{condensation\,rate} = k_g A\left(P_{v,bulk} - P_{v,i}\right) \tag{4.1}$$

$$P_{v,bulk} = y_{H_2O} * (P_{tot}) = y_{H_2O} * \left(P_{v,bulk} + P_{dry\,gas}\right) \tag{4.2}$$

$$P_{v,i} = P_{sat@T_i} \tag{4.3}$$

$$k_g = \frac{h_g M_{H_2O}}{Cp_g M_g Le^{2/3} P_{lm}} \tag{4.4}$$

Using Equations 4.1 through 4.4, calculated condensation rates and experimental measurements show that increasing the inlet moisture concentration increases the condensation rates. The parametric test listed in Table 4.1 is discussed here with a physical explanation for the performance observed. The table provides information about the tests including the mass transfer coefficient from Equation 4.4 and the difference in vapor partial pressures between the bulk flow and the condensate interface $\left(P_{v,bulk} - P_{v,i}\right)$. For an explanation of Equations 4.1 though 4.4, refer back to the Literature Review.

Figure 4.1 shows the condensation rate along with the inlet moisture concentration of the flue gas.

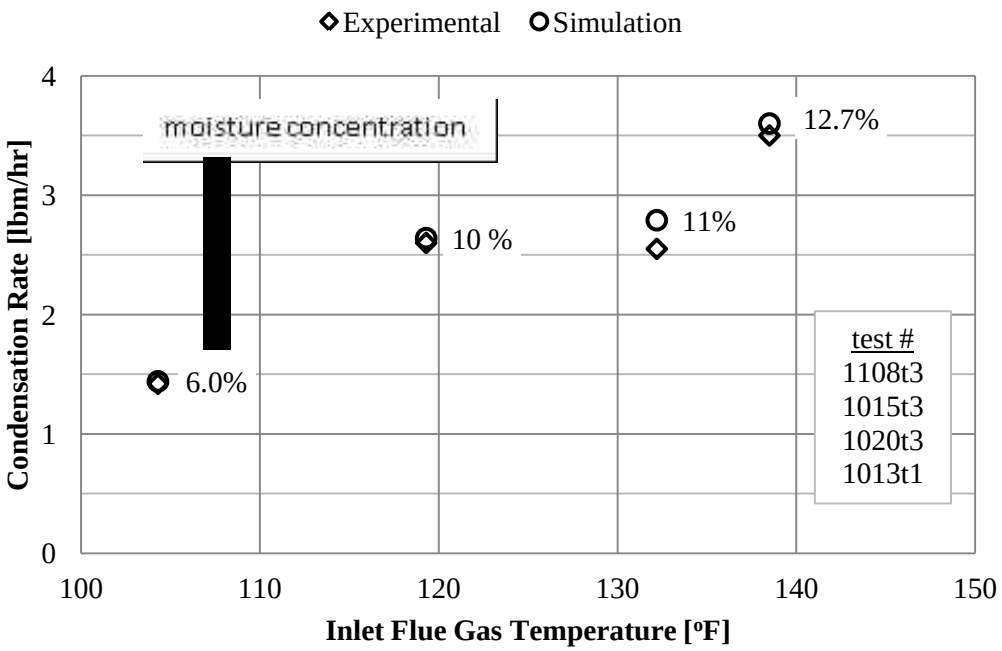

Figure 4.1 - Condensation rate versus inlet flue gas temperature for various inlet moisture concentrations.

The data shows that with increased inlet flue gas temperature the mass transfer coefficient was relatively constant, and the increased condensation rates were due to the increased difference in vapor partial pressures $(P_{v,bulk} - P_{v,i})$.

Table 4.1 – Parameters affecting condensation rates for a series of tests with varying inlet flue gas temperatures and inlet moisture concentrations.

Test Name	1108t3	1015t3	1020t3	1013t1
Inlet Gas Temperature [^{o}F]	104.3	119.3	132.2	138.5
Inlet Flue Gas Moisture Concentration y_{H2O} [percent wet-basis]	6	10	11	12.7
Water Condensation Rate in the ACC [lbm/hr]	1.42	2.6	2.55	3.5
Mass Transfer Coefficient k_g [lbm/hr-ft^2-psi]	1.4	1.57	1.58	1.54
($P_{v,bulk} - P_{v,i}$) [psia]	0.0471	0.663	0.8675	1.217

Figure 4.2 shows the sensible and latent heat transfer rates. Both components increase with increasing flue gas temperature and moisture concentration because the driving potentials $(T_g - T_s)$ and $(P_{v,bulk} - P_{v,i})$ increased. The respective heat transfer equations are shown below.

$$Q_{sensible} = h_g A_i (T_g - T_s) \tag{4.5}$$

$$Q_{latent} = h_{fg} k_g A_i (P_{v,bulk} - P_{v,i}) \tag{4.6}$$

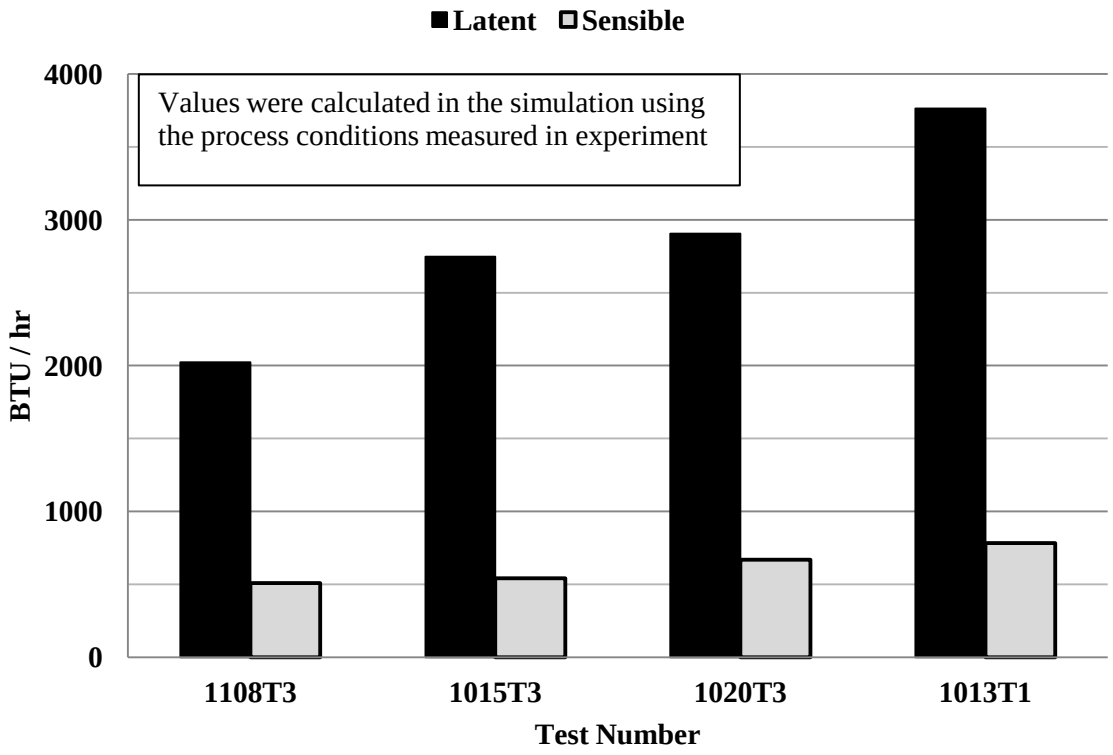

Figure 4.2 - Sensible and latent heat transfer rates for a parametric test with increasing inlet flue gas temperature and moisture concentration.

To observe the effects of just the inlet flue gas temperature the simulation was used and the inlet moisture concentration was kept constant and the inlet flue gas temperature was increased. The process conditions for these simulations were the average of the tests listed in Table 4.1 but with a constant inlet moisture concentration of 6 percent. Shown in Figure 4.3 are simulation

results that show the condensation rate slightly decreased with increased inlet flue gas temperature.

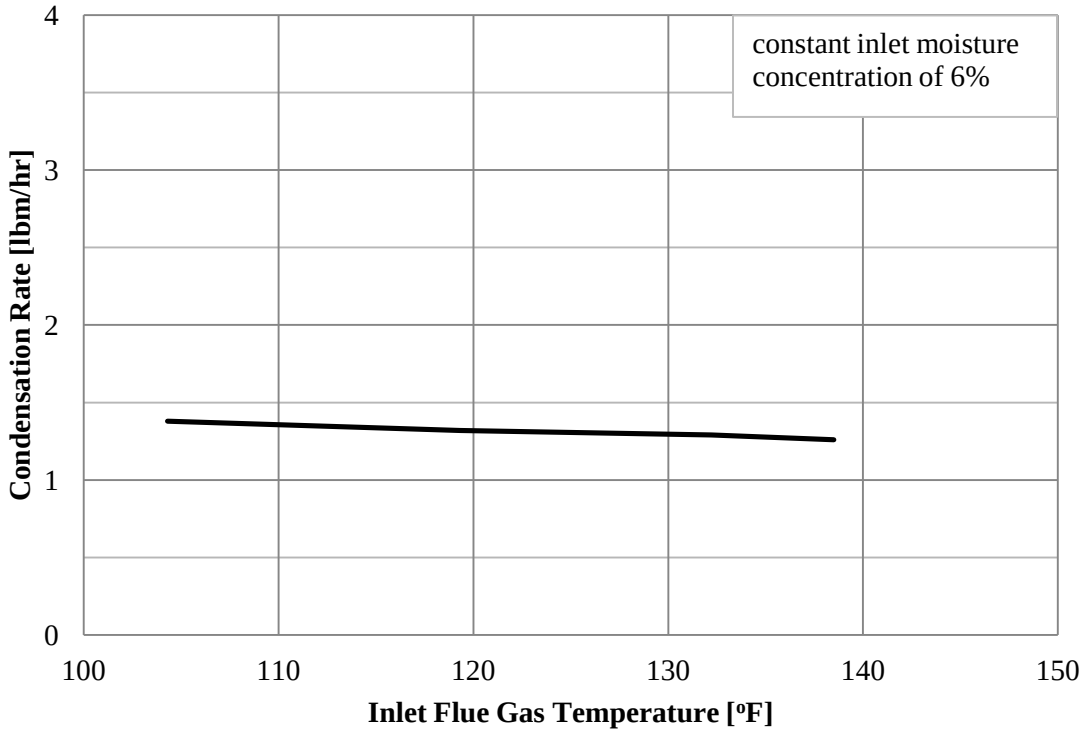

Figure 4.3 – Theoretical predictions for condensation rate versus inlet flue gas temperature.

The explanation for the reduced condensation rates is buried in the complex coupling of sensible and latent heat transfer from flue gas. The Colburn-Hougen equation, explained in Chapter 1 and shown again in Equation 4.7 shows that a balance exists between the sensible and latent heat transfer rates. Raising T_g caused an increased portion of the total heat transfer to be in form of sensible energy, which decreased the condensation rate. This decrease in latent heat transfer rates and increase in sensible heat transfer rates is shown in Figure 4.4.

$$h_g A_g\left(T_g - T_s\right) + h_{fg} k_g A_g\left(P_{v,bulk} - P_{v,i}\right) = h_a A_a (T_s - T_a) \tag{4.7}$$

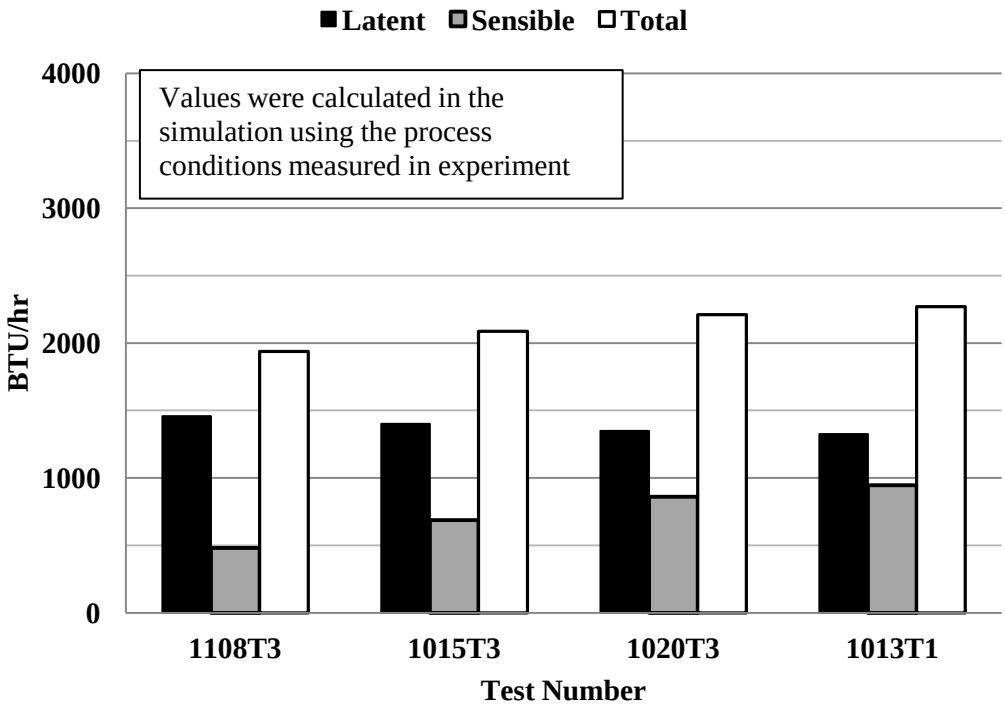

Figure 4.4 – Sensible and latent heat transfer rates for a parametric test with increasing inlet flue gas temperatures.

The explanation for the decreased latent heat transfer rates and increased sensible heat transfer rates is the slight increase in tube wall temperature. Tube wall temperature affects the condensation potential $\left(P_{v,bulk} - P_{v,i}\right)$, and water condensation rates. Figure 4.5 shows the slight increase in tube wall temperature, and Figure 4.6 shows the decrease in the condensation potential $\left(P_{v,bulk} - P_{v,i}\right)$.

To determine whether altering a process condition will increase water condensation rates, one needs to understand how the process condition affects the wall temperature. The benefit to processing a flue gas with a higher inlet temperature is to recover more energy and not more water.

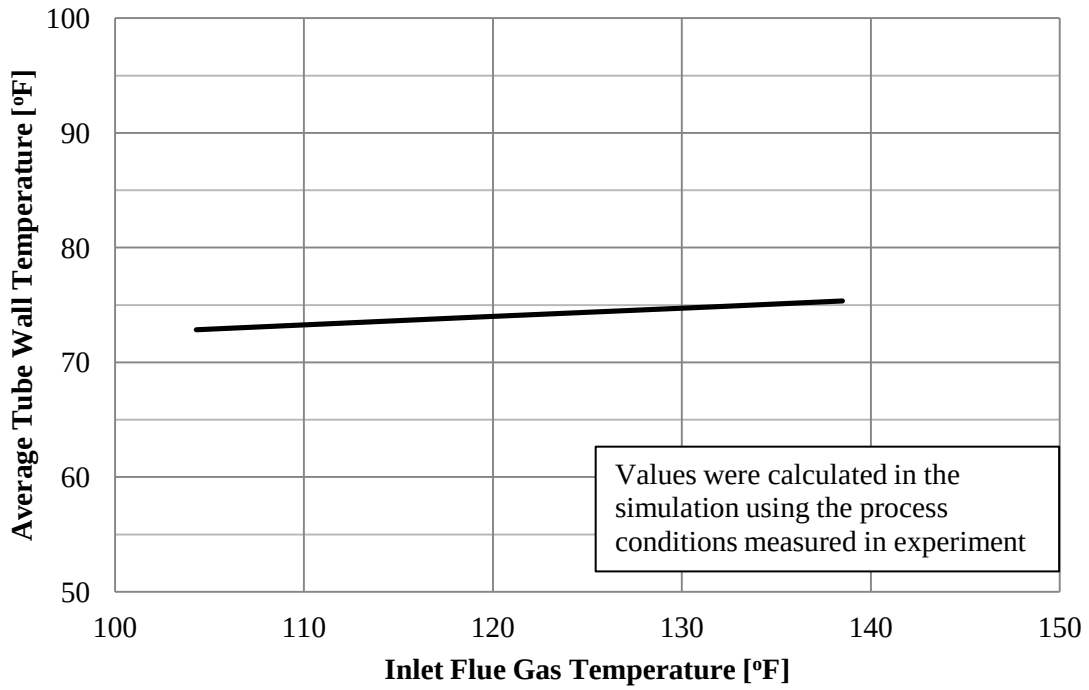

Figure 4.5 – Theoretical predictions for tube wall temperature versus inlet flue gas temperature.

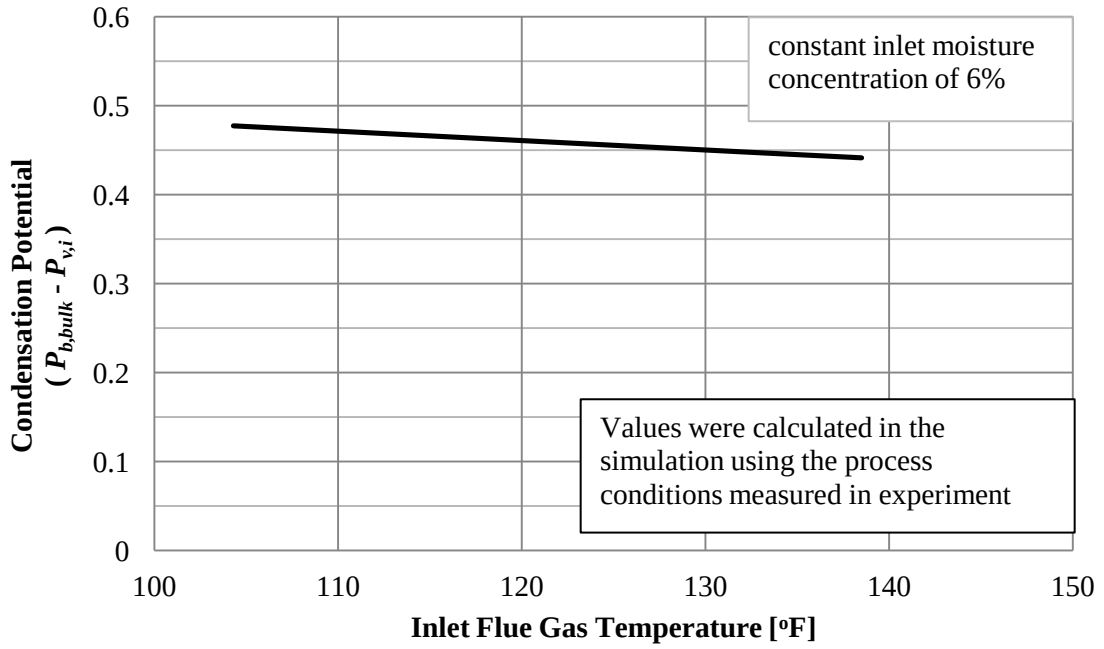

Figure 4.6 – Theoretical predictions for vapor partial pressure versus inlet flue gas temperature.

4.2 Effect of Cooling Air Temperature

Another approach to increase the efficiency of the heat exchanger is to lower the temperature of the cooling air. Decreasing the cooling air temperature creates a larger temperature difference between the heat exchanger tubes and the cooling air $(T_s - T_{air})$, which increases heat transfer (see Equation 4.8).

$$Q = h_g A_o \eta_o (T_s - T_a) \tag{4.8}$$

The following two figures show that the ACC will be more effective when installed at a location where the air is cool (Table 4.2 shows the process conditions for these simulations). Figure 4.7 shows results from the heat and mass transfer simulation for situations involving colder inlet cooling air, and Figure 4.8 shows how the average temperature of the tube wall changed for different inlet cooling air temperatures.

Table 4.2 - Process conditions for simulations that vary inlet cooling air temperature.

Process Conditions	
Inlet Flue Gas Temperature [^{o}F]	**146.4**
Flue Gas Velocity [ft/sec]	**30**
Moisture Concentration [percent wet-basis]	**13**
Cooling Air Velocity [ft/sec]	**30**

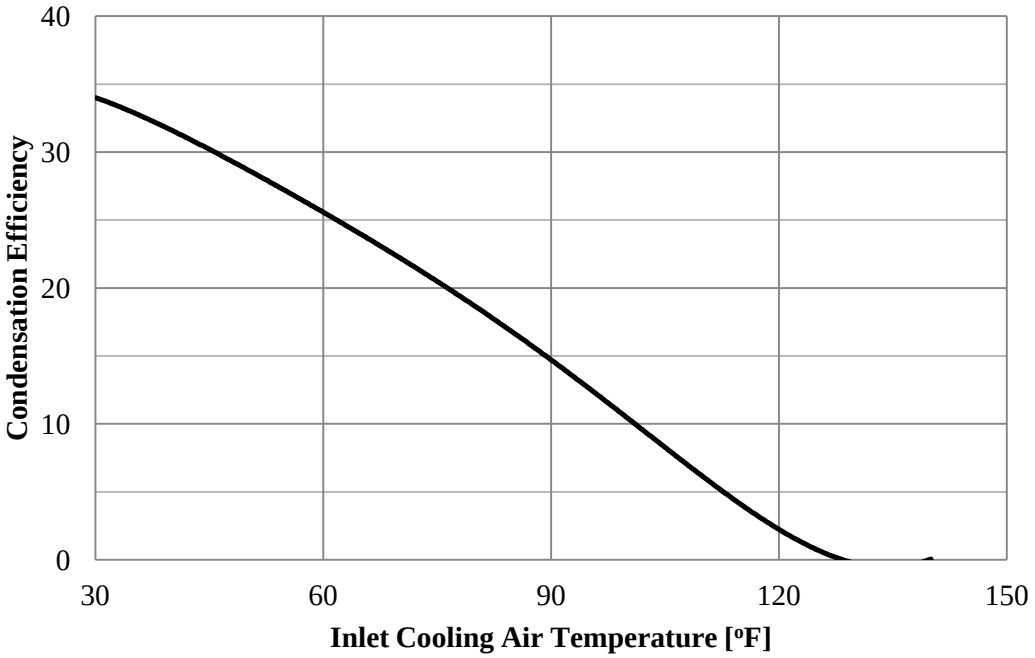

Figure 4.7 – Theoretical predictions for condensation efficiency versus inlet cooling air temperature.

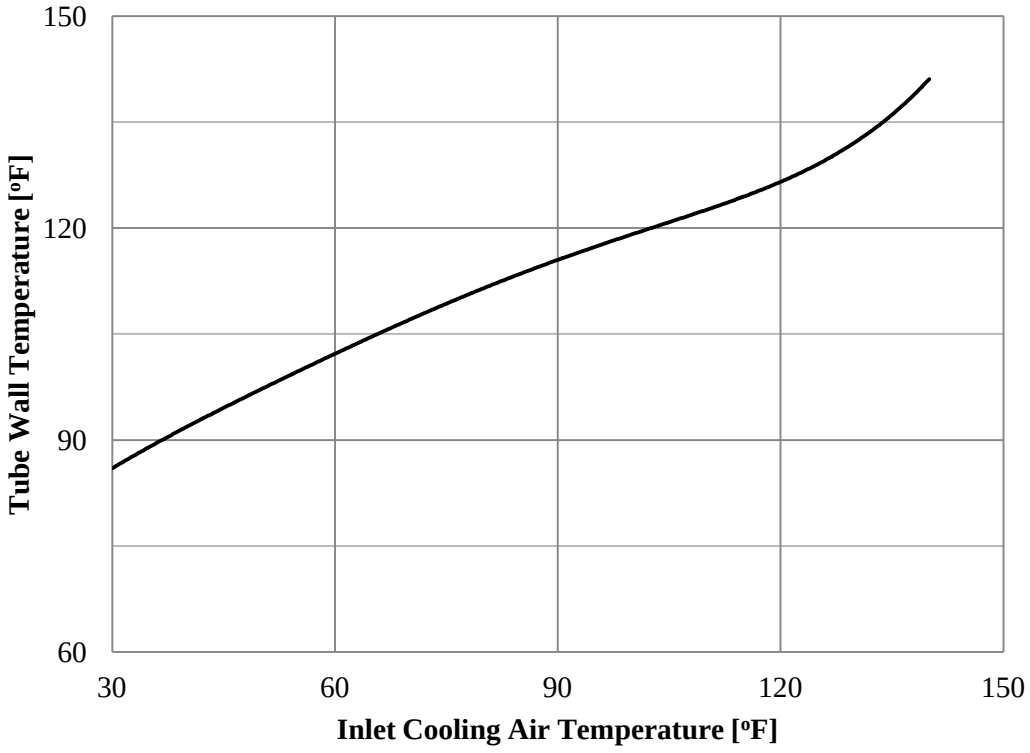

Figure 4.8 – Theoretical predictions for tube wall temperature versus inlet cooling air temperature.

Referring back to Equations 4.1 through 4.4, which describe the vapor condensation process, it was easily seen that lowering the tube wall temperature increased the driving potential for condensation. Figure 4.9 shows the increase in $(P_{v,bulk} - P_{v,i})$ with lower inlet cooling air temperature. This is because $P_{v,i}$ is the saturation pressure at the tube wall temperature, which was proportional to inlet cooling air temperature. The figure also shows the calculated mass transfer coefficient. It can be concluded that lowering the inlet cooling air temperature has a positive effect on the heat exchanger's performance. The increase in heat transfer rate for this parametric test is shown in Figure 4.10.

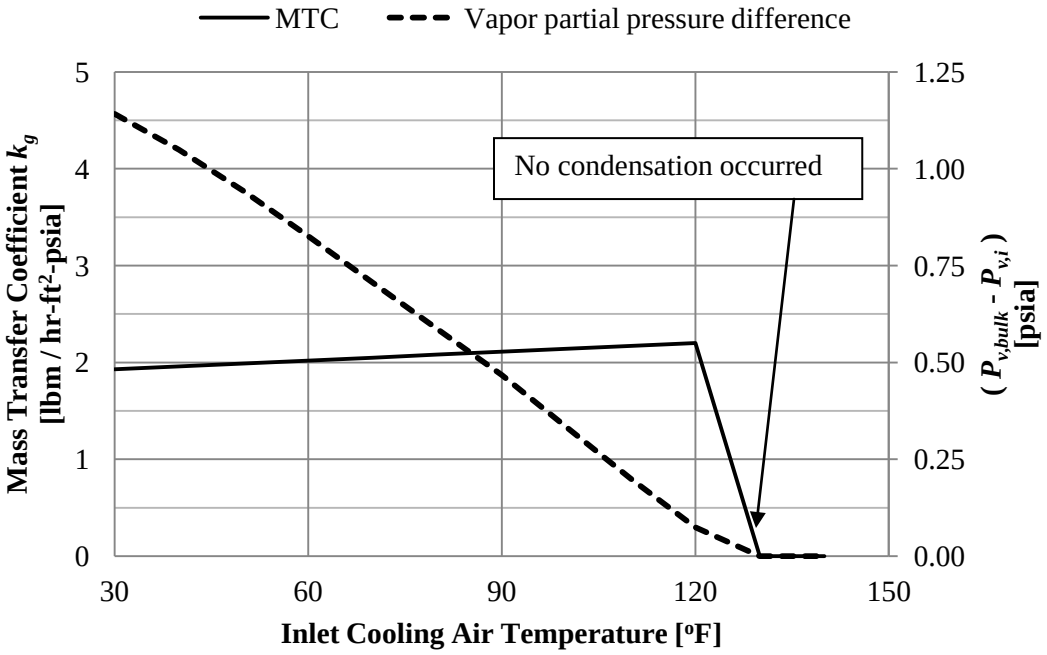

Figure 4.9 – Theoretical predictions for mass transfer coefficient and condensation potential versus inlet cooling air temperature.

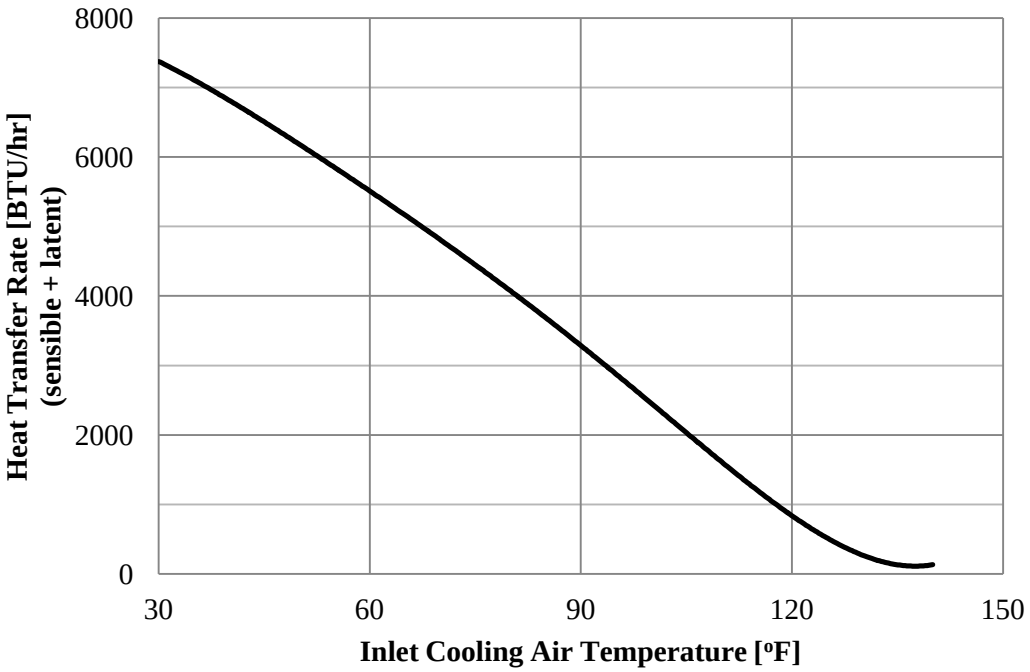

Figure 4.10 – Theoretical predictions for heat Transfer rate versus inlet cooling air temperature.

4.3 Effect of Flue Gas Velocity

Equations 4.1 to 4.4 suggest that increasing the mass transfer coefficient k_g will increase the rate of condensation. However, since k_g is analogous to the heat transfer coefficient, increasing k_g would ultimately require process conditions that increase the heat transfer coefficient. This was tested by increasing the gas-side velocity. The experiment shown in Table 4.3 was a case where flue gas velocity was increased while all other process conditions were held constant, and the results indicate that increasing velocity does not necessarily mean higher rates of water recovery.

The primary effects listed in Table 4.3 were a relatively constant rate of water recovery but a decrease in condensation efficiency. Also, a larger flue gas velocity means the heat exchanger would be smaller because each tube would process more flue gas and Figure 4.11 shows that more heat is recovered as the velocity was increased.

Figure 4.12 shows the increase in heat and mass transfer coefficients for the flue gas. One would expect the heat and mass transfer rates to both increase, but Figure 4.13 shows

Table 4.3 - Data from a parametric test of flue gas velocity.

Test Name	1013t1	1013t2	1013t3	1020t2	1020t1
Flue Gas Velocity [ft/sec]	27.9	38.6	44.5	50.4	59.7
Inlet Gas Temperature [^{o}F]	138.5	139.6	144	140.7	142.3
Inlet Flue Gas Moisture Concentration [% wet-basis]	12.7	12.2	12.4	12	11.2
Incoming Vapor Flow rate [lbm/hr]	11.1	14.7	17.1	18.6	20.4
Water Condensation Rate [lbm/hr]	3.5	3.42	3.53	3.48	3.67
Condensation Efficiency [%]	31.9	23.6	21.0	19.0	18.3
Mass Transfer Coefficient k_q [lbm/hr-ft^2-psia]	1.27	1.46	1.67	1.65	1.99
Gas-side HTC [BTU/hr-ft^2-^{o}F]	7.69	9.95	11.1	12.2	13.9
Air-side HTC [BTU/hr-ft^2-^{o}F]	10.2	10.2	10.2	9.42	9.45
($P_{v,bulk} - P_{v,i}$) [psia]	1.04	0.89	0.80	0.80	0.70

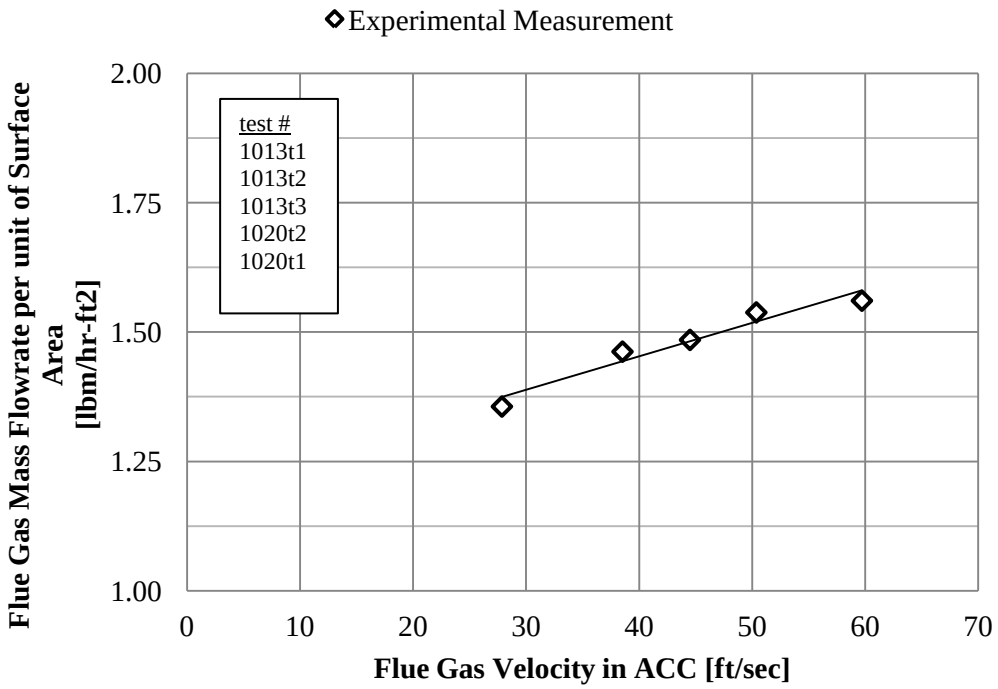

Figure 4.11 – Mass flow rate per unit of surface area versus flue gas velocity (experimental data and curve fit).

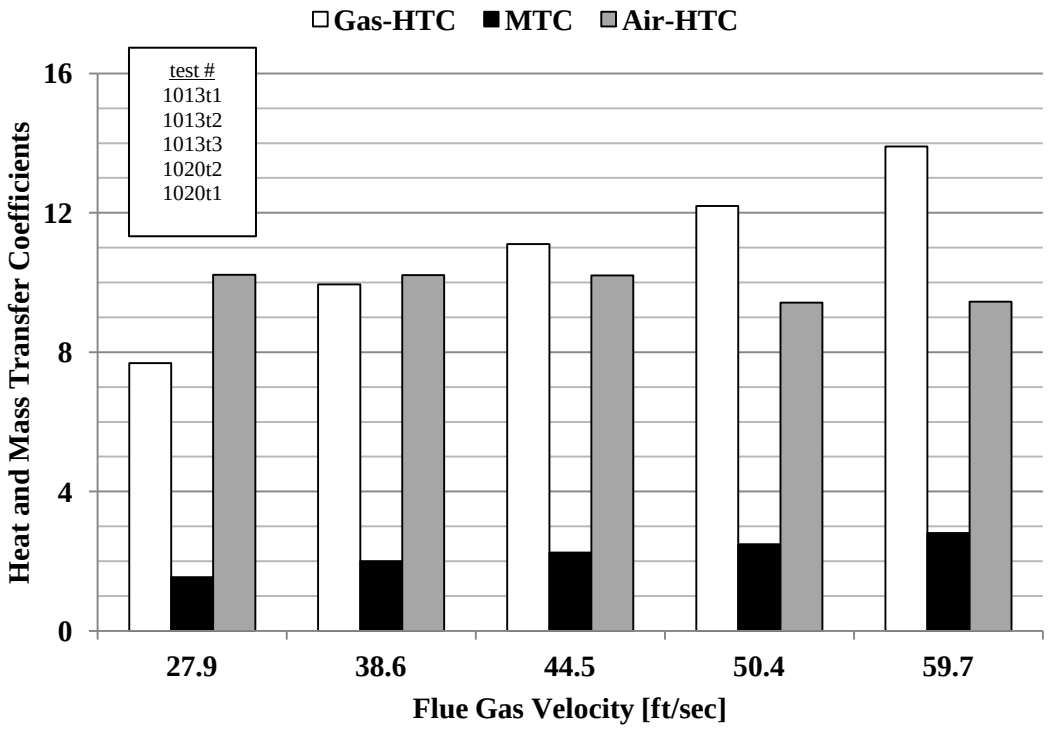

Figure 4.12 - Heat and mass transfer coefficients for various flue gas velocities

Figure 4.13 shows the mass transfer coefficient and vapor partial pressure difference from Equation 4.1. As the flue gas velocity was increased, the condensation efficiency of the ACC decreases because the driving potential for condensation $\left(P_{v,bulk} - P_{v,i}\right)$ decreased. These results underscore the importance of the tube wall temperature in characterizing the performance of the ACC. The data points in Figure 4.13 were obtained using experimental measurements.

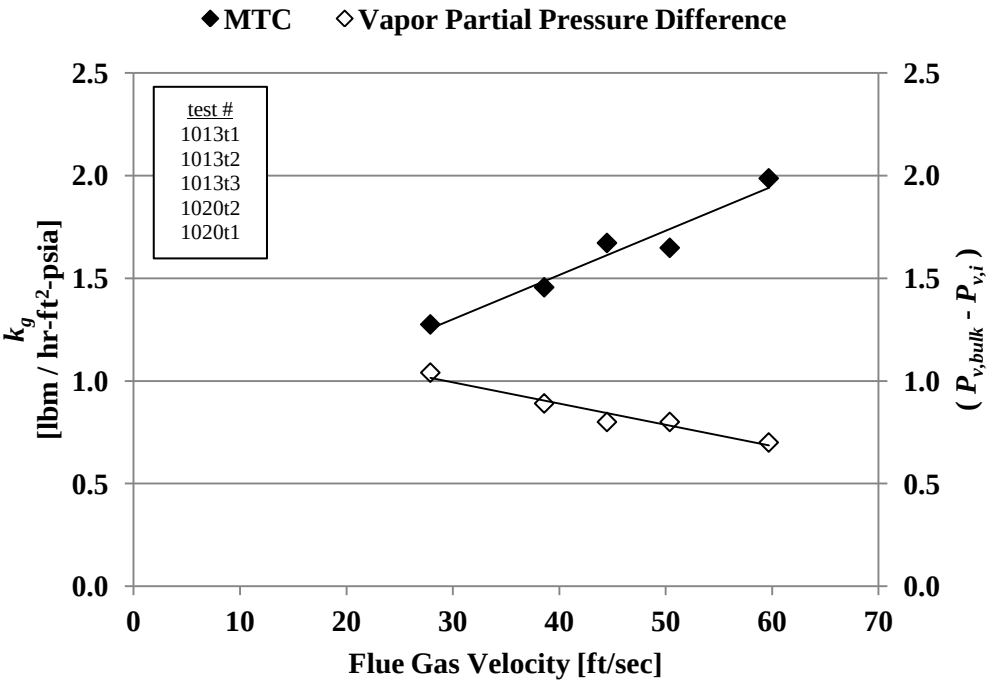

Figure 4.13 - Mass transfer coefficient and condensation potential versus flue gas velocity (experimental data and curve fit).

4.4 Effect of Cooling Air Velocity

The heat and mass transfer simulation was used to determine condensation efficiency when cooling air velocity ranged between 5 and 60 ft/sec. The process conditions used were similar to the experimental conditions described in Chapter 3 and were:

- Inlet flue gas temperature: 137.3 ^{o}F
- Flue gas velocity: 29.8 ft/sec
- Inlet moisture concentration: 13.1%
- Inlet cooling air temperature: 58.6 ^{o}F

It is shown in Figure 4.14 and Figure 4.15 that cooling air velocity and again, tube wall temperature, have a substantial impact on condensation efficiency. Referring back to Equations 4.1 to 4.4, the reason was the lower tube wall temperature decreased the partial pressure of vapor at the tube wall/condensate interface which increased the driving potential for condensation.

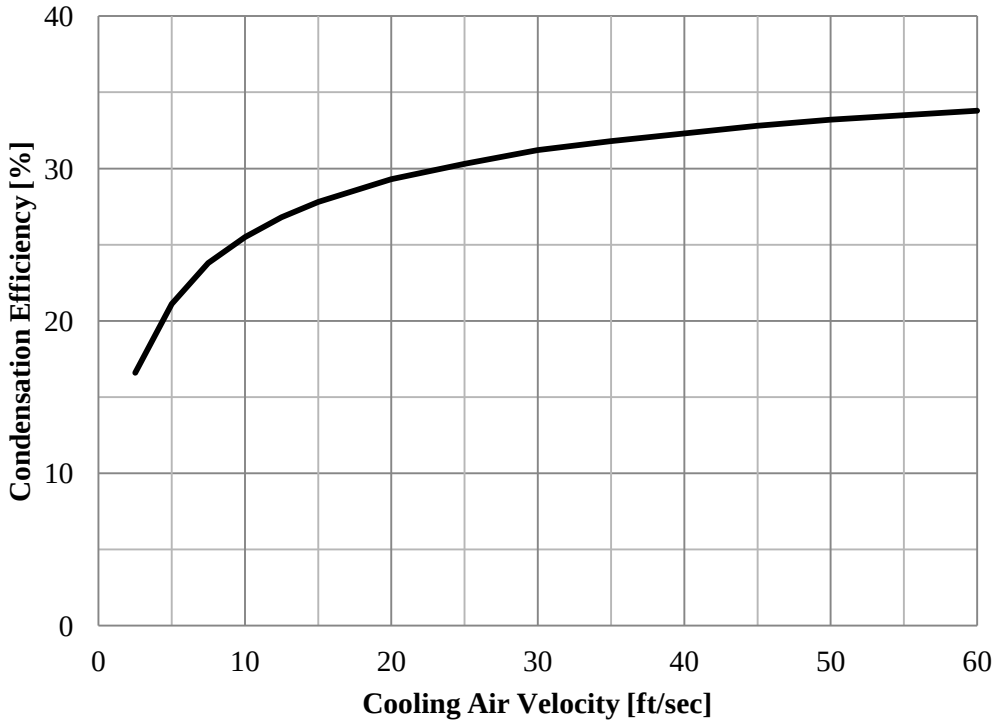

Figure 4.14 – Theoretical predictions for condensation efficiency versus cooling air velocity.

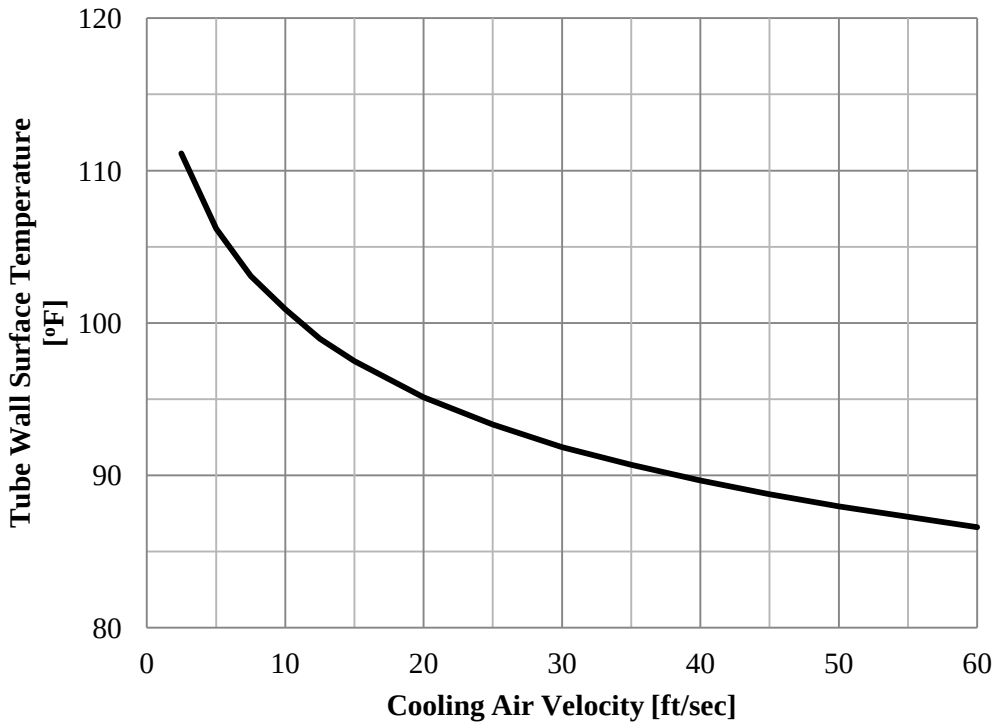

Figure 4.15 – Theoretical predictions for tube wall temperature versus cooling air velocity.

Figure 4.16 shows that the vapor partial pressure difference $\left(P_{v,bulk} - P_{v,i}\right)$ increased, which caused an increase in condensation rate. The mass transfer coefficient k_g decreased slightly, but this was due to a slight decrease in the heat transfer coefficient. Equation 4.4 shows how k_g and h_g are related and Figure 4.17 shows the slight decrease in the heat transfer coefficient, and this decrease was attributed to changing fluid properties due to changes in temperature.

As was shown in experiment, increasing the cooling air velocity increased the total heat transfer rate, and this is shown with results from the simulation in Figure 4.18. Ultimately, increasing cooling air velocity increases condensation rates and heat transfer rates, and this is because the heat transfer coefficient on the air-side h_a is increased, and both the sensible and latent heat potentials are increased on the gas-side $\left(T_s - T_g\right)$ and $\left(P_{v,bulk} - P_{v,i}\right)$.

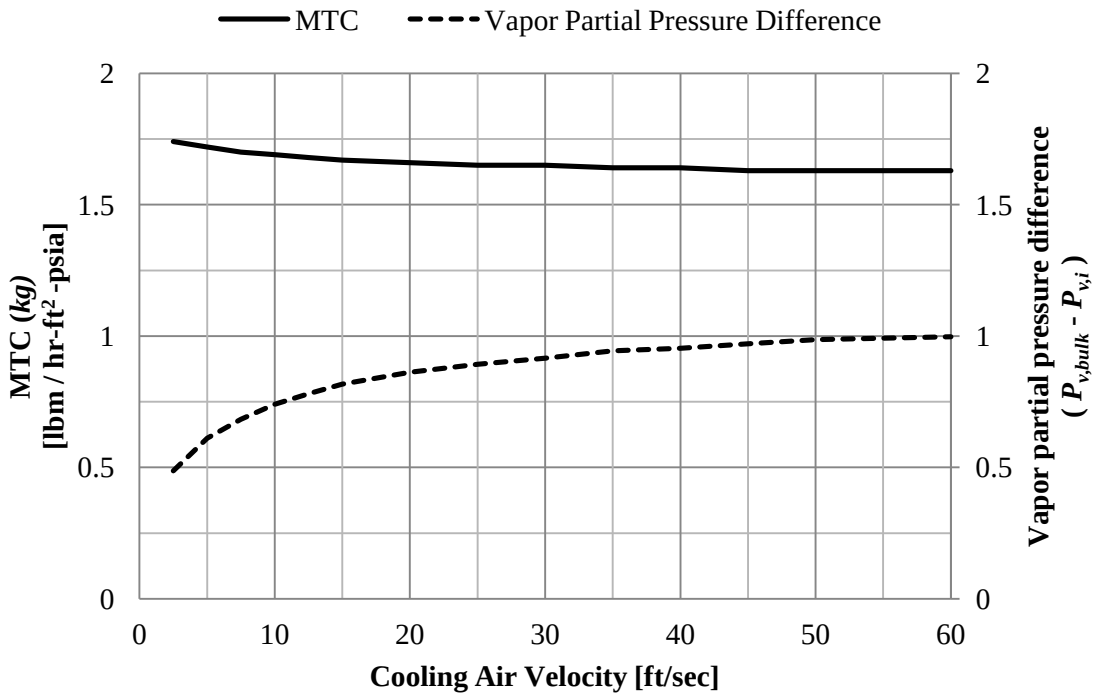

Figure 4.16 – Theoretical predictions for mass transfer coefficient and condensation potential versus cooling air velocity

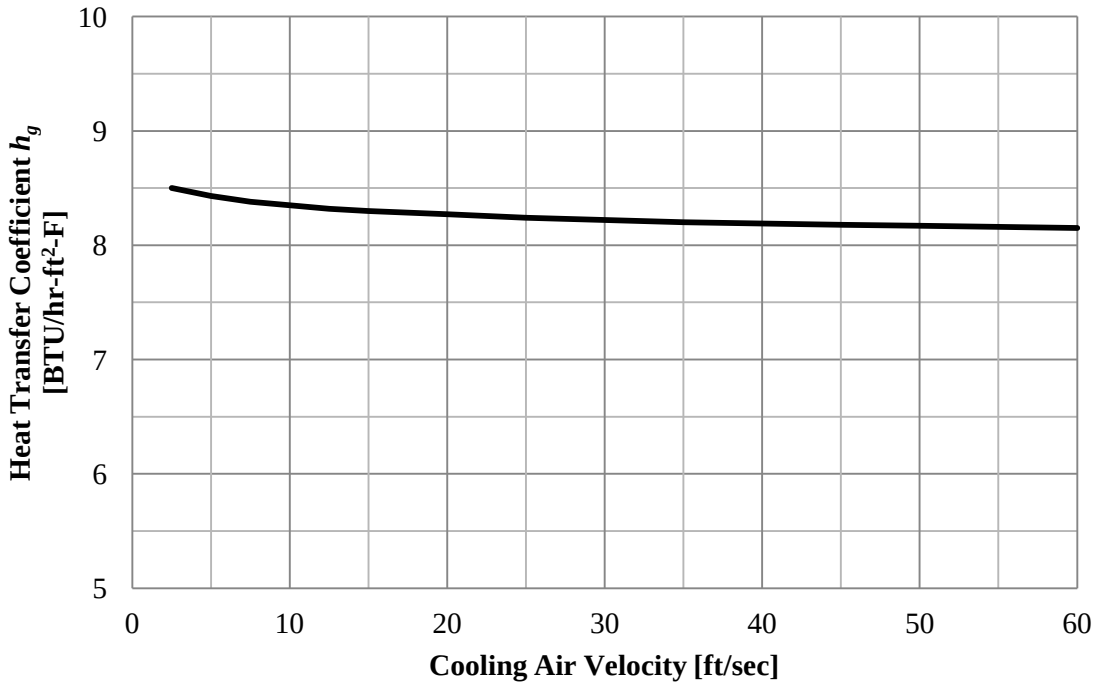

Figure 4.17 – Theoretical predictions for heat transfer coefficient variation for various cooling air velocity.

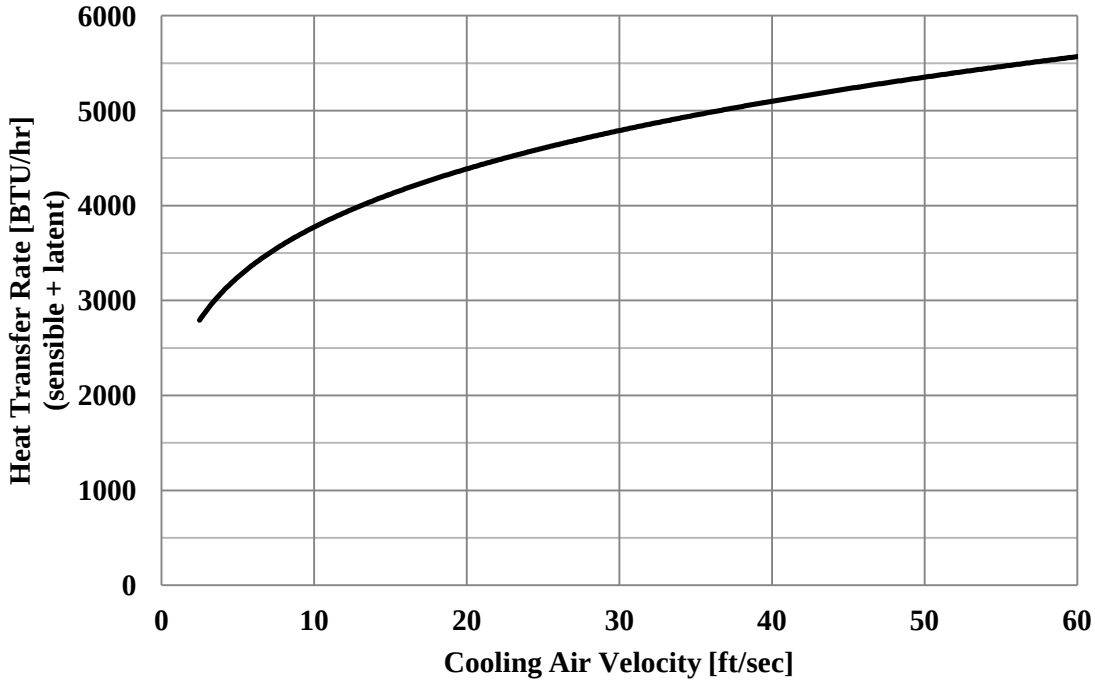

Figure 4.18 – Theoretical predictions for heat transfer rate versus cooling air velocity.

What has been discovered and shown up to this point is the importance of the tube wall temperature in affecting the performance of the ACC. Each process condition affects the tube wall temperature in a different way and it depends on the purpose of the ACC to choose the best process conditions.

4.5 Combined Effect of Increased Cooling Air Velocity and Flue Gas Velocity

The following parametric test listed in Table 4.4 is one where both the gas-side and air-side velocities were increased. Figure 4.19 shows the flue gas and cooling air velocities for this parametric test, and Figure 4.20 shows how this affected the heat transfer coefficients for each test.

Table 4.4 - Data from a parametric test of both cooling air velocity and flue gas velocity.

Test Name	1112t1	1013t2	1106t1	1104t4
Inlet Gas Temperature [^{o}F]	136.4	139.6	141.7	141.7
Flue Gas Flow rate [lbm/hr]	151.2	184.8	196.7	233.4
Flue Gas Velocity [ft/sec]	30.9	38.6	41	48.1
Incoming Vapor Flow rate [lbm/hr]	12.5	14.7	16.8	17.3
Flue Gas Moisture Concentration [% wet-basis]	12.7	12.2	13.2	11.5
Water Condensation Rate [lbm/hr]	2.97	3.42	4.03	4.11
Mass Transfer Coefficient [lbm/hr-ft^2-psia]	1.69	2	2.11	2.35
Gas-side HTC [BTU/hr-ft^2-^{o}F]	8.52	9.95	10.5	11.9
Air-side HTC [BTU/hr-ft^2-^{o}F]	9.7	10.2	11.4	12.2
($P_{v,bulk} - P_{v,i}$) [psia]	0.697	0.655	0.775	0.702
Condensation Efficiency [%]	24.1	23.6	24.4	24.3

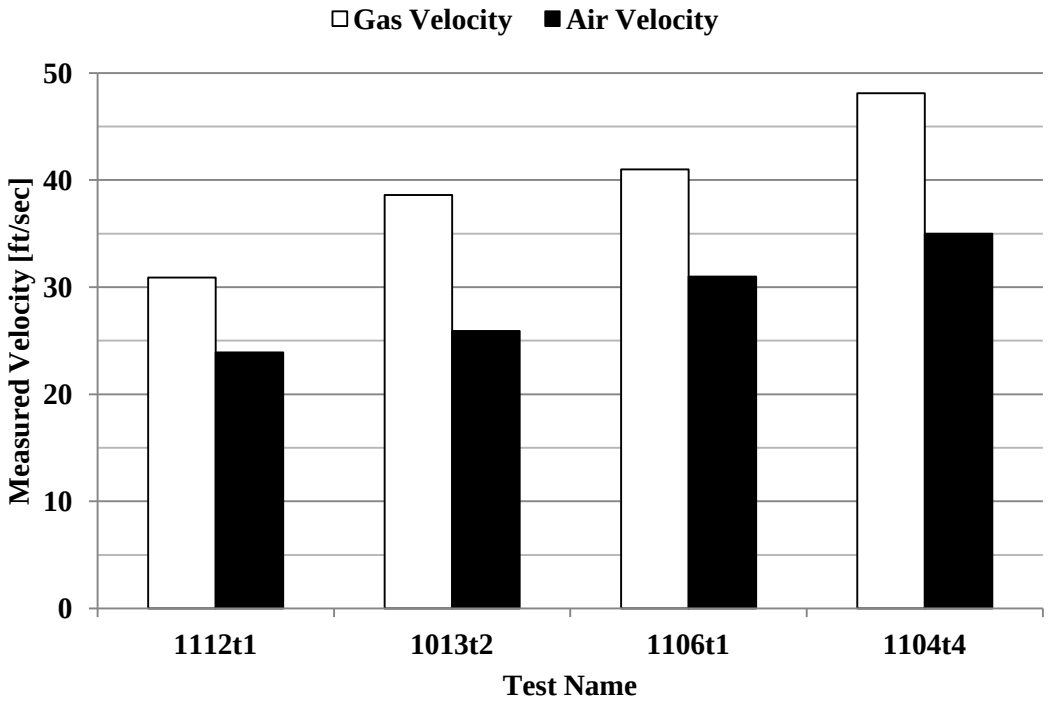

Figure 4.19 - Process conditions for parametric test for increasing both flue gas and air side velocities.

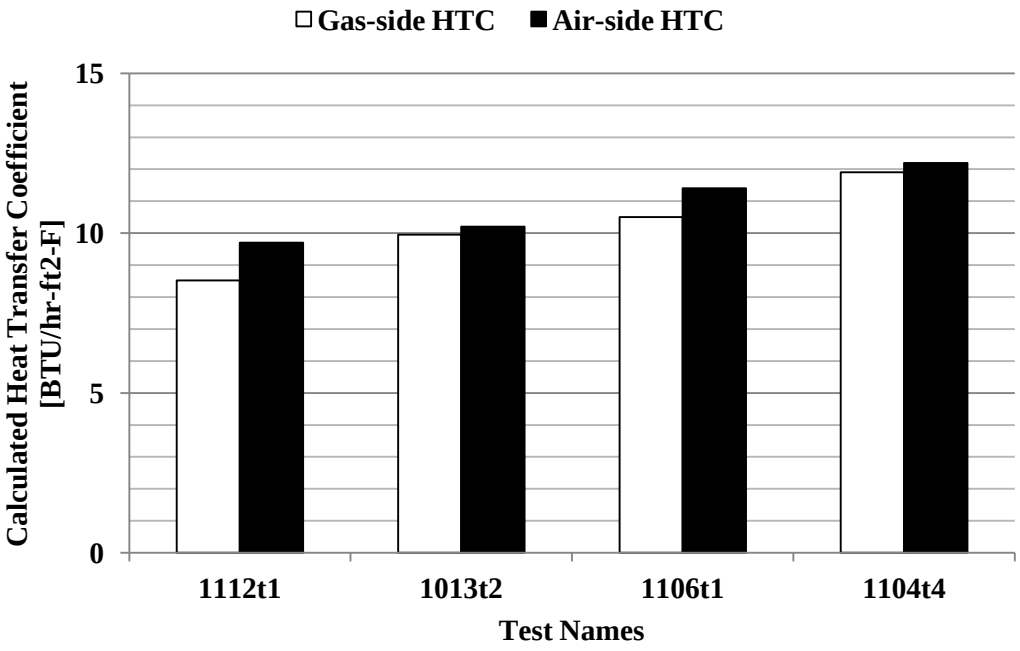

Figure 4.20 - Heat transfer coefficients as cooling air velocity and flue gas velocity were increased.

Figure 4.21 shows how the increased flue gas and cooling air velocities affected the mass transfer coefficient and vapor partial pressure difference. The experimental data in the figure indicates that increasing both cooling air velocity and flue gas velocity simultaneously has a positive impact on both sensible heat transfer and latent heat transfer.

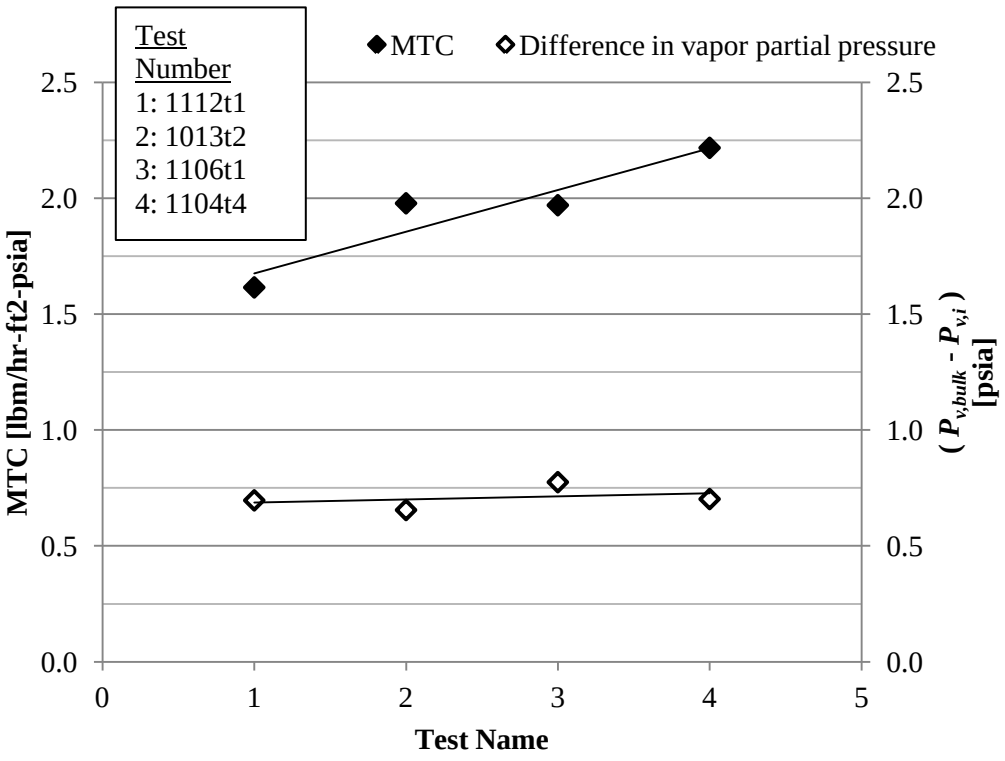

Figure 4.21 - Mass transfer coefficient and condensation potential for tests with varied cooling air and flue gas velocities (experimental data and curve fit).

4.6 Effect of Surface Area

Varying the amount of surface area on the air side has an effect on the resistance to heat transfer. Equation 4.9 is Newton's law of cooling which describes the sensible heat transfer on the air-side of the ACC and it shows that increasing the air-side surface area A_a promotes increased heat transfer.

$$Q_a = h_a A_a (T_s - T_a) \tag{4.9}$$

The surface area can be increased on the air-side by adding more fins. The next graph shows how the condensation efficiency changes due to the addition of more fins. This increase in surface area decreased the heat transfer resistance and lowered the tube wall temperature, which caused greater condensation efficiencies. Figure 4.22 shows the condensation efficiency increase

due to adding more fins, and shows how increasing the air-side surface area decreased the average tube wall temperature.

The process conditions for these experiments are listed in Table 4.5.

Table 4.5 - Process conditions for simulations that varied fin pitch.

Process Conditions	
Inlet Flue Gas Temperature [^{o}F]	**146.4**
Flue Gas Velocity [ft/sec]	**30**
Moisture Concentration [percent wet-basis]	**13**
Cooling Air Velocity [ft/sec]	**30**

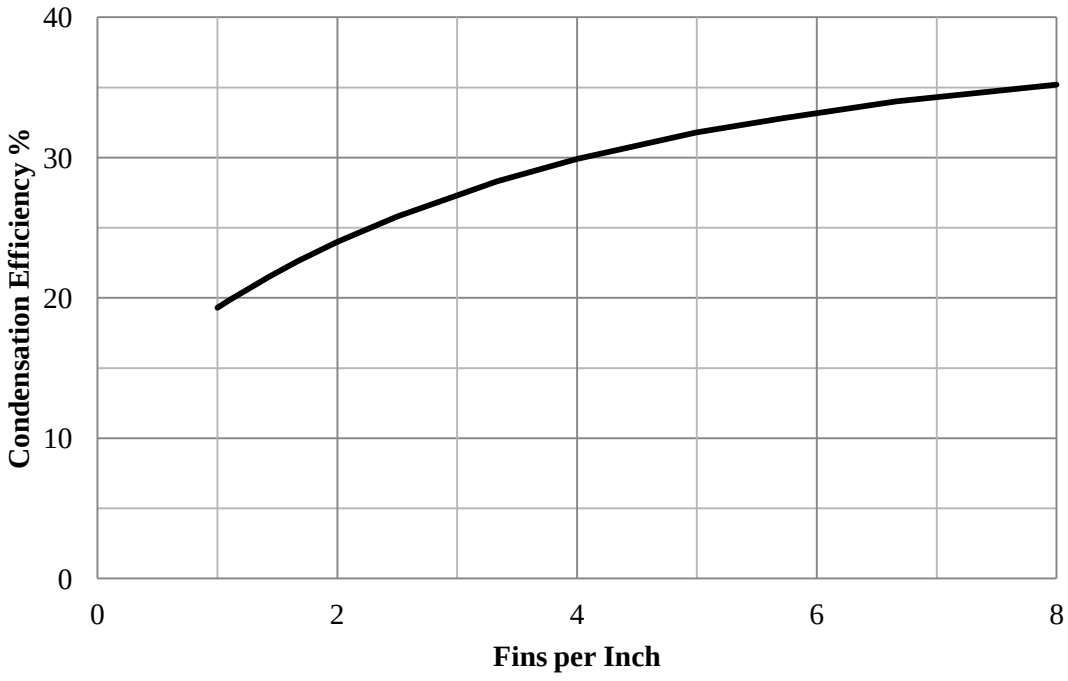

Figure 4.22 – Theoretical predictions for condensation efficiency versus fin pitch.

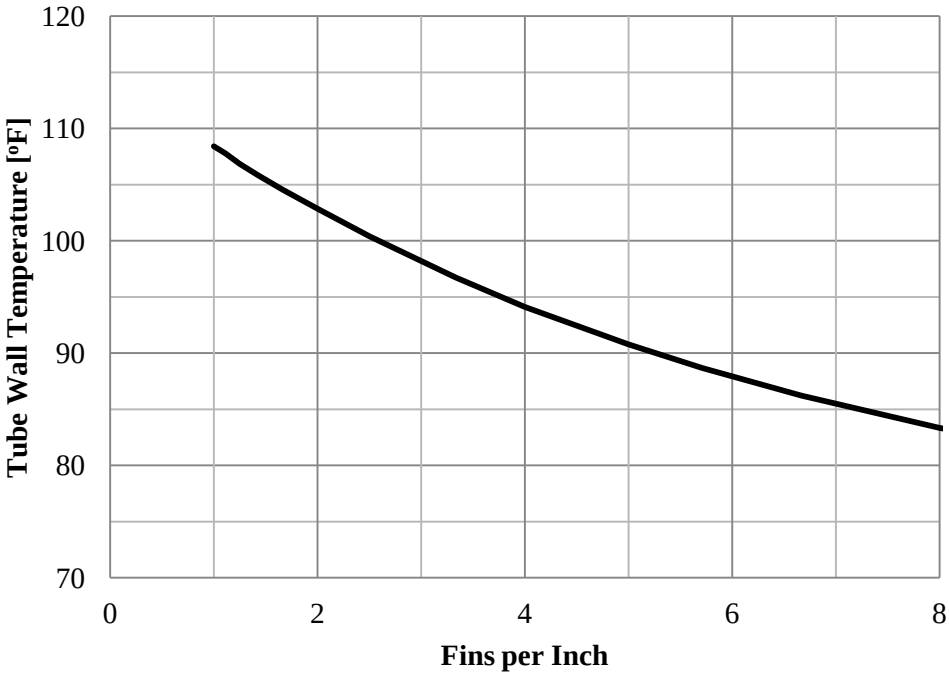

Figure 4.23 – Theoretical predictions for average tube wall temperature versus fin pitch.

5 Design of a Full-Scale Air-Cooled Condenser

The heat and mass transfer simulation described in Chapter 2 was used to size an air-cooled condenser for a power plant. This chapter describes the methodology to determine the size and cost of the full-scale ACC. Also discussed are the effects design variables have on the size and cost of the ACC.

The configuration of the flue gas air-cooled condenser was modeled after a type of air-cooled steam condensers shown in Figure 5.1. These steam condensers have an A-frame construction in which the steam is distributed to the tubes by a header and cooled as it flows downward through the tubes. These systems have a modular design and each module consists of tube banks, a fan, and headers and piping. Because the system has a modular design, different sized systems are built by combining modules. These systems work well as steam condensers in power plants [44] and this was the configuration considered for the flue gas air-cooled condenser.

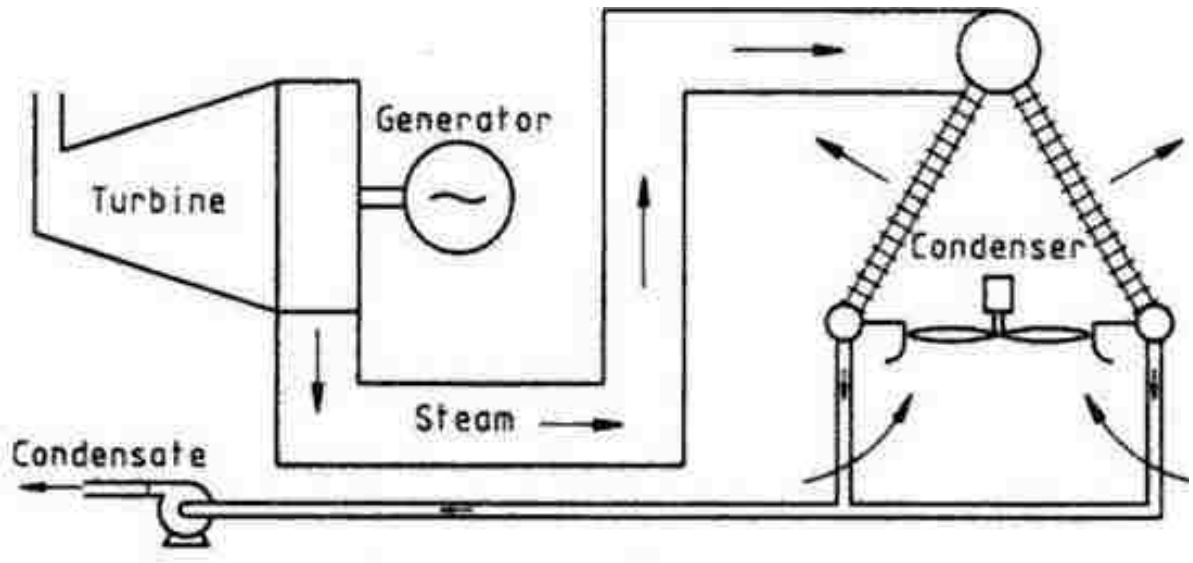

Figure 5.1 - Typical air-cooled steam condenser.

The entire flue gas cooling system consisted of water-cooled and air-cooled condensers, as shown in Figure 5.2. The flue gas was first cooled in the water-cooled condenser then it

flowed through the air-cooled condenser where the majority of the water recovery occurred. Details of the water-cooled condenser can found in Jeong et al. [13-14].

As mentioned, air-cooled condensers are typically a modular design, where a complete system consisted of multiple modules of the same design. Figure 5.3 shows a system which had four modules. The number of modules depended on the flue gas flow rate, the available space to build the ACC, and the flue gas and cooling air temperatures. The factors that affected the size of each module were process conditions and tube and fin geometries, and these design choices are discussed in this chapter.

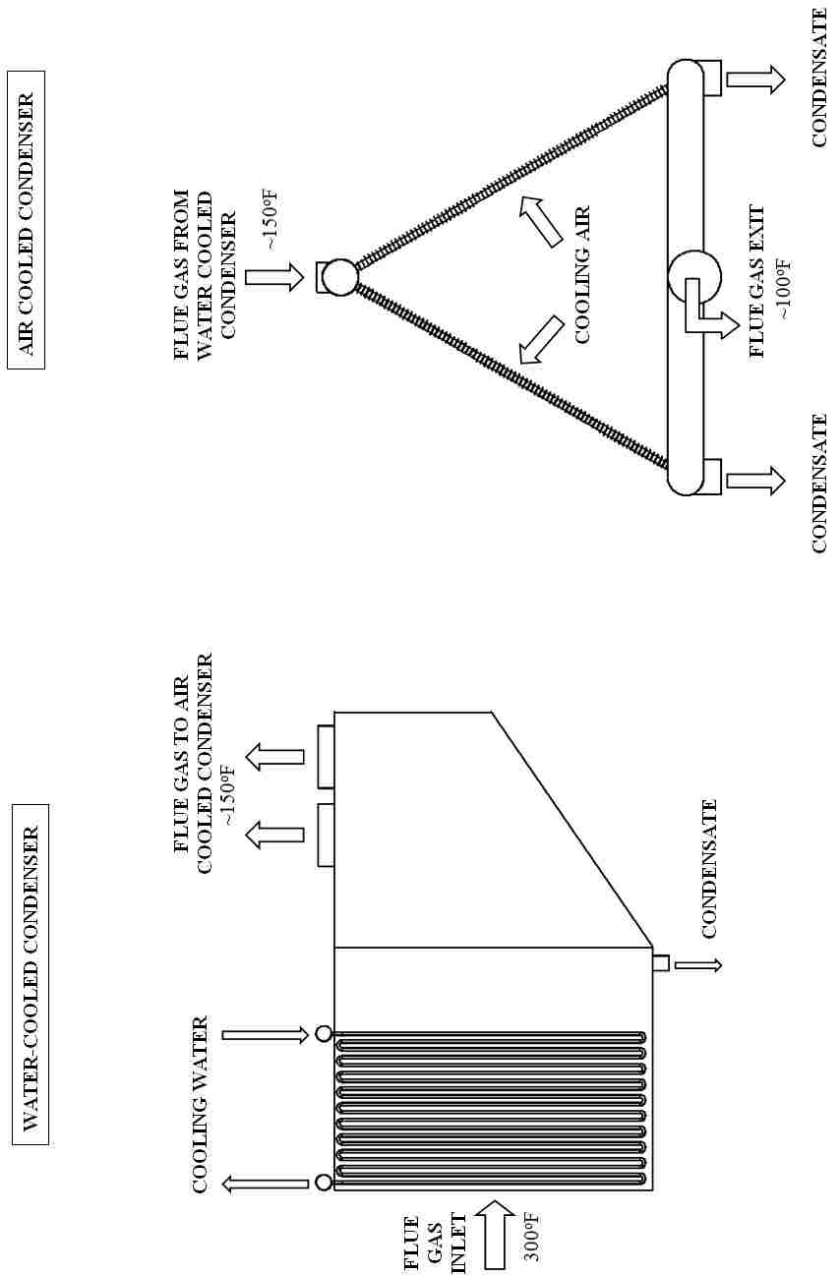

Figure 5.2 - Large scale design configuration of water-cooled and air-cooled flue gas condensers.

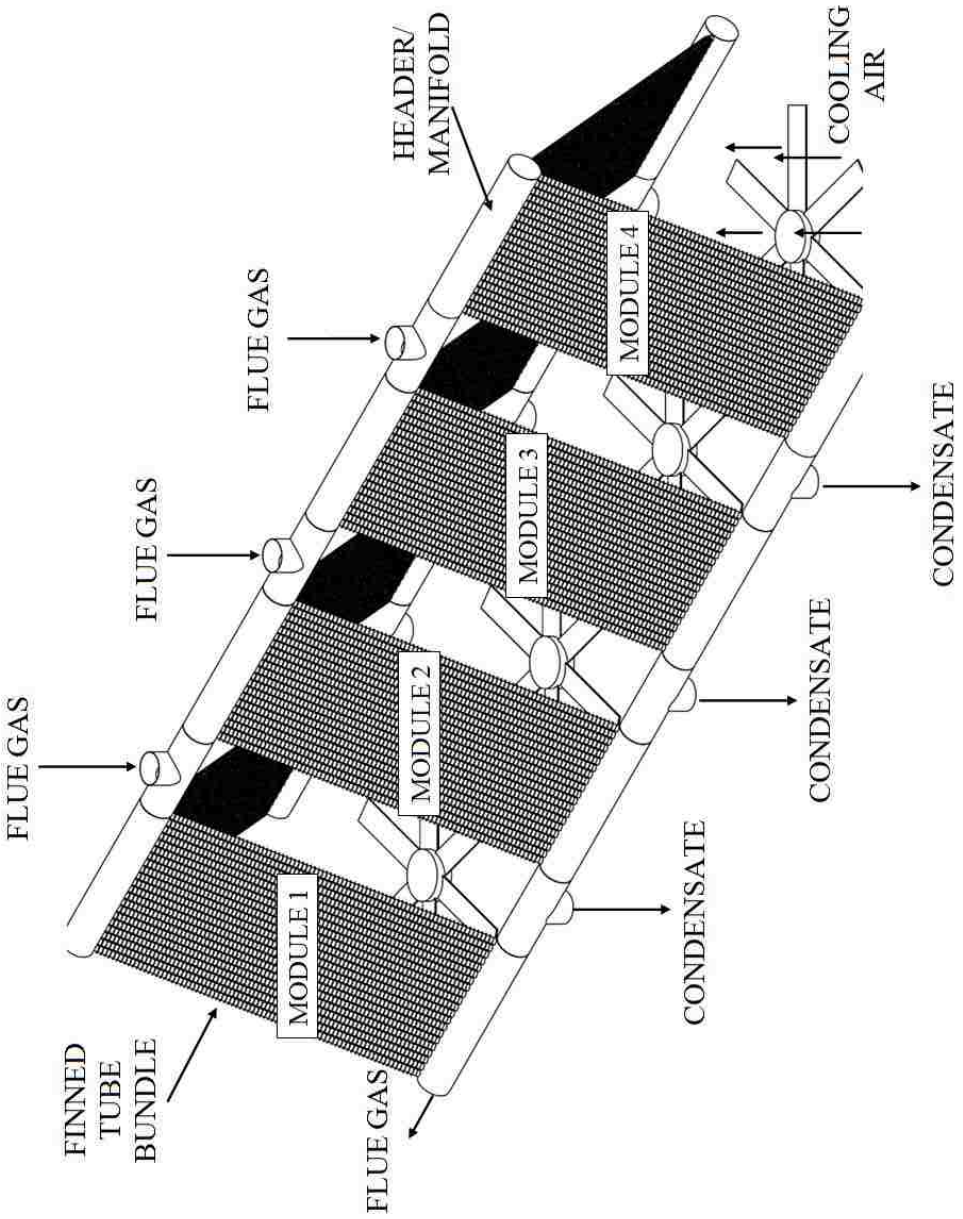

Figure 5.3 - Modular design of the air-cooled condenser.

Section 5.1 discusses the calculation procedure for the size and cost of a full-scale ACC. Section 5.2 describes parametric studies for the design factors, and Section 5.3 discusses the optimal designs.

5.1 Calculation Procedure to Determine the Size and Cost of an Air-Cooled Condenser

The heat and mass transfer simulation described in Chapter 2 simulated a single column of tubes. The size of the ACC was determined by calculating how many columns were necessary to process a specific flue gas load.

To size an ACC, the designer must choose the flue gas velocity and tube diameter. The flue gas flow rate for each tube can be calculated using Equation 5.1.

$$\dot{m}_{g,single\ tube} = \rho_g V_g CSA_{single\ tube} \tag{5.1}$$

where $CSA_{single\ tube}$ is the flow cross sectional area of one heat exchanger tube. The number of tubes for the ACC system can be calculated with Equation 5.2.

$$tubes = {\dot{m}_{g,total}}\Big/{\dot{m}_{g,single\ tube}} \tag{5.2}$$

By choosing the tube diameter and flue gas velocity, one can estimate how many tubes will be necessary for the heat exchanger. A typical 550 MW power plant has a flue gas flow rate of approximately 5,500,000 lbm/hr and Figure 5.4 shows the number of tubes needed to process the flue gas depending on flue gas velocity (inner tube diameter of 4 inches).

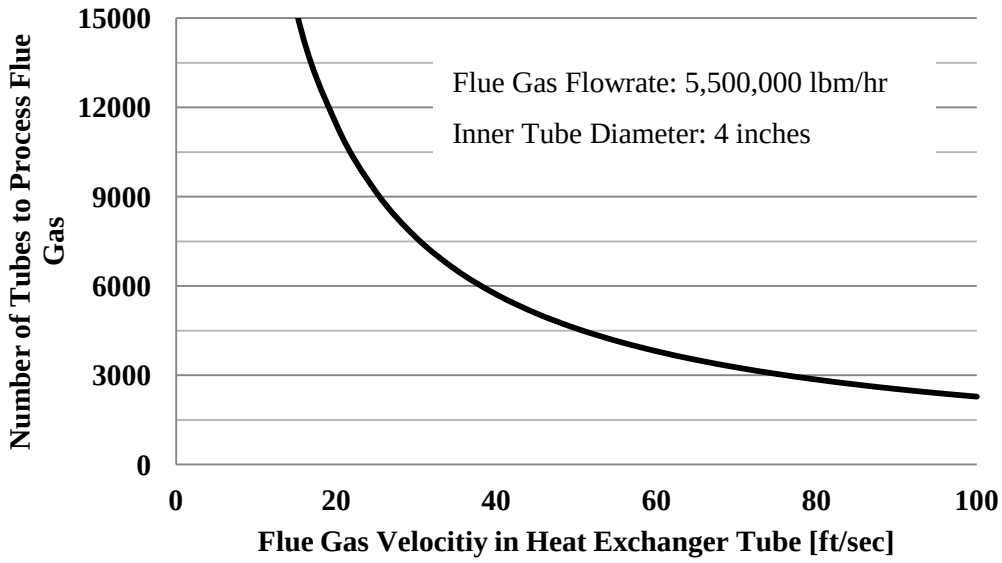

Figure 5.4 - Number of tubes in ACC for different flue gas velocities.

As shown in Figure 5.3, the tubes are placed in bundles, which are installed in modules. In Figure 5.3, each module hosts two tube bundles. The number of tube bundles can be determined by estimating the width of a bundle, choosing the transverse tube spacing, and the number of rows of tubes. For example, Table 5.1 is one possible layout of an ACC. Figure 5.5 and Figure 5.6 indicate what is a module, bundle, and tube row to correspond with Table 5.1.

Table 5.1 - Example configuration of a full-scale ACC.

Flue Gas Flow rate	5,500,000 lbm/hr
Flue Gas Velocity	40 ft/sec
Outer Tube Diameter / Fin Length	4 inches / 1 inch
Number of Tubes	4800
Transverse Tube Spacing [S_t] ($Tube\ Dimater + 2 * Fin\ Length$)	6 inches
Bundle Width	20 feet
Tubes per Row in a Bundle	40
Number of Tube Rows per Bundle	4
Number of Tubes per Bundle	160
Number of Tube Bundles	30

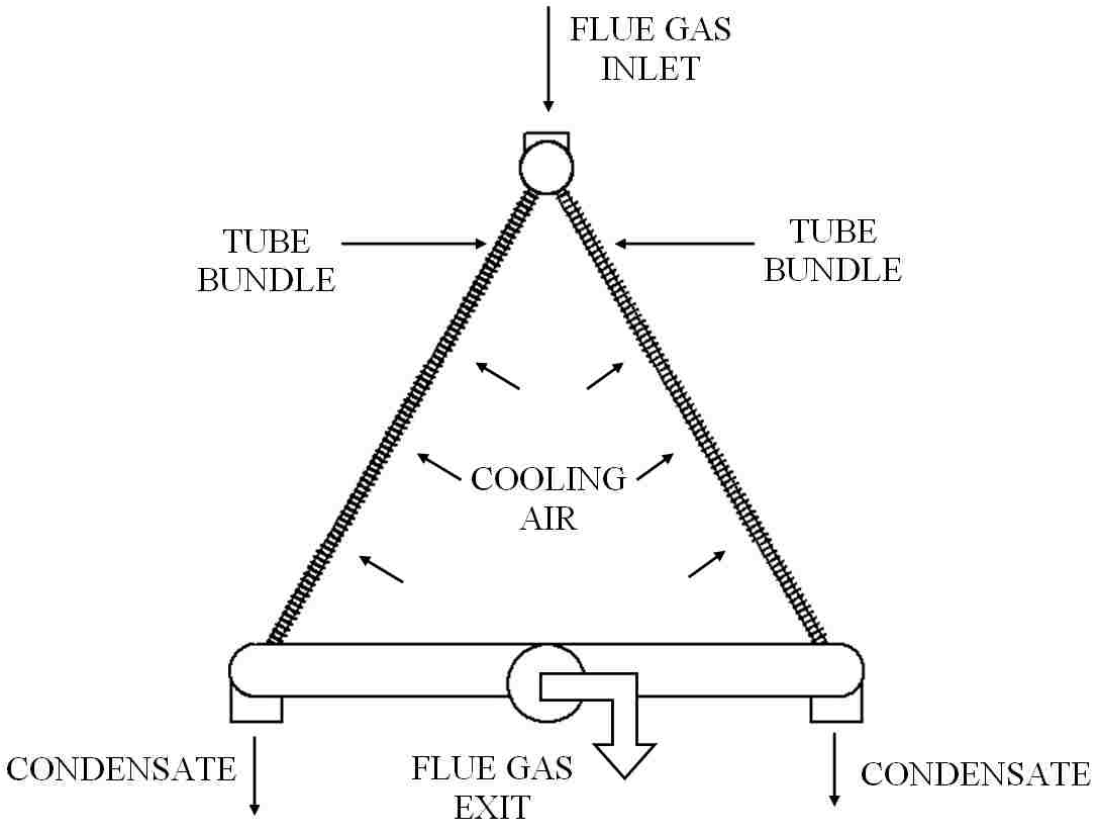

Figure 5.5 - Schematic of 1 module of the ACC which has 2 tube bundles and 1 row of tubes in each bundle.

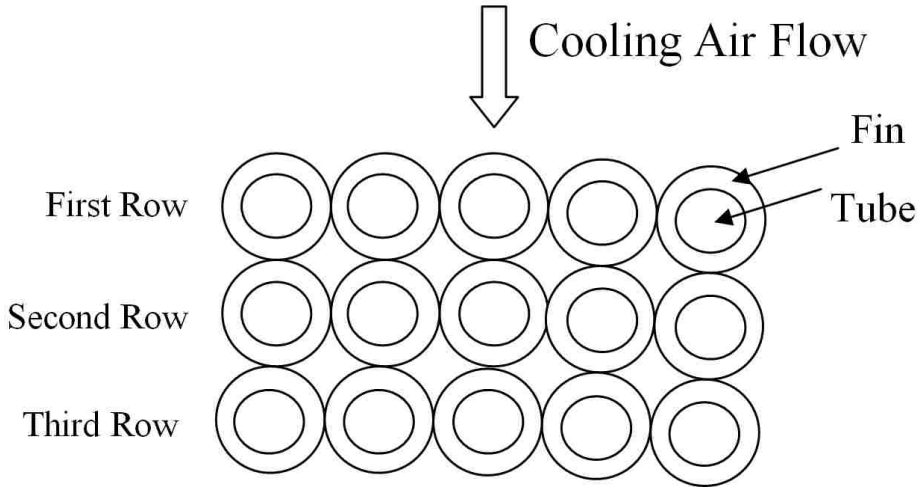

Figure 5.6 - Top view of a tube bundle which has 3 rows of tubes.

As shown in the Literature Review, the capital cost of the ACC was determined from Guthrie [64] using the gas-side surface area of the ACC. The following calculation procedure estimates the net annual cost of the ACC.

1. Calculate the number of tubes necessary to process the flue gas using Equation 5.2.
2. Calculate the length of tube necessary to condense the desired amount of water.
3. Calculate the surface are of the ACC using the tube and fin geometry.
4. Calculate installed capital cost of the ACC using the capital cost correlations from Gurthrie [64], or an alternative cost correlation from Smith [62] or Clerk [63]. Guthrie's is Equation 5.3.

$$Capital\ Cost_{1968} = 78.0(Surface\ Area)^{0.8} \tag{5.3}$$

5. Use *Chemical Engineering* indexes to determine the present value of the installed cost.

$$Capital\ Cost(year\ 2009) = Capital\ Cost(year\ 1968) * \frac{Index(year\ 2009)}{Index\ (year\ 1968)} \tag{5.4}$$

6. Determine the annualized installed capital cost of the ACC using Equation 5.5.

$$Cost_{annualized} = Cost_{capital} * \frac{i(1+i)^n}{(1+i)^n - 1} \tag{5.5}$$

7. Determine the annual operating costs of the ACC by assuming the contributions are from powering the air-side fans and the additional loads on the flue gas fans. The isentropic relation was used to calculate the fan power (Equation 5.6). Then it was assumed that the cost of electricity was \$0.05 per kilowatt-hour, and the plant operated for 7000 hours per year. The annual operating cost to operate the air-side fan and gas-side fan were calculated using Equation 5.7.

$$\mathbb{P} = k\Delta P \frac{\dot{m}_{g,total}}{\rho_g} \frac{1}{\eta_{fan}}$$

$$k = \frac{\gamma}{\gamma - 1} \frac{\left(\frac{P_2}{P_1}\right)^{\left(\frac{\gamma-1}{\gamma}\right)}}{\frac{P_2}{P_1} - 1} \tag{5.6}$$

$$Operating\ Cost_{fan} = \mathbb{P} * 7000\ \frac{hrs}{yr} * \frac{\$0.05}{kW - hr} \tag{5.7}$$

8. The annual savings due to recovering water were calculated from the water condensation rate and the fuel savings rate. In the simulations it was assumed that water cost $1.50 per 1000 gallons and fuel cost $50 per ton.

$$Operating\ Savings = \dot{m}_{condensate} * 7000 \frac{hrs}{yr} * \frac{\$1.50}{1000\ Gallons} \tag{5.8a}$$

$$Operating\ Savings = \dot{m}_{fuel\ savings} * 7000 \frac{hrs}{yr} * \frac{\$50}{ton} \tag{5.8b}$$

9. The net annual cost of the air-cooled condenser was calculated using Equation 5.9.

$$\begin{aligned} &Net\ Annual\ Cost \\ &= Capital\ Cost_{annualized} + Operating\ Cost_{fans} \\ &- Operating\ Savings \end{aligned} \tag{5.9}$$

5.2 Parametric Study for the Design of the Air-Cooled Condenser

The process conditions and tube and fin geometry design choices are listed in Table 5.2. This section discusses how each affects the size and cost of the ACC. This information was generated using the heat and mass transfer simulation and parametrically varying the parameters in Table 5.2.

Table 5.2 - Factors included in the parametric studies of ACC design.

Design Parameters		
Flue Gas Velocity	**Fin Pitch**	**Tube Diameter**
Flue Gas Temperature	**Fin Length**	**Transverse Tube Spacing**
Cooling Air Velocity	**Fin Thickness**	**Number of Tube Rows**
Cooling Air Temperature	**-**	**-**

For the simulations in this section, the flue gas flow rate and moisture concentration are listed in Table 5.3. The flue gas flow rate is typical for power plants in the 600 MW range and the moisture level of flue gas can range from 6 to 15 volume percent depending on the coal rank. In experiments performed at power plants by Jeong et al. it was not uncommon to have moisture concentrations of 11 percent. An 11 percent moisture concentration translates to approximately 400,000 lbm/hr of water vapor for a typical 600 MW power plant.

Table 5.3 - Flue gas flow rate for parametric simulations.

Flue gas flow rate [lbm/hr]	6,000,000
Moisture concentration [% wet basis]	11
Moisture flow rate [lbm/hr]	400,000

Table 5.4 provides the nominal values for these simulations. The length of the heat exchanger tubes was determined by the condensation efficiency. The tubes were the necessary length to condense 50% of the incoming water vapor, or approximately 200,000 lbm/hr. The 50% value for condensation efficiency can be any value, depending on the desired water recovery. There was no particular reason for 50% in this study.

Table 5.4 – Nominal conditions for full-scale simulations.

Inlet Flue Gas Temperature [^{o}F]	135^{o}F
Flue Gas Velocity [ft/sec]	40
Inlet Cooling Air Temperature [^{o}F]	75^{o}F
Air Velocity between Tubes [ft/sec]	30
Condensation Efficiency (see Equation 2.6)	50%
Number of tube rows in heat exchanger banks (See Figure 5.6)	3
Tube Inner Diameter [inches]	4
Tube Outer Diameter [inches]	4.4
Fin Pitch [inches]	0.25
Fin Length [inches]	1.0
Fin Thickness [inches]	0.0625
Transverse Tube Spacing [inches]	6.4

Tube diameter was the first parameter that was varied and Figure 5.7 shows how changing the tube diameter had an effect on how long the tube must be to condense 50 percent of the water vapor from the flue gas. The figure shows it is impractical to design an ACC with a tube diameter greater than four inches (for the conditions in Table 5.4) because the tubes would be over 35 feet long.

In Figure 5.8 the gas-side surface area is plotted against increasing inner tube diameter. The graph shows that for these particular process conditions the surface area ranges from roughly 130,000 ft^2 to 300,000ft^2. The heat exchanger condensed 50% of the moisture, which is 200,000 lbm/hr. At $1.50 per 1000 gallons of water, the water savings were $242,000. The operating costs and annualized net annual costs varied with tube diameter and this is shown in Figure 5.9. The three costs, annualized capital cost, operating costs, and annual savings are summed and plotted in Figure 5.10.

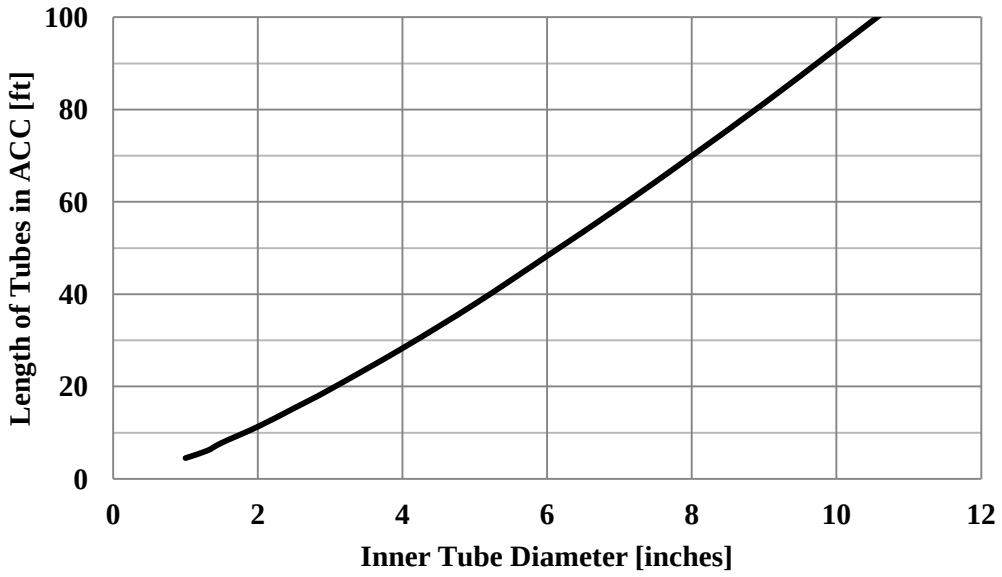

Figure 5.7 – Length of heat exchanger tubes versus inner tube diameter for flue gas inlet temperature of 135°F.

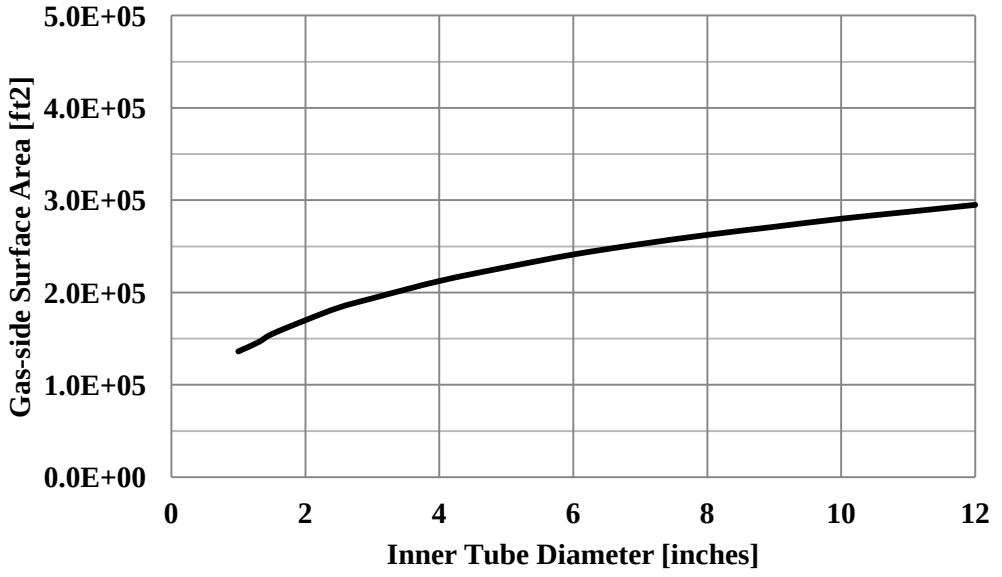

Figure 5.8 – Gas-side surface area versus inner tube diameter for flue gas inlet temperature of 135°F.

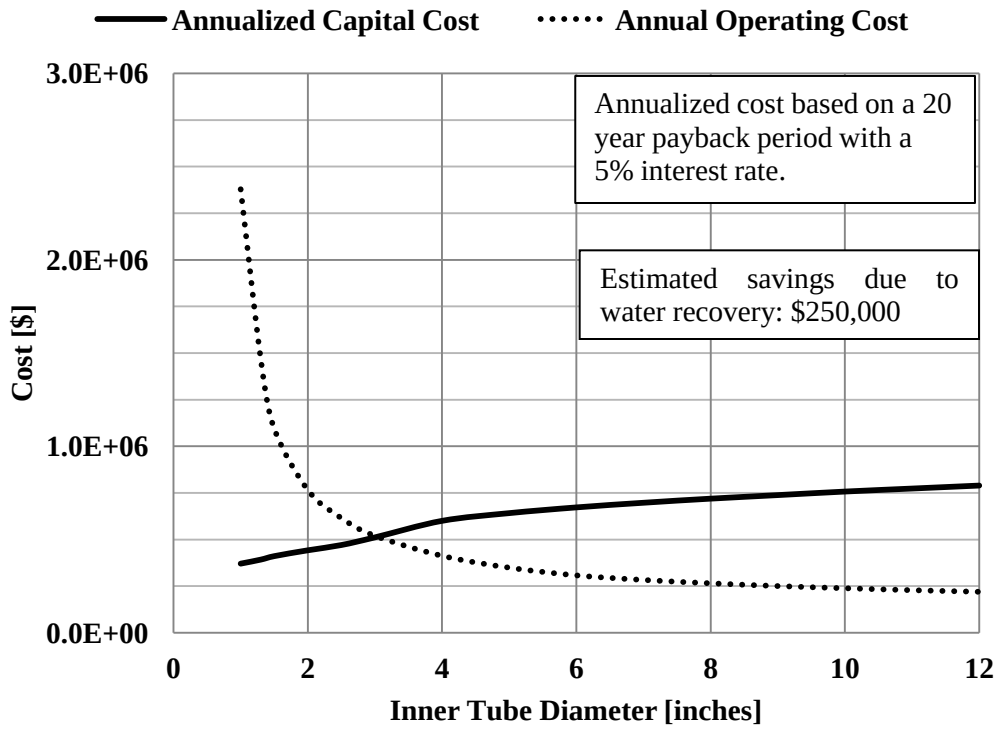

Figure 5.9 – Annual costs of ACC versus inner tube diameter for inlet flue gas temperature of 135°F.

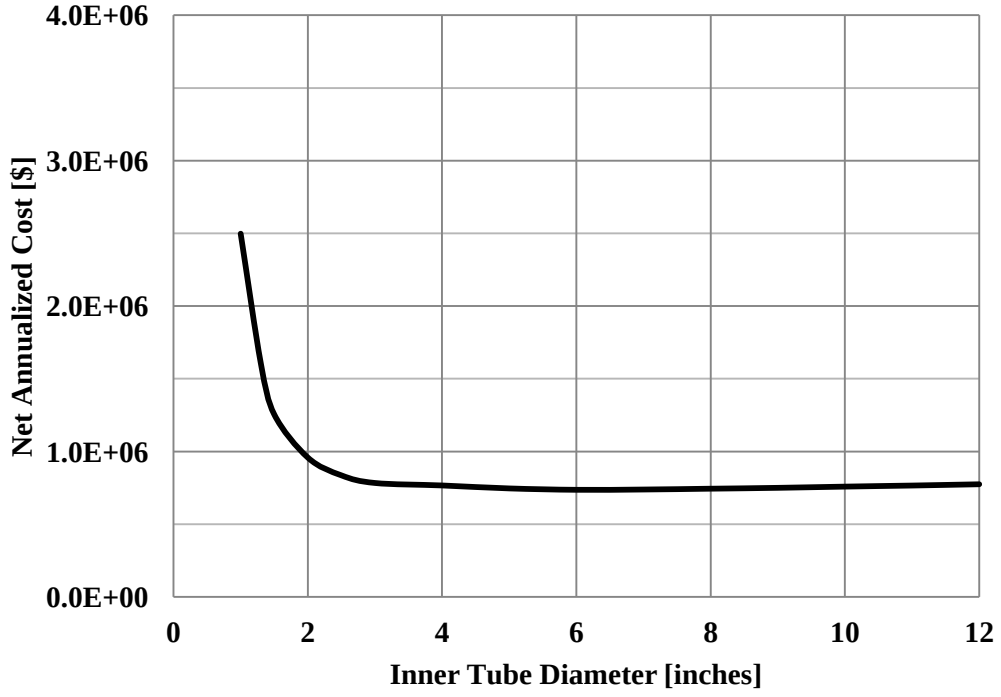

Figure 5.10 – Net annualized cost versus inner tube diameter for flue gas inlet temperature of 135°F.

Even though the net annual cost is the least with a large tube diameter, an additional constraint is the length of tubing that can be manufactured and installed into a power plant system. An inner tube diameter between two inches and four inches has reasonable performance and has short tubes.

The next design factors that were varied were transverse tube spacing, fin pitch, and fin length. Figure 5.12 through Figure 5.15 shows how increasing the transverse tube spacing affected the size and cost of the ACC. In the figures, the abscissa on the graphs is a transverse tube spacing factor F_{st} defined in Figure 5.11 and Equation 5.10.

$$S_t = F_{St}(OD + 2F_L) \tag{5.10}$$

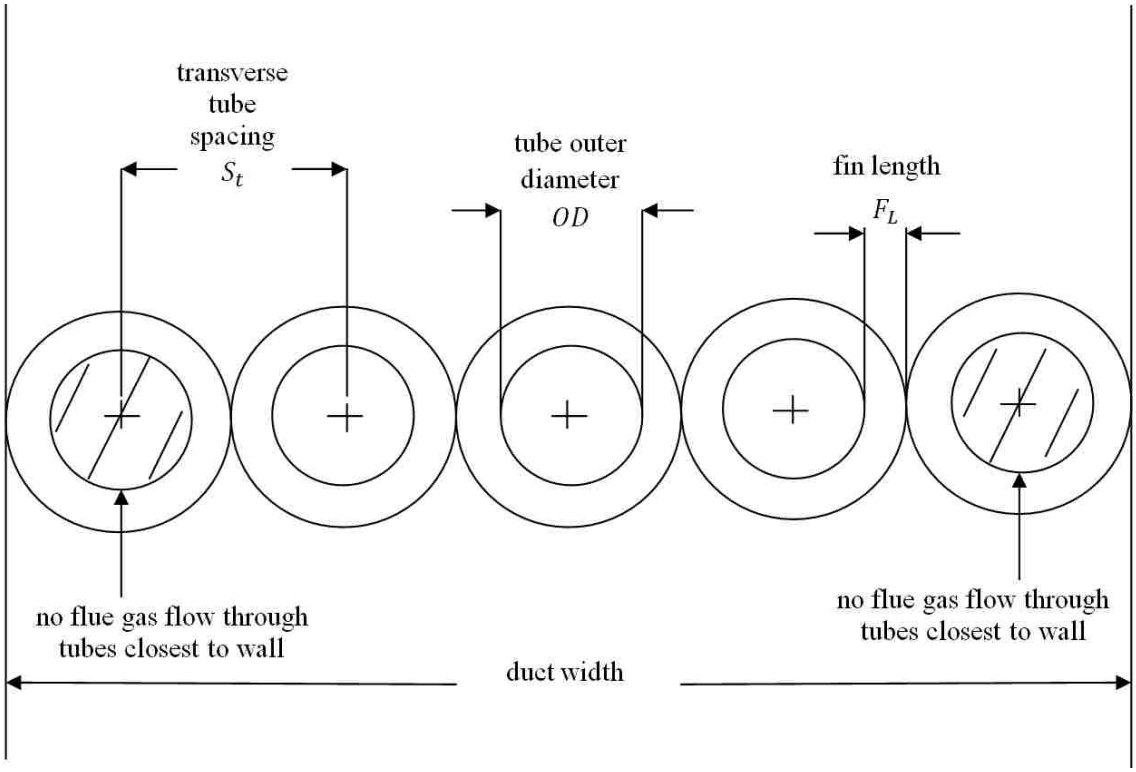

Figure 5.11 – Transverse tube spacing of the heat exchanger tube bundle.

In the simulations, the cooling air velocity was constant and increased transverse tube spacing increased the cooling air flow rate. According to Equation 5.11, a larger mass flow rate of cooling air decreased the temperature change from row to row.

$$Q = \dot{m}_{air} C_{p,air} \Delta T \tag{5.11}$$

The thermodynamic effects of transverse tube spacing were small. There was a six percent decrease in the necessary tube length (Figure 5.13). However, the operating costs of the ACC increased substantially due to the increased cooling air flow rate that was required to fill the spaces between the tubes to maintain the same velocity. In summary, the least expensive design was the most compact arrangement where $S_t = OD + 2 * F_L$

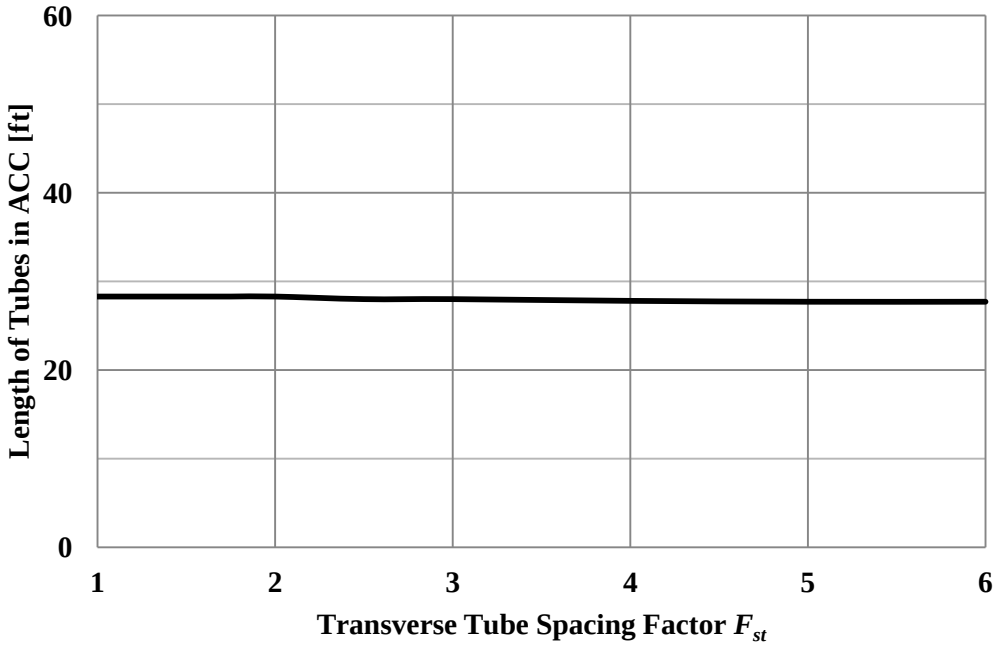

Figure 5.12 – Length of heat exchanger tubes versus transverse tube spacing for inlet flue gas temperature of 135°F.

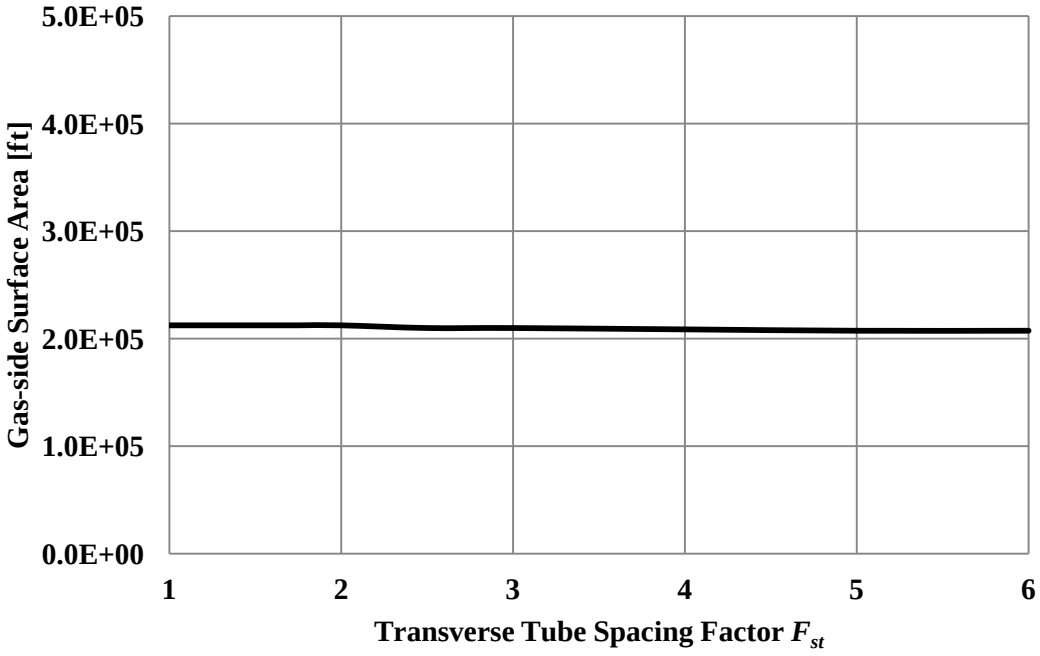

Figure 5.13 – Gas-side surface area versus transverse tube spacing for inlet flue gas temperature of 135°F.

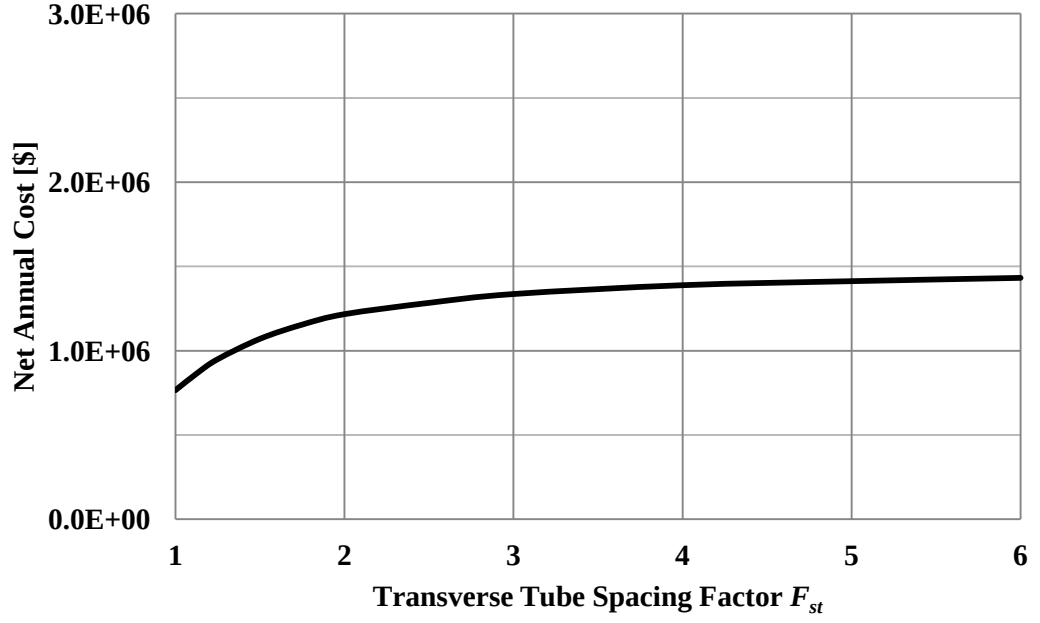

Figure 5.14 – Net annual cost versus transverse tube spacing for inlet flue gas temperature of 135°F.

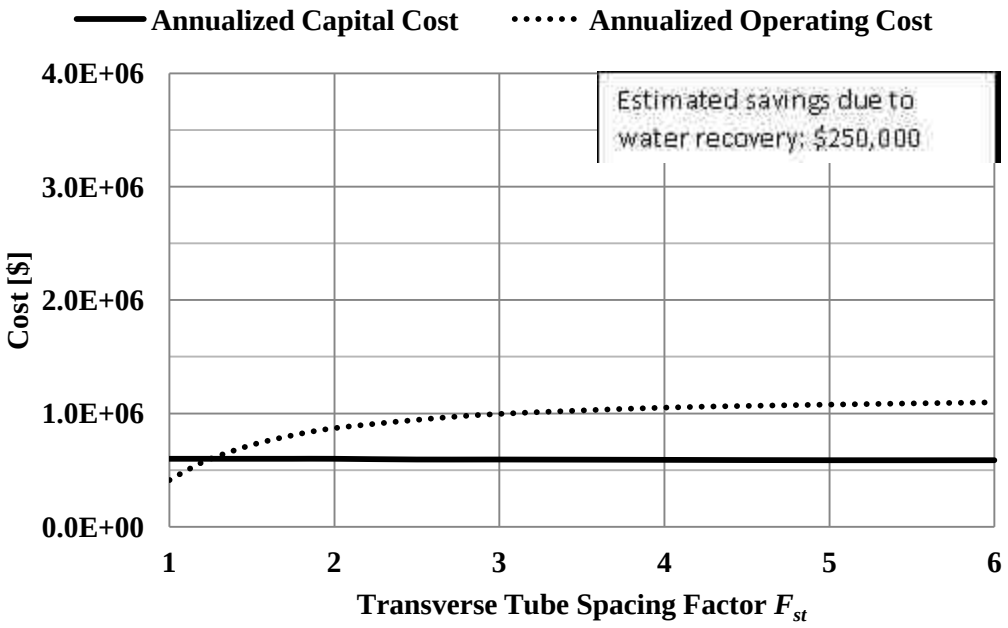

Figure 5.15 – Annualized costs of ACC versus transverse tube spacing for inlet flue gas temperature of 135°F.

Fin length affected both the heat transfer and pressure drop of the system. The optimal fin length balanced flow resistance with heat transfer. Figure 5.16 through Figure 5.19show the effects on size and cost of the ACC due to different fin lengths. There was an optimal length of the fin length around one inch, shown in Figure 5.18. Figure 5.18 is the net sum of all associated costs including the estimated savings due to water recovery, and the operating costs and capitalized costs shown in Figure 5.19.

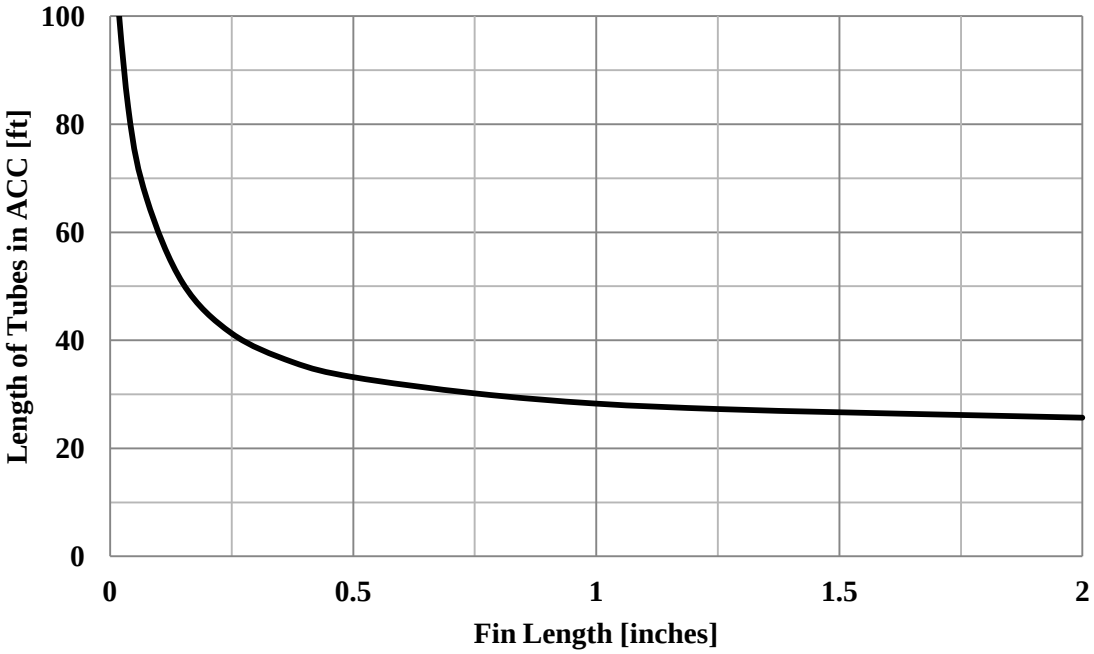

Figure 5.16 – Length of heat exchanger tubes versus fin length for inlet flue gas temperature of 135°F.

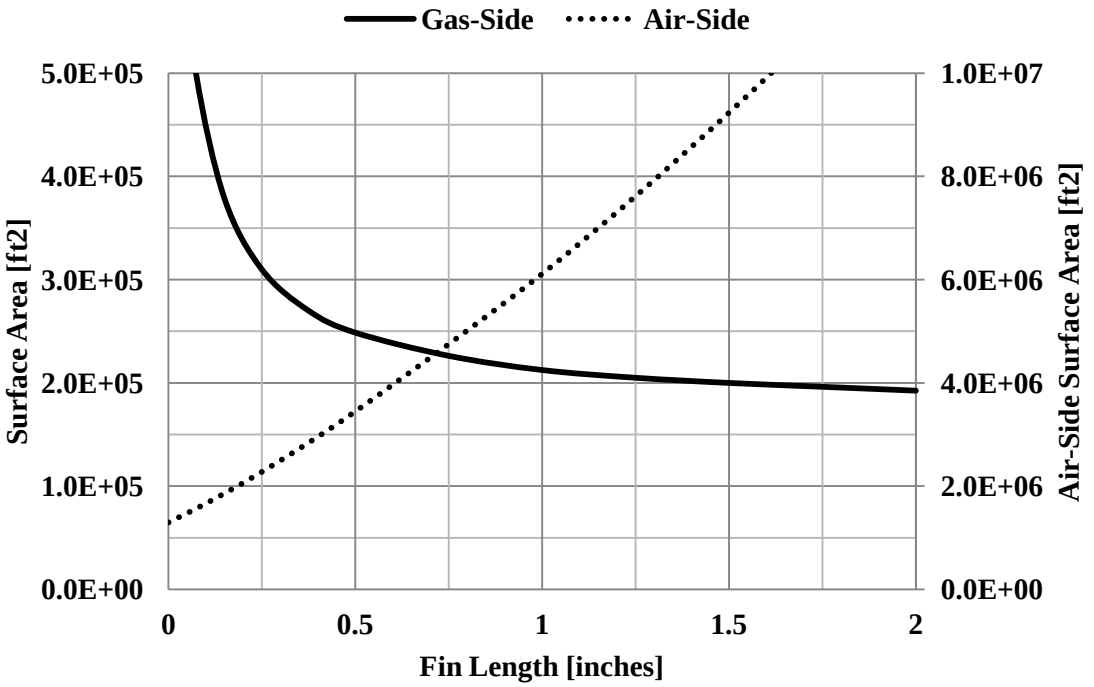

Figure 5.17 – Surface area versus fin length for inlet flue gas temperature of 135°F.

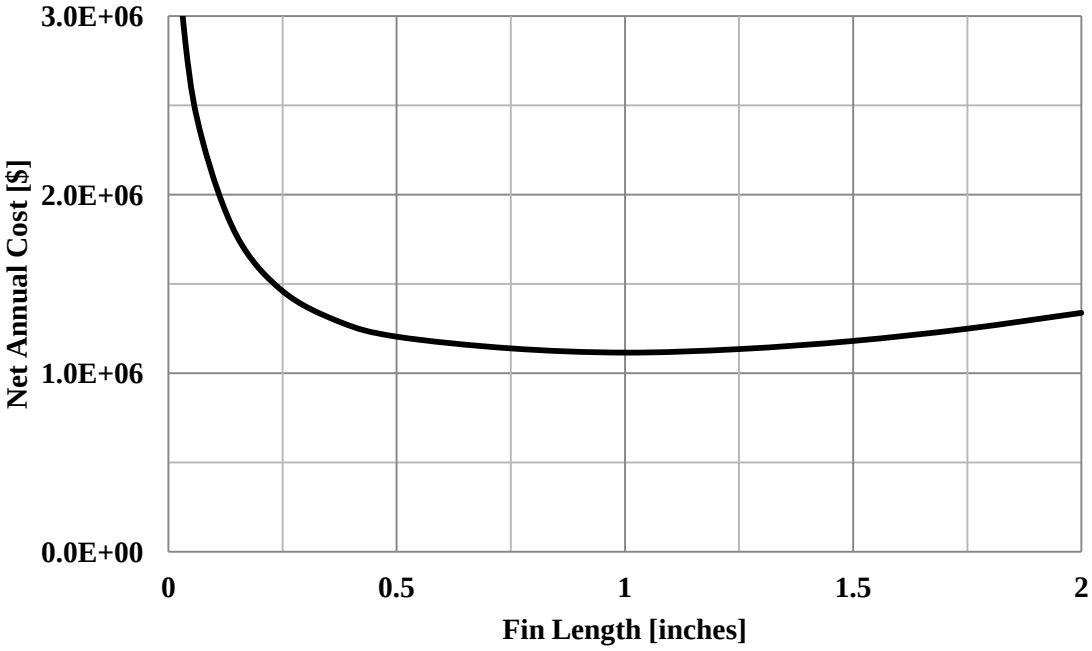

Figure 5.18 – Net annual cost versus fin length for inlet flue gas temperature of 135°F.

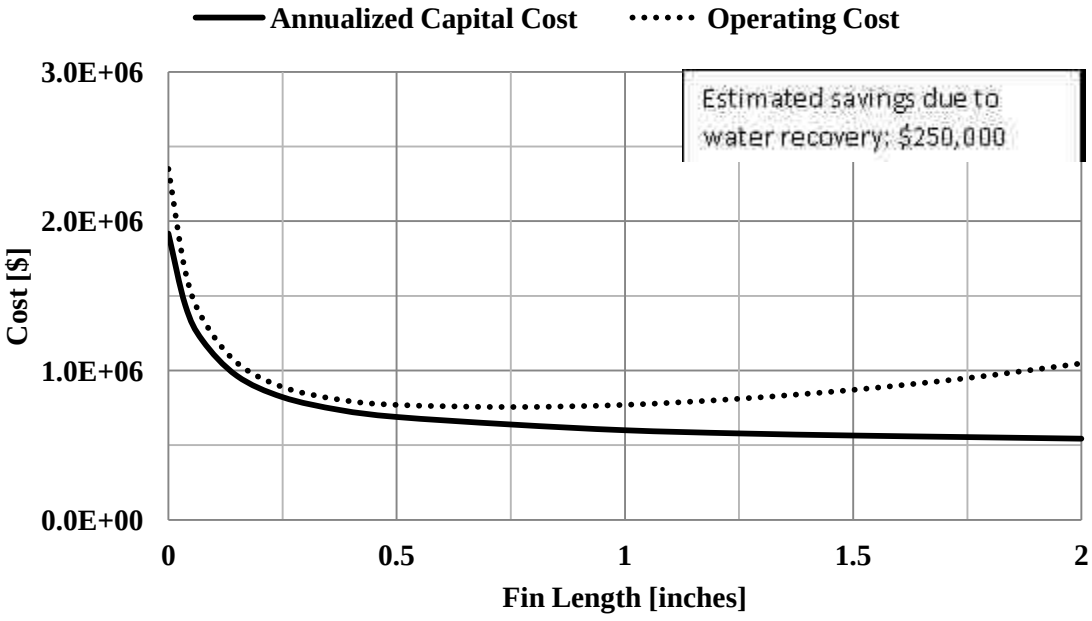

Figure 5.19 – Annualized costs of the ACC versus fin length for inlet flue gas temperature of 135°F.

Changing the fin pitch had a substantial impact on the ACC's performance and the effects on size and cost are shown in Figure 5.20 through Figure 5.23. For a fin pitch of 0.20 inches, the tubes were 28 feet long, and when fin pitch was 1 inch and 3 inches, the required tube length increased to 45 feet and 76 feet respectively. Such tube lengths are impractical even though Figure 5.22 indicates that the net annual cost was less.

The heat exchanger condensed 50% of the moisture, which is 200,000 lbm/hr. At $1.50 per 1000 gallons of water, the water savings were $242,000. The operating costs and annualized net annual costs varied with tube diameter and this is shown in Figure 5.23. The three costs, annualized capital cost, operating costs, and annual savings are summed and plotted in Figure 5.22.

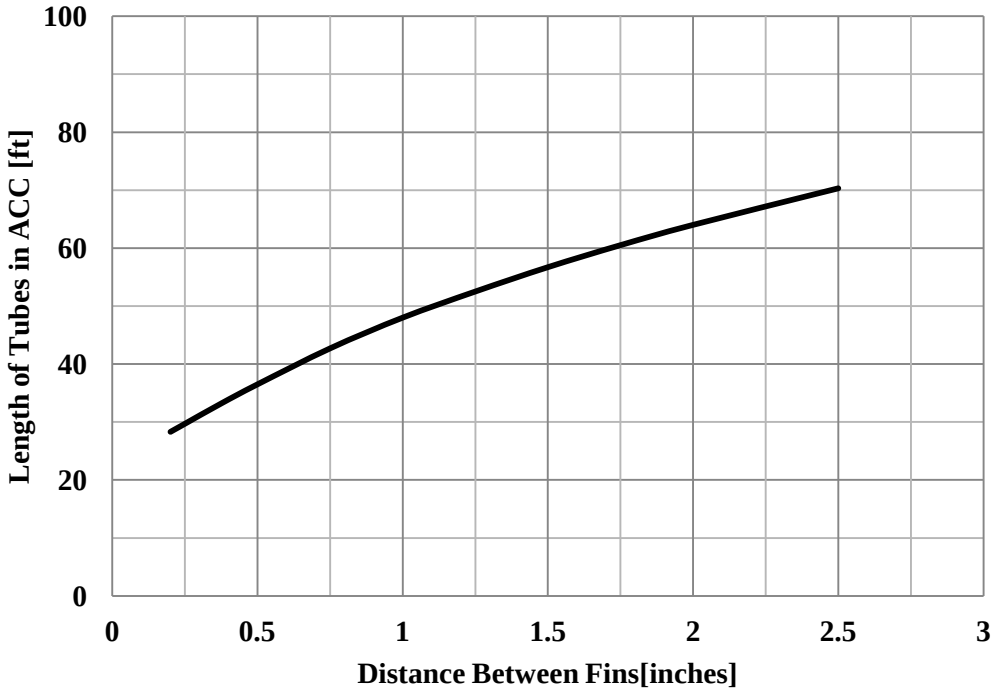

Figure 5.20 – Length of heat exchanger tubes versus fin pitch for inlet flue gas temperature of 135°F.

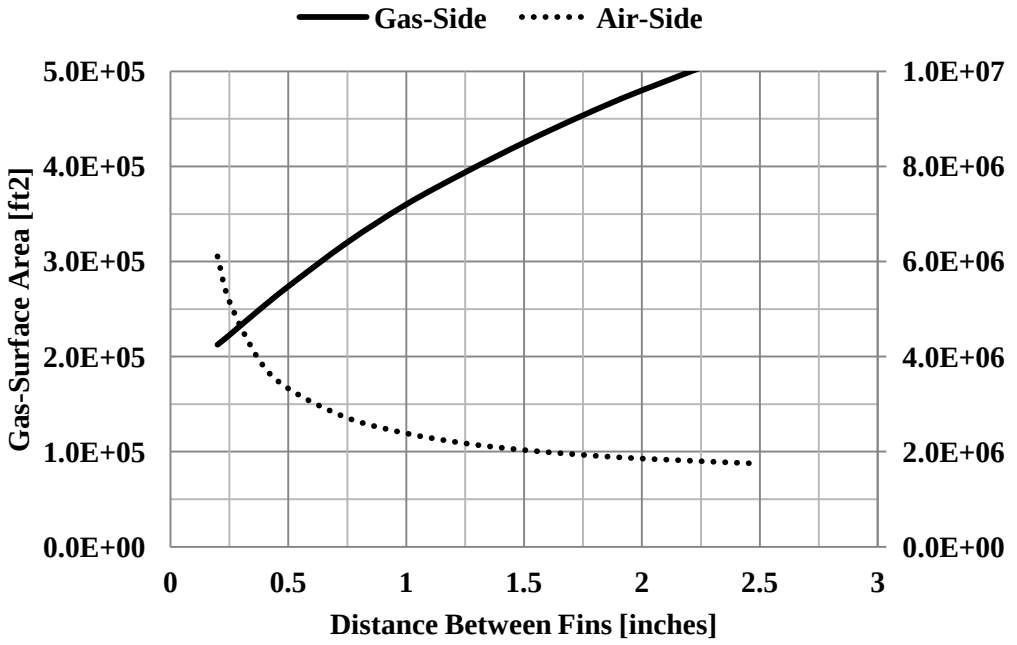

Figure 5.21 – Heat exchanger surface area versus fin pitch for inlet flue gas temperature of 135°F.

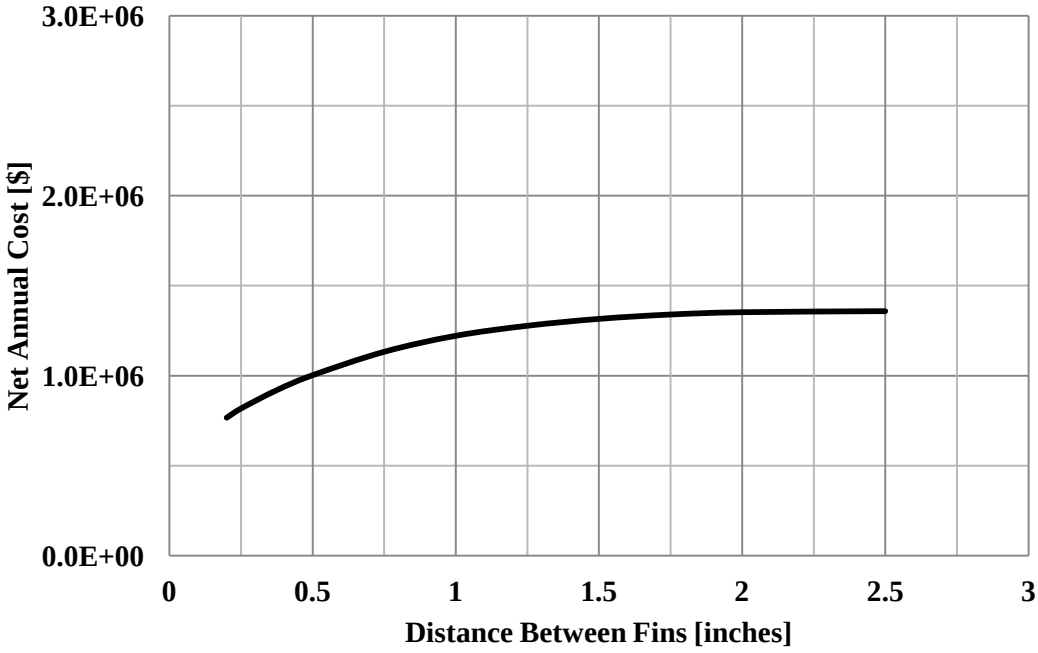

Figure 5.22 – Net annual cost of ACC versus fin pitch for inlet flue gas temperature of 135°F.

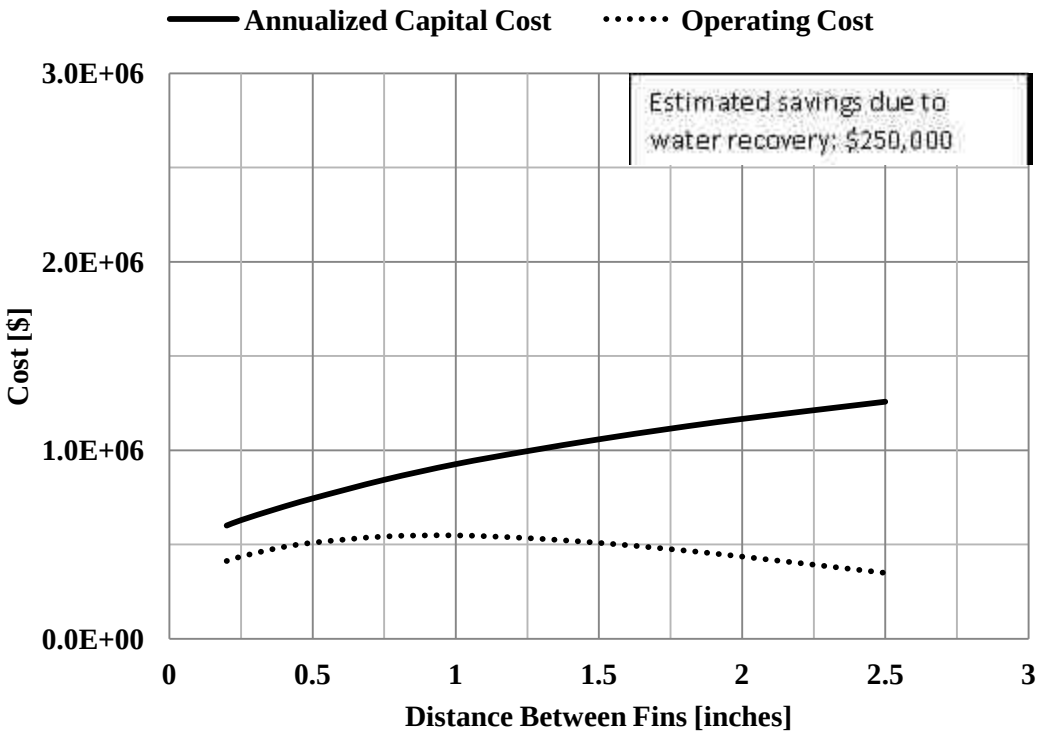

Figure 5.23 – Annualized costs of ACC versus fin pitch for inlet flue gas temperature of 135°F.

Thickness of the fin affected how efficiently the fin distributed heat. Figure 5.24 through Figure 5.26 show the effects fin thickness had on size and cost of the ACC. Fin thickness had a relatively small affect on the size of the heat exchanger and tube length remained relatively constant. However, fin thickness affected the operating costs because increasing the fin thickness decreased the spacing between the fins. This decreased the flow area, and thus less cooling air was necessary which lessened the operating costs. Figure 5.25 shows the net annual cost of the ACC, which is the sum of the operating savings due to water recovery and the operating costs and capital cost shown in Figure 5.26.

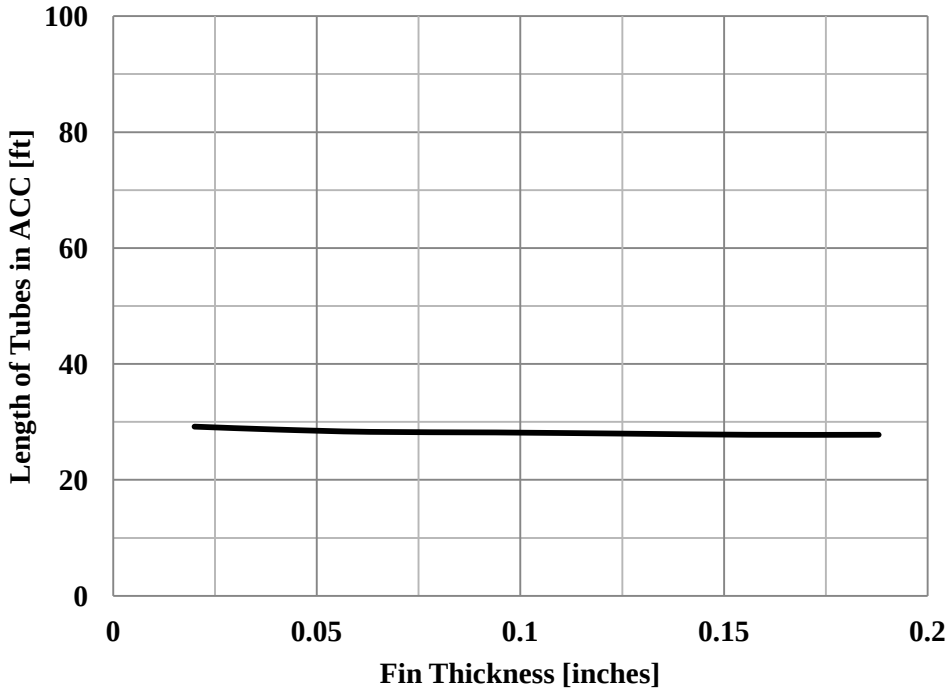

Figure 5.24 – Length of heat exchanger tubes versus fin thickness for inlet flue gas temperature of 135°F.

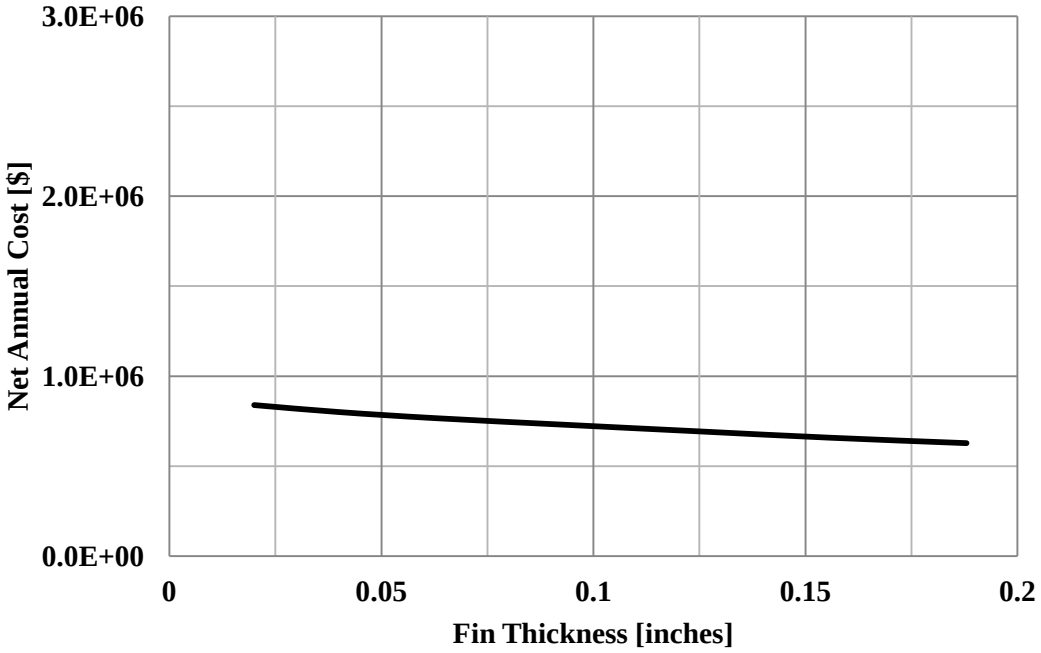

Figure 5.25 – Net annual cost versus fin pitch for inlet flue gas temperature of 135°F.

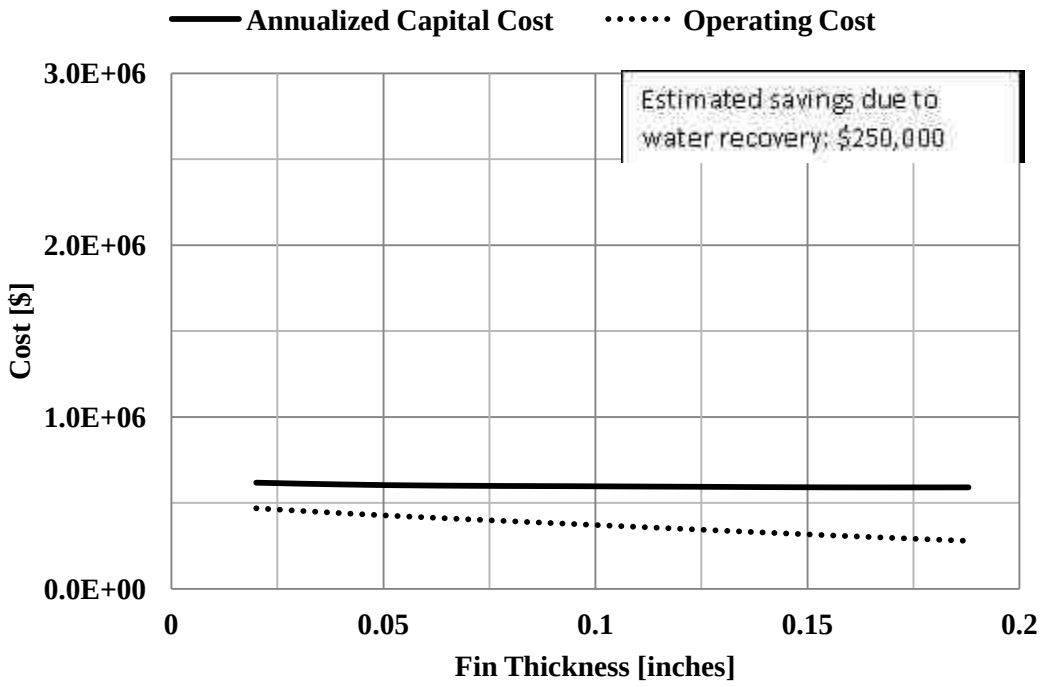

Figure 5.26 – Annualized costs of the ACC versus fin thickness for inlet flue gas temperature of 135°F.

Other design choices that affected the size and cost of the ACC were the process conditions: flue gas velocity, cooling air velocity, inlet flue gas temperature, and inlet cooling air temperature. The following 4 parametric studies show the effects of process conditions on size and cost of the ACC.

Figure 5.27 through Figure 5.30 show the effects of flue gas velocity. Increasing the flue gas velocity increased the flue gas flow rate in each tube, which reduced the overall number of tubes required to process the flue gas. The increased velocity also increased the heat transfer coefficient and rate of heat and mass transfer. However, the increase in heat and mass transfer did not compensate for the decrease in surface area and longer tubes were necessary to maintain 50 percent condensation efficiency. Increasing the velocity from 5 to 60 ft/sec changed the heat exchanger from one that had 57,000 tubes that were 15 feet long to one that had 4800 tubes that were 35 feet long.

The effects on cost are seen in Figure 5.29 and Figure 5.30. Figure 5.29 shows the net annualized cost of the ACC, which accounts for the savings associated with recovering water and the operating costs and capital cost of the ACC shown in Figure 5.30. In this case the results indicated that specifying a higher flue gas velocity would lead to lower annual costs of the ACC.

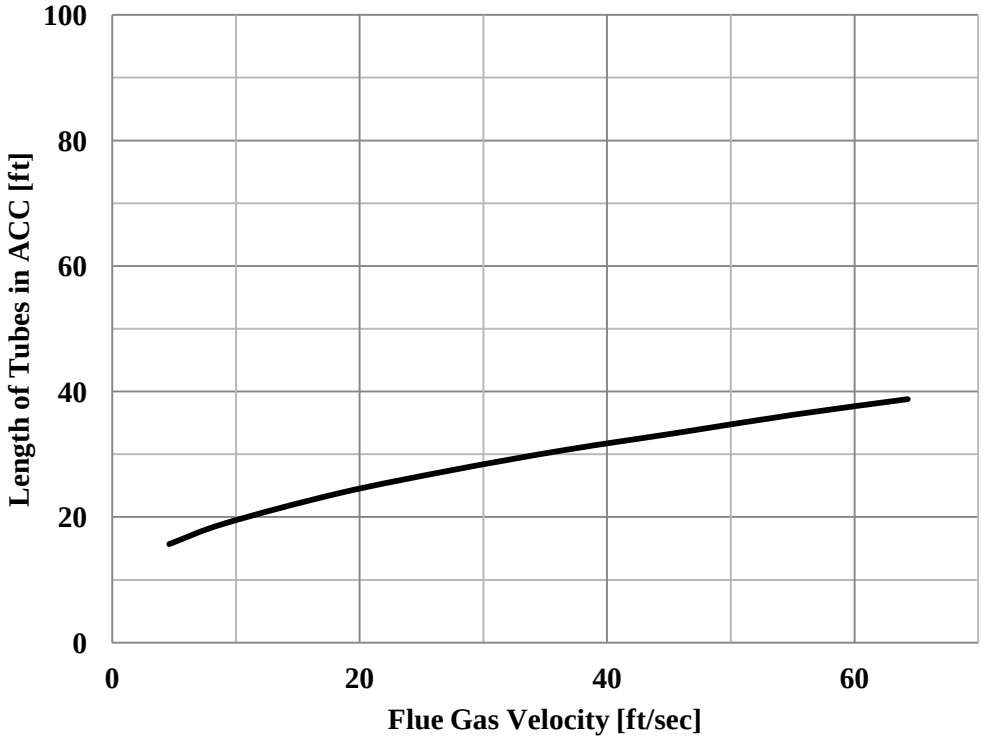

Figure 5.27 – Length of heat exchanger tubes versus flue gas velocity for inlet flue gas temperature of 135°F.

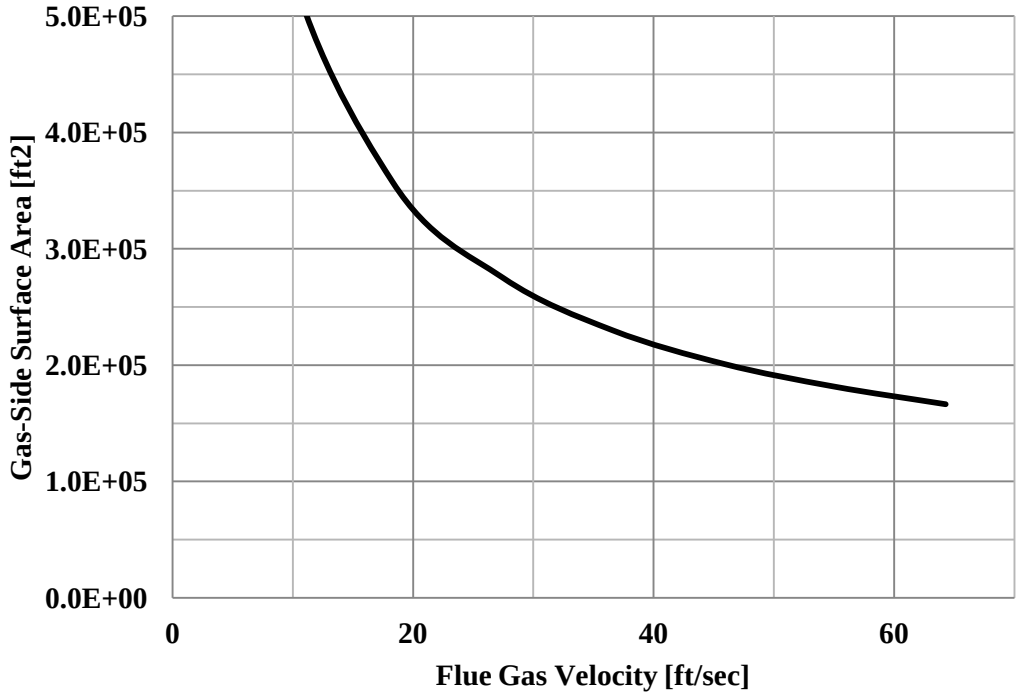

Figure 5.28 – Gas-side surface area versus flue gas velocity for inlet flue gas temperature of 135°F.

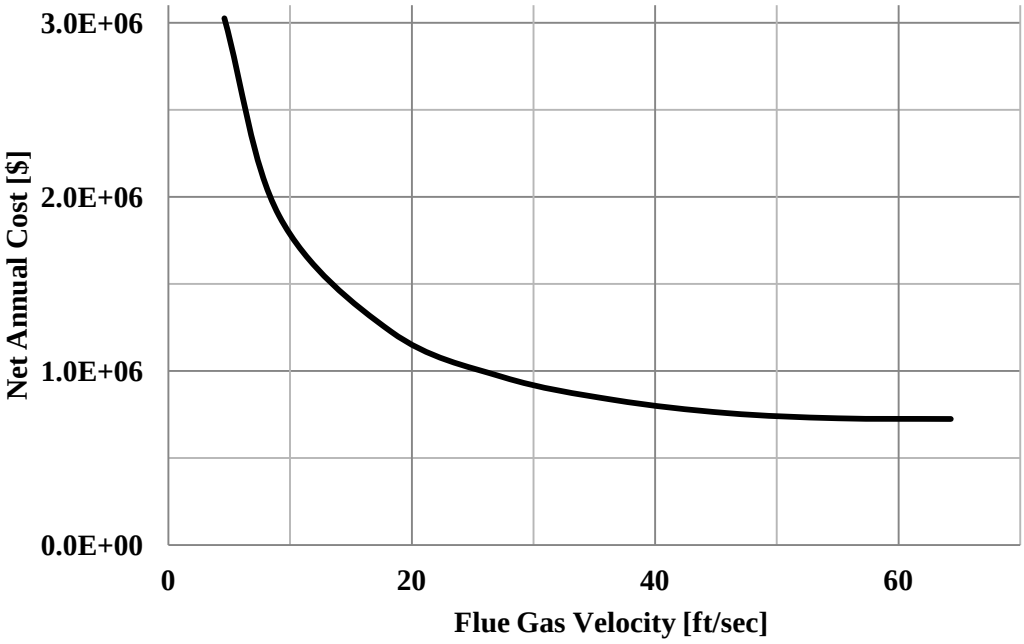

Figure 5.29 – Net annual cost versus flue gas velocity for inlet flue gas temperature of 135°F.

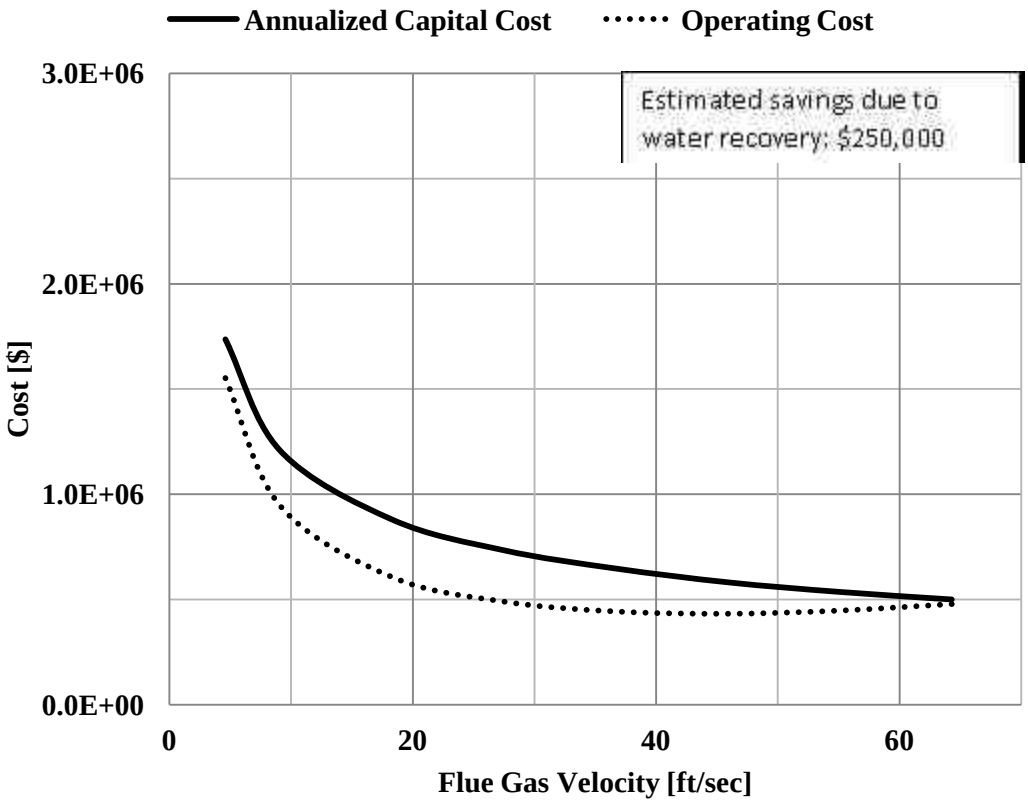

Figure 5.30 – Annualized costs for the ACC versus flue gas velocity for inlet flue gas temperature of/ 135°F.

Figure 5.31 through Figure 5.34 shows the effect of increased cooling air velocity. As was observed during the experiments discussed in Chapters 3 and 4, increasing the cooling air velocity lowered the tube wall temperature which increased the driving mechanisms for condensation. Figure 5.31 shows that when the cooling air velocity was increased, a shorter tube condensed the same quantity of water. Figure 5.32 shows the reduction in surface area associated with a higher cooling air velocity.

There was an optimal cooling air velocity of approximately 12 ft/sec. Figure 5.33 shows the net annual cost versus cooling air velocity. The net annual cost was the sum of the estimated savings due to recovering water and the operating and capital cost of the ACC shown in Figure 5.34.

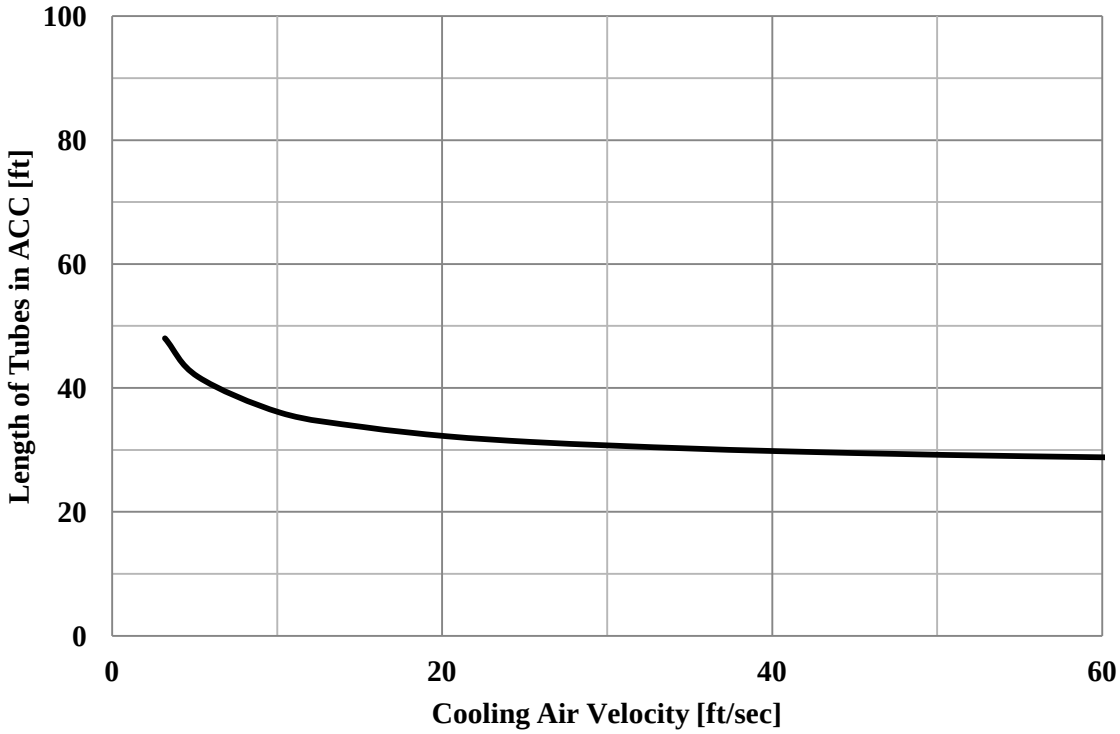

Figure 5.31 – Length of heat exchanger tubes versus cooling air velocity for inlet flue gas temperature of 135°F.

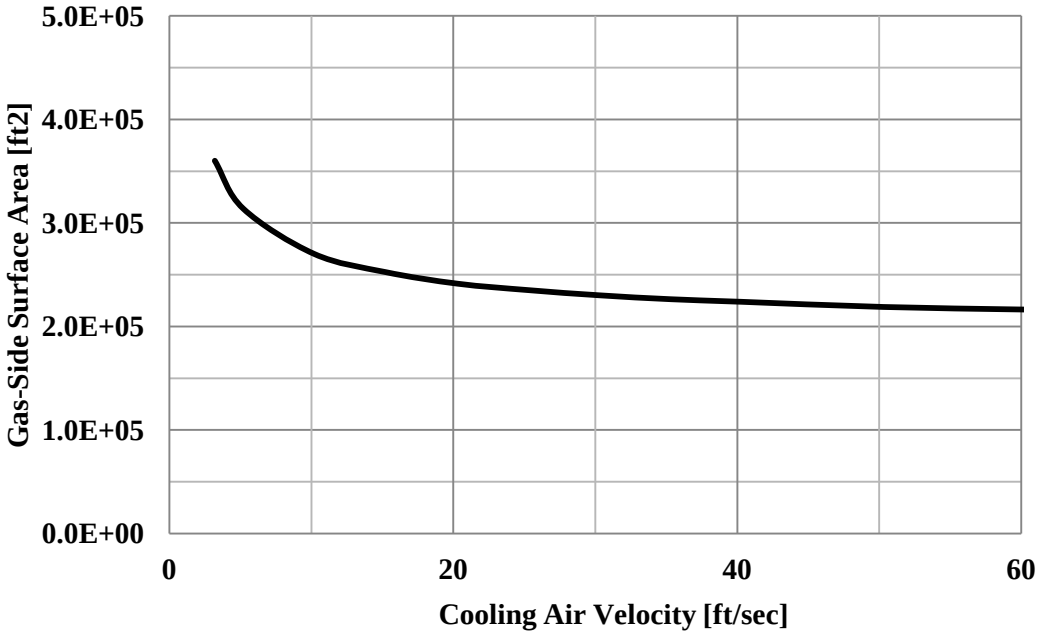

Figure 5.32 – Gas-side surface area versus cooling air velocity for inlet flue gas temperature of 135°F.

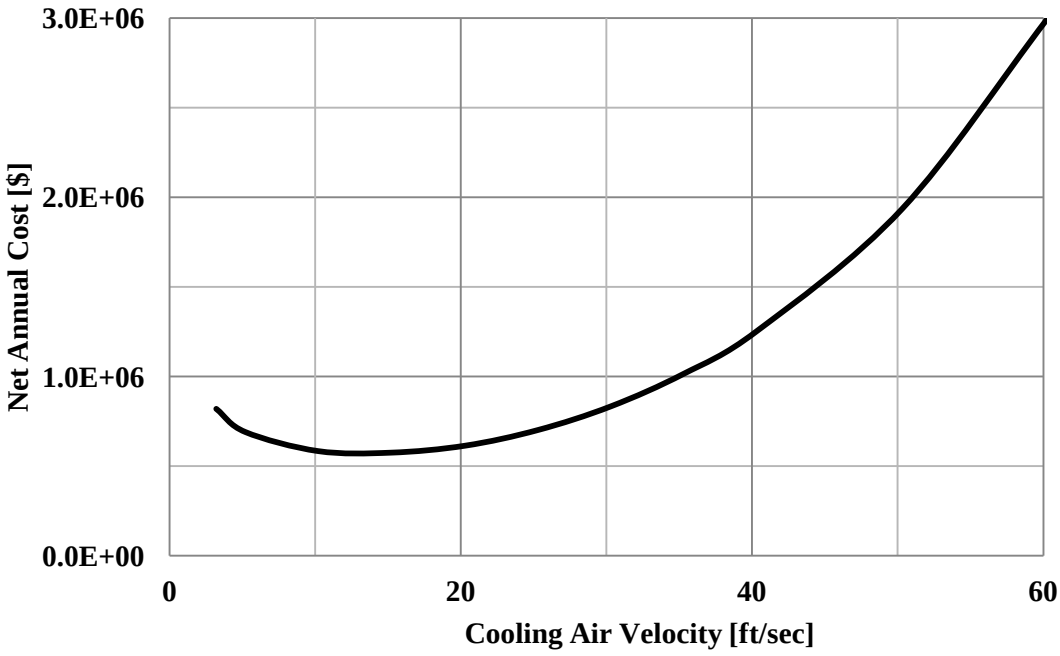

Figure 5.33 – Net annual cost versus cooling air velocity for inlet flue gas temperature of 135°F.

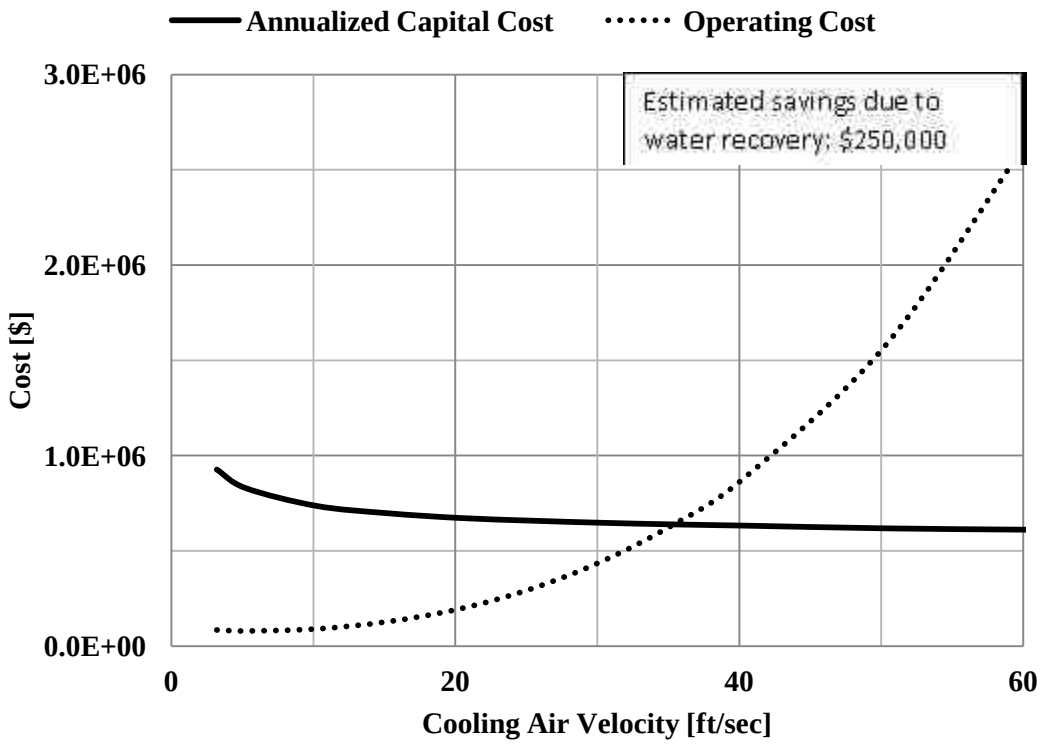

Figure 5.34 – Annualized costs versus cooling air velocity for inlet flue gas temperature of 135°F.

Figure 5.35 through Figure 5.38 shows how inlet flue gas temperature affected size and cost of the ACC. The effects, also discussed in Chapters 3 and 4, were that inlet flue gas temperature had little impact on water condensation rate. Comparing the heat transfer resistances on the gas-side and the air-side, the gas-side has a higher resistance, and so changing the flue gas temperature had a relatively small affect on the tube wall temperature. And, since condensation rate is driven by tube wall temperature, the performance of the ACC has a weak dependence on inlet flue gas temperature. (When reviewing the experimental results discussed in Chapter 3, it is important to consider the variations in moisture concentrations because moisture concentration greatly affects condensation rate.)

Figure 5.35 shows the length of the tubes in the ACC, and Figure 5.36 shows the surface area of the ACC. The net annual cost in Figure 5.37 is the sum of the estimated savings due to recovering water and the operating costs and capital cost of the ACC shown in Figure 5.38.

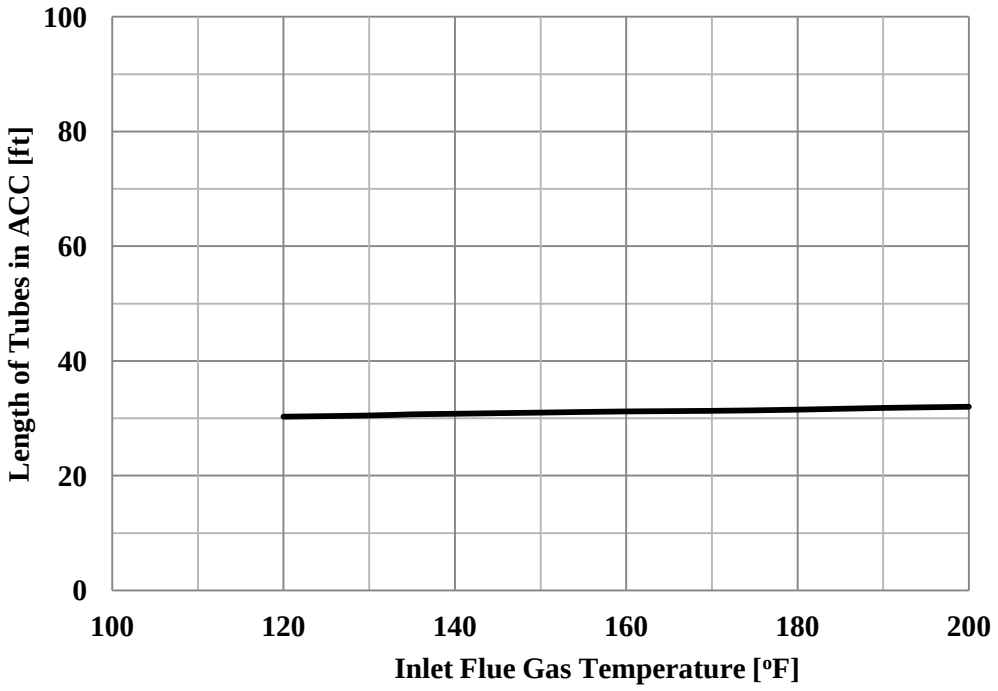

Figure 5.35 – Length of heat exchanger tubes versus inlet flue gas temperature.

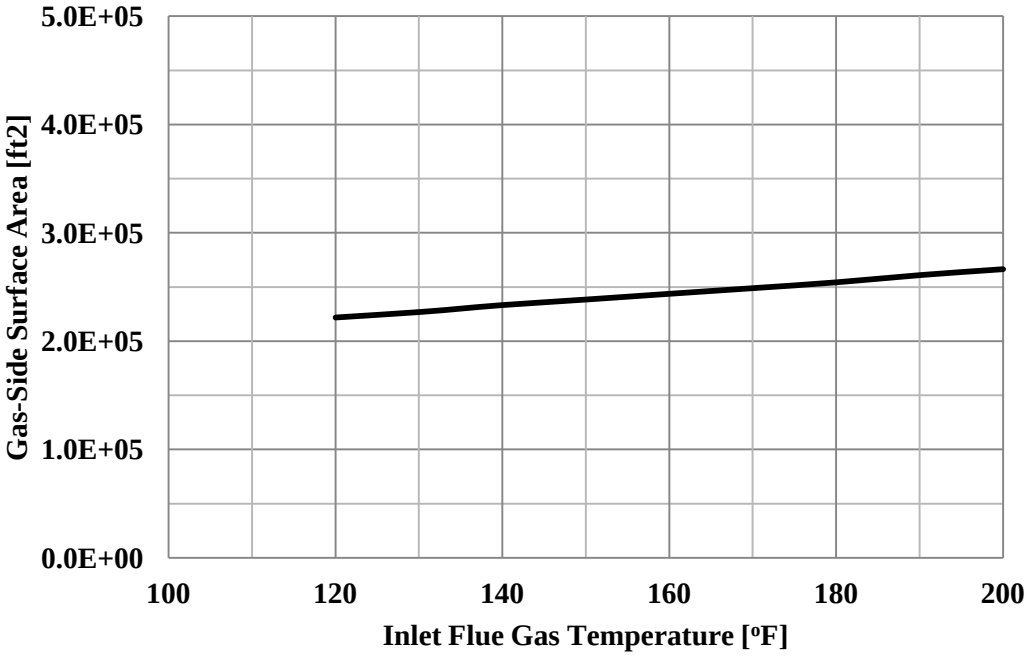

Figure 5.36 – Gas-side surface area versus inlet flue gas temperature.

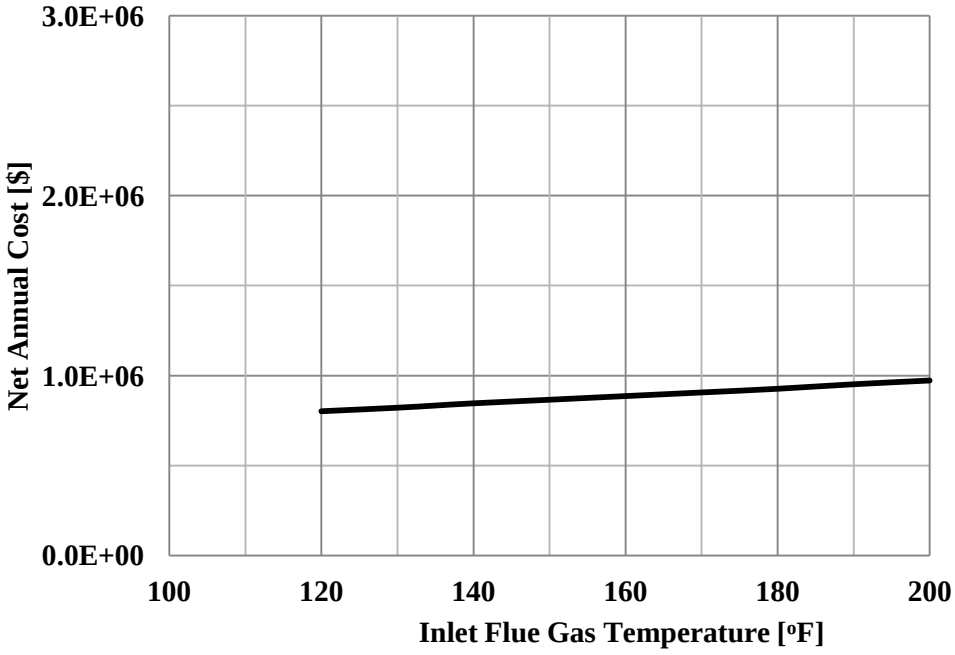

Figure 5.37 – Net annual cost versus inlet flue gas temperature.

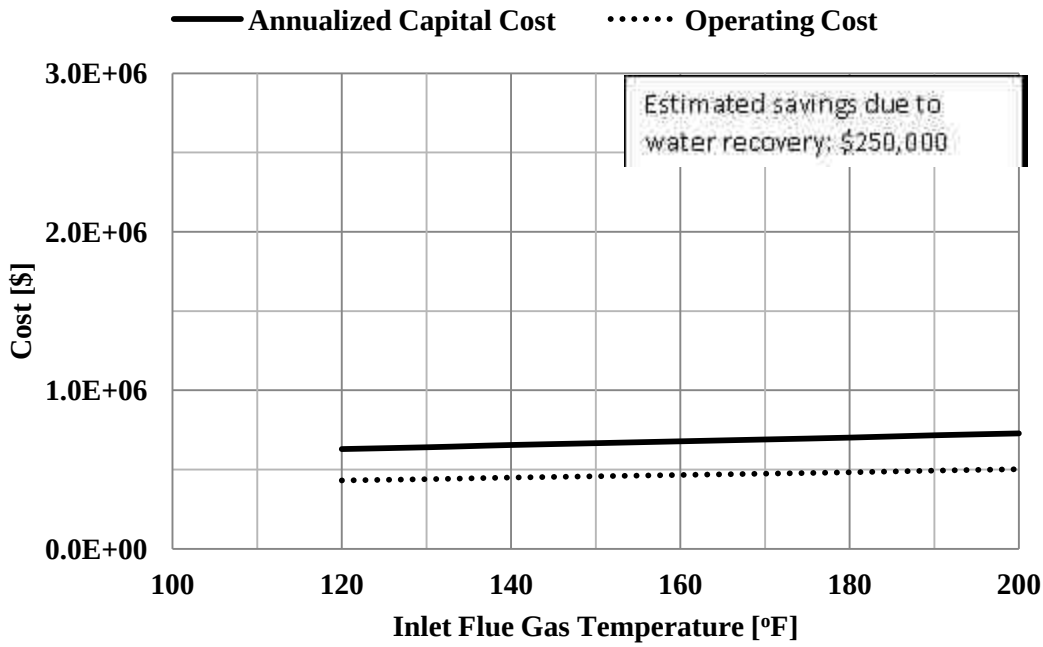

Figure 5.38 – Annualized costs for the ACC versus inlet flue gas temperature.

The next parameter that was varied was inlet cooling air temperature. The decreased inlet cooling air temperature lowered the required length of tubing and the overall surface area. This is shown in Figure 5.39 and Figure 5.40. As was discussed in Chapters 3 and 4, lowering the inlet cooling air temperature lowers the tube wall temperature, hence increasing the potential for condensation. A low inlet cooling air temperature increased the performance of the ACC and lowered the cost. The net annual cost of the ACC is shown in Figure 5.41, which is the sum of the estimated annual savings due to recovering water and the annual operating costs and capital cost shown in Figure 5.42.

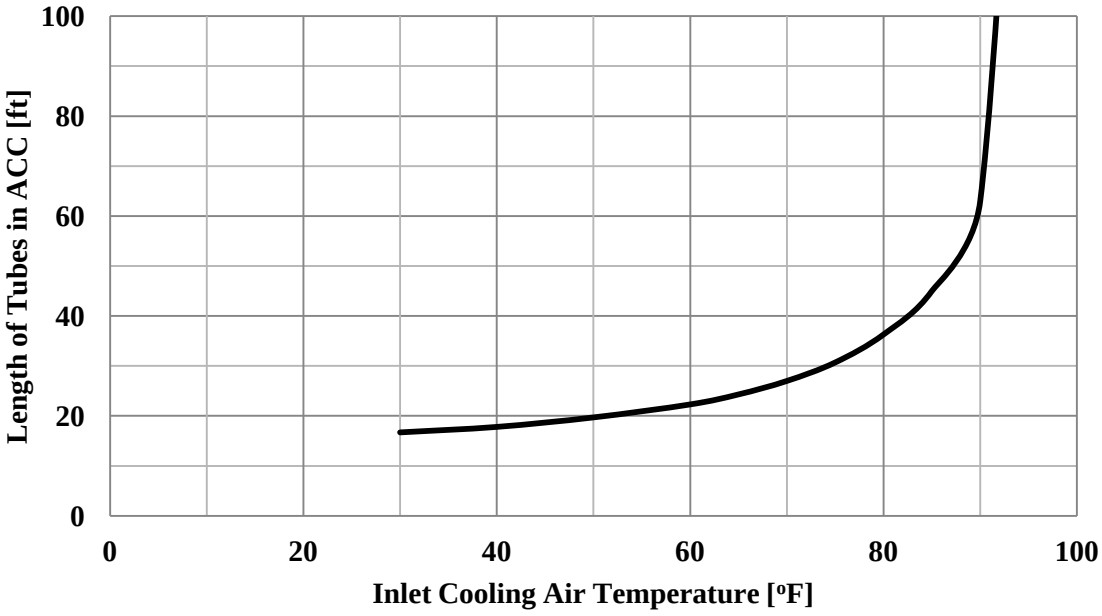

Figure 5.39 – Length of heat exchanger tubes versus inlet air temperature for inlet flue gas temperature of 135°F.

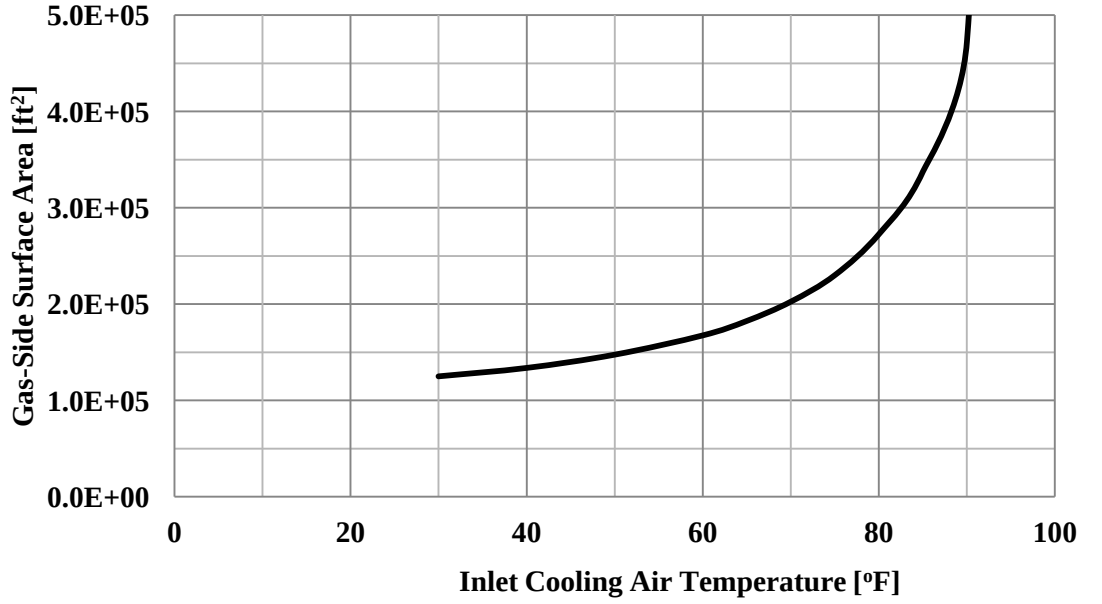

Figure 5.40 – Gas-side surface area versus inlet air temperature for inlet flue gas temperature of 135°F.

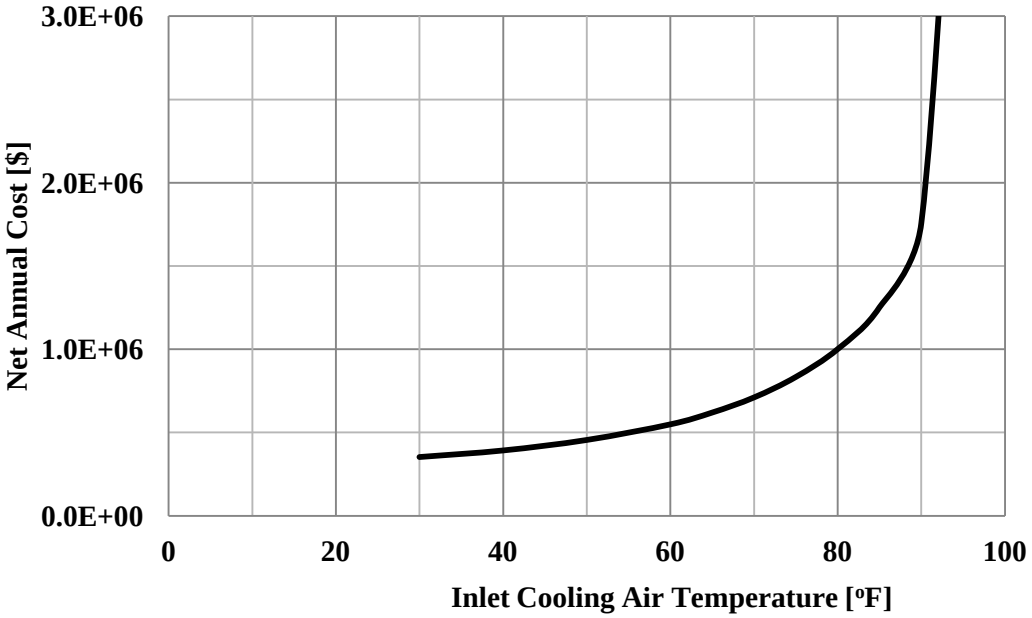

Figure 5.41 – Net annual cost versus inlet air temperature for inlet flue gas temperature of 135°F.

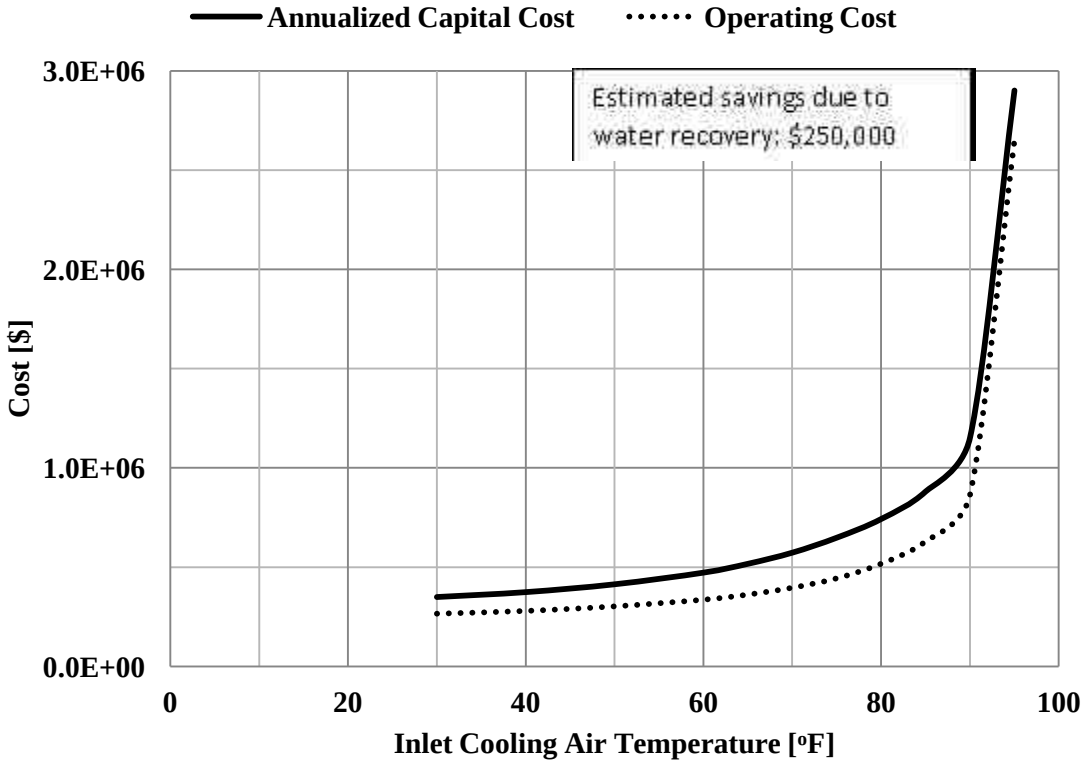

Figure 5.42 – Annualized costs of ACC versus inlet air temperature for inlet flue gas temperature of 135°F.

The last parameter varied was the number of tube rows in the direction of the cooling air flow. Figure 5.43 shows that increasing the number of tube rows increased the length of the ACC. This was due to the increase in cooling air temperature in subsequent rows, which reduced the mean temperature difference.

The effect on net annual cost is shown in Figure 5.45, which is the sum of the estimated savings due to recovering water and the operating costs and capital cost shown in Figure 5.46. Increasing the number of tube rows from 1 to 10 increased the capital cost by 20 percent and the annual operating cost by 30 percent. Five rows compared to one row increased the capital cost by 7 percent and the annual operating costs by 10 percent. The benefit to having more rows is less tube bundles and a more compact heat exchanger

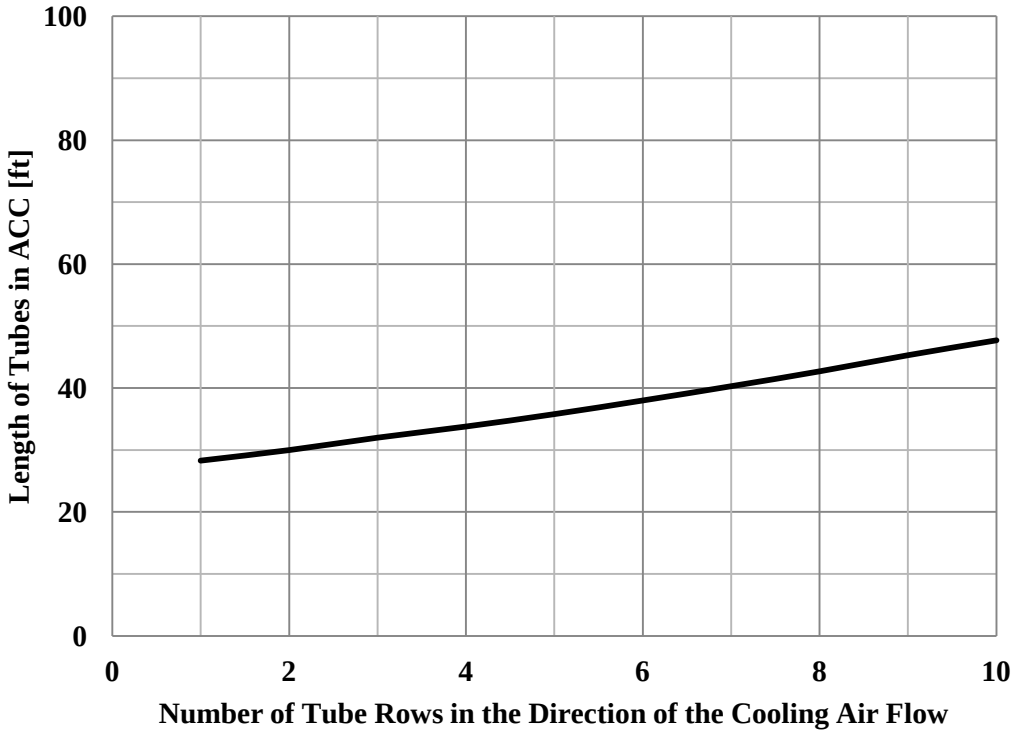

Figure 5.43 – Length of heat exchanger tubes versus number of tube rows for inlet flue gas temperature of 135°F.

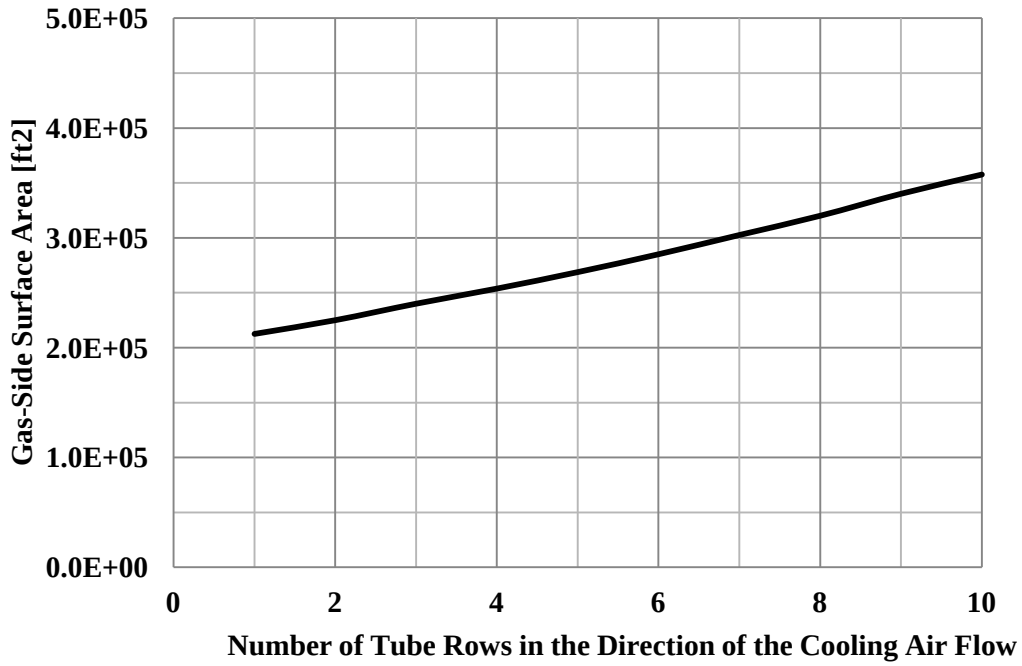

Figure 5.44 – Gas-side surface area versus number of tube rows for inlet flue gas temperature of 135°F.

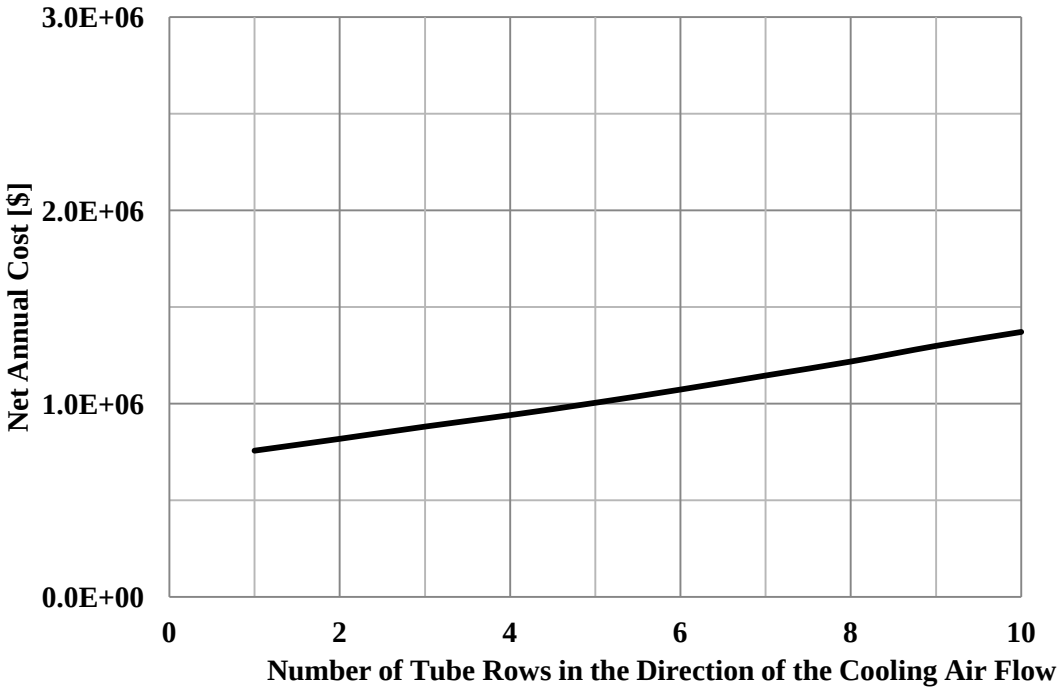

Figure 5.45 – Net annual cost versus number of tube rows for inlet flue gas temperature of 135°F.

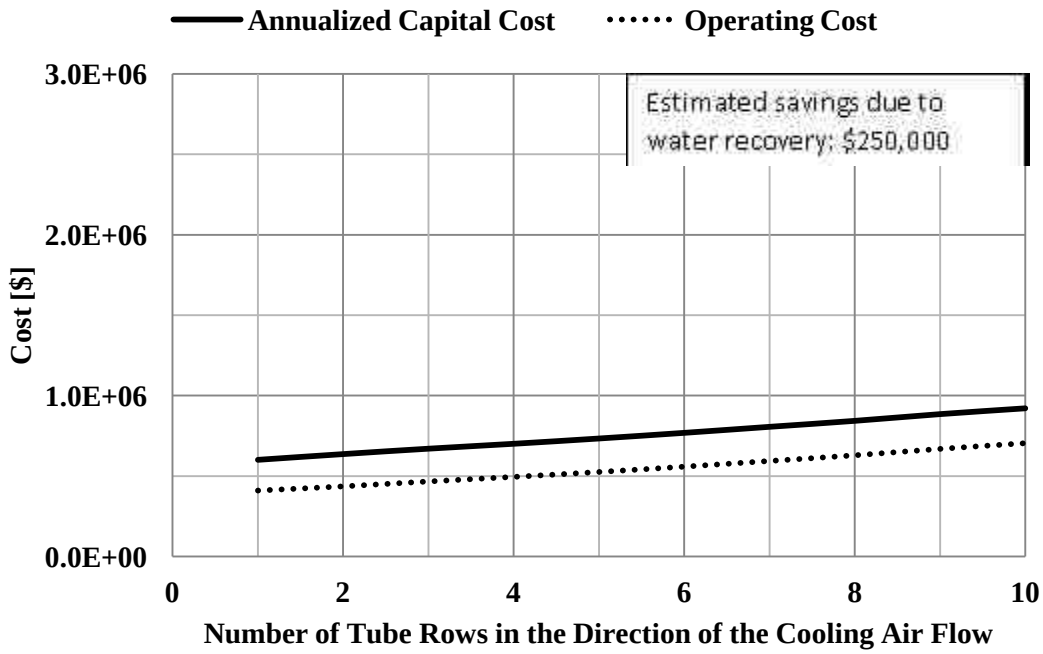

Figure 5.46 – Annualized capital costs versus number of tube rows for inlet flue gas temperature of 135°F.

The remaining sections of the chapter discuss how to optimize these design parameters. Section 5.3 begins with optimizing 4 geometry parameters, and then incorporates the flue gas and cooling air velocities into the optimization. Then the heat exchanger is optimized for various case studies. The last section discusses the optimal ACC for desired condensation efficiencies different than 50 percent.

5.3 Optimal Design of the Flue Gas Air-Cooled Condenser for the Case with no Flue Gas Desulfurization System

The Nelder-Mead method described in the Literature Review was used to optimize the full-scale design. The purpose of the optimization was to determine values for design variables which minimized the annualized cost of the air-cooled condenser. To reiterate what was described in Chapters 1 and 2, the function that was minimized was Equation 5.12.

$$Annual\ Cost = Annualized\ Capital\ Cost + Operating\ Costs - Operating\ Savings \tag{5.12}$$

Section 5.3.1 discusses the progression of finding an optimal design. First just the geometry was optimized, then the flow rates were optimized, and finally the geometry and flow rates were optimized simultaneously. This shows that the latter procedure of optimizing all variables simultaneously provided the least expensive design.

Section 5.3.2 discusses tube row effects because tube rows were not included as an optimization variable. The Nelder-Mead method required all variables be continuous, and tube rows was a discreet parameter in the simulation.

Sections 5.3.3 and 5.3.4 discuss the effects of the inlet flue gas temperature and inlet cooling air temperature.

5.3.1 Optimal Design Values of the Parametric Simulations

Process conditions for the ACC are listed in Table 5.5, these process conditions mirror those of Table 5.4 because this optimization sought the best design choices for the parametric tests presented in Section 5.2, with the exception of the number of tube rows. Tube rows was changed to 2 to shorten the duration of the simulations.

Table 5.5 – Process conditions used for the optimization of the parametric simulations in section 5.2.

Inlet Flue Gas Temperature [^{o}F]	135^{o}F
Inlet Moisture Concentration [wet vol %]	11.0
Flue Gas Velocity [ft/sec]	40
Inlet Cooling Air Temperature [^{o}F]	75^{o}F
Air Velocity between Tubes [ft/sec]	30
Condensation Efficiency (Equation 2.6)	50%
Number of tube rows in heat exchanger banks	2

The parameters that were varied were tube diameter, fin spacing, fin length, and fin thickness. Tube rows was not included because the Nelder-Mead technique requires the variables be continuous. The cooling air and flue gas velocity were considered following the first optimization of the geometry. The ranges of the parameters for the optimization are listed in Table 5.6. These ranges were in part determined by Equations 1.17 and 1.18, to avoid singularity. (In general these ranges are selected by the designer and can be any value which keeps the governing equations from becoming singular or applying to conditions outside the recommended ranges for heat transfer correlations, mass transfer correlations, etc…)

It was assumed that the transverse tube spacing of the tubes S_t must be as small as possible. The tube spacing was calculated according to the diagram in Figure 5.11, in which the tube spacing is equal to the tube diameter plus the length of the fins. This constraint was imposed because the heat exchanger was expected to have approximately 10,000 tubes and it will need to be as compact as possible. The longitudinal tube spacing was set equal to the transverse tube spacing. Moreover, the parametric simulations for transverse tube spacing showed that it was more efficient for the tubes to be close-packed (See Figure 5.14).

The optimization began by building the initial simplex of the Nelder-Mead method. Table 5.6 lists the variables that were optimized along with the ranges during the optimization. Table 5.7 lists the information to build the initial simplex. The column labeled Starting Value was the guessed heat exchanger design. The column labeled Si in Table 5.7 was the parameter used to build the remaining vertices of the initial simplex. The tilted initial simplex method of Walters [42] utilized the guessed heat exchanger design and the parameter Si to build the entire initial simplex, shown in matrix form in Table 5.8.

Table 5.6 – Range of variables for the optimization of the parametric simulations from section 5.2.

Parameter	Minimum	Maximum
Tube Diameter [inches]	1.75	6
Fin Spacing [inches]	0.20	1.0
Fin Length [inches]	0.25	1.25
Fin Thickness [inches]	0.0625	0.125

Table 5.7 – Parameters to build the initial simplex for the optimization.

	Starting Values		Si from [42]
Optimization Parameters	**Normalized**	**Actual [inches]**	
Fin Pitch	0.1	0.28	0.125
Fin Length	0.5	0.625	-0.2
Inner Tube Diameter	0.2	2.6	0.25
Fin Thickness	0.25	0.0781	0.5
Net Annual Cost	$778,529		

Table 5.8 – Initial simplex for optimization of four geometric parameters.

	Fin Pitch (normalized)	Fin Length (normalized)	Inner Tube Diameter (normalized)	Fin Thickness (normalized)	Net Annual Cost (normalized)
Vertex 1	0.1	0.5	0.2	0.25	$778,529
Vertex 2	0.2207	0.4482	0.2647	0.3794	$883,279
Vertex 3	0.1295	0.3114	0.2589	0.3679	$843,284
Vertex 4	0.1273	0.4563	0.4314	0.3593	$838,239
Vertex 5	0.1256	0.459	0.2512	0.706	$781,654

The results of the optimization are listed in Table 5.9 and the details of the final simplex are listed in Table 5.10. The optimal design values had an annual operating cost that was approximately $175,000 less than the initial guess. The repeated values in Table 5.10 indicate convergence.

Table 5.9 – Results of the optimal tube geometry for the parametric simulations from section 5.2.

	Design Values	
Optimization Parameters	**Guess**	**Optimal**
Fin Pitch [inches]	0.28	0.2056
Fin Length [inches]	0.625	0.34638
Inner Tube Diameter [inches]	2.6	1.86433
Fin Thickness [inches]	0.07813	0.125
Cost	$778,529	$601,940

Table 5.10 – Final simplex of the optimization.

	Fin Pitch (normalized)	Fin Length (normalized)	Inner Tube Diameter (normalized)	Fin Thickness (normalized)	Net Annual Cost (normalized)
Vertex 1	0.007	0.771	0.0269	1.000	$601,939.15
Vertex 2	0.007	0.771	0.0269	1.000	$601,939.15
Vertex 3	0.007	0.771	0.0269	1.000	$601,939.15
Vertex 4	0.007	0.771	0.0269	1.000	$601,939.15
Vertex 5	0.007	0.771	0.0269	1.000	$601,939.15

The details of the optimal heat exchanger design are listed in Table 5.11. The condensation efficiency of the heat exchanger was 48% which resulted in a condensation rate of approximately 192,000 lbm/hr, or 383 GPM. In this design, the length of the heat exchanger tubes was 13.6 feet. An interesting conclusion from the optimization was that the simulation converged to a relatively small tube diameter. Recall from Figure 5.9 that as the tube diameter becomes large the capital costs because increasingly large, and as the tube diameter approaches very small values, the operating costs increase due to large fluid pressure drops.

Also listed in Table 5.11 are the costs associated with the ACC. The estimated field-erected capital cost was 6.7 million. The estimate was calculated using the correlation of Guthrie [64] and it included all costs associated with fabrication and installation. The annualized capital cost based on a 20 year repayment at a five percent fixed interest rate was $540,000. The costs to operate the cooling air fans and the additional load on the flue gas fan was $303,000 per year, and the estimated annual savings due to condensing water was $242,000 at $1.50 per 1000 gallons of water. The net annual cost of this design was $602,000. To break even with this design, water would need to be valued at $5.25 per 1000 gallons. A discussion about the cost of water is in Section 5.4.2.

Table 5.11 – Details of the optimal tube geometry for the parametric simulations from section 5.2.

Flue Gas Flow Rate [lbm/hr]	6,000,000
Vapor Flow Rate [lbm/hr]	403,720
Cooling Air Flow Rate [lbm/hr]	72,128,375
Flue Gas Velocity [ft/sec]	36.9
Cooling Air Velocity [ft/sec]	30.4
Inlet Flue Gas Temperature [^{o}F]	135
Inlet Moisture Concentration [% vol wet]	11.0
Inlet Cooling Air Temperature [^{o}F]	75
Tube Inner Diameter [inch]	1.86
Tube Thickness [inch]	0.2
Fin Length [inches]	0.35
Fin Pitch [inches]	0.206
Fin Thickness [inches]	0.125
Number of Tube Rows	2
Transverse Tube Spacing [inches]	2.96
Longitudinal Tube Spacing [inches]	2.96
Tube Length [ft]	13.6
Number of Tubes	32,970
Gas-side Surface Area [ft^2]	218,742
Air-side Surface Area [ft^2]	2,598,804
Field Erected Capital Cost	$6,742,011
Annualized Capital Cost	$540,996
Annualized Operating Cost	$303,281
Estimated Annual Savings due to Water Recovery (water costs estimated as $1.50 per 1000 gallons)	$242,338
Net Annualized Cost [20 yrs @ 5%]	$601,939
PERFORMANCE	
Sensible Heat Transfer [BTU/hr]	52,091,510
Latent Heat Transfer [BTU/hr]	200,311,307
Condensation Rate [lbm/hr]	192,526
Condensation Efficiency	48%

Next, the flue gas velocity and cooling air velocity were optimized. In this optimization, geometry was fixed and flue gas and cooling air velocities were optimized for the ranges listed in Table 5.12.

Table 5.12 - Range of velocities for optimizing the cooling air and flue gas velocities for the parametric simulations in section 5.2.

	Range		
Parameter	**Min**	**Max**	**Fixed**
Flue Gas Velocity [ft/sec]	7.5	80	
Cooling Air Velocity [ft/sec]	7.5	50	
Fin Pitch [inch]			0.206
Fin Length [inch]			0.35
Inner Tube Diameter [inch]			1.86
Fin Thickness [inch]			0.125

The results of the optimization are shown in Table 5.13. The net annualized cost of the ACC decreased by $110,000 compared to the design listed in Figure 5.10.

Table 5.13 - Optimal flue gas and cooling air velocities for the parametric simulations in section 5.2 (50% condensation efficiency).

	Simulation Values	
Optimization Parameters	**Guess**	**Optimal**
Gas Velocity [ft/sec]	58.25	43.76
Air Velocity [ft/sec]	20.25	18.32
Net annualized Cost	$529,268	$491,525

The last step was to optimize the system for both the geometry and the process conditions simultaneously. The details of the optimizations are listed in Appendix B, and summarized in

Table 5.14. The optimal design corresponded to a net annual cost of $307,000, compared to the first guess which corresponded to a net annual cost of $779,000.

Table 5.14 - Final optimization of the ACC with an inlet flue gas temperature of 135°F and inlet cooling air temperature of 75°F (50% condensation efficiency).

	Range		Design Values	
Optimization Parameters	**Min**	**Max**	**Guess**	**ACC-1**
Gas Velocity [ft/sec]	7.5	80	43.76	49.9
Air Velocity [ft/sec]	7.5	50	18.32	7.5
Fin Pitch [inch]	0.2	1.0	0.206	0.20
Fin Length [inch]	0	1.25	0.35	1.25
Inner Tube Diameter [inch]	1.75	6	1.86	1.75
Fin Thickness [inch]	0.0625	0.125	0.125	0.109
Cost			$491,525	$306,748

The details of the optimal design are listed in Table 5.15. The field-erected capital cost was estimated to be $5,287,000, using Guthrie's estimate for stainless steel air-cooled condensers. The annual operating costs were estimated to be $119,000 and the estimated savings due to water recovery were $237,000, assuming water costs $1.50 per 1000 gallons. Assuming the capital cost is paid off over a period of 20 years with a 5 percent fixed interest rate, the net annual cost of the ACC would be $307,000.

In this design the tubes were 11.7 feet long. As a comparison, ACCs used for condensing steam can have tubes up to 30 feet long. There is potential for the tubes to be longer than 11.7 feet and the ACC would then condense more water vapor.

Table 5.15 - Details of optimal design of the ACC for an inlet flue gas temperature of 135°F and inlet cooling air temperature of 75°F (further details listed in the appendix).

Flue Gas Flow Rate [lbm/hr]	6,000,000
Vapor Flow Rate [lbm/hr]	403,720
Cooling Air Flow Rate [lbm/hr]	53,638,732
Inlet Flue Gas Temperature [°F]	135
Inlet Moisture Concentration [% vol wet]	11.0
Inlet Cooling Air Temperature [°F]	75
Tube Inner Diameter [inches]	1.75
Tube Thickness [inches]	0.2
Fin Length [inches]	1.25
Fin Pitch [inches]	0.2
Fin Thickness [inches]	0.109
Number of Tube Rows	2
Transverse Tube Spacing [inches]	4.65
Longitudinal Tube Spacing [inches]	4.65
Tube Length [ft]	11.7
Number of Tubes	30,000
Gas-side Surface Area [ft^2]	161,416
Air-side Surface Area [ft^2]	8,404,383
Field Erected Capital Cost	$5,286,886
Annualized Capital Cost	$424,233
Annualized Operating Cost	$118,771
Estimated Annual Savings due to water recovery	$236,256
Net Annualized Cost [20 yrs @ 5%]	$306,749
PERFORMANCE	
Sensible Heat Transfer [BTU/hr]	50,670,814
Latent Heat Transfer [BTU/hr]	195,779,374
Condensation Rate [lbm/hr]	187,691
Condensation Efficiency	47%

One design choice left out of the optimization was the number of tube rows. Figure 5.47 shows how this affects the net annual cost, and while one tube row was the least expensive, a heat exchanger that is only one row would require an impractical amount of space. Choosing the appropriate number of tube rows is specific to each application and the choice should be made based on factors associated with installation and how much space is available.

Increasing the number of tube rows increased the cost due to two factors, the additional pressure drop and the additional surface area. The additional pressure drop was due to more tube rows and longer tubes, and the additional surface area was necessary because the overall temperature difference between the flue gas and cooling air decreased in subsequent rows. The next section discusses optimizing the ACC with different numbers of tube rows.

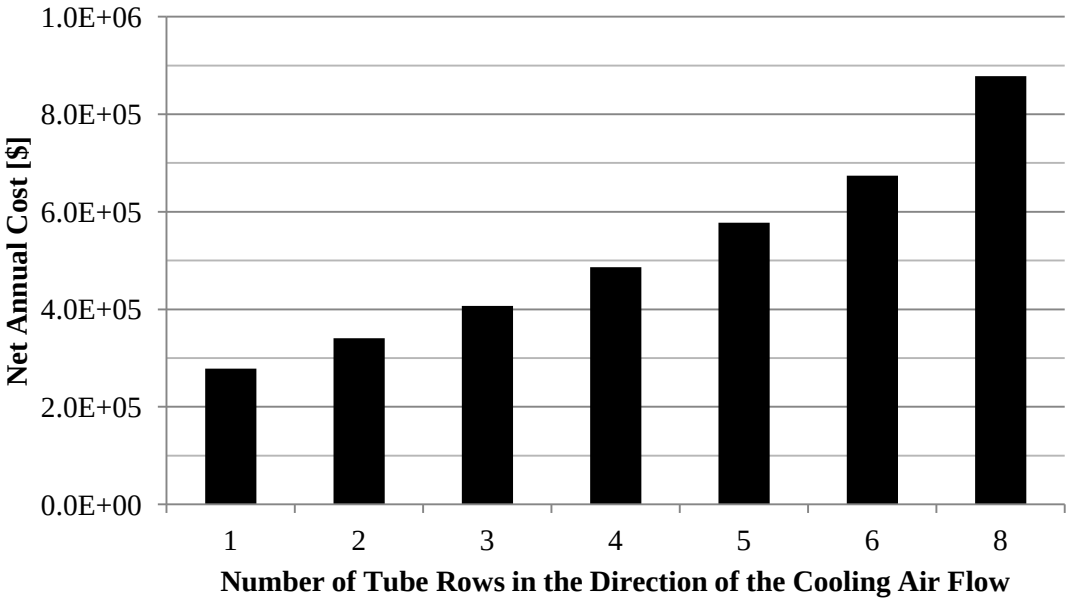

Figure 5.47 - Net annual cost of optimal ACC with increased tube rows.

5.3.2 Optimal Design for ACCs with Additional Tube Rows

The designs in Figure 5.47 all have the same tube geometry and fluid velocities, which are listed in Table 5.15. In this section, the designs were optimized for two, four, six, and eight rows of tubes. This set of optimizations answered the question: does an air-cooled condenser

with multiple rows of tubes have an optimal design different than an air-cooled condenser with one row of tubes?

The process conditions for this investigation were

- Inlet Air Temperature: 75^{o}F
- Inlet Flue Gas Temperature: 135^{o}F
- Inlet Flue Gas Moisture Concentration: 11 percent (wet-basis)

The optimal designs for the four cases are summarized in Table 5.16, and additional details are provided in Appendix B.2. The results indicated that the designs were the same with the exception of increased cooling air velocity for ACCs with more tube rows. In addition, ACCs with more tube rows required longer tubes to maintain condensation efficiency (see Figure 5.43).

Table 5.16 - Optimal design of the ACC with different number of tube rows (50% condensation efficiency).

	ROWS-Case I	**ROWS-Case II**	**ROWS-Case III**	**ROWS-Case IV**
	2	**4**	**6**	**8**
Flue Gas Velocity [ft/sec]	49.9	44	49.7	49
Cooling Air Velocity [ft/sec]	7.5	8.8	9.5	9.4
Fin Pitch [inch]	0.2	0.2	0.2	0.2
Fin Length [inch]	1.25	1.18	1.25	1.25
Inner Tube Diameter [inch]	1.75	1.77	1.75	1.75
Fin Thickness [inch]	0.109	0.104	0.108	0.107
Tube Length [ft]	12	14.3	17.7	22.4
Gas-side Surface Area [ft^2]	157,134	203,798	226,432	289,243
Net Annual Cost	$307,000	$415,000	$537,000	$726,000

The difference in net annual costs is significant between a design that has 2 rows of tubes and one that has 8 rows. This design choice must be made according to the specific application and depends on how large or compact of an ACC is desired. An ACC with two rows of tubes

will require much more space than an ACC with eight rows of tubes. Table 5.17 shows the frontal area of the four designs listed in Table 5.16. The heat exchanger height and width are measured according to Table 5.17. The calculations show that it may be necessary to have many rows in order to package the heat exchanger within a practical amount of space.

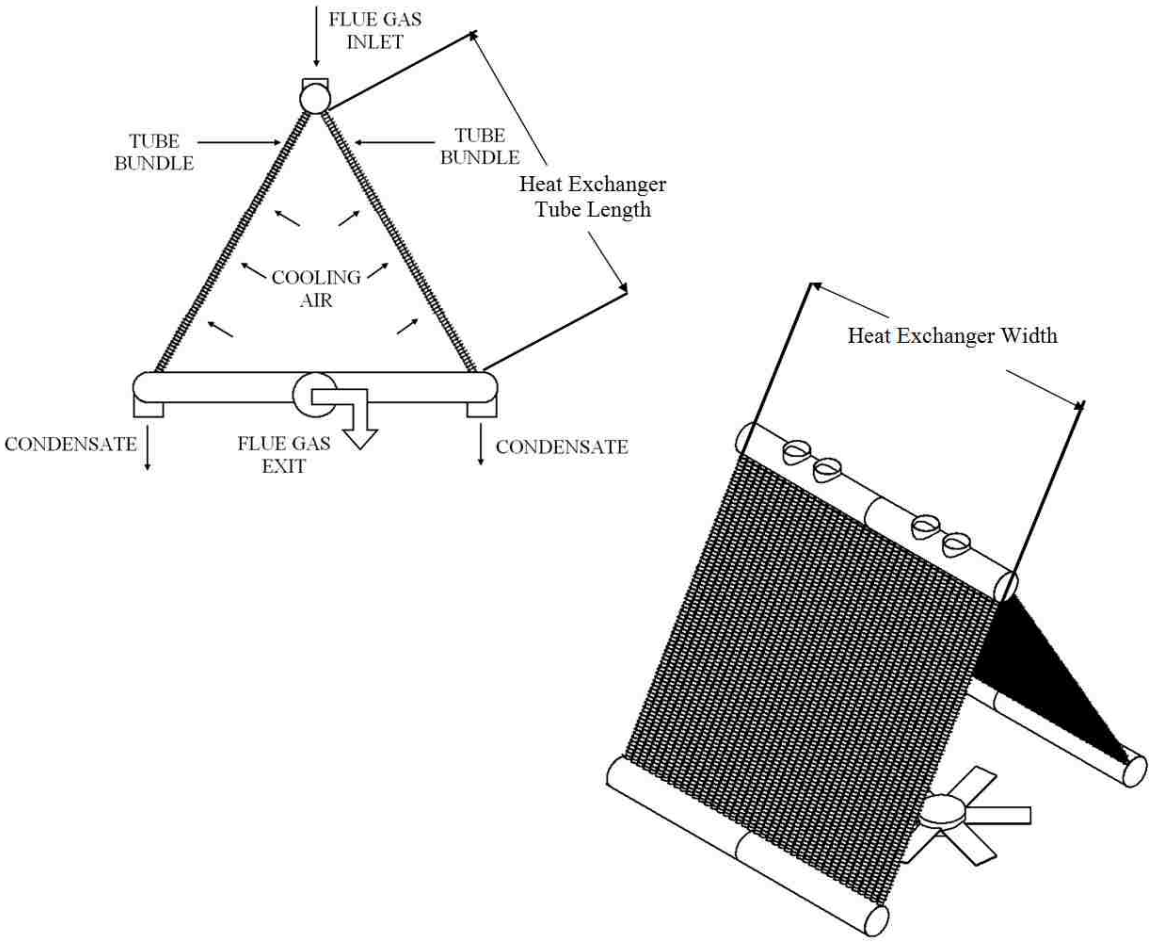

Figure 5.48 - ACC Dimensions.

Table 5.17 - Frontal area of an ACC with increasing numbers of tube rows (see Figure 5.49).

Rows	St	Heat Exchanger Tube Length [ft]	Number of Tubes	Number of Tube Columns	Heat Exchanger Frontal Area (Width * Height)	Heat Exchanger Width [ft]
2	4.65	12	30,000	15,000	69750	2906
4	4.54	14.3	30,000	7,500	40576	1419
6	4.65	17.7	30,000	5,000	34294	969
8	4.64	22.4	30,000	3,750	32480	725

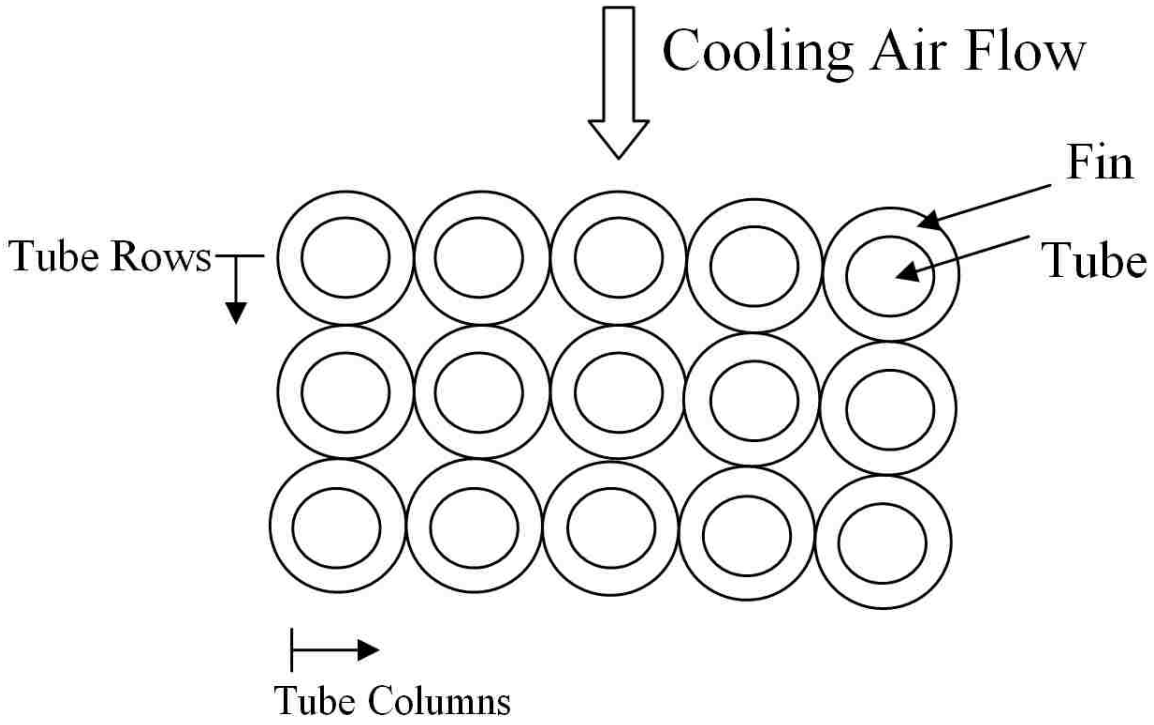

Figure 5.49 - Tube bundle schematic showing 3 tube rows and 5 tube bundles.

5.3.3 Effect of Inlet Cooling Air Temperature on the Optimal Design

The inlet flue gas temperature was held constant at 135^{o}F for subsequent optimizations in which the inlet cooling air temperature was 40^{o}F, 60^{o}F, 75^{o}F, and 90^{o}F. The ACC was optimized for the process conditions listed below.

- Flue Gas Flow Rate: 6,000,000 lbm/hr
- Inlet Flue Gas Temperature: 135^{o}F
- 11 Percent Moisture Concentration
- Two tube rows in each bundle
- Minimum Transverse and Longitudinal Tube Spacing

The range for the six variables being optimized is listed in Table 5.18.

Table 5.18 - Range of variables for the optimization simulations of the ACC for the cases in section 0 and section 5.3.4.

	Minimum	Maximum
Flue gas velocity [ft/sec]	7.5	80
Air velocity [ft/sec]	7.5	50
Fin pitch [inch]	0.20	1.0
Fin length [inch]	0.05	1.25
Inner tube diameter [inch]	1.75	6.0
Fin thickness [inch]	0.0625	0.125
Tube length	Determined by how long the tube must be to condense 50 percent of the water vapor	

The results from the optimizations are summarized in Table 5.19, and details are in Appendix B.3. Notable conclusions from the optimizations were the increase in net annual cost and the increase in the required tube length for cases with higher inlet cooling air temperatures. Power plants in warmer climates will need ACCs with longer tubes. It is important to notice the fact that a different inlet cooling air temperature does not change the optimal design choices for the geometry of the fins or the diameter of the tubes. The details of each of the four heat exchanger designs along with the details of the net annual cost can be found in Appendix B.3.

Table 5.19 - Summary of results from optimization of the ACC for various inlet cooling air temperatures (50% condensation efficiency).

		AIR-Case I	AIR-Case II	AIR-Case III	AIR-Case IV
Inlet cooling air temperature [^{o}F]	Fixed	40	60	75	90
Flue gas velocity [ft/sec]	Optimal	48	53	50	48
Cooling air velocity [ft/sec]	Optimal	7.5	7.5	7.5	7.9
Fin pitch [inch]	Optimal	0.20	0.20	0.20	0.20
Fin length [inch]	Optimal	1.23	1.25	1.25	1.25
Inner tube diameter [inch]	Optimal	1.75	1.75	1.75	1.75
Fin thickness [inch]	Optimal	0.122	0.121	0.109	0.115
Tube length [ft]	Calculated	6.9	8.8	11.7	22.4
Net annual cost	Calculated	$125,764	$193,458	$306,748	$732,000

5.3.4 Effect of Inlet Flue Gas Temperature on the Optimal Design

The temperature of the flue gas entering the ACC will be determined by the design of the water-cooled condenser upstream of the ACC. Figure 5.2 shows the overall flue gas cooling system which consists of the water-cooled heat exchanger followed by the air-cooled heat exchanger. The capacity at which the water-cooled heat exchanger can cool the flue gas will determine the inlet flue gas temperature to the ACC. Therefore, it was of interest to investigate the effect of inlet flue gas temperature on the optimal tube geometry and fluid velocities.

The process conditions for the optimization simulations are listed in Table 5.20, and the ranges for the variables during the optimization were the same as what is listed in Table 5.18.

Table 5.20 - Process conditions for optimization simulations for ACCs with various inlet flue gas temperatures (50% condensation efficiency).

	FG-Case I	FG-Case II	FG-Case III	FG-Case IV	FG-Case V
Inlet Flue Gas Temperature [^{o}F]	135	150	175	200	225
Inlet Cooling Air Temperature [^{o}F]	75	75	75	75	75
Inlet Flue Gas Moisture Concentration (wet-basis)	11 %	11 %	11 %	11 %	11 %

The details of the optimizations are tabulated in Appendix B.4 and summarized in Table 5.21. The results indicated that increasing the inlet flue gas temperature from 135^{o}F to 200^{o}F had very little effect on the overall performance and size of the ACC. The surface area requirements increased slightly with increased inlet flue gas temperature but the amount was relatively small. This net annual cost of the ACC with varying inlet flue gas temperatures remains relatively constant.

Table 5.21 - Summary of results for the optimal design of the ACC with increasing inlet flue gas temperature (50% condensation efficiency).

Test name	NominalTfg 1d	NominalTfg 2d	NominalTfg 3c	NominalTfg 4b	NominalTfg 4b
	FG-Case I	FG-Case II	FG-Case III	FG-Case IV	FG-Case V
Inlet Flue Gas Temperature [^{o}F]	**135**	**150**	**175**	**200**	**225**
Flue gas velocity [ft/sec]	51	50	51	55	50
Cooling air velocity [ft/sec]	7.8	7.7	7.6	8.0	7.9
Fin pitch [inch]	0.20	0.20	0.20	0.20	0.20
Fin length [inch]	1.25	1.25	1.25	1.25	1.25
Inner tube diameter [inch]	1.75	1.75	1.75	1.75	1.76
Fin thickness [inch]	0.112	0.111	0.111	0.121	0.112
Surface Area [ft^{2}]	158,472	165,867	175,747	177,019	196,499
Tube length [ft]	11.8	11.9	12.2	12.7	12.6
Net annual cost	$306,641	$320,045	$342,666	$364,298	$388,339

The recurring result from the optimization simulations were that a small tube diameter with close-packed fins was optimal. A benefit of such a design was that the heat exchanger tubes were relatively short. Recall from Section 5.2 and Figure 5.7 that larger tube diameters required the heat exchanger tubes to be longer to maintain 50 percent condensation efficiency. Ultimately, small diameter tubes resulted in an ACC that was less expensive and more compact. A discussion of the heat transfer and pressure drop is after the following two figures.

Simulations were carried out to show the lower limit of inner tube diameter. Figure 5.50 shows the net annual cost of the ACC when the inner tube diameter of the design "FG-Case I" from Table 5.21 was varied. There was a minimum when the inner tube diameter was approximately 1.50 inches. Figure 5.51 separates the net annual cost into its components, annual operating costs, capital cost, and estimated savings due to water recovery. During the optimization simulations, the inner tube diameter was limited to a minimum of 1.75 inches. This minimum was to avoid singularity in Equations 1.17 and 1.18.

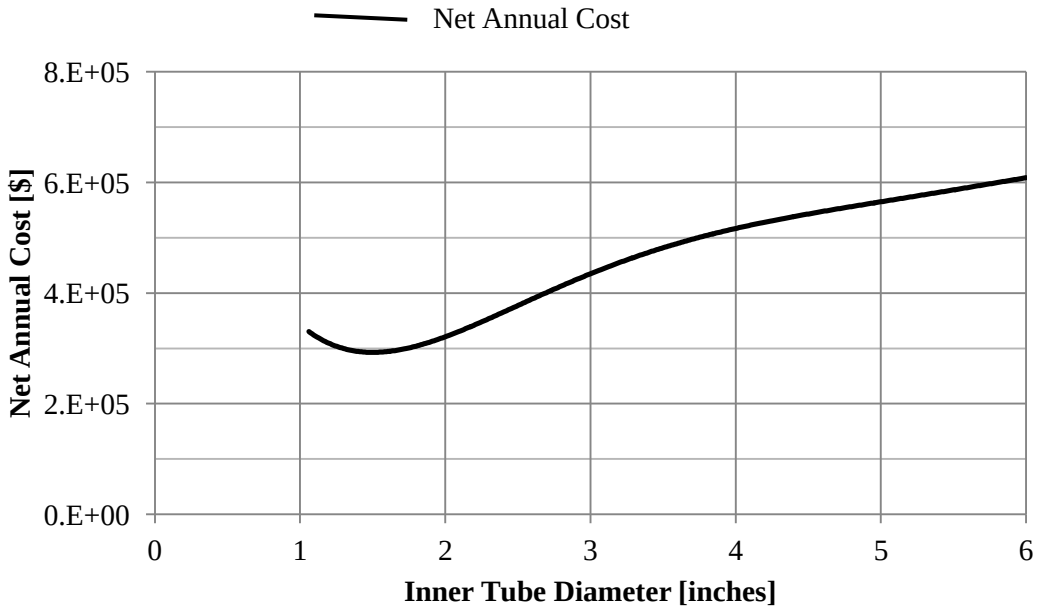

Figure 5.50 - Parametric simulation for FG-Case I from Table 5.21.

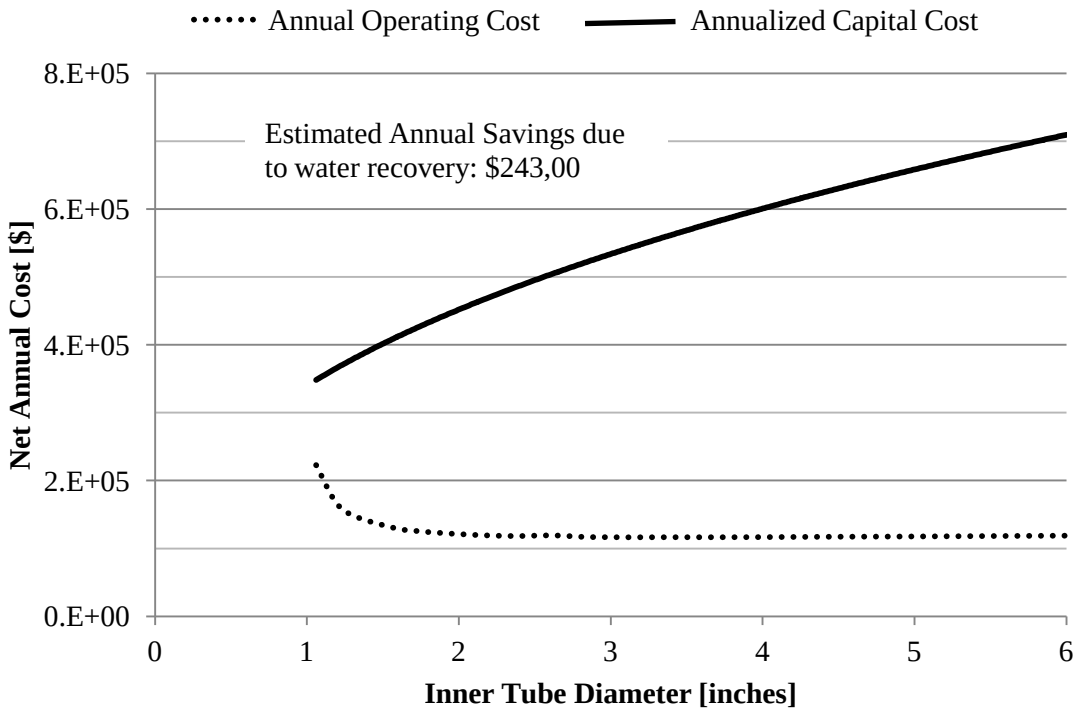

Figure 5.51 - Parametric simulation for FG-Case I from Figure 5.20.

Increasing the tube diameter had the effect of decreasing the heat transfer coefficients for both the gas side and the air side. The respective heat transfer coefficients for the simulations shown in Figure 5.50 and Figure 5.51 is in Figure 5.52. With increasing tube diameter, the heat transfer coefficient does decrease. For turbulent flow, the heat transfer coefficient is proportional to the tube diameter as $1/OD^{0.4}$ (seen from Equations 1.12 and 1.13).

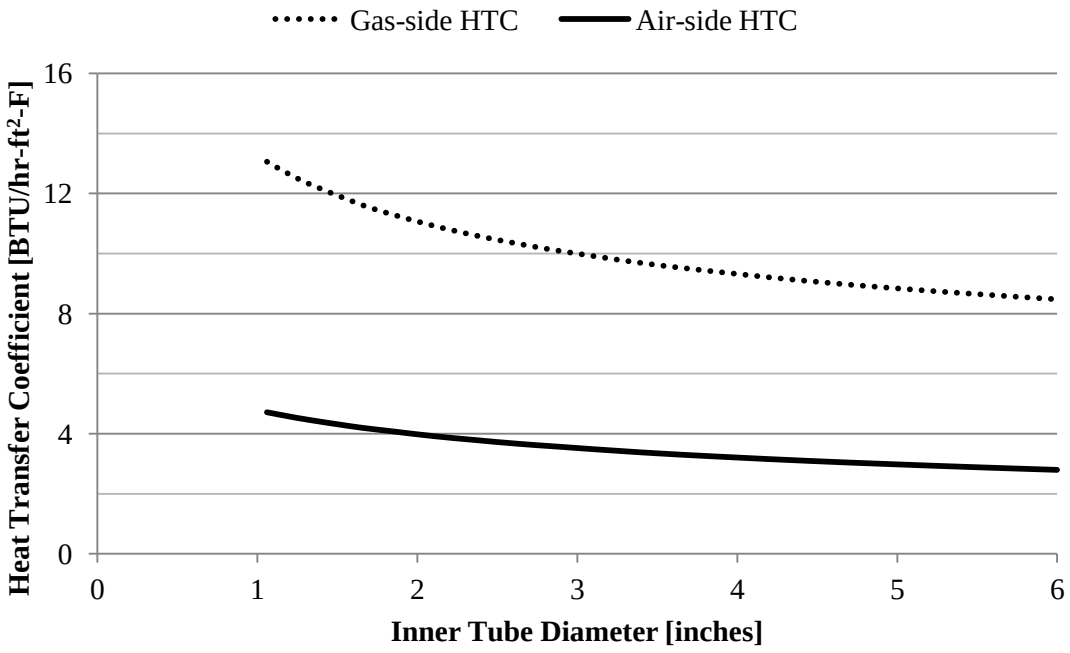

Figure 5.52 - Heat transfer coefficients for increasing tube diameter.

The pressure drop of both the cooling air and flue gas is affected by a change in tube diameter. Equation 1.21 shows the pressure gradient of the flue gas inside the tubes, and the pressure gradient increases with decreasing tube diameter. This is shown in Figure 5.53. However, decreasing the tube diameter also means that the tubes can be shorter and still condense the same quantity of water. Figure 5.54 shows the tube length to condense 50% of the water vapor. A 1 inch diameter tube requires much less tubing than a 6 inch diameter tube. Therefore, even though the pressure gradient is larger for a small diameter tube, the tubes are much shorter, and the two effects counteract. Figure 5.55 shows the overall pressure drop in inches of water.

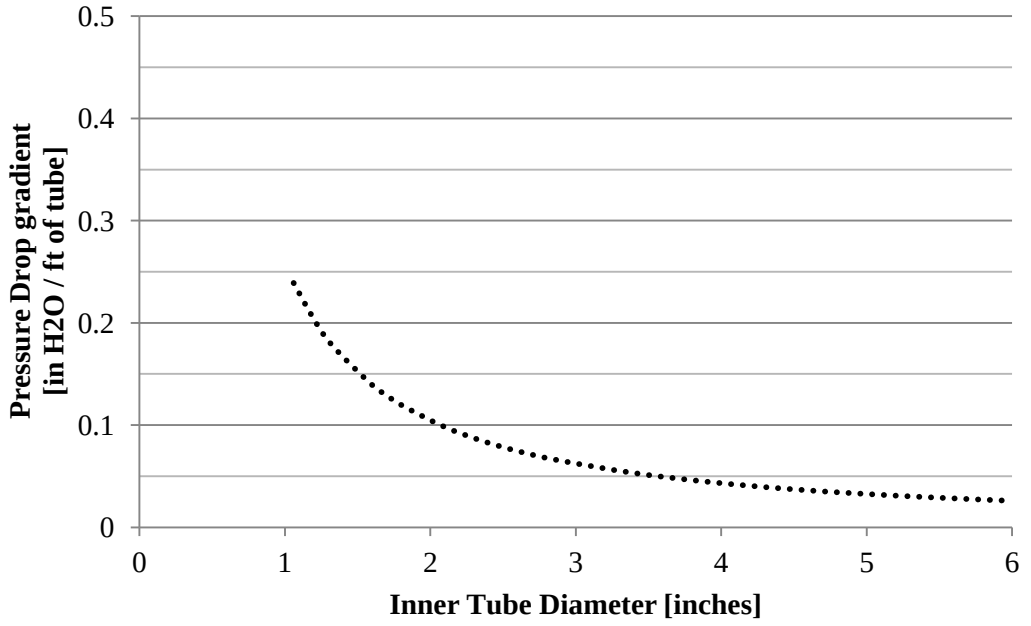

Figure 5.53 - Pressure gradient of flue gas for various tube diameters.

Figure 5.54 - Tube length necessary to condense 50% of the water vapor.

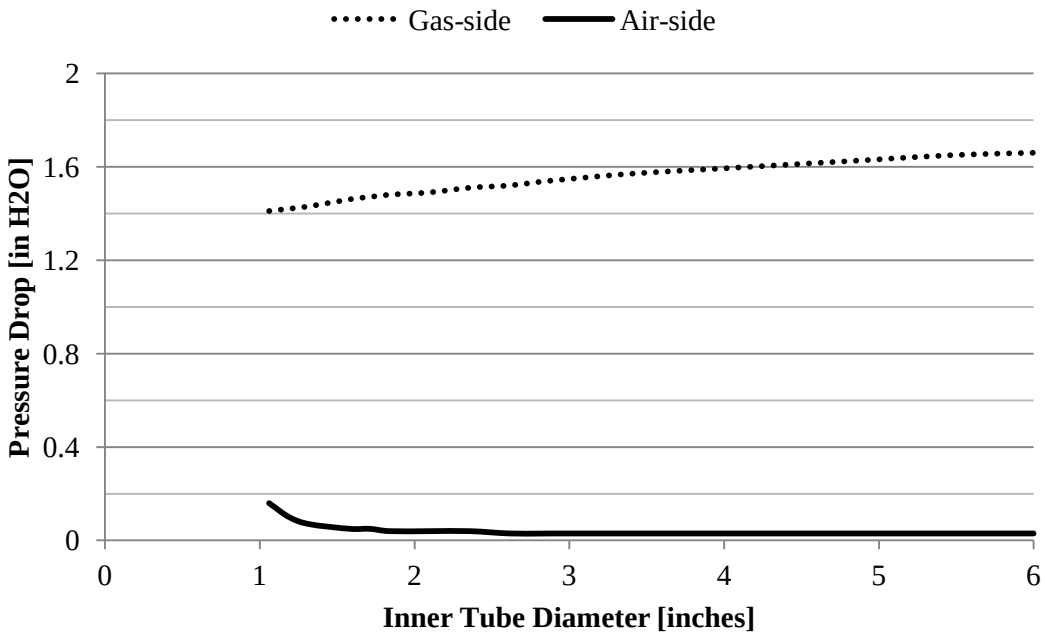

Figure 5.55 - Pressure drop of the cooling air and flue gas for the ACC when 50% of the water is condensed.

5.4 Optimal Design of the Flue Gas Air-Cooled Condenser for the Case with a Flue Gas Desulfurization System

Section 5.3 discussed optimizing the flue gas condenser for the case in which the flue gas enters the air-cooled condenser (ACC) with a moisture concentration of 11 percent. Another case, which is described in this section, is where the flue gas enters the ACC saturated with water vapor. Such a case exists when there is a wet flue gas desulfurization (FGD) system to remove SO_2 from the flue gas. In an FGD system, the flue gas is scrubbed with a slurry mixture of limestone and water and when the flue gas exits the FGD system it is saturated with water at a temperature of approximately 135°F. After exiting the wet FGD system, the flue gas would be processed by a series of flue gas condensers to recover water vapor and energy.

The complete flue gas condenser system is shown conceptually in Figure 5.56. First the flue gas flows through a water-cooled heat exchanger, then is processed by the ACC. The proposed configuration of the heat exchangers is shown in Figure 5.57. Boiler feed-water is used as the coolant for the water cooled heat exchanger and ambient air is used as the coolant for the ACC. An analysis of the water-cooled condensers using the model developed by Jeong et al. [13-14] showed that the water cooled condenser could cool the flue gas from 135°F to 128°F. For the present study, the flue gas was assumed to be saturated at 128°F when entering the ACC.

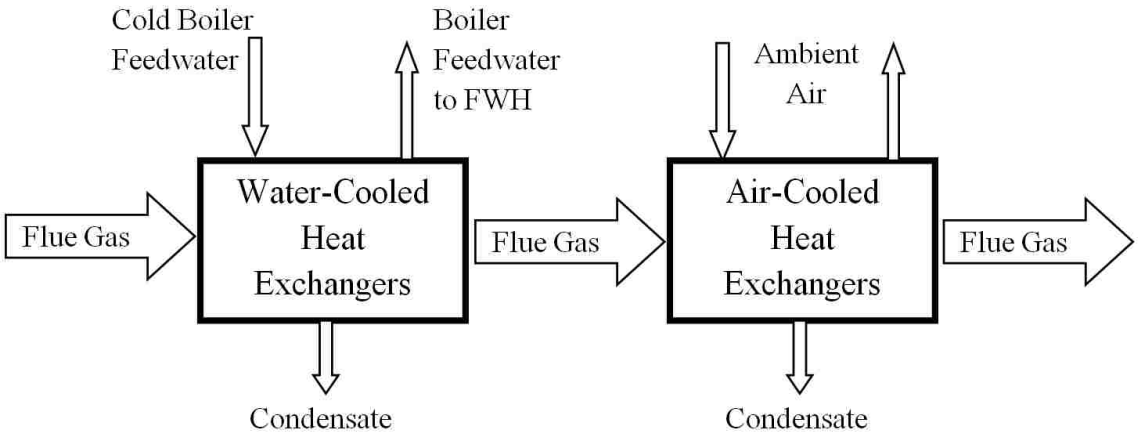

Figure 5.56 - Conceptual design of water-cooled and air-cooled heat exchanger system

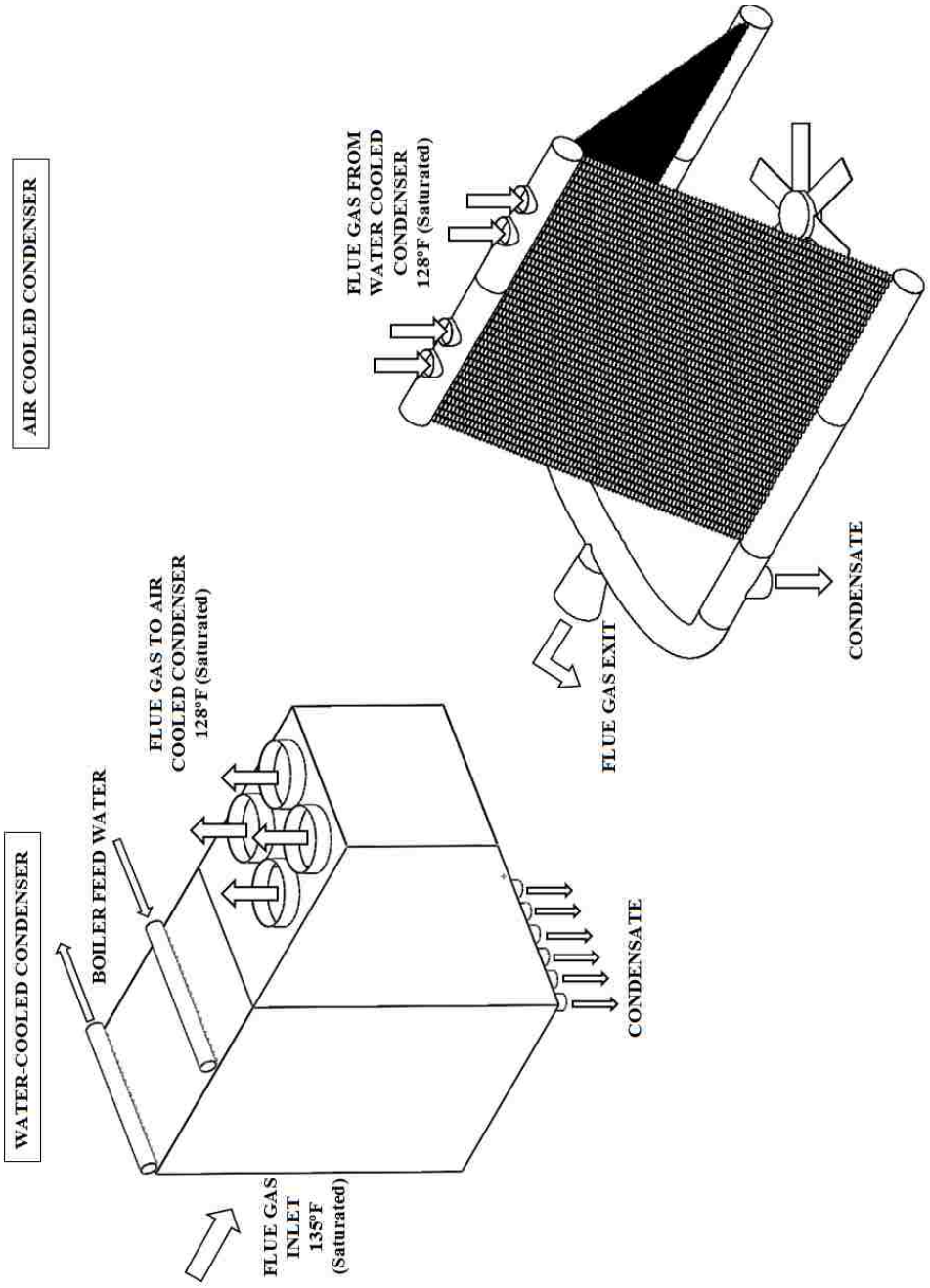

Figure 5.57 - Proposed design of water-cooled and air-cooled heat exchanger system when a wet FGD system is installed

The design discussed in this section utilized the cost calculation procedure presented in Section 5.1. One optimization simulation studied in the present research had the process conditions listed below.

- Inlet Flue Gas Temperature: 128^{o}F
- Inlet Flue Gas Moisture Concentration: 14.4% (saturated on a wet-basis)
- Inlet Cooling Air Temperature: 75^{o}F
- Flue Gas Flow Rate: 6,000,000 lbm/hr
- Desired Condensation Efficiency - approximately 55 percent.

Recall that the optimization simulation required the user to select a desired condensation efficiency to determine how long the tubes must be. This was discussed in Section 5.1

The results from this optimization are summarized in Table 5.22. The geometry of the tubes was the same as the case with no wet FGD scrubber (described in Section 5.3), which is a small diameter tube with small spacing between fins. The cooling air velocity was approximately 8 ft/sec and the flue gas velocity was 46 ft/sec, which are comparable velocities to the case with no wet FGD system.

The cost of this ACC, also tabulated in Table 5.22, does not include potential water treatment costs. The net annual cost for this design was estimated to be $241,000 when water is valued at $1.50 per 1000 gallons.

In the next discussion in Section 5.4.1, the desired condensation efficiency was varied to determine how the condensation efficiency affected the optimal design

Table 5.22 - Optimal ACC when there is a wet FGD system. Additional details in the Appendix.

Test name: Nominal128_saturated_60d	
Flue Gas Flow Rate [lbm/hr]	6,000,000
Vapor Flow Rate [lbm/hr]	532,881
Cooling Air Flow Rate [lbm/hr]	63,700,259
Flue Gas Velocity [ft/sec]	46.2
Cooling Air Velocity [ft/sec]	7.8
Inlet Flue Gas Temperature [^{o}F]	128
Inlet Cooling Air Temperature [^{o}F]	75
Tube Inner Diameter [inch]	1.75
Tube Thickness [inch]	0.2
Fin Length [inch]	1.25
Fin Pitch [inch]	0.2
Fin Thickness [inch]	0.11
Number of Tube Rows	2
Transverse Tube Spacing [inch]	4.65
Longitudinal Tube Spacing [inch]	4.65
Number of Tubes	29000
Tube Length [ft]	14.2
Gas-side Surface Area [ft^2]	190,136
Air-side Surface Area [ft^2]	9,899,044
Field Erected Capital Cost	$6,026,921
Annualized Capital Cost for 20 years repayment at 5% interest.	$483,616
Annualized Operating Cost	$135,538
Estimated Annual Savings in Water Costs @ $1.50 per 1000 gallon	$378,408
Net Annualized Cost [20 yrs @ 5%]	$240,746
Sensible Heat Transfer [BTU/hr]	44,181,735
Latent Heat Transfer [BTU/hr]	312,946,275
Condensation Rate [lbm/hr]	300,623
Condensation Efficiency	56%

5.4.1 Effect of Changing the Desired Condensation Efficiency

In the optimization simulations the size of the air-cooled condenser (ACC) was determined by how much surface area was required to condense a certain quantity of water vapor. Increasing the required condensation efficiency of the ACC required more surface area, and this section discusses the effects on cost. Process conditions for optimization simulations to determine the effect of varying the condensation efficiency were:

- Inlet Flue Gas Temperature – 128^{o}F
- Inlet Flue Gas Moisture Concentration – 14.4% (saturated on a wet-basis)
- Inlet Cooling Air Temperatures – two cases: 75^{o}F and 60^{o}F

The optimal designs of the ACC for this application are listed in Table 5.23 and Table 5.24, with details in Appendix B.5. The two tables correspond to inlet cooling air temperatures of 75^{o}F and 60^{o}F respectively. In the tables, each column represents different condensation efficiencies. For example, the first column, which the desired condensation efficiency was 23 percent, was the least expensive design, and as the desired condensation efficiency was increased, so was the net annual cost.

Figure 5.58 shows how it becomes increasingly more expensive to recover larger quantities of water vapor from the flue gas. To increase condensation efficiency over 60 percent required substantial increases in net annual cost. For example, increasing the condensation efficiency from 60 percent to 70 percent required doubling the net annual cost of the ACC when the inlet cooling air temperature was 75^{o}F. Figure 5.59 plots the corresponding condensation rates. Nonetheless, this design, which corresponds to a 600 MW power plant, can recover up to 400,000 lbm/hr (800 GPM) or water vapor.

Figure 5.60 shows the total heat transfer to the cooling air. This information is useful should the energy recovered be used in another process in the power plant (e.g. pre-heating combustion air). In addition, the graph shows that a lower inlet cooling air temperature substantially reduced the cost of recovering the energy.

Table 5.23 – Summary of results for the optimal design of the ACC with the inlet flue gas in a saturated state and inlet cooling air temperature of 75^{o}F. Additional information found in Appendix

Test Name	75_25d	75_40d	75_50d	75_60d	75_69d	75_75a
Condensation Efficiency	22.6%	36.7%	46.2%	56.4%	66.3%	73.2%
Inlet Flue Gas Moisture Concentration [wet-basis]	14.4%	14.4%	14.4%	14.4%	14.4%	14.4%
Exit Flue Gas Moisture Concentration [wet-basis]	11.60%	9.67%	8.34%	6.86%	5.39%	4.33%
Flue Gas Velocity [ft/sec]	39	43	50.7	50.4	45.3	53.2
Cooling Air Velocity [ft/sec]	9.4	9	8.2	7.6	7.8	7.5
Fin Pitch [inch]	0.2	0.2	0.2	0.2	0.2	0.2
Fin Length [inch]	1.25	1.25	1.25	1.25	1.25	1.25
Inner Tube Diameter [inch]	1.75	1.75	1.75	1.75	1.75	1.75
Fin Thickness [inch]	0.099	0.111	0.114	0.110	0.110	0.117
Gas-Side Surface Area [ft^2]	50,087	94,705	130,636	190,136	271,240	354,471
Tube Length [ft]	3	6.3	9.8	14.2	20.2	27.9
Total Heat Transfer to Cooling Air [MBTU/hr]	141	230	291	357	423	470
Net Annual Cost	$67,892	$113,574	$162,861	$240,746	$404,031	$647,151

Table 5.24 - Summary of results for the optimal design of the ACC with the inlet flue gas in a saturated state and inlet cooling air temperature of 60^{o}F

Test Name	60_25c	60_40d	60_50d	60_60a	60_69a	60_75c
Condensation Efficiency	23.1%	37.1%	47.0%	56.6%	66.3%	72.8%
Inlet Flue Gas Moisture Concentration [wet-basis]	14.4%	14.4%	14.4%	14.4%	14.4%	14.4%
Exit Flue Gas Moisture Concentration [wet-basis]	11.5%	9.63%	8.23%	6.84%	5.40%	4.40%
Flue Gas Velocity [ft/sec]	37.8	43.6	46	46	47.6	45
Cooling Air Velocity [ft/sec]	9	8.6	8.2	7.8	8.2	7.7
Fin Pitch [inch]	0.2	0.2	0.2	0.2	0.2	0.2
Fin Length [inch]	1.25	1.25	1.25	1.25	1.25	1.25
Inner Tube Diameter [inch]	1.75	1.75	1.75	1.75	1.75	1.75
Fin Thickness [inch]	0.0973	0.111	0.111	0.119	0.115	0.109
Gas-Side Surface Area [ft^2]	42,867	77,000	107,895	148,238	194,333	251,996
Tube Length [ft]	2.5	5.3	7.9	11	15.2	19
Total Heat Transfer to Cooling Air [MBTU/hr]	147	237	301	365	430	475
Net Annual Cost	$37,593	$60,075	$87,321	$129,745	$198,949	$300,223

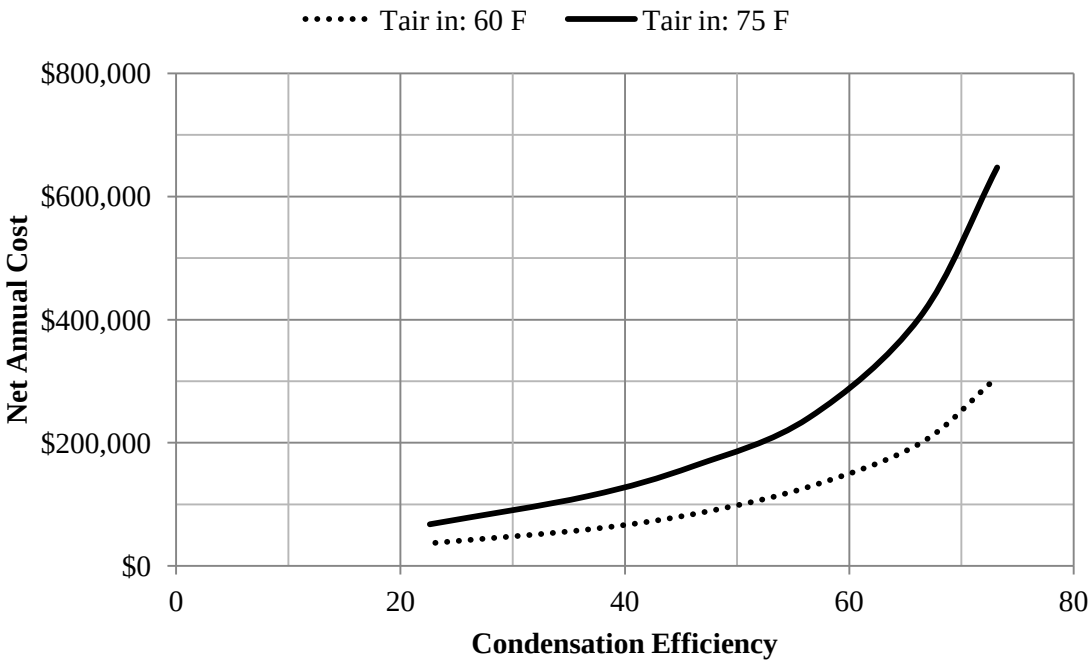

Figure 5.58 – Net annual cost versus condensation efficiency for the case with a saturated flue gas.

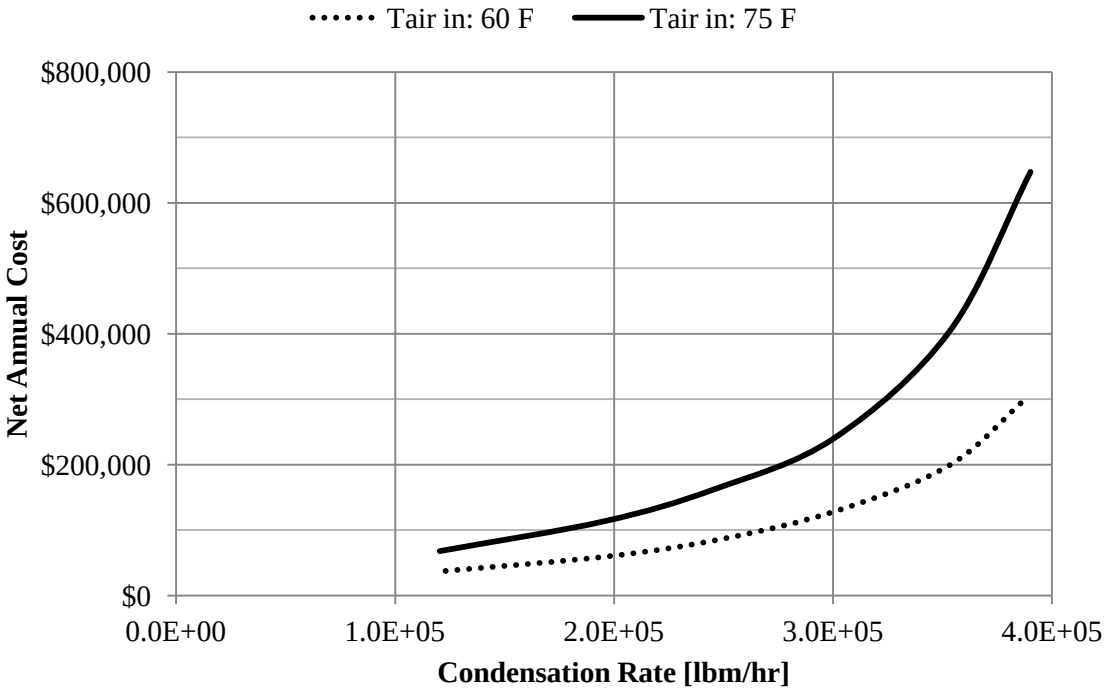

Figure 5.59 – Net annual cost versus condensation rate for the case with a saturated flue gas.

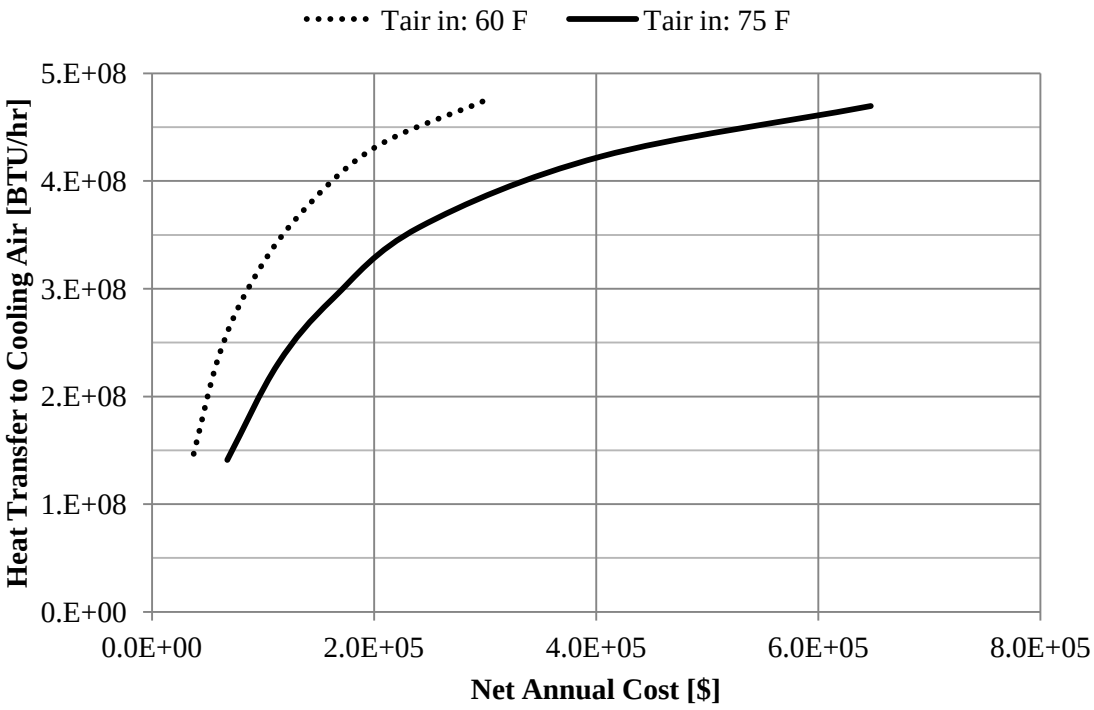

Figure 5.60 - Heat transfer to cooling air versus net annual cost for the case with a saturated flue gas.

5.4.2 The Effect due to Rising Costs of Water

One assumption made throughout the simulations presented in this dissertation was that water will cost $1.50 per 1000 gallons. However, in reality the cost of water depends on the location of the power plant and many other factors, and a single value cannot be assumed to represent all applications.

Table 5.25 describes the details of two ACCs which were used to investigate the effects of changing the value of recovering water. The difference between the two designs is the inlet cooling air temperature. In both cases, the condensation efficiency was approximately 57 percent, or 300,000 lbm/hr (600 GPM). The net annualized cost of the two heat exchangers was $130,00 and $240,000 for an inlet cooling air temperature of 60 and 75^{o}F respectively.

Table 5.25 - Heat exchanger designs to study effects of water costs (taken from Appendix B.5 for the cases with a condensation efficiency of approximately 60 perecnt).

Inlet Cooling Air Temperature [^{o}F]	**60**	**75**
Flue Gas Flow Rate [lbm/hr]	6,000,000	6,000,000
Vapor Flow Rate [lbm/hr]	532,881	532,881
Cooling Air Flow Rate [lbm/hr]	49,252,766	63,700,259
Flue Gas Velocity [ft/sec]	46.0	46.2
Cooling Air Velocity [ft/sec]	7.8	7.8
Inlet Flue Gas Temperature [^{o}F]	128	128
Inlet Cooling Air Temperature [^{o}F]	60	75
Tube Inner Diameter [inch]	1.75	1.75
Tube Thickness [inch]	0.2	0.2
Fin Length	1.25.	1.25
Fin Pitch [inch]	0.2	0.2
Fin Thickness [inch]	0.119	0.11
Number of Tube Rows	2	2
Transverse Tube Spacing [inch]	4.65	4.65
Longitudinal Tube Spacing [inch]	4.65	4.65
Number of Tubes	29,000	29,000
Tube Length [ft]	11.0	14.2
Gas-side Surface Area [ft^2]	148,238	190,136
Air-side Surface Area [ft^2]	7,749,020	9,899,044
Field Erected Capital Cost	$4,938,680	$6,026,921
Annualized Capital Cost	$396,292	$483,616
Annualized Operating Cost	$113,375	$135,538
Estimated Annual Savings if Water Costs @ $1.50 per 1000 gallon	$379,922	$378,408
Net Annualized Cost [20 yrs @ 5%]	$129,745	$240,746
Sensible Heat Transfer [BTU/hr]	49,215,407	44,181,735
Latent Heat Transfer [BTU/hr]	315,866,487	312,946,275
Condensation Rate [lbm/hr]	301,826	300,623
Condensation Efficiency	57%	56%

Table 5.25 lists the estimated annual savings by recovering water at $1.50 per 1000 gallons. If the cost of water was a different rate, this would affect the net annualized cost of the

ACC. Figure 5.61 shows how the net annualized cost varied based on what water is worth. However, an additional cost associated with recovering water that was not assessed in this model was water treatment costs.

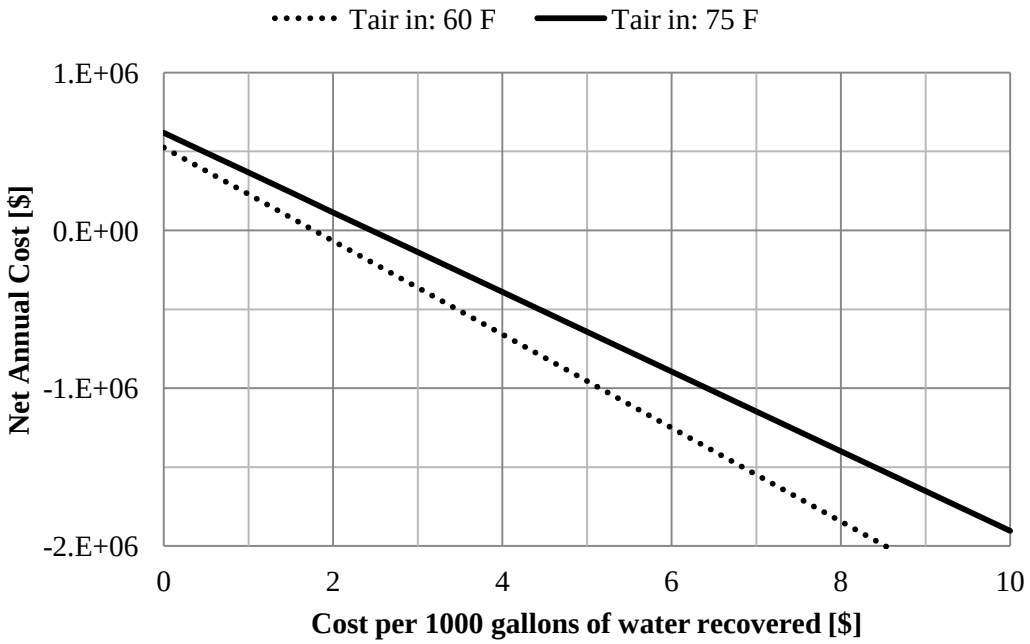

Figure 5.61 - Net annual cost of the ACC for increased values of water recovery.

These investigations were extended to the cases when the water vapor condensation efficiency varied from 22 percent to 73 percent, and this is shown in Table 5.26 for the case when the inlet cooling air temperature was 60^{o}F, and Table 5.27 when the inlet cooling air temperature was 75^{o}F. The columns represent heat exchangers with more surface area and a greater condensation efficiency, and the rows list what the water savings could be if the value of water increased, neglecting water treatment costs. The last two rows of the tables list the annualized capital cost of the ACC over 20 years at a 5 percent interest rate and the operating costs of the flue gas and cooling air fans.

Table 5.26 - Costs associated with operating the ACC for cases when water is increasingly expensive (inlet cooling air temperature of 60°F).

Test Name	60_25c	60_40d	60_50d	60_60a	60_69a	60_75c
Condensation Efficiency [%]	**23.1**	**37.1**	**47**	**56.6**	**66.3**	**72.8**
Condensation Rate [lbm/hr]	123,022	197,726	250,598	301,826	353,090	387,808
Inlet Water Vapor Flow Rate [lbm/hr]	533,000	533,000	533,000	533,000	533,000	533,000
Annual Savings in Water Recovery at $0.0 per 1000 Gallons	$0	$0	$0	$0	$0	$0
Annual Savings in Water Recovery at $0.50 per 1000 Gallons	$51,618	$82,962	$105,146	$126,641	$148,150	$162,717
Annual Savings in Water Recovery at $1.00 per 1000 Gallons	$103,236	$165,925	$210,293	$253,282	$296,301	$325,435
Annual Savings in Water Recovery at $1.50 per 1000 Gallons	$154,854	$248,887	$315,439	$379,922	$444,451	$488,152
Annual Savings in Water Recovery at $2.00 per 1000 Gallons	$206,471	$331,849	$420,586	$506,563	$592,601	$650,869
Annual Savings in Water Recovery at $3.00 per 1000 Gallons	$309,707	$497,774	$630,879	$759,845	$888,902	$976,304
Annual Savings in Water Recovery at $5.00 per 1000 Gallons	$516,178	$829,623	$1,051,465	$1,266,408	$1,481,503	$1,627,173
Annual Savings in Water Recovery at $10.00 per 1000 Gallons	$1,032,357	$1,659,246	$2,102,929	$2,532,816	$2,963,005	$3,254,346
Annualized Capital Cost over 20 years	$146,874	$234,661	$307,361	$396,292	$492,136	$628,255
Operating Costs of the Flue Gas and Cooling Air Fans	$45,572	$74,301	$95,399	$129,745	$151,263	$160,120

Table 5.27 - Costs associated with operating the ACC for cases when water is increasingly expensive (inlet cooling air temperature of 75°F).

Test Name	75_25	75_40	75_50	75_60	75_69	75_75
Condensation Efficiency [%]	**22.6**	**36.7**	**46.2**	**56.4**	**66.3**	**73.2**
Condensation Rate [lbm/hr]	120,403	195,603	246,150	300,623	353,251	390,086
Inlet Water Vapor Flow Rate [lbm/hr]	533,000	533,000	533,000	533,000	533,000	533,000
Annual Savings in Water Recovery at $0.0 per 1000 Gallons	$0	$0	$0	$0	$0	$0
Annual Savings in Water Recovery at $0.50 per 1000 Gallons	$50,519	$82,072	$103,280	$126,136	$148,218	$163,673
Annual Savings in Water Recovery at $1.00 per 1000 Gallons	$101,038	$164,143	$206,560	$252,272	$296,436	$327,346
Annual Savings in Water Recovery at $1.50 per 1000 Gallons	$151,557	$246,215	$309,840	$378,408	$444,653	$491,019
Annual Savings in Water Recovery at $2.00 per 1000 Gallons	$202,076	$328,286	$413,121	$504,544	$592,871	$654,693
Annual Savings in Water Recovery at $3.00 per 1000 Gallons	$303,114	$492,429	$619,681	$756,816	$889,307	$982,039
Annual Savings in Water Recovery at $5.00 per 1000 Gallons	$505,190	$820,715	$1,032,801	$1,261,360	$1,482,178	$1,636,731
Annual Savings in Water Recovery at $10.00 per 1000 Gallons	$1,010,379	$1,641,431	$2,065,603	$2,522,721	$2,964,356	$3,273,463
Annualized Capital Cost over 20 years	$166,352	$276,915	$358,177	$483,616	$676,304	$901,165
Operating Costs of the Flue Gas and Cooling Air Fan	$53,097	$82,873	$114,525	$135,538	$172,380	$237,003

6 Design of a Full Scale Flue Gas Air-Heater

This chapter discusses the application of the air-cooled condenser pre-heating boiler combustion air. The efficiency of a boiler is affected by the inlet temperature of the combustion air, and an increase in the inlet temperature of the combustion air would positively affect the efficiency of the boiler and subsequently the heat rate of the power plant.

The proposed configuration is shown in Figure 6.1 and Figure 6.2. The flue gas flows first through a water-cooled condenser to pre-heat boiler feed water then enters the air heater to pre-heat combustion air. In the air heater the flue gas flows inside vertical tubes and combustion air flows through a duct around the tubes. Since moisture is condensing from the flue gas into a collection basin, flue gas will flow downward through the tubes to prevent the possibility of slug or churn flow. To offset the imbalance in heat transfer coefficients between the combustion air and flue gas, the circular tubes will have fins on the air side. The air heater would be placed downstream of any baghouse, ESP, FGD system, and water-cooled flue gas condenser, and the state of the flue gas would be dependent on which of these systems are installed.

Section 6.1 discusses the calculation procedure to determine the size and cost of the air heater and Section 6.2 discusses two different case studies, each with a different inlet flue gas temperature. Detailed results from the optimizations in Section 6.2 can be found in Appendix B.6. Section 6.3 discusses the reduction in fuel consumption due to incorporating the air heater into a power plant.

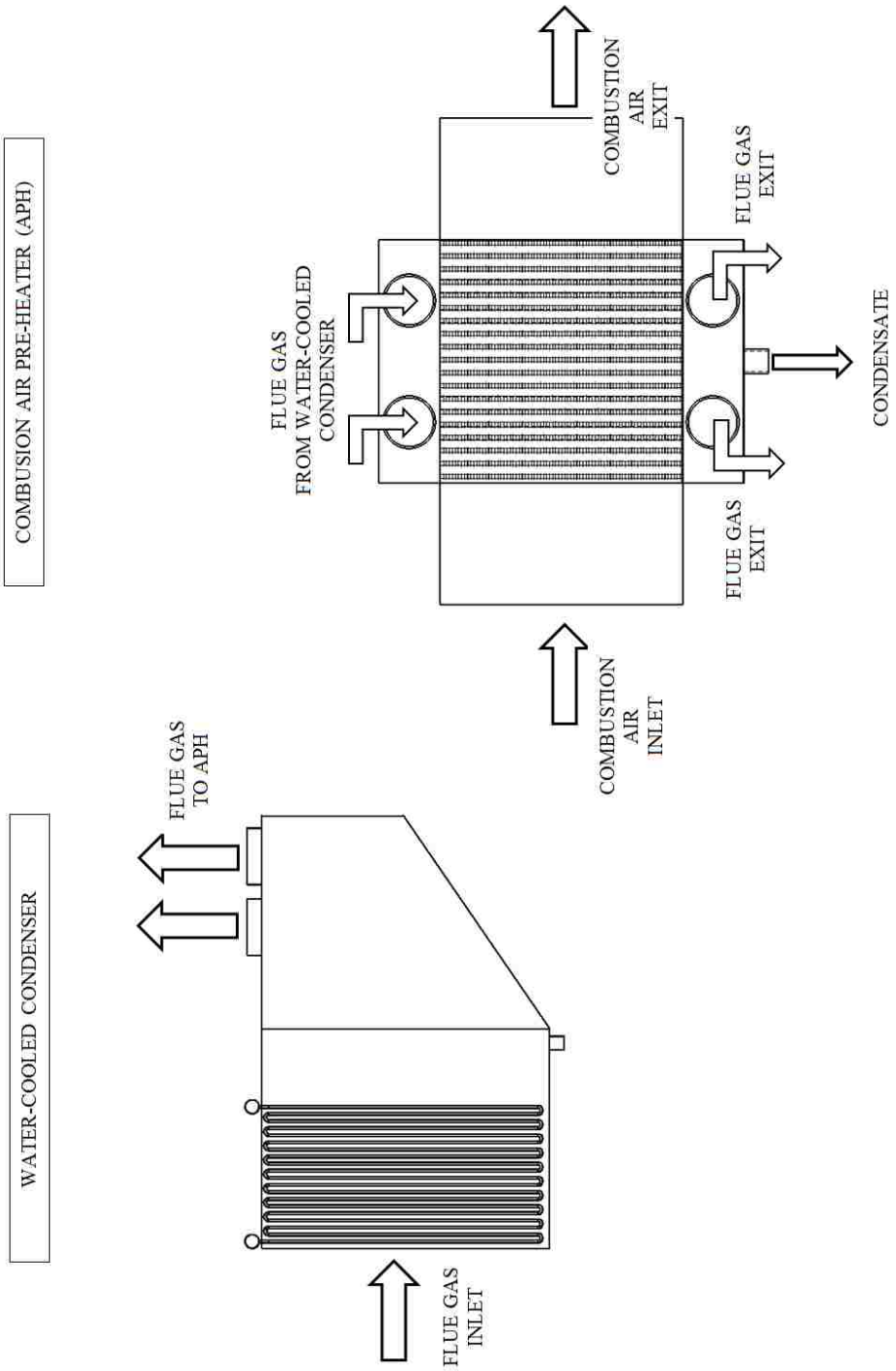

Figure 6.1 - Side view of flue gas condensing system when the combustion air is pre-heated.

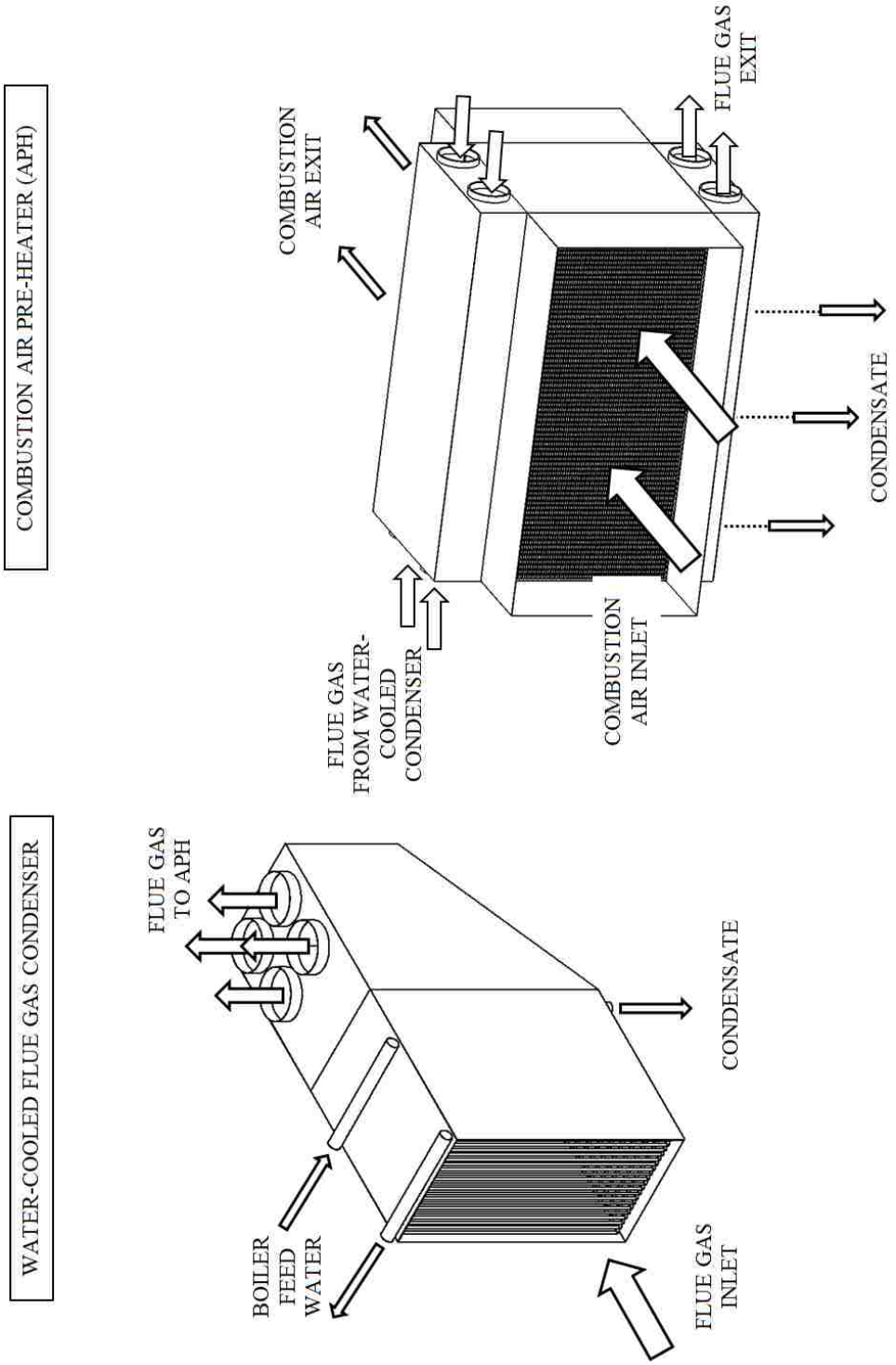

Figure 6.2 - Isometric view of flue gas condensing system when combustion air is pre-heated.

6.1 Calculation Procedure to Determine the Size and Cost of the Air Heater

The size of the air heater was determined by the tube geometry and combustion air velocity. Equations 6.1 and 6.2 show how the cross sectional area and duct width were calculated.

$$CSA_{duct} = \frac{\dot{m}_{air}}{\rho_{air} V_{air}} \tag{6.1}$$

$$Duct\ Height = \frac{CSA_{duct}}{Tube\ Length} \tag{6.2}$$

$$Duct\ Width = \frac{CSA_{duct}}{Duct\ Height} \tag{6.3}$$

where CSA_{duct} is the cross sectional area of the duct carrying the combustion air.

The number of rows in the air heater was determined using the heat and mass transfer simulation described in Chapter 2, employing the condition that the number of tube rows in the direction of the air flow was the necessary amount to increase the combustion air temperature to the desired value. As a result, all of the flue gas is not processed. In some cases, only 25 or 40 percent of the flue gas would be necessary. The benefit of this is a smaller and less expensive system. The total flue gas flow rate of the ACC was calculated after determining the number of tubes and flow rate of flue gas through each tube.

The configuration of the air heater was inline finned tubes as opposed to the ACC described in Chapter 5, which had staggered fin tubes. The air heater had more rows of tubes than the design proposed in Chapter 5, and according to experiments performed by Zhukauskus, the ratio of heat transfer to pressure drop for inline configurations is higher than staggered configurations for bundles that have more than 10 rows of tubes [47].

The heat transfer correlations used for the combustion air side were Equations 6.4 and 6.5, dependent on air-side Reynolds number.

$$Nu_{N_L>16} = 0.3 + \frac{0.62 * {Re_{film}}^{1/2} {Pr_{film}}^{1/3}}{\left[1 + \left(0.4/Pr_{film}\right)^{2/3}\right]^{1/4}} \left[1 + \left(\frac{Re_{film}}{282000}\right)^{5/8}\right]^{4/5}$$
$$Re_{film} = \frac{\rho_{film} V * OD}{\mu_{film}} < 1000 \tag{6.4}$$

$$Nu_{N_L>16} = 0.27 {Re_{mean}}^{0.63} {Pr_{mean}}^{0.36} \left(\frac{Pr_{mean}}{Pr_s}\right)^{1/4}$$
$$1000 < Re_{film} < 2{,}000{,}000 \tag{6.5}$$
$$S_t/S_l > 0.7$$

where $Nu_{N_L>16}$ is the fully developed Nusselt number, *film* refers to evaluating the properties at the film temperature, which is the average of the air and tube surface temperatures, *mean* refers to evaluating the property at the average of the inlet and exit air temperatures, and '*s*' corresponds to the property being evaluated at the tube surface temperature, S_t and S_l refer to the transverse and longitudinal tube spacing respectively. The correction for bundles with less than 16 rows was given by Equation 6.6 using the correction factors in Table 6.1, where N_L is the number of rows.

$$Nu = C_2 Nu_{N_L>16} \tag{6.6}$$

Table 6.1 – Correction factors C_2 for Nusselt Numbers when there are less than 17 rows of tubes.

	C_2								
N_L	**1**	**2**	**3**	**4**	**5**	**7**	**10**	**13**	**16**
Aligned Tubes	0.7	0.8	0.86	0.9	0.92	0.95	0.97	0.98	0.99
Staggered Tubes	0.64	0.76	0.84	0.89	0.92	0.95	0.97	0.98	0.99

The heat transfer coefficient for the air-side is Equation 6.7.

$$h_a = \frac{Nu * OD}{k} \tag{6.7}$$

The fins were accounted for by determining the fin efficiency (Equation 6.8) [39].

$$\eta_F = \frac{2r_1}{m(r_{2c}^2 - r_1^2)} \frac{K_1(mr_1)I_1(mr_{2c}) - I_1(mr_1)K_1(mr_{2c})}{I_0(mr_1)K_1(mr_{2c}) - K_0(mr_1)I_1(mr_{2c})} \tag{6.8}$$

where I_0 and K_0 are modified, zero-order Bessel functions of the first and second kind, and I_1 and K_1 are modified, first-order Bessel functions of the first and second kind, $r_1$refers to the inner radius of the fin and r_{2c} refers to the summation of the outer radius of the fin and half the fin thickness. The overall surface efficiency η_o was calculated using Equation 6.9 to account for the number of fins on the tube and the spacing between them.

$$\eta_o = 1 - \frac{NA_F}{A_t}(1 - \eta_F) \tag{6.9}$$

where N is the total number of fins, A_F is the surface area of one fin, A_t is the total exterior surface area of the tube including the fins. The overall heat transfer is Equation 6.10.

$$Q = h_a \eta_o A_t (T_a - T_s) \tag{6.10}$$

where A_t is the combined surface area of the tube and fins, and this is how the air-side heat transfer is calculated.

The method to calculate the air-side pressure loss for the air heater was estimated using Equation 6.11 because pressure-drop correlations for inline finned tubes were not available in the literature or in heat transfer handbooks. It was assumed the flow structure differences between bare tube bundles and finned tube bundles were equally proportional for the cases with fins and without fins. (See Equation 6.11)

$$\Delta P_{inline\ finned} = \Delta P_{inline\ bare} \left(\frac{\Delta P_{staggered\ fin}}{\Delta P_{staggered\ bare}} \right) \tag{6.11}$$

The three terms $\Delta P_{inline\ bare}$, $\Delta P_{staggered\ fin}$, and $\Delta P_{staggered\ bare}$ correspond to the pressure loss for heat exchanger tube bundles of inline bare tubes, staggered finned tubes, and staggered bare tubes, respectively.

The terms $\Delta P_{inline\ bare}$ and $\Delta P_{staggered\ bare}$ were calculated using Equation 6.12, which was developed by Zhukauskus [46-47].

$$\Delta P = N_L \chi \left(\frac{\rho V_{max}^2}{2} \right) f \tag{6.12}$$

where N_L is the number of tube rows, f and χ were the friction factor and tube correction factor, respectively, and these values were plotted in [46-47].

The term $\Delta P_{staggered\ fin}$ in Equation 6.11 was calculated using Equation 6.13. It was experimentally determined by Stasiulevičius and Skrinska [34].

$$\frac{\Delta P}{\rho V_{max}^2} = \frac{6.55\left(1 - F_p/OD\right)^{1.8} Re^{-0.25}}{\left(\frac{S_t}{OD}\right)^{0.55} \left(\frac{S_l}{OD}\right)^{0.5} \left(1 - \frac{F_h}{OD}\right)^{1.4}} Z \tag{6.12}$$

The correlations and procedure to calculate the flue gas heat transfer and pressure loss were the same as what was described in Section 5.1, and the cost of the air heater was estimated using the method described in Section 5.1. However, unlike the calculation procedure in Section 5.1, the length of the tubes is fixed and does not change during the optimization. Recall that in Section 5.1 the tube length was decided by the primary objective of those simulations, which was to condense 50 percent of the water vapor. The primary objective for the air heater optimization is to increase the combustion air temperature the desired amount. Therefore the tube lengths are fixed and the number of rows of tubes in the direction of the air flow is the variable. The simulation of the air heater performs a check after each row to determine if the combustion air is the desired value.

6.2 Optimal Design of a Combustion Air Heater (ACC) for the case with a wet flue gas desulphurization system

The case studies described in this section had the process conditions listed in Table 6.2, and represent a typical 600 MW power plant that has a wet flue gas desulphurization system (FGD). Air first passed through the FD fan before entering the ACC. The inlet cooling air temperature to the ACC, which was combustion air, was 80^{o}F and the optimization was performed to find an ACC design that increased the combustion air temperature to about 3^{o}F less than the temperature of the flue gas entering the air-cooled condenser (ACC). Since the design was a single-pass, cross-flow configuration with cooling air flowing around the tubes (see Figure 6.2), there were only as many rows as necessary to increase the combustion air temperature to the desired value (tube rows was defined in Figure 5.49).

Table 6.2 – Process conditions and fixed design choices for the optimization of the flue gas condenser that preheats combustion air.

	Case I (with water-cooled condenser)	Case II (w/o water-cooled condenser)
Combustion Air Flow Rate [lbm/hr]	5,300,000	5,300,000
Inlet Flue Gas Temperature to ACC [^{o}F]	128	135
Inlet Cooling Air Temperature to ACC [^{o}F]	80	80
Inlet Flue Gas Moisture Concentration [% wet basis]	14.4	17.4
Tube Length [ft]	30	30
Target Exit Cooling Air Temperature [^{o}F]	125	132

The variables that were optimized in case 1 and case 2 are listed in Table 6.3. The inlet flue gas temperature for the two cases was 128^{o}F and 135^{o}F. It was expected that the actual temperature of the flue gas exiting a wet FGD would be 135^{o}F. Case 1 represents the case shown in Figure 6.1 and Figure 6.2. Case 2 is without the water-cooled condenser and the flue gas

would directly enter the ACC after exiting the wet FGD. In both cases, the desired temperature of the air exiting the ACC was 3°F less than the temperature of the flue gas entering the ACC.

The results from the optimizations of cases 1 and 2 are listed in Table 6.3. More details of the designs and optimizations are listed in Table 6.5 and Table 6.6 and in Appendix B.6. The flue gas velocity of roughly 50 feet per second was expected. 50 ft/sec was the flue gas velocity seen in the optimizations presented in Chapter 5. This value of 50 feet per second was a balance between heat transfer and pressure drop. The cooling air velocity was 8.3 and 12.9 ft/sec respectively for the two cases. These velocities also correspond to values determined in Chapter 5.

Where the two designs cases 1 and 2 differ with those discussed Chapter 5 was the tube diameter. In Chapter 5 the resultant tube geometry determined by the optimization was the smallest possible tube diameter because the small diameter increased rates of condensation and condensation was the primary objective. For the air heater the primary objective was heating the air and the net cost of the ACC that heated the air most did not always correspond to the smallest tube diameter. This is seen in Table 6.3. The remaining optimal variables, fin pitch, fin length, and fin thickness were as expected and matched with the designs discussed in Chapter 5.

Also shown in Table 6.3 is the amount of flue gas that was processed. In both cases, all of the flue gas was not utilized. For case 1 the flue gas flow rate was 1,545,000 lbm/hr and for case 2 the flue gas flow rate was 1,824,000 lbm/hr. In both cases, the cooling air flow rate was 5,300,000 lbm/hr. The reason that only a fraction of the flue gas was processed is because the heat capacity of the flue gas relatively larger due to the flue gas being saturated with moisture.

Table 6.3 – Optimized design values for the cases when the ACC is used to pre heat combustion air.

Variable	Case I	Case II
Flue Gas Velocity [ft/sec]	49.5	52.7
Cooling Air Velocity [ft/sec]	8.3	12.9
Fin Pitch [inches]	0.20	0.20
Fin Length [inches]	1.25	1.25
Inner Tube Diameter [inches]	2.33	3.54
Fin Thickness [inches]	0.113	0.125
Flue Gas Flow Rate [lbm/hr]	1,545,000	1,824,000
Surface Area [ft^2]	80,955	58,023
Net Annual Cost	$ 267,933	$ 201,000

Further details of the optimal designs for case 1 and case 2 are listed in Table 6.5 and Table 6.6. In the tables, it is seen that a fraction of the flue gas was processed in the ACC. Approximately 30 percent of the flue gas was necessary to pre-heat the combustion air for case 1 and 25 percent for case 2. By only processing a fraction of the total flue gas, the heat exchanger could be smaller which would reduce capital investment. The surface area for the two heat exchangers was 81,000 ft^2 for case 1 and 58,000 for case 2, compared to approximately 200,000 ft^2 for the designs presented in Chapter 5. The reason for case 2 having less surface area than case 1 is that case 2 had larger amounts of latent energy in the flue gas (the flue gas is saturated with water vapor at 135^{o}F compared to 128^{o}F), and thus it was a more effective heat exchanger. In addition, because case 2 had less surface area, its net cost was less than case 1.

The following section, Section 6.3, discusses the effect on fuel consumption from increasing the temperature of the entering combustion air. Recall that the primary objective of the ACC in this section was to increase the temperature of the combustion air. The secondary objective was to recover water. Table 6.4 lists the estimated savings due to decreasing fuel consumption (calculations outlined in Section 6.3) and recovering water. The cost of coal was estimated at $50 dollars per ton.

Table 6.4 - Cost savings associated with using the ACC to pre-heat combustion air.

	Case I	**Case II**
Annual Cost Savings due to decreased Fuel Consumption	$234,000	$270,000
Annual Cost Savings due to Recovering Water at $1.50 per 1000 gallons	$ 62,300	$ 73,750

Table 6.5 - Optimal design of the flue gas condenser used to pre-heat combustion air (for the case with an inlet flue gas temperature of 128°F).

optimalAPH_125d	
Flue Gas Flow Rate [lbm / hr]	1,545,807
Vapor Flow Rate [lbm / hr]	139,751
Cooling Air Flow Rate [lbm / hr]	5,300,000
Flue Gas Velocity [ft/sec]	47.2
Cooling Air Velocity [ft/sec]	8.7
Inlet Flue Gas Temperature [°F]	128
Exit Flue Gas Temperature [°F]	113
Inlet Cooling Air Temperature [°F]	80
Exit Cooling Air Temperature [°F[	125
Inlet Moisture Concentration [% wet basis]	14.4
Exit Moisture Concentration [% wet basis]	9.8
Tube Inner Diameter [inches]	2.33
Tube Thickness [inches]	0.2
Fin Length [inches]	1.25
Fin Pitch [inches]	0.2
Fin Thickness [inches]	0.113
Number of Tube Rows in the direction of the Air Flow	5
Transverse Tube Spacing [inches]	5.23
Longitudinal Tube Spacing [inches]	5.23
Number of Tubes	4425
Tube Length [ft]	30
Gas-Side Surface Area [ft^2]	80,955
Air-Side Surface Area [ft^2]	1,873,582
Air-Side Fan Power [kW]	10.8
Additional Gas-Side Fan Power [kW]	89
Field Erected Capital Cost	$3,500,531
Annualized Capital Cost	$280,892
Annualized Operating Cost	$49,372
Estimated Annual Savings in Water Costs @ $1.50 per 1000 gallon	$62,331
Estimated Annual Fuel Savings @ $50 per ton	$234,000
Net Annualized Cost [20 yrs @ 5%]	$33,933
Sensible Heat Transfer [BTU/hr]	6,177,588
Latent Heat Transfer [BTU/hr]	51,127,139
Condensation Rate [lbm / hr]	49,518
Condensation Efficiency of Processed Glue Gas	35%
Condensation Efficiency of Total Flue Gas	9.6%

Table 6.6 – Optimal design of the flue gas condenser used to pre-heat combustion air (for the case with an inlet flue gas temperature of 135°F).

optimalAPH_135a	
Flue Gas Flow Rate [lbm/hr]	1,823,864
Vapor Flow Rate [lbm/hr]	201,994
Cooling Air Flow Rate [lbm/hr]	5,300,000
Flue Gas Velocity [ft/sec]	52.7
Cooling Air Velocity [ft/sec]	12.9
Inlet Flue Gas Temperature [°F]	135
Exit Flue Gas Temperature [°F]	123
Inlet Cooling Air Temperature [F]	80
Exit Cooling Air Temperature [°F]	132
Inlet Moisture Concentration [% wet basis]	17.4
Exit Moisture Concentration [% wet basis]	13.0
Tube Inner Diameter [inch]	3.54
Tube Thickness [inch]	0.2
Fin Length [inches]	1.25
Fin Pitch [inches]	0.2
Fin Thickness [inches]	0.125
Number of Tube Rows in the direction of the Air Flow	3
Transverse Tube Spacing [inches]	6.43
Longitudinal Tube Spacing [inches]	6.43
Number of Tubes	2088
Tube Length [ft]	30
Gas-side Surface Area [ft^2]	58,023
Air-side Surface Area [ft^2]	1,149,016
Air-Side Fan Power [kW]	16.3
Gas-Side Fan Power [kW]	90.4
Field Erected Capital Cost	$2,681,759
Annualized Capital Cost	$215,191
Annualized Operating Cost	$60,003
Estimated Annual Savings in Water Costs @ $1.50 per 1000 gallon	$73,747
Estimated Annual Savings in Fuel @ $50 per ton	$270,000
Net Annualized Cost [20 yrs @ 5%]	-$32,553
Sensible Heat Transfer [BTU/hr]	5,892,501
Latent Heat Transfer [BTU/hr]	60,299,506
Condensation Rate [lbm/hr]	58,587
Condensation Efficiency of Processed Flue Gas	29%
Condensation Efficiency of Total Flue Gas	9.3%

6.3 Effect on Fuel Consumption due to the ACC Pre-Heating Combustion Air

In contrast to the designs presented in Chapter 5, the design presented in this chapter utilized the recovered energy to heat combustion air. This would improve the boiler efficiency because less fuel energy will be spent to heat the combustion air. Currently, large high temperature Ljungstrom type air pre-heaters exist in power plants to increase combustion air temperature to roughly 500 to 600°F. In the present study, an additional air pre-heater is proposed to operate as a low-temperature air-heater, pre-heating the combustion before it enters the main, Ljungstrom type air pre-heater.

This section begins by describing the main, high-temperature air pre-heater and typical inlet and outlet temperatures. Then the effect the air-heater of the present study is discussed, and finally results are presented to show how fuel consumption is affected.

Temperatures typical of a main air pre-heater are given in Figure 6.3. These temperatures were obtained from previous tests at power plants involving main APHs. The 80°F inlet temperature can vary depending on the situation. The air-heater of the present study would affect the temperature of the combustion air entering the main air pre-heater (labeled 80°F in Figure 6.3), and Figure 6.4 shows the proposed design of a configuration with both air heaters.

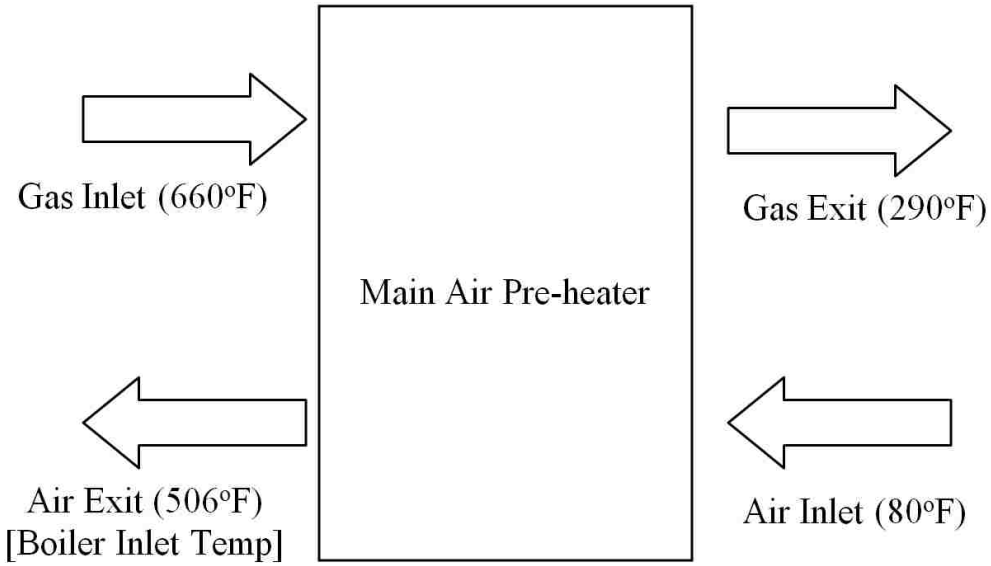

Figure 6.3 – Example of temperatures of a high temperature air pre-heater.

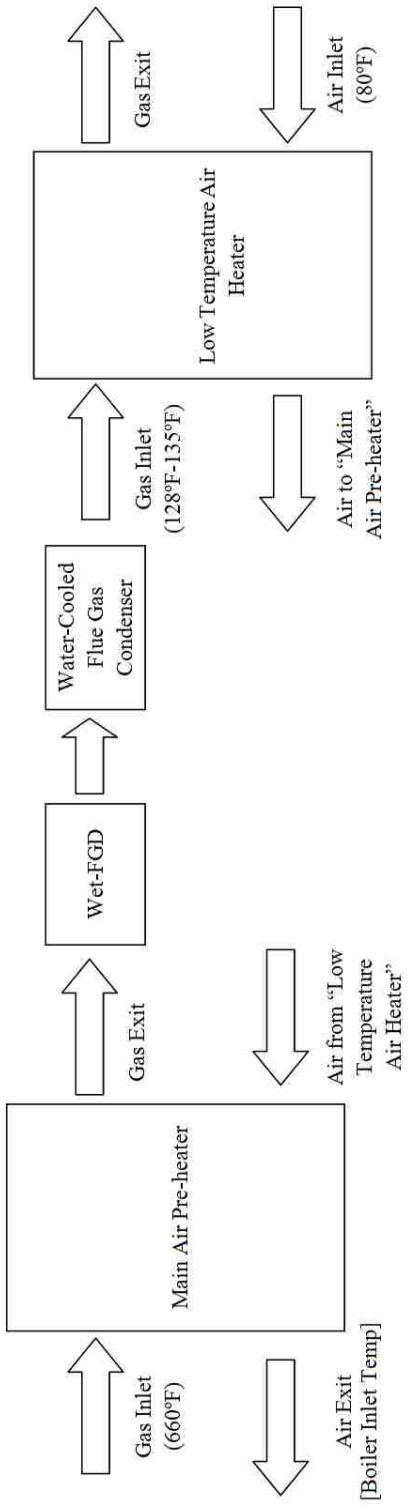

Figure 6.4 - Conceptual integration of the air heater developed in the current study.

The effect the air-heater developed in the present study had on fuel consumption was determined using the control volume defined in Figure 6.5. Calculations were carried out for cases with and without the presence of the air-heater. Within Figure 6.5 the temperature labeled "Air To Main APH" is the temperature exiting the ACC of the present study. This temperature and the temperature of the flue gas exiting the boiler, which was taken as 660^{o}F, was used to determine the temperature labeled "Gas Exiting Main APH" in Figure 6.5. Since the water and steam flow rates do not change, the coal flow rate was then readily calculated.

-

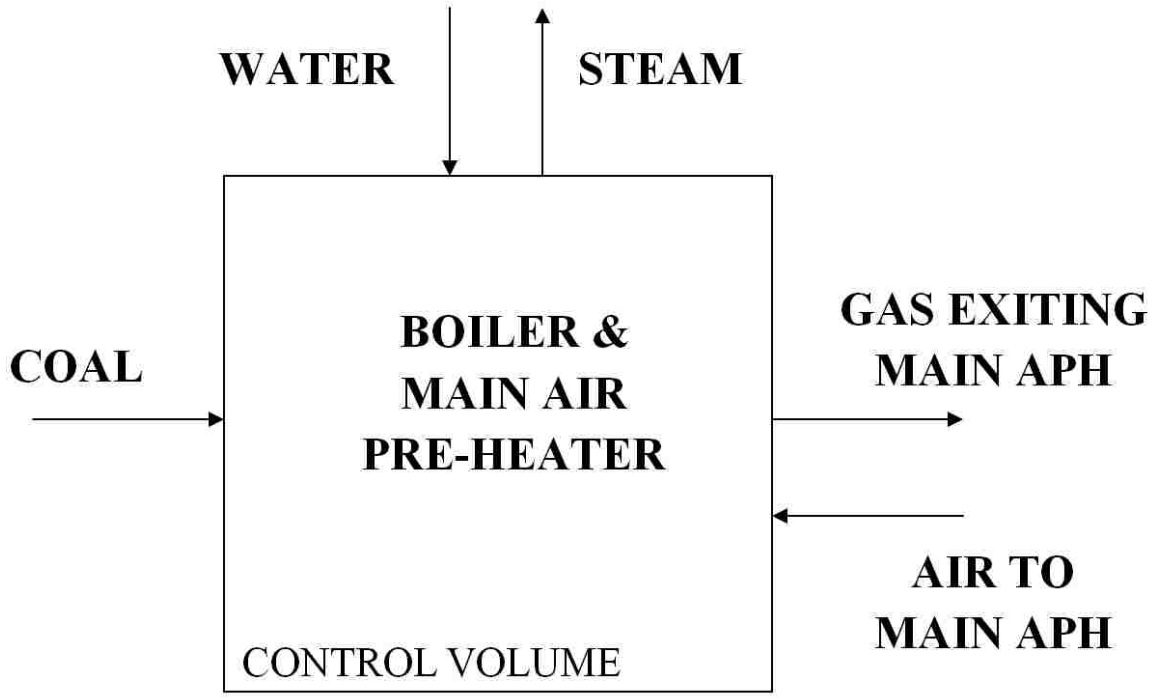

Figure 6.5 - Control volume of the boiler and main air pre-heater which was used to calculate the change in fuel consumption.

With the air-cooled condenser (ACC) incorporated into system as an air heater, the temperature of the combustion air entering the main air pre-heater is the temperature of the air exiting the air-heater. The flue gas temperature exiting the main air pre-heater was calculated

with an ε-NTU analysis of the main air pre-heater. The effectiveness ε of the main APH shown in Figure 6.3 was calculated to be 0.74. The temperature values in the figure were taken from data obtained from a coal fired power plant.

The air cooled condenser was capable of increasing the combustion air from 80 to 125°F in Case I and from 80 to 132°F in Case II. This was shown in Section 6.2. Increasing the inlet temperature of the combustion air alters the exiting temperatures from the main APH and these changes are tabulated in Table 6.7. The results for Case I were the air entering the boiler increased by 12 degrees and the flue gas temperature exiting the main air pre-heater increased 29 degrees (see Figure 6.6). For Case II, the air entering the boiler increased by 14 degrees and the flue gas temperature exiting the main air pre-heater increased by 33 degrees.

Table 6.7 - Inlet and exit temperatures of the main APH when the ACC is used to pre-heat combustion air.

	Without ACC as an Air Pre-Heater	With ACC as Air-Heater (Case I) **(Figure 6.6**)	With ACC as Air-Heater (Case II)
Flue Gas Flow Rate [lbm/hr]	6,000,000	6,000,000	6,000,000
Cooling Air Flow Rate [lbm/hr]	5,540,000	5,540,000	5,540,000
Gas Inlet [°F]	660	660	660
Gas Exit [°F]	290	319	323
Air Inlet [°F]	80	125	132
Air Exit [°F]	506	518	520
Heat Exchanger Effectiveness*	0.74	0.74	0.74

* $Effectiveness\ \varepsilon = \frac{q}{q_{max}} = \frac{\dot{m}_{gas}(T_{gas,in} - T_{gas,exit})}{\dot{m}_{air}(T_{gas,in} - T_{air,in})}$ [39]

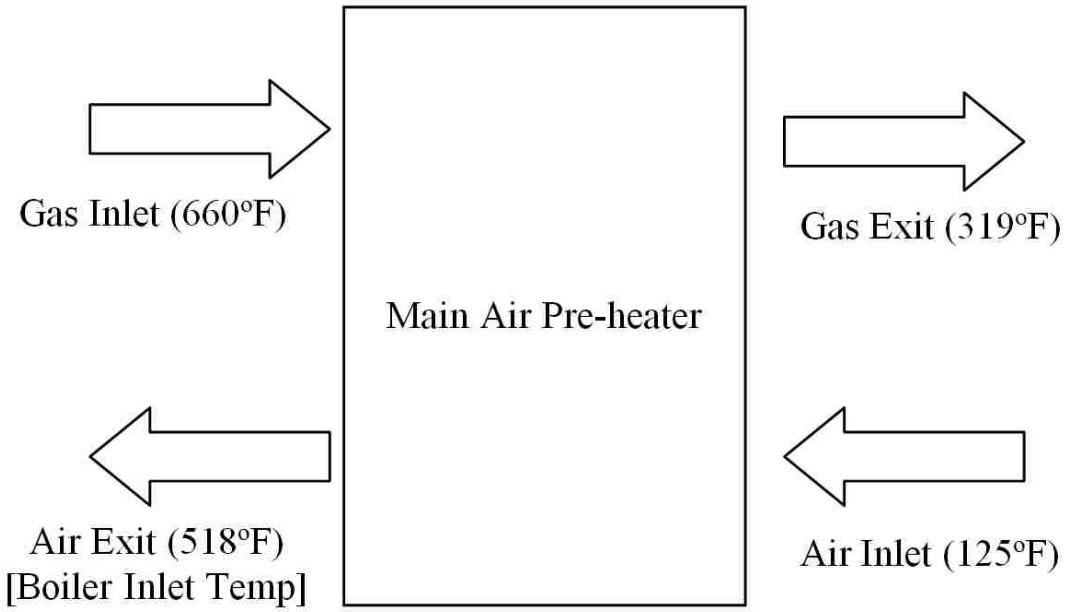

Figure 6.6 - Inlet and exit temperatures of main air pre-heater when the ACC is used as an air-heater developed in the present study is incorporated into the power plant (Case I).

The net energy added to the control volume shown in Figure 6.5 was calculated using the values in Table 6.7. There was a "loss" and a "credit" associated with incorporating the ACC as an air heater, and on a unit hour basis, the loss and credit were calculated using Equations 6.13 through 6.15.

Credit $$\Delta h_{credit} = Cp_{air} * \dot{m}_{cooling\ air} * (\Delta T_{in}) \quad (6.13)$$

Loss $$\Delta h_{loss} = Cp_{flue\ gas} * \dot{m}_{flue\ gas} * (\Delta T_{exit}) \quad (6.14)$$

Net $$\Delta h_{net} = \Delta h_{credit} - \Delta h_{loss} \quad (6.15)$$

The values for the specific heats in Equations 6.13 and 6.14 were obtained from the simulations and based on the composition of the flue gas and for air the specific heat was taken from a reference book. The effect preheating combustion air had on fuel consumption was found using the higher heating value of coal, which can typically be 12,000 BTU/lbm (see Equation 6.16).

$$Fuel\ Savings = \frac{\Delta h_{net}}{Higher\ Heating\ Value} \tag{6.16}$$

The fuel flow rate was approximately 460,000 lbm/hr (calculated in Appendix C), and Table 6.8 shows the reductions in fuel for the two cases. Note, these annual reductions reflect a power plant in operation for 7000 hours per year and other assumptions listed in Appendix C.

Table 6.8 - Reduction in fuel consumption due to incorporating the ACC as a combustion air pre-heater.

Case I (ΔT Combustion Air: 45°F)	**4,680 tons/yr**	**0.29 %**	**$234,000**
Case II (ΔT Combustion Air: 52°F)	**5,400 tons/yr**	**0.34 %**	**$270,000**

In case 1, the reduction in fuel flow consumption was approximately 4,680 tons per year, or 0.29%. At $50 per ton, the fuel savings were $234,000. If the temperature of the combustion air entering the main APH were further increased, as in case 2, the fuel saved increased to 0.34% or $270,000 per year. There was a linear relationship between the temperature exiting the ACC and decrease in fuel consumption. Figure 6.7 and Figure 6.8 show this relationship. The calculations in the figures were an extension of the calculations in Table 6.8.

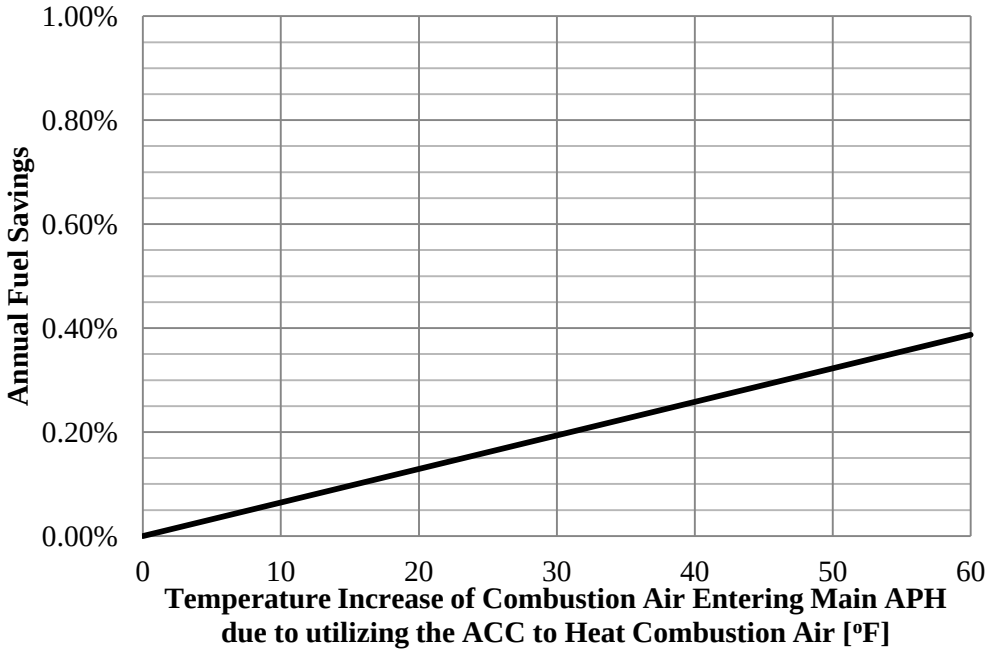

Figure 6.7 - Fuel savings as a function of increased combustion air temperature. (Base combustion air inlet temperature was 80°F.)

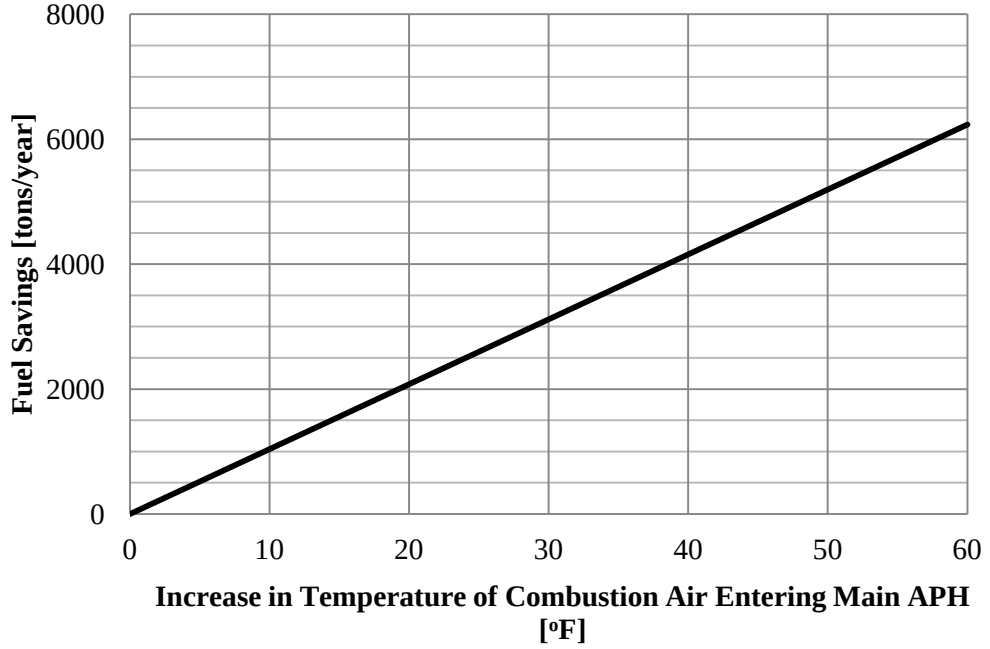

Figure 6.8 - Fuel savings as a function of increased combustion air temperature. (Base combustion air inlet temperature was 80°F.)

7 Concluding Remarks: Cost-Benefit Analysis

The applications of the ACC developed in the present study are categorized into four cases. Case 1 involves the ACC processing flue gas using ambient air as the heat sink, and Case 2 involves the ACC processing flue gas downstream of a wet FGD using ambient air as the heat sink. Case 3 involves using the ACC as a combustion air heater and processing flue gas downstream of a wet FGD and boiler feedwater heater which processes flue gas. Case 4 involves using the ACC as a combustion air heater and processing flue gas downstream of a wet FGD, no boiler feedwater heater.

Cases 1 and 2 were discussed in Chapter 5 and Cases 3 and 4 were discussed in Chapter 6. The cases differ in their primary objective, which for Cases 1 and 2 is to recover water and for Cases 3 and 4 is to increase the combustion air temperature.

Case 1: Case 1 processes a flue gas just downstream of a baghouse or ESP. The idea behind Case 1 is to recover water from flue gas then treat the water so it can be used as makeup water for a cooling tower. The water condensed from the flue gas is acidic and should be treated. The costs associated with the treatment process have not been included in the analysis. This application of the ACC is beneficial to a plant in a dry region where it is difficult to procure necessary amounts of water to meet the plant's needs.

Case 2: The objectives are the same as Case 1 but for a power plant that a wet FGD system. The ACC would be installed downstream of the FGD and process a low temperature, high moisture concentration flue gas. The objective is to recover water that can be used as cooling tower makeup water. Compared to Case 1, the flue gas temperature is 97 degrees cooler and the system is smaller because less sensible heat is recovered. Case 2 condenses more water than Case 1 and it is less expensive to build and operate.

Case 3: In this case, shown in Figure 6.1 and Figure 6.2, the ACC is used to heat combustion air, and this limits the flow rate of cooling air. In this design the primary objective is to increase the temperature of the combustion air to approximately 3 degrees less than the

incoming flue gas. For a power plant with a wet FGD system the flue gas can exit the wet FGD at 135^{o}F and then be cooled to 128^{o}F using boiler feedwater. After the flue gas exits the boiler feedwater heater it would enter the ACC and heat the combustion air from 80^{o}F to 125^{o}F. In Case 3, only 25 percent of the flue gas is necessary to preheat the air, allowing for a smaller heat exchanger.

Case 4: In contrast to Case 3, there is no boiler feedwater heater after the wet FGD. In this case, the flue gas enters the ACC at 135^{o}F and saturated. The combustion air temperature increases from 80 to 132^{o}F and this results in a fuel savings that are estimated at $234,000 per year. Combined with the estimated savings due to recovering water and neglecting costs associated with treating the condensed water, there is a net benefit to installing the ACC.

Table 7.1 summarizes the four cases' cost-to-benefit. Values used for key parameters include 20 year equipment life, 5 percent annual interest rate, electrical power at $50/MWhr, water at $1.50/1000 gallons, and fuel at $50/ton.

These results suggest that in some cases incorporating the ACC into a power plant can provide a net benefit, including financial savings and reduced consumption of water and fuel. In addition, stack emissions including mercury, and sulfuric, hydrochloric, and nitric acid emissions would be reduced and there may be a cost/credit associated with the emission reductions.

In conclusion, using an air-cooled condenser to condense boiler flue gas will address some increasing concerns about generating power from coal. The amount of water that a power plant consumes to meet daily cooling needs would be reduced, in some cases the amount of fuel necessary to maintain gross power generation can be reduced, and stack emissions can be reduced. The study presented in this dissertation showed that designs can be optimized depending on the primary objective of the ACC and in doing so the costs of building and operating the ACC are manageable and in some cases the power plant can realize a net financial benefit.

Table 7.1 - Summary of ACC designs.

Parameter	Case 1	Case 2	Case 3	Case 4
Tfg,in [^{o}F]	225	128	128	135
Tfg,out [^{o}F]	123.8	105.4	113	123
Tair, in [^{o}F]	75.0	75.0	80.0	80
Tair, out [^{o}F]	96.5	101	125	132
Inlet H_2O Concentration [%]	11	14.4	14.4	17.4
Flue Gas Flow Rate [Million lbm/hr]	6.0	6.0	1.5	1.8
Cooling Air Flow Rate [Million lbm/hr]	67.2	46.5	5.3	5.3
Condensation Rate [Million lbm/hr]	0.185	0.246	0.049	0.059
Condensation Efficiency of Processed Flue Gas [%]	46	46	35	29
Condensation Efficiency of Total Flue Gas Flow [%]	46	46	9.3	9.6
Heat Transfer Rate [Million BTU/hr]	343	290	57	66
Power Consumption of Gas and Air Fans[kW]	370	280	99.8	106
Gas-Side Surface Area [ft^2]	197,000	130,000	81,000	58,000
Installed Cost [$ Million]	6.1	4.4	3.5	2.6
Annualized Installed Cost [$ Million / year]	0.496	0.358	0.281	0.215
Annual Operating Cost [$ Million / year]	0.125	0.114	0.049	0.060
Estimated Savings in Water Recovery [$ Million /year]	0.233	0.309	0.062	0.073
Estimated Fuel Savings [$ Million / year]	-	-	0.234	0.270
Estimated Net Annual Cost [$ Million / year]	0.388	0.162	0.033	-0.032

8 References Cited

[1] –"Estimating Freshwater Needs to Meet Future Thermoelectric Generation Requirements: 2009 Update," DOE/NETL Report 400/2009/1339, September 30, 2009

[2] - Cho, S.M., Dietz, D., Kandis, M., Carbonara, J., Heaphy, J., Kressner, A., Carrigan, J., Heat Rate Improvement with Condensing Heat Exchangers, *International Exhibition & Conference for the Power Generation Industries*, *Fossil Plant Retrofit & Repowering and Fossil Plant Performance Improvemen,* **11-12** (1992) 448 – 463

[3] - Johnson, D.W., DiVitto, J.G., Rakocy, M.E., Condensing Heat Exchangers for Maximum Boiler Efficiency, *ASME Power Division,Heat Exchanger Technologies for the Global Environment*, **25** (1994) 127-130

[4] - Johnson, D.W., Rowley, D.R., Schulze, K.H., Carrigan, J.F., Integrated Flue Gas Treatment and Heat Recovery Using a Condensing Heat Exchanger. *Proceedings of the American Power Conference,* **56:2** (1994) 965-970

[5] - Smith, Peter V., Bailey, Ralph T., Johnson, Dennis W., Testing Condensing Heat Exchangers for Energy Efficiency and Pollution Control. *Proceedings of the Air & Waste Management Association's Annual Meeting & Exhibition,* (1996)

[6] - Butcher, Thomas A; Litzke, Wai Lin; Schulze, Karl; Bailey Ralph; Condensing Economizers for Efficiency Improvement and Emissions Control in Industrial Boilers. *Conference: Combustion Canada 1996*, DOE Contract Number: AC02-76CH00016, Report Numbers: BNL--62939; CONF-9606183 --1

[7] - Kudlac, G.A., Multiple Pollutant Removal Using The Condensing Heat Exchanger – Task 3 Topical Report: Long Term Wear Tests, DOE/PC/95255--T6-Add.2

[8] – Johnson, Dennis W., Schulze, Karl H., "Two Stage Downflow Flue Gas Treatment Condensing Heat Exchanger." Patent 5,510,087. 23 April 1996.

[9] - Hossfeld, Lawrence M., Hawkins, David J., A Cost-Effective Technology for Flue Gas Condensation Heat Recovery. *American Society of Mechanical Engineers (paper),* Jt. ASME/IEEE Power Generation Conference., Milwaukee, WI, USA, 1985

[10] - Dinulescu, Mircea, Combustion Air Preheating For Refinery Heaters Using Plate-Type Heat Exchangers. *Energy Progress*, **8:2** (1988) 103-108

[11] - Svedberg, Gunnar, Advanced heat recovery from flue gases, Fernwärme international – FWI, Jg. 15 (1986) 128-132

[12] - Thorn, William F., Waste heat Recovery From Stacks Using Direct-Contact Condensing heat Exchange. *Official proceedings, annual conference of the International District Heating and Cooling Association*, **76** (1985) 431-466

[13] – Jeong, Kwangkook, Condensation of Water Vapor and Sulfuric Acid in Boiler Flue Gas, Ph.D. Dissertation, Lehigh 2009

[14] – Jeong, K., Kessen, M., Bilirgen, H., Levy, E., Analytical Modeling of water condensation in condensing heat exchanger, *Int. J. Heat and Mass Transfer*, accepted but not yet published

[15] – Kroger, Detlev G., Air-Cooled Heat Exchangers and Cooling Towers, PennWell, 2004

[16] – Colburn, Allan P., Relation between Mass Transfer (Absorption) and Fluid Friction, *Industrial and Engineering Chemistry*, **22:9** (1930) 967-970

[17] – Chilton, T.H., Colburn, A.P., du Pont, E.I., Mass Transfer (Absorption) Coefficients, *Industrial and Engineering Chemistry*, **26**:**11** (1934) 1183-1187

[18] – Colburn, A.P., du Pont, E.I., Design of Cooler condensers for Mixtures of Vapors with Noncondensing Gases, **26:11** (1934) 1178-1185

[19] – Stewart, Paul B., Clayton, James L., Loya, Benigno, Hurd, Stanley E., Condensing Heat Transfer in Steam –Air Mixtures in Turbulent Flow, *I&EC Process Design and Development*, **3:1** (1964) 48-54

[20] – Levy, E., Bilirgen, H., Jeong, K., Kessen, M., Samuelson, C., Whitcombe, C., Recovery of Water From Boiler Flue Gas: Final Technical Report DOE Award Number DE-FC26-06NT42727 (2008)

[21] – Paikert, P., 3.8: Air-Cooled Heat Exchangers. In Heat Exchanger Design Handbook, Hemisphere Publishing Company, 1983

[22] – Mueller, A.C. 3.4: Condensers. In Heat Exchanger Design Handbook, Hemisphere Publishing Company, 1983

[23] – Bejan, Adrian, Kraus, Allan D., (Eds.), Heat Transfer Handbook, New Jersey, John Wiley & Sons, Inc., 2003.

[24] – Rohsenow, Warren M., Hartnett, James P., Cho, Young I., (Eds.)., Handbook of Heat Transfer, New York, McGraw-Hill, 1998.

[25] – Webb, Ralph L., Wanniarachchi, A.S., The Effect of Noncondensible Gases in Water Chiller Condensers – Literature Survey and Theoretical Predictions, ASHRAE Trans, 1980.

[26] – Osakabe, Masahiro, Yagi, Kiyoyuki, Itoh, Tsugue, Ohmasa, Kunimitsu, Condensation Heat Transfer on Tubes in Actual Flue Gas, *Heat Transfer – Asian Research*, **32:2** (2003) 153-166.

[27] – Gnielinski, V., New Equations for Heat and Mass Transfer in Turbulent Pipe and Channel Flow, *Int. Chem. Eng*., **16** (1976) 359-368.

[28] – Al-Arabi, M., Turbulent Heat Transfer in the Entrance Region of a Tube, *Heat Transfer Engineering*, **3:3-4** (1981) 76-83.

[29] – Munson, B.R., Young, D.A., Okiishi, T.H., Fundamentals of Fluid Mechanics, John Wiley & Sons, 2002.

[30] – Mirkovic, Z., Heat Transfer and Flow Resistance Correlation for helically Finned and Staggered Tube Banks in Crossflow, in heat Exchanger: Design and Theory Source Book, eds. N.H.Afgan and E.U. Schlunder, McGraw Hill,1974, 559-584.

[31] – Ganguli, A., Tung, S.S., Taborek, J., Parametric Study of Air-cooled Heat Exchanger Finned Tube Geometry, AIChE Symposium Series, **81:245** (1985) 122-128.

[32] – Gianolio, E., Cuti, F., Heat Transfer Coefficienct and Pressure Drops for Air Coolers with Different Numbers of Rows Under Induced and Forced Draft, *Heat Transfer Engineering*, **3:1** (1981) 38-47.

[33] – Briggs, D.E., Young, E.H., Convection Heat Transfer and Pressure Drop of Air Flowing Across Triangular Pitch Banks of Finned Tubes, *Chemical Engineering Progress Symposium Series*, **59:41** (1963) 1-10.

[34] – Stasiulevicius, J., Skrinska, A., Heat Transfer of Finned Tube Bundles in Crossflow, Eds. A. Zhukauskas and G. Hewitt, Washington, Hemisphere Publishing Corporation, 1988.

[35] – Robinson, K.K., Briggs, D.E., Pressure Drop of Air Flowing across Triangular Pitch Banks of Finned Tubes, *Chemicacl Engineering Progress Symposium Series*, **62:64** (1966) 177-182.

[36] – Carey, V.P., Liquid-Vapor Phase-Change Phenomena, Hemisphere Publishing Corporation, 1992.

[37] – Lockhart, R.W., Martinelli, R.C., Proposed correlation of data for isothermal two-phase, two-component flow in pipes, *Chemical Engineering Progress*, **45:1** (1949) 39-48.

[38] – Kolev, N,. Multiphase Flow Dynamics 2: Mechanical and Thermal Interactions, Springer, 2002.

[39] – Incropera, F.P., DeWitt, D.P., *Introduction to Heat Transfer 4th ed*., John Wiley and Sons, 2002.

[40] – Nelder, J.A., Mead, R., A Simplex Method for Function Minimization, *Computer Journal*, **7** (1965) 308-313.

[41] – Lagarias, J., Reeds, J. A., Wright, M. H., Wright P.E., Convergence Properties of the Nelder-Mead Simplex Method in Low Dimensions, *SIAM Journal of Optimization*, **9:1** (1998) 112-147.

[42] – Walters, F.H., Parker, L.R. Jr., Morgan, S.L., Deming, S.N., *Sequential Simplex Optimization*, CRC Press, 1991.

[43] – Idelchik, I.E., *Handbook of Hydraulic Resistance 3rd ed*., Jaico Publishing House, 2003.

[44] - Wurtz, W., Peltier, R., Air-cooled condensers eliminate plant water use, *Power*, September 15, 2008.

[45] - Colburn, A.P., Hougen, O.A., Studies in Heat Transmission, *Industrial and Engineering Chemistry*, **22:5** (1930) 522-524.

[46] - Zhukauskas, A., Ulinskas, R., *Heat Transfer in Tube Banks in Crossflow*, Washington, Hemisphere Publishing Corporation, 1988.

[47] - Zhukauskas, A., Heat Transfer from Tubes in Crossflow, *Advances in Heat Transfer*, **8** (1972) 93-160.

[48] - Bird, R B., Stewart, W. E., Lightfoot, E.N., *Transport Phenomena*, J. Wiley, 1962.

[49] - ASME PTC 4-2008, *Fired Steam Generators Performance Test Codes*, The American Society of Mechanical Engineers, New York, 2009.

[50] – Wildi-Tremblay, P., Gosselin, L., "Minimizing shell-and-tube heat exchanger cost with genetic algorithms and considering maintenance", *International Journal of Energy Research*, **31** (2007) 867 – 885.

[51] – Allen, B., Gosselin, L., "Optimal geometry and flow arrangement for minimizing the cost of shell-and-tube condensers", *International Journal of Energy Research*, **32** (2008) 958 – 969.

[52] – Xie, G.N., Sunden, B., Wang, Q.W., "Optimization of compact heat exchangers by a genetic algorithm", *Applied Thermal Engineering*, **28** (2008) 895 – 906.

[53] – Doodman, A.R., Fesanghary, M., Hosseini, R., "A robust stochastic approach for design optimization of air cooled heat exchangers", *Applied Energy*, **86** (2009) 1240 – 1245.

[54] – Caputo, A.C., Pelagagge, P.M., Salini, P., "Heat exchanger design based on economic optimization", *Applied Thermal Engineering*, **28** (2008) 1151 – 1159.

[55] – Selbas, R., Kizilkan, O., Reppich, M., "A new design approach for shell-and-tube heat exchangers using genetic algorithms from economic point of view", *Chemical Engineering and Processing*, **45** (2006) 268 – 275.

[56] – Ponce-Ortega, J.M., Serna-Gonzalez, M., Jimenez-Gutierrez, A., "Use of genetic algorithms for the optimal design of shell-and-tube heat exchangers", *Applied Thermal Engineering*, **29** (2009) 203 – 209.

[57] – Patel, V.K., Rao, R.V., "Design optimization of shell-and-tube heat exchanger using particle swarm optimization technique", *Applied Thermal Engineering*, **30** (2010) 1417 – 1425.

[58] – Ozcelik, Y., "Exergetic optimization of shell-and-tube heat exchangers using a genetic based algorithm", *Applied Thermal Engineering*, **27** (2007) 1849 – 1856.

[59] - Wilke, C.R., A Viscosity Equation for Gas Mixtures, *The Journal of Chemical Physics*, **18:4** (1950) 517-519.

[60] - Wilke, C.R., Diffusional Properties of Multicomponent Gases, *Chemical Engineering Progress*, **46:2** (1950) 95-104.

[61] – Hewitt, G.F., Hall-Taylor, N.S., *Annular Two-Phase Flow*, Pergamon Press, 1970.

[62] – Smith, R., *Chemical Process*, John Wiley and Sons, 2005.

[63] – Clerk, J., "Costs of Air vs. Water Cooling", *Modern Cost Engineering Techniques*, McGraw-Hill, 1970.

[64] – Guthrie, K.M., "Capital Cost Estimating", *Modern Cost Engineering Techniques*, McGraw-Hill, 1970.

[65] – *Steam*, Babcock and Wilcox Handbook, 2002.

[66] – Dunbar, Stephen, *Experimental and Numerical Studied of Condensing Heat Exchangers used in Flue Gas water Recovery Systems*, M.S. Thesis, Lehigh University, 2010.

Appendix A

The data listed in Appendix A is from the research discussed in Chapter 3. Table A1 lists measured data for water-cooled and air-cooled condenser experiments. Each row the table represents a different experiment having different process conditions. Table A2 compares the experimental measurements with the heat and mass transfer simulation developed in the present study. Each experiment was simulated using the heat and mass transfer simulation to validate the simulation by showing agreement.

TABLE A1 - Measured data for water-cooled and air-cooled condenser experiments.

		FLOW			CONDENSATE			MOISTURE		TEMPERATURE MEASUREMENTS						
		lbm/hr		ft/sec	lbm/hr		%	% wet-basis		degree Fahrenheit						
Date	**#**	**Flue Gas**	**Water**	**Max Air Velocity**	**WCC***	**ACC***	**Recovery Efficiency**	**Inlet to WCC**	**Exit**	**Inlet to WCC**	**Exit of WCC**	**Inlet to ACC**	**Exit of ACC**	**Water In**	**Water Exit**	**Air Inlet**
10/11/2010	1	180	367	23.5	1.35	2.56	21.6	15.6	12.6	317	153	146.8	127.5	130	111	79.4
10/11/2010	2	210	403	23.5	2.43	2.7	24.1	15.7	12.4	311	159	152.7	130.3	126	107	76.5
10/13/2010	1	135	333	26.2	0.53	3.5	35.0	13.2	9	245	146	138.5	115.7	127	118	55.8
10/13/2010	2	187	372	26.2	1.71	3.42	31.7	13.5	9.6	255	143	139.6	118.9	123	109	59.3
10/13/2010	3	213	354	26.2	1.85	3.53	28.8	13.6	10.1	260	145	144	122.6	124	108	62.6
10/15/2010	1	212	648	23.2	5.87	3.43	45.8	14.8	8.6	268	143	133.1	114.6	105	88	56.8
10/15/2010	2	211	669	23.2	8.43	2.56	56.6	14.3	6.7	270	123	120.3	105.7	110	88	58.2
10/15/2010	3	139	421	23.2	3.48	2.6	50.2	13.5	7.2	248	122	119.3	106.2	123	106	59.5
10/20/2010	1	292	582	22.7	8.29	3.67	42.3	15.1	9.3	282	155	142.3	121.5	115	89	55
10/20/2010	2	243	404	22.7	4.36	3.48	34.5	14.5	10	274	152	140.7	121.6	124	101	58.7
10/20/2010	3	140	404	22.7	2.39	2.55	41.2	13.3	8.3	330	140	132.2	111.9	122	104	62.7
10/20/2010	4	185	367	22.7	1.28	3.24	26.7	14.2	10.8	378	159	147.2	123.3	137	111	64.5
10/22/2010	1	150	360	31.4	1.35	3.25	38.0	12.5	8.1	405	138	131.6	111.6	136	114	58.3
10/22/2010	2	146	786	31.4	5.98	1.32	65.2	11.9	4.5	359	109	105.5	91.3	99	83	58.8
10/22/2010	3	145	488	31.4	3.28	2.51	49.5	12.6	6.8	346	125	120	102.7	117	99	59.7

*WCC: water-cooled condenser*ACC: air-cooled condenser

TABLE A1 continued - Measured data for water-cooled and air-cooled condenser experiments.

		FLOW			CONDENSATE			MOISTURE		TEMPERATURE MEASUREMENTS						
		lbm/hr		ft/sec	lbm/hr		%	% wet-basis		degree Fahrenheit						
Date	**#**	**Flue Gas**	**Cooling Water**	**Max Air Velocity**	**WCC**	**ACC**	**Recovery Efficiency**	**Inlet to WCC**	**Exit**	**Inlet to WCC**	**Exit of WCC**	**Inlet to ACC**	**Exit of ACC**	**Water In**	**Water Exit**	**Air Inlet**
10/27/2010	1	354	705	29.5	13.83	3.13	43.5	17	10.4	267	148	142.1	123.2	118	83	65.8
10/27/2010	2	314	391	29.5	5.74	3.8	32.1	14.6	10.4	266	146	140.6	123.3	128	99	66
10/27/2010	3	283	658	29.5	5.34	3.1	34.4	13.4	9.2	309	147	141.4	120.6	115	86	63.5
10/27/2010	4	248	425	29.5	3.56	4.09	31.0	15.4	11.2	325	151	144.2	123.6	132	102	61.6
10/31/2010	1	145	532	36.2	6	2.07	65.6	13.2	4.9	242	107	105.7	93.6	103	88	56.7
10/31/2010	2	147	373	36.2	3.3	3.02	50.6	13.2	7	248	125	120	104.6	121	106	55.6
10/31/2010	3	146	364	36.2	2.12	3.45	45.7	13.1	7.6	375	134	127	107.8	130	108	54.1
11/4/2010	1	146	361	35	2.27	4.25	44.4	15.6	9.3	385	144	136.2	114.3	138	114	56.4
11/4/2010	2	145	429	35	3.4	3.44	49.2	14.8	8.1	371	139	131.9	109.5	128	106	58.6
11/4/2010	3	186	367	35	2.68	4.8	39.4	15.8	10.2	377	149	142	119	139	110	58.4
11/4/2010	4	243	554	35	9.11	4.11	50.8	16.6	8.9	334	147	141.7	118.4	122	91	58
11/4/2010	5	284	745	35	11.69	3.97	52.9	16.1	8.3	324	148	142.6	119	113	83	57.1
11/6/2010	1	201	423	30.9	4.18	4.03	39.7	16	10.3	396	150	141.7	118.7	133	101	59.3
11/6/2010	2	147	362	30.9	2.8	3.9	44.4	15.9	9.5	377	145	138.2	115.6	135	106	58.8
11/8/2010	1	189	345	26.4	1.25	4.4	29.4	15.8	11.7	400	154	145.9	122.7	145	114	55.7

TABLE A1 continued - Measured data for water-cooled and air-cooled condenser experiments.

		FLOW			CONDENSATE			MOISTURE		TEMPERATURE MEASUREMENTS						
		lbm/hr		ft/sec	lbm/hr		%	% wet-basis		degree Fahrenheit						
Date	**#**	**Flue Gas**	**Cooling Water**	**Max Air Velocity**	**WCC**	**ACC**	**Recovery Efficiency**	**Inlet to WCC**	**Exit**	**Inlet to WCC**	**Exit of WCC**	**Inlet to ACC**	**Exit of ACC**	**Water In**	**Water Exit**	**Air Inlet**
11/8/2010	2	131	630	26.4	6.9	1.42	72.3	13.7	4.2	357	108	104.3	88.5	106	86	55.1
11/8/2010	3	130	507	18.8	6.26	1.6	68.3	13.7	4.7	325	110	106.5	91.7	108	88	55
11/8/2010	4	133	388	18.8	3.6	2.52	52.3	13.6	7	358	127	121.2	104.5	120	101	57.6
11/8/2010	5	129	348	18.8	1.66	3.16	41.2	14	8.8	410	137	129.5	112.5	137	113	59.4
11/12/2010	1	153	358	23.9	1.6	2.97	32.9	14.1	9.9	410	148	136.4	117.7	135	109	61.8
11/12/2010	2	203	489	23.9	3.83	2.28	33.4	14	9.8	391	151	140.1	118.5	115	90	67.4
11/12/2010	3	252	574	23.9	6.1	2.14	34.5	14.8	10.2	329	147	140.8	121.1	112	87	68.7
11/12/2010	4	302	591	23.9	8.76	2.53	39.8	14.6	9.4	292	142	139.6	120.9	114	85	63.9

TABLE A2 – Comparisons of the experimental measurements with the heat and mass transfer simulation developed in the present study.

			Water Recovery Rate in ACC			Decrease in Flue Gas Temp			Surface Temperature [F]			
Date	**Temp**	**Gas**	**lbm/hr**			**degree Fahrenheit**			**12''**	**24''**	**12''**	**24''**
	F	**ft/sec**	**Exp**	**Sim**	**Diff**	**Exp**	**Sim**	**Diff**	**Simulation**		**Experiment**	
10/11/2010	146.8	38.7	2.56	3.26	-0.272	19.4	15.1	0.219	113.3	110.0	111.1	108.7
10/11/2010	152.7	45.2	2.7	3.39	-0.255	22.4	17.1	0.235	113.2	110.0	111.7	109.3
10/13/2010	138.5	27.9	3.5	3.58	-0.023	22.8	21.9	0.04	92.9	86.6	99.2	91.2
10/13/2010	139.6	38.5	3.42	3.86	-0.129	20.8	18.6	0.106	98.8	93.5	101.6	95.8
10/13/2010	144	44.5	3.53	3.92	-0.11	21.4	18.1	0.156	102.9	98.4	105.0	100.6
10/15/2010	133.1	43.1	3.43	3.63	-0.056	18.5	16.6	0.102	95.6	91.4	96.7	93.5
10/15/2010	120.3	41.2	2.56	2.67	-0.046	14.5	14.4	0.011	88.3	84.5	90.3	87.5
10/15/2010	119.3	27.5	2.6	2.61	-0.002	13	15.3	-0.177	87.8	83.3	91.0	86.3
10/20/2010	142.3	59.7	3.67	4.12	-0.122	20.8	17.2	0.174	101.0	96.8	100.7	97.5
10/20/2010	140.7	50.4	3.48	4.06	-0.165	19.1	16.5	0.135	102.2	98.2	102.5	99.0
10/20/2010	132.2	28.4	2.55	2.75	-0.079	20.2	18.5	0.087	93.3	88.9	96.8	91.8
10/20/2010	147.2	39.3	3.24	3.73	-0.151	23.9	19	0.206	104.6	100.6	105.1	101.1
10/22/2010	131.6	30.3	3.25	3.31	-0.018	20	19.4	0.031	90.6	85.2	95.3	88.2
10/22/2010	105.5	27.3	1.32	1.41	-0.072	14.3	14.6	-0.025	74.9	71.5	80.1	75.3
10/22/2010	120	28.4	2.51	2.55	-0.016	17.3	16.6	0.039	85.0	81.0	89.4	84.2

TABLE A2 continued - Comparisons of the experimental measurements with the heat and mass transfer simulation developed in the present study.

			Water Recovery Rate in ACC			Decrease in Flue Gas Temp			Surface Temperature [F]			
Date	**Temp**	**Gas**	**lbm/hr**			**degree Fahrenheit**			**12''**	**24''**	**12''**	**24''**
	F	**ft/sec**	**Exp**	**Sim**	**Diff**	**Exp**	**Sim**	**Diff**	**Simulation**		**Experiment**	
10/27/2010	142.1	72	3.13	4.06	-0.297	18.9	14.2	0.25	106.2	103.8	103.9	102.8
10/27/2010	140.6	65.4	3.8	4.19	-0.102	17.3	13.8	0.204	106.5	103.9	104.5	102.7
10/27/2010	141.4	58.6	3.1	3.66	-0.181	20.8	16.6	0.201	101.0	98.1	99.4	97.3
10/27/2010	144.2	52.1	4.09	4.7	-0.15	20.6	16.3	0.211	105.6	102.3	101.5	99.4
10/31/2010	105.7	27.1	2.07	1.94	0.063	12.1	14.4	-0.187	76.0	72.0	82.1	76.5
10/31/2010	120	28.8	3.02	3.01	0.003	15.4	17.4	-0.131	83.3	78.7	90.0	83.6
10/31/2010	127	29	3.45	3.4	0.015	19.1	19.7	-0.027	85.2	80.2	92.3	85.4
11/4/2010	136.2	29.2	4.25	4.15	0.024	21.9	20.3	0.072	94.7	86.8	95.5	86.7
11/4/2010	131.9	28.6	3.44	3.33	0.033	22.4	19.6	0.122	92.6	85.6	92.0	82.8
11/4/2010	142	37.9	4.8	4.66	0.028	23	18.8	0.184	102.1	95.6	99.7	92.4
11/4/2010	141.7	48.1	4.11	4.16	-0.013	23.3	18.7	0.196	99.4	93.8	96.3	91.5
11/4/2010	142.6	56.2	3.97	3.97	0.001	23.6	18.9	0.197	97.9	93.3	95.1	91.1
11/6/2010	141.7	41	4.03	4.32	-0.071	22.9	17.9	0.22	102.1	98.0	101.5	95.7
11/6/2010	138.2	29.5	3.9	3.83	0.017	22.6	19.6	0.134	97.3	92.7	99.3	92.6
11/8/2010	145.9	40.1	4.4	4.88	-0.108	23.1	18.6	0.198	104.9	100.0	103.7	98.9

TABLE A2 continued - Comparisons of the experimental measurements with the heat and mass transfer simulation developed in the present study.

			Water Recovery Rate in ACC			Decrease in Flue Gas Temp			Surface Temperature [F]			
Date	**Temp**	**Gas**	**lbm/hr**			**degree Fahrenheit**			**12''**	**24''**	**12''**	**24''**
	F	**ft/sec**	**Exp**	**Sim**	**Diff**	**Exp**	**Sim**	**Diff**	**Simulation**		**Experiment**	
11/8/2010	104.3	24.1	1.42	1.35	0.048	15.8	15.4	0.024	73.7	69.4	75.9	69.8
11/8/2010	106.5	25.1	1.6	1.51	0.054	14.8	15.2	-0.023	76.4	72.0	79.3	72.8
11/8/2010	121.2	26.3	2.52	2.43	0.036	16.6	16.4	0.015	88.0	83.7	91.0	83.9
11/8/2010	129.5	26.4	3.16	3.04	0.036	17	16.8	0.016	95.4	91.2	99.0	91.8
11/12/2010	136.4	30.9	2.97	3.53	-0.189	18.7	17.8	0.044	99.2	93.7	102.5	94.6

Appendix B – Optimization Simulations for the Case with no Wet FGD Scrubber

This section of the Appendix discusses the optimizations presented in Chapter 5. Multiple optimizations were carried out for each case to build confidence in the results. As discussed in the Literature Review, the Nelder-Mead method is susceptible to converging to a local minimum and the way to ensure the optimization located a global minimum is through repeated trials using different simplexes.

Appendix B.1 - Details of the Optimizations of the Parametric Tests Discussed in Section 5.3.1.

These four tables list the optimization simulations which led to the results listed in Table 5.15. Each table corresponds to an optimization simulation which began with a different initial simplex. For each simulation, the columns labeled" Starting Value" list the details of a first heat exchanger design, which corresponds to one vertex of the simplex. The entire simplex was built using the values listed in the column "Starting Values" and the parameter Si, which is the last column of the Table. Si is the parameter used by Walters [42] to build initial simplexes.

The second and third columns list the domain of each variable during the optimization. For the "Starting Value" and "Optimal Value", there are "Normalized" and "Actual" values. These correspond to the dimensionless and absolute values of the variables. Recall from Section 2.4, the variables were normalized during the optimization to remove the units from the optimization equations.

test name: NominalALL1a							
	Range		**Starting Value**		**Optimal Value**		**Si**
	Min	**Max**	**Normalized**	**Actual**	**Normalized**	**Actual**	
Gas-side Surface Area						161,416	
Tube Length						11.7	
Gas Velocity	7.5	80.0	0.500	43.8	0.584	49.9	0.125
Air Velocity	7.5	50.0	0.255	18.3	0.001	7.5	-0.125
Fin Pitch	0.20	1.00	0.007	0.21	0.000	0.20	0.05
Fin Length	0.00	1.25	0.277	0.35	1.000	1.25	0.15
Inner Tube Diameter	1.75	6.00	0.027	1.86	0.000	1.75	0.9
Fin Thickness	0.063	0.125	1.000	0.125	0.749	0.109	-0.1
Net Annual Cost			$476,078		$306,748		

test name: NominalALL2a							
	Range		Starting Value		Optimal Value		Si
	Min	Max	Normalized	Actual	Normalized	Actual	
Gas-side Surface Area						194,978	
Tube Length						12.5	
Gas Velocity	7.5	80.0	0.500	43.8	0.501	43.9	0.25
Air Velocity	7.5	50.0	0.255	18.3	0.063	10.2	0.25
Fin Pitch	0.20	1.00	0.007	0.21	0.000	0.20	0.5
Fin Length	0.00	1.25	0.277	0.35	0.596	0.75	0.15
Inner Tube Diameter	1.75	6.00	0.027	1.86	0.003	1.76	0.125
Fin Thickness	0.063	0.125	1.000	0.125	0.056	0.066	-0.5
Net Annual Cost			$476,078		$364,417		

test name: NominalALL4a							
	Range		Starting Value		Optimal Value		Si
	Min	Max	Normalized	Actual	Normalized	Actual	
Surface Area						162,212	
Tube Length						11.9	
Gas Velocity	7.5	80.0	0.500	43.8	0.590	50.2	-0.5
Air Velocity	7.5	50.0	0.255	18.3	0.003	7.6	0.5
Fin Pitch	0.20	1.00	0.007	0.21	0.007	0.21	0.5
Fin Length	0.00	1.25	0.277	0.35	0.999	1.25	0.5
Inner Tube Diameter	1.75	6.00	0.027	1.86	0.000	1.75	0.5
Fin Thickness	0.063	0.125	1.000	0.125	0.629	0.102	-0.5
Net Annual Cost			$476,078		$310,776		

test name: NominalALL5a							
	Range		Starting Value		Optimal Value		Si
	Min	Max	Normalized	Actual	Normalized	Actual	
Gas-side Surface Area						185,583	
Tube Length						12.9	
Gas Velocity	7.5	80.0	0.500	43.8	0.473	41.8	-0.133
Air Velocity	7.5	50.0	0.255	18.3	0.038	9.1	0.133
Fin Pitch	0.20	1.00	0.007	0.21	0.021	0.22	0.133
Fin Length	0.00	1.25	0.277	0.35	1.000	1.25	0.133
Inner Tube Diameter	1.75	6.00	0.027	1.86	0.058	1.99	0.133
Fin Thickness	0.063	0.125	1.000	0.125	1.000	0.125	-0.133
Net Annual Cost			$476,078		$335,280		

Appendix B.2 - Effect the Number of Tube Rows has on the Optimal Design

This section details the optimization simulations of the ACC described in Section 5.3.2, which discussed row effects. Two optimizations were carried out for each case with two, four, six, and eight tube rows. In each case the optimization converged to very similar design choices and process conditions.

Each table represents one optimization simulation. The variables optimized are listed in the Table and the range of each variable is given in the second and third columns. The columns labeled "Starting Value" list the variables used as the initial guess, which was one vertex of the initial simplex. The column labeled "Si" is the parameter assigned to each variable which built the remaining vertexes of the simplex using the Tilted Initial Simplex Method described in Walters [42]. The columns labeled "Optimal Value" list the values of the optimal heat exchanger design. Under the headings "Starting Value" and "Optimal Value", there are "Normalized" and "Actual" values. These correspond to the dimensionless and absolute values of the variables, respectively. Recall from Section 2.4, the variables were normalized during the optimization to remove the units from the optimization equations.

Appendix B.2.1 - Two Tube Rows

Test name: OptimalALL1a							
	Range		**Starting Value**		**Optimal Value**		**Si**
	Min	**Max**	**Normalized**	**Actual**	**Normalized**	**Actual**	
Gas-side Surface Area						161,416	
Tube Length [ft]						11.7	
Gas Velocity	7.5	80.0	0.500	43.8	0.584	49.9	0.125
Air Velocity	7.5	50.0	0.255	18.3	0.001	7.5	-0.125
Fin Pitch	0.20	1.00	0.007	0.21	0.000	0.20	0.05
Fin Length	0.00	1.25	0.277	0.35	1.000	1.25	0.15
Inner Tube Diameter	1.75	6.00	0.027	1.86	0.000	1.75	0.9
Fin Thickness	0.063	0.125	1.000	0.125	0.749	0.109	-0.1
Net Annual Cost			$476,078		$306,748		

Test name: NominalALL2r_2							
	Range		**Starting Value**		**Optimal Value**		**Si**
	Min	**Max**	**Normalized**	**Actual**	**Normalized**	**Actual**	
Gas-side Surface Area						157,134	
Tube Length [ft]						12.0	
Gas Velocity	7.5	80.0	0.500	43.8	0.561	48.2	-0.1
Air Velocity	7.5	50.0	0.255	18.3	0.012	8.0	-0.1
Fin Pitch	0.20	1.00	0.007	0.21	0.000	0.20	0.1
Fin Length	0.00	1.25	0.277	0.35	1.000	1.24	0.4
Inner Tube Diameter	1.75	6.00	0.027	1.86	0.000	1.75	0.1
Fin Thickness	0.063	0.125	1.000	0.125	0.712	0.107	-0.25
Net Annual Cost			$476,078		$308,323		

The details of the optimal ACC having two tube rows are:

OptimalALL1a	
Flue Gas Flow Rate [lbm/hr]	6,000,000
Vapor Flow Rate [lbm/hr]	403,720
Cooling Air Flow Rate [lbm/hr]	53,638,732
Flue Gas Velocity [ft/sec]	46.1
Cooling Air Velocity [ft/sec]	7.7
Inlet Flue Gas Temperature [F]	135
Exit Flue Gas Temperature [F]	101.7
Inlet Cooling Air Temperature [F]	75
Exit Cooling Air Temperature [F]	94.1
Tube Inner Diameter [inch]	1.75
Tube Thickness [inch]	0.2
Fin Length [inches]	1.25
Fin Pitch [inches]	0.2
Fin Thickness [inches]	0.109
Number of Tube Rows	2
Transverse Tube Spacing [inches]	4.65
Longitudinal Tube Spacing [inches]	4.65
Number of Tubes	30,000
Tube Length	12
Gas-side Surface Area [ft2]	161,416
Air-side Surface Area [ft2]	8,404,383
Field Erected Capital Cost	$5,286,886
Annualized Capital Cost	$424,233
Annualized Operating Cost	$118,771
Estimated Annual Savings in Water Costs @ $1.50 per 1000 gallon	$236,256
Net Annualized Cost [20 yrs @ 5%]	$306,749
Gas-Side Fan Power [kW]	233
Air-Side Fan Power [kW]	55
Sensible Heat Transfer [BTU/hr]	50,670,814
Latent Heat Transfer [BTU/hr]	195,779,374
Condensation Rate [lbm/hr]	187,691
Condensation Efficiency	47%
Inlet/Exit Moisture Concentration [% wet-basis]	11/6.2

Appendix B.2.2 - Four Tube Rows

Test name: NominalALL4r							
	Range		**Starting Value**		**Optimal Value**		**Si**
	Min	**Max**	**Normalized**	**Actual**	**Normalized**	**Actual**	
Gas-side Surface Area						241,468	
Tube Length [ft]						17.6	
Gas Velocity	7.5	80.0	0.584	49.9	0.585	49.9	-0.5
Air Velocity	7.5	50.0	0.001	7.5	0.001	7.5	0.5
Fin Pitch	0.20	1.00	0.000	0.20	0.000	0.20	0.5
Fin Length	0.00	1.25	1.000	1.25	1.000	1.25	-0.5
Inner Tube Diameter	1.75	6.00	0.000	1.75	0.000	1.75	0.75
Fin Thickness	0.063	0.125	0.749	0.109	0.749	0.109	-0.5
Net Annual Cost			$498,092		$497,999		

Test name: NominalALL4r_2							
	Range		**Starting Value**		**Optimal Value**		**Si**
	Min	**Max**	**Normalized**	**Actual**	**Normalized**	**Actual**	
Gas-side Surface Area						203,798	
Tube Length [ft]						14.3	
Gas Velocity	7.5	80.0	0.584	49.9	0.503	44.0	0.1
Air Velocity	7.5	50.0	0.001	7.5	0.031	8.8	-0.4
Fin Pitch	0.20	1.00	0.000	0.20	0.000	0.20	-0.4
Fin Length	0.00	1.25	1.000	1.25	0.944	1.18	0.4
Inner Tube Diameter	1.75	6.00	0.000	1.75	0.005	1.77	-0.4
Fin Thickness	0.063	0.125	0.749	0.109	0.664	0.104	0.25
Net Annual Cost			$498,092		$414,488		

The details of the optimal ACC having four tube rows are:

NominalAll4r_2	
Flue Gas Flow Rate [lbm/hr]	6,000,000
Vapor Flow Rate [lbm/hr]	403,720
Cooling Air Flow Rate [lbm/hr]	36,268,379
Flue Gas Velocity [ft/sec]	44.0
Cooling Air Velocity [ft/sec]	8.8
Inlet Flue Gas Temperature [F]	135
Inlet Cooling Air Temperature [F]	75
Exit Flue Gas Temperature [F]	101.5
Exit Cooling Air Temperature [F]	102.9
Tube Inner Diameter [inch]	1.77
Tube Thickness [inch]	0.2
Fin Length [inches]	1.18
Fin Pitch [inches]	0.2
Fin Thickness [inches]	0.104
Number of Tube Rows	4
Transverse Tube Spacing [inches]	4.54
Longitudinal Tube Spacing [inches]	4.54
Number of Tubes	30000
Tube Length [ft]	14.3
Gas-side Surface Area [ft2]	203,798
Air-side Surface Area [ft2]	9,805,690
Field Erected Capital Cost	$6,370,924
Annualized Capital Cost	$511,219
Annualized Operating Cost	$135,567
Estimated Annual Savings in Water Costs @ $1.50 per 1000 gallon	$232,299
Net Annualized Cost [20 yrs @ 5%]	$414,488
Gas-Side Fan Power [kW]	240
Air-Side Fan Power [kW]	93
Sensible Heat Transfer [BTU/hr]	51,030,259
Latent Heat Transfer [BTU/hr]	192,166,206
Condensation Rate [lbm/hr]	184,548
Condensation Efficiency	46%
Inlet/Exit Moisture Concentration [% wet-basis]	11/6.3

Appendix B.2.3 - Six Tube Rows

Test name: NominalALL6r							
	Range		**Starting Value**		**Optimal Value**		**Si**
	Min	**Max**	**Normalized**	**Actual**	**Normalized**	**Actual**	
Gas-side Surface Area						241,983	
Tube Length [ft]						17.5	
Gas Velocity	7.5	80.0	0.584	49.9	0.581	49.6	-0.5
Air Velocity	7.5	50.0	0.001	7.5	0.012	8.0	0.5
Fin Pitch	0.20	1.00	0.000	0.20	0.000	0.20	0.5
Fin Length	0.00	1.25	1.000	1.25	0.979	1.22	-0.5
Inner Tube Diameter	1.75	6.00	0.000	1.75	0.000	1.75	0.75
Fin Thickness	0.063	0.125	0.749	0.109	0.693	0.106	-0.5
Cost			$538,679		$537,233		

Test name: NominalALL6r_2							
	Range		**Starting Value**		**Optimal Value**		**Si**
	Min	**Max**	**Normalized**	**Actual**	**Normalized**	**Actual**	
Gas-side Surface Area						226,432	
Tube Length [ft]						17.7	
Gas Velocity	7.5	80.0	0.584	49.9	0.582	49.7	0.1
Air Velocity	7.5	50.0	0.001	7.5	0.045	9.5	-0.4
Fin Pitch	0.20	1.00	0.000	0.20	0.000	0.20	-0.4
Fin Length	0.00	1.25	1.000	1.25	1.000	1.25	0.4
Inner Tube Diameter	1.75	6.00	0.000	1.75	0.000	1.75	-0.4
Fin Thickness	0.063	0.125	0.749	0.109	0.728	0.108	0.25
Cost			$538,679		$536,853		

The details of the optimal ACC having six tube rows are:

NominalAll6r_2	
Flue Gas Flow Rate [lbm/hr]	6,000,000
Vapor Flow Rate [lbm/hr]	403,720
Cooling Air Flow Rate [lbm/hr]	36,239,875
Flue Gas Velocity [ft/sec]	49.7
Cooling Air Velocity [ft/sec]	9.5
Inlet Flue Gas Temperature [F]	135
Inlet Cooling Air Temperature [F]	75
Exit Flue Gas Temperature [F]	100.7
Exit Cooling Air Temperature [F]	108.4
Tube Inner Diameter [inch]	1.75
Tube Thickness [inch]	0.2
Fin Length [inches]	1.25
Fin Pitch [inches]	0.2
Fin Thickness [inches]	0.108
Number of Tube Rows	6
Transverse Tube Spacing [inches]	4.65
Longitudinal Tube Spacing [inches]	4.65
Number of Tubes	30000
Tube Length [ft]	17.7
Gas-side Surface Area [ft2]	52,151,492
Air-side Surface Area [ft2]	190,804,257
Field Erected Capital Cost	$7,079,873
Annualized Capital Cost	$568,107
Annualized Operating Cost	$199,623
Estimated Annual Savings in Water Costs @ $1.50 per 1000 gallon	$230,877
Net Annualized Cost [20 yrs @ 5%]	$536,853
Gas-Side Fan Power [kW]	346
Air-Side Fan Power [kW]	147
Sensible Heat Transfer [BTU/hr]	52,151,492
Latent Heat Transfer [BTU/hr]	190,804,257
Condensation Rate [lbm/hr]	183,418
Condensation Efficiency	45%
Inlet/Exit Moisture Concentration [% wet-basis]	11/6.3

Appendix B.2.4 - Eight Tube Rows

Test name: NominalALL8r							
	Range		**Starting Value**		**Optimal Value**		**Si**
	Min	**Max**	**Normalized**	**Actual**	**Normalized**	**Actual**	
Gas-side Surface Area						308,993	
Tube Length [ft]						21.9	
Gas Velocity	7.5	80.0	0.584	49.9	0.568	48.7	-0.5
Air Velocity	7.5	50.0	0.001	7.5	0.005	7.7	0.5
Fin Pitch	0.20	1.00	0.000	0.20	0.000	0.20	0.5
Fin Length	0.00	1.25	1.000	1.25	0.997	1.25	-0.5
Inner Tube Diameter	1.75	6.00	0.000	1.75	0.000	1.75	0.75
Fin Thickness	0.063	0.125	0.749	0.109	0.731	0.108	-0.5
Cost			$731,148		$726,919		

Test name: NominalALL8r_2							
	Range		**Starting Value**		**Optimal Value**		**Si**
	Min	**Max**	**Normalized**	**Actual**	**Normalized**	**Actual**	
Gas-side Surface Area						289,243	
Tube Length [ft]						22.4	
Gas Velocity	7.5	80.0	0.584	49.9	0.572	49.0	0.1
Air Velocity	7.5	50.0	0.001	7.5	0.045	9.4	-0.4
Fin Pitch	0.20	1.00	0.000	0.20	0.000	0.20	-0.4
Fin Length	0.00	1.25	1.000	1.25	1.000	1.25	0.4
Inner Tube Diameter	1.75	6.00	0.000	1.75	0.000	1.75	-0.4
Fin Thickness	0.063	0.125	0.749	0.109	0.712	0.107	0.25
Cost			$731,148		$726,390		

The details of the optimal ACC having eight tube rows are:

NominalAll8r_2	
Flue Gas Flow Rate [lbm/hr]	6,000,000
Vapor Flow Rate [lbm/hr]	403,720
Cooling Air Flow Rate [lbm/hr]	28,413,286
Flue Gas Velocity [ft/sec]	49.0
Cooling Air Velocity [ft/sec]	9.4
Inlet Flue Gas Temperature [F]	135
Inlet Cooling Air Temperature [F]	75
Exit Flue Gas Temperature [F]	98.9
Exit Cooling Air Temperature [F]	111.7
Tube Inner Diameter [inch]	1.75
Tube Thickness [inch]	0.2
Fin Length [inches]	1.25
Fin Pitch [inches]	0.2
Fin Thickness [inches]	0.107
Number of Tube Rows	8
Transverse Tube Spacing [inches]	4.64
Longitudinal Tube Spacing [inches]	4.64
Number of Tubes	30000
Tube Length [ft]	22.4
Gas-side Surface Area [ft2]	289,243
Air-side Surface Area [ft2]	14,980,590
Field Erected Capital Cost	$9,103,401
Annualized Capital Cost	$730,480
Annualized Operating Cost	$237,154
Estimated Annual Savings in Water Costs @ $1.50 per 1000 gallon	$233,063
Net Annualized Cost [20 yrs @ 5%]	$726,390
Gas-Side Fan Power [kW]	398
Air-Side Fan Power [kW]	175
Sensible Heat Transfer [BTU/hr]	54,791,629
Latent Heat Transfer [BTU/hr]	195,889,856
Condensation Rate [lbm/hr]	188,405
Condensation Efficiency	47%
Inlet/Exit Moisture Concentration [% wet-basis]	11/6.2

Appendix B.3 – Effect of Inlet Cooling Air Temperature on the Optimal Design

This section details the optimization simulations of the ACC described in Section 0, which discusses inlet cooling air effects. Four optimizations were carried out for each case with inlet cooling air temperatures of 40^{o}F, 60^{o}F, 75^{o}F, and 90^{o}F. In each case the optimization converged to similar design choices and process conditions.

Each table represents one optimization simulation. The variables optimized are listed in the Table and the range of each variable is given in the second and third columns. The columns labeled "Starting Value" list the variables used as the initial guess, which was one vertex of the initial simplex. The column labeled "Si" is the parameter assigned to each variable which built the remaining vertexes of the simplex using the Tilted Initial Simplex Method described in Walters [42]. The columns labeled "Optimal Value" list the values of the optimal heat exchanger design. Under the headings "Starting Value" and "Optimal Value", there are "Normalized" and "Actual" values. These correspond to the dimensionless and absolute values of the variables, respectively. Recall from Section 2.4, the variables were normalized during the optimization to remove the units from the optimization equations.

Appendix B.3.1 – Inlet Cooling Air Temperature: 40°F

The following tables are the four optimization simulations performed with an inlet cooling air temperature of 40°F, and the details of the ACC's design for the best of the four optimizations follows.

Test name: NominalALL5c							
	Range		**Starting Value**		**Optimal Value**		**Si**
	Min	**Max**	**Normalized**	**Actual**	**Normalized**	**Actual**	
Gas-side Surface Area						98,332	
Tube Length						7.1	
Gas Velocity	7.5	80.0	0.621	52.5	0.577	49.3	0.125
Air Velocity	7.5	50.0	0.000	7.5	0.000	7.5	0.125
Fin Pitch	0.20	1.00	0.500	0.60	0.000	0.20	0.125
Fin Length	0.00	1.25	1.000	1.25	0.947	1.18	-0.125
Inner Tube Diameter	1.75	6.00	0.000	1.75	0.003	1.76	0.125
Fin Thickness	0.063	0.125	0.941	0.121	0.699	0.106	-0.125
Net Annual Cost			$193,109		$127,300		

Test name: NominalALL6c							
	Range		**Starting Value**		**Optimal Value**		**Si**
	Min	**Max**	**Normalized**	**Actual**	**Normalized**	**Actual**	
Gas-side Surface Area						93,086	
Tube Length						7.1	
Gas Velocity	7.5	80.0	0.621	52.5	0.627	52.9	-0.5
Air Velocity	7.5	50.0	0.000	7.5	0.032	8.8	0.5
Fin Pitch	0.20	1.00	0.000	0.20	0.000	0.20	0.5
Fin Length	0.00	1.25	1.000	1.25	0.930	1.16	-0.5
Inner Tube Diameter	1.75	6.00	0.000	1.75	0.000	1.75	0.5
Fin Thickness	0.063	0.125	0.941	0.121	0.849	0.116	-0.5
Net Annual Cost			$193,109		$129,276		

Test name: NominalALL7c							
	Range		**Starting Value**		**Optimal Value**		**Si**
	Min	**Max**	**Normalized**	**Actual**	**Normalized**	**Actual**	
Gas-side Surface Area						96,274	
Tube Length						7.4	
Gas Velocity	7.5	80.0	0.500	43.8	0.620	52.5	0.125
Air Velocity	7.5	50.0	0.500	28.8	0.012	8.0	-0.125
Fin Pitch	0.20	1.00	0.500	0.60	0.009	0.21	-0.125
Fin Length	0.00	1.25	0.500	0.63	0.856	1.07	0.125
Inner Tube Diameter	1.75	6.00	0.500	3.88	0.001	1.75	-0.125
Fin Thickness	0.063	0.125	0.500	0.094	0.277	0.080	-0.125
Net Annual Cost			$469,928		$133,108		

Test name: NominalALL8c							
	Range		**Starting Value**		**Optimal Value**		**Si**
	Min	**Max**	**Normalized**	**Actual**	**Normalized**	**Actual**	
Gas-side Surface Area						99,289	
Tube Length						6.9	
Gas Velocity	7.5	80.0	0.500	43.8	0.556	47.8	0.125
Air Velocity	7.5	50.0	0.500	28.8	0.001	7.5	-0.4
Fin Pitch	0.20	1.00	0.500	0.60	0.000	0.20	-0.4
Fin Length	0.00	1.25	0.500	0.63	0.987	1.23	0.4
Inner Tube Diameter	1.75	6.00	0.500	3.88	0.000	1.75	-0.4
Fin Thickness	0.063	0.125	0.500	0.094	0.957	0.122	0.4
Net Annual Cost			$469,928		$125,764		

The details of the optimal ACC having an inlet cooling air temperature of 40^{o}F are:

NominalAll8c	
Flue Gas Flow Rate [lbm/hr]	6,000,000
Vapor Flow Rate [lbm/hr]	403,720
Cooling Air Flow Rate [lbm/hr]	33,289,734
Flue Gas Velocity [ft/sec]	44.0
Cooling Air Velocity [ft/sec]	7.8
Inlet Flue Gas Temperature [F]	135
Inlet Cooling Air Temperature [F]	40
Exit Flue Gas Temperature [F]	97.2
Exit Cooling Air Temperature [F]	72.7
Tube Inner Diameter [inch]	1.75
Tube Thickness [inch]	0.2
Fin Length [inches]	1.23
Fin Pitch [inches]	0.2
Fin Thickness [inches]	122
Number of Tube Rows	2
Transverse Tube Spacing [inches]	4.62
Longitudinal Tube Spacing [inches]	4.62
Number of Tubes	31000
Tube Length [ft]	6.9
Gas-side Surface Area [ft2]	99,289
Air-side Surface Area [ft2]	5,111,628
Field Erected Capital Cost	$3,583,961
Annualized Capital Cost	$287,586
Annualized Operating Cost	$80,997
Estimated Annual Savings in Water Costs @ $1.50 per 1000 gallon	$242,819
Net Annualized Cost [20 yrs @ 5%]	$125,765
Gas-Side Fan Power [kW]	165
Air-Side Fan Power [kW]	42
Sensible Heat Transfer [BTU/hr]	57,612,908
Latent Heat Transfer [BTU/hr]	203,959,346
Condensation Rate [lbm/hr]	192,905
Condensation Efficiency	48%
Inlet/Exit Moisture Concentration [% wet-basis]	11/6.1

Appendix B.3.2 - Inlet Cooling Air Temperature: 60°F

The following tables are the 4 optimization simulations performed with an inlet cooling air temperature of 60°F, and the details of the ACC's design for the best of the four optimizations.

Test name: NominalALL5b							
	Range		**Starting Value**		**Optimal Value**		**Si**
	Min	**Max**	**Normalized**	**Actual**	**Normalized**	**Actual**	
Gas-side Surface Area						127,936	
Tube Length						8.5	
Gas Velocity	7.5	80.0	0.500	43.8	0.527	45.7	0.125
Air Velocity	7.5	50.0	0.255	18.3	0.000	7.5	-0.125
Fin Pitch	0.20	1.00	0.007	0.21	0.015	0.21	0.05
Fin Length	0.00	1.25	0.277	0.35	0.994	1.24	0.15
Inner Tube Diameter	1.75	6.00	0.027	1.86	0.000	1.75	1
Fin Thickness	0.063	0.125	1.000	0.125	0.778	0.111	-0.1
Net Annual Cost			$306,401		$196,723		

Test name: NominalALL6b							
	Range		**Starting Value**		**Optimal Value**		**Si**
	Min	**Max**	**Normalized**	**Actual**	**Normalized**	**Actual**	
Gas-side Surface Area						123,966	
Tube Length						9.1	
Gas Velocity	7.5	80.0	0.473	41.8	0.559	48.0	0.5
Air Velocity	7.5	50.0	0.038	9.1	0.000	7.5	0.5
Fin Pitch	0.20	1.00	0.021	0.22	0.003	0.20	0.5
Fin Length	0.00	1.25	1.000	1.25	1.000	1.25	-0.5
Inner Tube Diameter	1.75	6.00	0.058	1.99	0.019	1.83	0.5
Fin Thickness	0.063	0.125	1.000	0.125	0.798	0.112	-0.5
Net Annual Cost			$216,010		$196,910		

Test name: NominalALL7b							
	Range		**Starting Value**		**Optimal Value**		**Si**
	Min	**Max**	**Normalized**	**Actual**	**Normalized**	**Actual**	
Gas-side Surface Area						120,506	
Tube Length						9.3	
Gas Velocity	7.5	80.0	0.500	43.8	0.623	52.7	0.125
Air Velocity	7.5	50.0	0.500	28.8	0.062	10.1	-0.125
Fin Pitch	0.20	1.00	0.500	0.60	0.000	0.20	-0.125
Fin Length	0.00	1.25	0.500	0.63	0.806	1.01	0.125
Inner Tube Diameter	1.75	6.00	0.500	3.88	0.000	1.75	-0.125
Fin Thickness	0.063	0.125	0.500	0.094	0.412	0.088	-0.125
Net Annual Cost			$693,968		$207,000		

Test name: NominalALL8b							
	Range		**Starting Value**		**Optimal Value**		**Si**
	Min	**Max**	**Normalized**	**Actual**	**Normalized**	**Actual**	
Gas-side Surface Area						115,194	
Tube Length						8.8	
Gas Velocity	7.5	80.0	0.500	43.8	0.621	52.5	0.125
Air Velocity	7.5	50.0	0.500	28.8	0.000	7.5	-0.4
Fin Pitch	0.20	1.00	0.500	0.60	0.000	0.20	-0.4
Fin Length	0.00	1.25	0.500	0.63	1.000	1.25	0.4
Inner Tube Diameter	1.75	6.00	0.500	3.88	0.000	1.75	-0.4
Fin Thickness	0.063	0.125	0.500	0.094	0.941	0.121	0.4
Net Annual Cost			$693,968		$193,458		

The details of the optimal ACC having an inlet cooling air temperature of 60^{o}F are:

NominalAll8b	
Flue Gas Flow Rate [lbm/hr]	6,000,000
Vapor Flow Rate [lbm/hr]	403,720
Cooling Air Flow Rate [lbm/hr]	37,625,756
Flue Gas Velocity [ft/sec]	48.6
Cooling Air Velocity [ft/sec]	7.7
Inlet Flue Gas Temperature [F]	135
Inlet Cooling Air Temperature [F]	60
Exit Flue Gas Temperature [F]	101.1
Exit Cooling Air Temperature [F]	87.5
Tube Inner Diameter [inch]	1.75
Tube Thickness [inch]	0.2
Fin Length [inches]	1.25
Fin Pitch [inches]	0.2
Fin Thickness [inches]	0.121
Number of Tube Rows	2
Transverse Tube Spacing [inches]	4.65
Longitudinal Tube Spacing [inches]	4.65
Number of Tubes	29000
Tube Length [ft]	8.8
Gas-side Surface Area [ft2]	115,194
Air-side Surface Area [ft2]	6,014,738
Field Erected Capital Cost	$4,036,337
Annualized Capital Cost	$323,886
Annualized Operating Cost	$106,162
Estimated Annual Savings in Water Costs @ $1.50 per 1000 gallon	$236,590
Net Annualized Cost [20 yrs @ 5%]	$193,458
Gas-Side Fan Power [kW]	222
Air-Side Fan Power [kW]	39
Sensible Heat Transfer [BTU/hr]	51,681,997
Latent Heat Transfer [BTU/hr]	197,045,865
Condensation Rate [lbm/hr]	187,957
Condensation Efficiency	47%
Inlet/Exit Moisture Concentration [% wet-basis]	11/6.2

Appendix B.3.3 – Inlet Cooling Air Temperature: 75°F

The following tables are the 4 optimization simulations performed with an inlet cooling air temperature of 75°F, and the details of the ACC's design for the best of the four optimizations.

Test name: NominalALL1a							
	Range		**Starting Value**		**Optimal Value**		**Si**
	Min	**Max**	**Normalized**	**Actual**	**Normalized**	**Actual**	
Surface Area						161,416	
Tube Length						11.7	
Gas Velocity	7.5	80.0	0.500	43.8	0.584	49.9	0.125
Air Velocity	7.5	50.0	0.255	18.3	0.001	7.5	-0.125
Fin Pitch	0.20	1.00	0.007	0.21	0.000	0.20	0.05
Fin Length	0.00	1.25	0.277	0.35	1.000	1.25	0.15
Inner Tube Diameter	1.75	6.00	0.027	1.86	0.000	1.75	1
Fin Thickness	0.063	0.125	1.000	0.125	0.749	0.109	-0.1
Net Annual Cost			$476,078		$306,748		

Test name: NominalALL2a							
	Range		**Starting Value**		**Optimal Value**		**Si**
	Min	**Max**	**Normalized**	**Actual**	**Normalized**	**Actual**	
Surface Area						194,978	
Tube Length						12.5	
Gas Velocity	7.5	80.0	0.500	43.8	0.501	43.9	0.25
Air Velocity	7.5	50.0	0.255	18.3	0.063	10.2	0.25
Fin Pitch	0.20	1.00	0.007	0.21	0.000	0.20	0.5
Fin Length	0.00	1.25	0.277	0.35	0.596	0.75	0.15
Inner Tube Diameter	1.75	6.00	0.027	1.86	0.003	1.76	0.125
Fin Thickness	0.063	0.125	1.000	0.125	0.056	0.066	-0.5
Net Annual Cost			$476,078		$364,417		

Test name: NominalALL4a							
	Range		**Starting Value**		**Optimal Value**		**Si**
	Min	**Max**	**Normalized**	**Actual**	**Normalized**	**Actual**	
Surface Area						162,212	
Tube Length						11.9	
Gas Velocity	7.5	80.0	0.500	43.8	0.590	50.2	-0.5
Air Velocity	7.5	50.0	0.255	18.3	0.003	7.6	0.5
Fin Pitch	0.20	1.00	0.007	0.21	0.007	0.21	0.5
Fin Length	0.00	1.25	0.277	0.35	0.999	1.25	0.5
Inner Tube Diameter	1.75	6.00	0.027	1.86	0.000	1.75	0.5
Fin Thickness	0.063	0.125	1.000	0.125	0.629	0.102	-0.5
Net Annual Cost			$476,078		$310,776		

Test name: NominalALL5a							
	Range		Starting Value		Optimal Value		Si
	Min	Max	Normalized	Actual	Normalized	Actual	
Surface Area						185,583	
Tube Length						12.9	
Gas Velocity	7.5	80.0	0.500	43.8	0.473	41.8	-0.133
Air Velocity	7.5	50.0	0.255	18.3	0.038	9.1	0.133
Fin Pitch	0.20	1.00	0.007	0.21	0.021	0.22	0.133
Fin Length	0.00	1.25	0.277	0.35	1.000	1.25	0.133
Inner Tube Diameter	1.75	6.00	0.027	1.86	0.058	1.99	0.133
Fin Thickness	0.063	0.125	1.000	0.125	1.000	0.125	-0.133
Net Annual Cost			$476,078		$335,280		

The details of the optimal ACC having an inlet cooling air temperature of 75^{o}F are:

OptimalALL1a	
Flue Gas Flow Rate [lbm/hr]	6,000,000
Vapor Flow Rate [lbm/hr]	403,720
Cooling Air Flow Rate [lbm/hr]	53,638,732
Inlet Flue Gas Temperature [F]	135
Inlet Cooling Air Temperature [F]	75
Exit Flue Gas Temperature [F]	101.7
Exit Cooling Air Temperature [F]	94.1
Tube Inner Diameter [inch]	1.75
Tube Thickness [inch]	0.2
Fin Length [inches]	1.25
Fin Pitch [inches]	0.2
Fin Thickness [inches]	0.109
Number of Tube Rows	2
Transverse Tube Spacing [inches]	4.65
Longitudinal Tube Spacing [inches]	4.65
Number of Tubes	30000
Tube Length [ft]	11.7
Gas-side Surface Area [ft2]	161,416
Air-side Surface Area [ft2]	8,404,383
Field Erected Capital Cost	$5,286,886
Annualized Capital Cost	$424,233
Annualized Operating Cost	$118,771
Estimated Annual Savings in Water Costs @ $1.50 per 1000 gallon	$236,256
Net Annualized Cost [20 yrs @ 5%]	$306,749
Gas-Side Fan Power [kW]	233
Air-Side Fan Power [kW]	55
Sensible Heat Transfer [BTU/hr]	50,670,814
Latent Heat Transfer [BTU/hr]	195,779,374
Condensation Rate [lbm/hr]	187,691
Condensation Efficiency	47%
Inlet/Exit Moisture Concentration [% wet-basis]	11/6.2

Appendix B.3.4 - Inlet Cooling Air Temperature: 90°F

The following tables are the 4 optimization simulations performed with an inlet cooling air temperature of 90°F, and the details of the ACC's design for the best of the four optimizations.

Test name: NominalALL5d_2							
	Range		**Starting Value**		**Optimal Value**		**Si**
	Min	**Max**	**Normalized**	**Actual**	**Normalized**	**Actual**	
Surface Area						331,780	
Tube Length						21.4	
Gas Velocity	7.5	80.0	0.6	52.5	0.5	44.2	0.1
Air Velocity	7.5	50.0	0.0	7.5	0.0	8.4	0.1
Fin Pitch	0.20	1.00	0.50	0.60	0.00	0.20	0.13
Fin Length	0.00	1.25	1.00	1.25	0.98	1.23	-0.13
Inner Tube Diameter	1.75	6.00	0.00	1.75	0.00	1.75	0.13
Fin Thickness	0.063	0.125	0.941	0.121	0.975	0.123	-0.125
Net Annual Cost			$1,184,809		$733,028		

Test name: NominalALL6d_2							
	Range		**Starting Value**		**Optimal Value**		**Si**
	Min	**Max**	**Normalized**	**Actual**	**Normalized**	**Actual**	
Surface Area						317,747	
Tube Length						22.4	
Gas Velocity	7.5	80.0	0.6	52.5	0.6	48.3	-0.5
Air Velocity	7.5	50.0	0.0	7.5	0.0	7.9	0.5
Fin Pitch	0.20	1.00	0.50	0.60	0.00	0.20	0.50
Fin Length	0.00	1.25	1.00	1.25	1.00	1.25	-0.50
Inner Tube Diameter	1.75	6.00	0.00	1.75	0.00	1.75	0.50
Fin Thickness	0.063	0.125	0.941	0.121	0.836	0.115	-0.500
Net Annual Cost			$1,184,809		$732,000		

Test name: NominalALL7d_2							
	Range		**Starting Value**		**Optimal Value**		**Si**
	Min	**Max**	**Normalized**	**Actual**	**Normalized**	**Actual**	
Surface Area						259,434	
Tube Length						27.7	
Gas Velocity	7.5	80.0	0.5	43.8	0.9	72.7	0.1
Air Velocity	7.5	50.0	0.5	28.8	0.0	7.8	-0.1
Fin Pitch	0.20	1.00	0.50	0.60	0.00	0.20	-0.13
Fin Length	0.00	1.25	0.50	0.63	1.00	1.24	0.13
Inner Tube Diameter	1.75	6.00	0.50	3.88	0.00	1.77	-0.13
Fin Thickness	0.063	0.125	0.500	0.094	0.785	0.112	0.125
Net Annual Cost			$2,065,606		$824,839		

Test name: NominalALL8d_2							
	Range		**Starting Value**		**Optimal Value**		**Si**
	Min	**Max**	**Normalized**	**Actual**	**Normalized**	**Actual**	
Surface Area						297,940	
Tube Length						23.4	
Gas Velocity	7.5	80.0	0.5	43.8	0.6	53.9	0.1
Air Velocity	7.5	50.0	0.5	28.8	0.0	8.3	-0.4
Fin Pitch	0.20	1.00	0.50	0.60	0.00	0.20	-0.40
Fin Length	0.00	1.25	0.50	0.63	1.00	1.24	0.40
Inner Tube Diameter	1.75	6.00	0.50	3.88	0.00	1.75	-0.40
Fin Thickness	0.063	0.125	0.500	0.094	0.849	0.116	0.400
Net Annual Cost			$2,065,606		$736,307		

The details of the optimal ACC having an inlet cooling air temperature of 90^{o}F are:

NominalAll6d_2	
Flue Gas Flow Rate [lbm/hr]	6,000,000
Vapor Flow Rate [lbm/hr]	403,720
Cooling Air Flow Rate [lbm/hr]	106,294,869
Flue Gas Velocity [ft/sec]	44.2
Cooling Air Velocity [ft/sec]	8.0
Inlet Flue Gas Temperature [F]	135
Inlet Cooling Air Temperature [F]	90
Exit Flue Gas Temperature [F]	99.5
Exit Cooling Air Temperature [F]	99.9
Tube Inner Diameter [inch]	1.75
Tube Thickness [inch]	0.2
Fin Length [inches]	1.25
Fin Pitch [inches]	0.2
Fin Thickness [inches]	0.115
Number of Tube Rows	2
Transverse Tube Spacing [inches]	4.65
Longitudinal Tube Spacing [inches]	4.65
Number of Tubes	31000
Tube Length [ft]	22.4
Gas-side Surface Area [ft2]	317,747
Air-side Surface Area [ft2]	1,648,941
Field Erected Capital Cost	$9,814,342
Annualized Capital Cost	$787,528
Annualized Operating Cost	$186,226
Estimated Annual Savings in Water Costs @ $1.50 per 1000 gallon	$241,754
Net Annualized Cost [20 yrs @ 5%]	$732,001
Gas-Side Fan Power [kW]	331
Air-Side Fan Power [kW]	136
Sensible Heat Transfer [BTU/hr]	53,838,611
Latent Heat Transfer [BTU/hr]	199,365,760
Condensation Rate [lbm/hr]	192,059
Condensation Efficiency	48%
Inlet/Exit Moisture Concentration [% wet-basis]	11/6.1

Appendix B.4 - Effect of Inlet Flue Gas Temperature on the Optimal Design

The following sections tabulate the optimization results and initial simplexes for the simulations discussed in Section 5.3.4, which discussed inlet flue gas temperature effects. Four inlet flue gas temperatures were investigated: 135^{o}F, 150^{o}F, 175^{o}F, 200^{o}F, and 225^{o}F.

Each table represents one optimization simulation. The variables optimized are listed in the Table and the range of each variable is given in the second and third columns. The columns labeled "Starting Value" list the variables used as the initial guess, which was one vertex of the initial simplex. The column labeled "Si" is the parameter assigned to each variable which built the remaining vertexes of the simplex using the Tilted Initial Simplex Method described in Walters [42]. The columns labeled "Optimal Value" list the values of the optimal heat exchanger design. Under the headings "Starting Value" and "Optimal Value", there are "Normalized" and "Actual" values. These correspond to the dimensionless and absolute values of the variables, respectively. Recall from Section 2.4, the variables were normalized during the optimization to remove the units from the optimization equations.

Appendix B.4.1 - Inlet Flue Gas Temperature: 135°F

The following tables are the 4 optimization simulations performed with an inlet flue gas temperature of 135°F, and the details of the ACC's design for the best of the four optimizations.

Test name: NominalTfg1a							
	Range		**Starting Value**		**Optimal Value**		**Si**
	Min	**Max**	**Normalized**	**Actual**	**Normalized**	**Actual**	
Gas-side Surface Area						157,276	
Tube Length						12	
Gas Velocity	7.5	80.0	0.500	43.8	0.620	52.5	0.125
Air Velocity	7.5	50.0	0.500	28.8	0.001	7.6	-0.4
Fin Pitch	0.20	1.00	0.500	0.60	0.000	0.20	-0.4
Fin Length	0.00	1.25	0.500	0.63	0.986	1.23	0.4
Inner Tube Diameter	1.75	6.00	0.500	3.88	0.000	1.75	-0.4
Fin Thickness	0.063	0.125	0.500	0.094	0.842	0.115	0.4
Net Annual Cost			$1,026,852		$308,419		

Test name: NominalTfg1b							
	Range		**Starting Value**		**Optimal Value**		**Si**
	Min	**Max**	**Normalized**	**Actual**	**Normalized**	**Actual**	
Gas-side Surface Area						161,005	
Tube Length						12	
Gas Velocity	7.5	80.0	0.500	43.8	0.599	50.9	0.125
Air Velocity	7.5	50.0	0.500	28.8	0.002	7.6	-0.125
Fin Pitch	0.20	1.00	0.500	0.60	0.011	0.21	-0.125
Fin Length	0.00	1.25	0.500	0.63	1.000	1.25	0.125
Inner Tube Diameter	1.75	6.00	0.500	3.88	0.001	1.75	-0.125
Fin Thickness	0.063	0.125	0.500	0.094	0.856	0.116	0.125
Net Annual Cost			$1,026,852		$310,612		

Test name: NominalTfg1c							
	Range		**Starting Value**		**Optimal Value**		**Si**
	Min	**Max**	**Normalized**	**Actual**	**Normalized**	**Actual**	
Gas-side Surface Area						161,342	
Tube Length						11.7	
Gas Velocity	7.5	80.0	0.584	49.9	0.585	49.9	-0.5
Air Velocity	7.5	50.0	0.001	7.5	0.001	7.5	0.5
Fin Pitch	0.20	1.00	0.000	0.20	0.000	0.20	0.5
Fin Length	0.00	1.25	1.000	1.25	1.000	1.25	-0.5
Inner Tube Diameter	1.75	6.00	0.000	1.75	0.000	1.75	0.5
Fin Thickness	0.063	0.125	0.749	0.109	0.768	0.110	-0.5
Net Annual Cost			$308,376		$306,652		

Test name NominalTfg1d							
	Range		**Starting Value**		**Optimal Value**		**Si**
	Min	**Max**	**Normalized**	**Actual**	**Normalized**	**Actual**	
Gas-side Surface Area						158,472	
Tube Length						11.8	
Gas Velocity	7.5	80.0	0.584	49.9	0.602	51.1	0.125
Air Velocity	7.5	50.0	0.001	7.5	0.006	7.8	0.125
Fin Pitch	0.20	1.00	0.000	0.20	0.000	0.20	0.125
Fin Length	0.00	1.25	1.000	1.25	1.000	1.25	-0.125
Inner Tube Diameter	1.75	6.00	0.000	1.75	0.000	1.75	0.125
Fin Thickness	0.063	0.125	0.749	0.109	0.789	0.112	0.125
Net Annual Cost			$308,377		$306,641		

Test name: NominalTfg1c	
Flue Gas Flow rate [lbm/hr]	6,000,000
Vapor Flow rate [lbm/hr]	403,720
Cooling Air Flow rate [lbm/hr]	53,372,673
Flue Gas Velocity [ft/sec]	46.1
Cooling Air Velocity [ft/sec]	7.7
Inlet Flue Gas Temperature [F]	135
Inlet Cooling Air Temperature [F]	75
Exit Flue Gas Temperature [F]	101.7
Exit Cooling Air Temperature [F]	94.2
Tube Inner Diameter [inch]	1.75
Tube Thickness [inch]	0.2
Fin Length [inches]	1.25
Fin Pitch [inches]	0.2
Fin Thickness [inches]	0.11
Number of Tube Rows	2
Transverse Tube Spacing [inches]	4.65
Longitudinal Tube Spacing [inches]	4.65
Number of Tubes	30000
Tube Length [ft]	11.7
Gas-side Surface Area [ft2]	161,342
Air-side Surface Area [ft2]	8,402,692
Field Erected Capital Cost	$5,284,960
Annualized Capital Cost	$424,079
Annualized Operating Cost	$118,717
Estimated Annual Savings in Water Costs @ $1.50 per 1000 gallon	$236,144
Net Annualized Cost [20 yrs @ 5%]	$306,652
Gas-Side Fan Power [kW]	235
Air-Side Fan Power [kW]	55
Sensible Heat Transfer [BTU/hr]	50,649,913
Latent Heat Transfer [BTU/hr]	195,685,511
Condensation Rate [lbm/hr]	187,603
Condensation Efficiency	47%
Inlet/Exit Moisture Concentration [% wet-basis]	11/6.2

Appendix B.4.2 - Inlet Flue Gas Temperature: 150°F

The following tables are the 4 optimization simulations performed with an inlet flue gas temperature of 150°F, and the details of the ACC's design for the best of the four optimizations.

Test name: NominalTfg2a							
	Range		**Starting Value**		**Optimal Value**		**Si**
	Min	**Max**	**Normalized**	**Actual**	**Normalized**	**Actual**	
Gas-side Surface Area						160,195	
Tube Length						12.1	
Gas Velocity	7.5	80.0	0.500	43.8	0.629	53.1	0.125
Air Velocity	7.5	50.0	0.500	28.8	0.011	7.9	-0.4
Fin Pitch	0.20	1.00	0.500	0.60	0.000	0.20	-0.4
Fin Length	0.00	1.25	0.500	0.63	1.000	1.25	0.4
Inner Tube Diameter	1.75	6.00	0.500	3.88	0.000	1.75	-0.4
Fin Thickness	0.063	0.125	0.500	0.094	0.871	0.117	0.4
Net Annual Cost			1,079,520		320,199		

Test name: NominalTfg2b							
	Range		**Starting Value**		**Optimal Value**		**Si**
	Min	**Max**	**Normalized**	**Actual**	**Normalized**	**Actual**	
Gas-side Surface Area						143,362	
Tube Length						13	
Gas Velocity	7.5	80.0	0.500	43.8	0.774	63.6	0.125
Air Velocity	7.5	50.0	0.500	28.8	0.029	8.7	-0.125
Fin Pitch	0.20	1.00	0.500	0.60	0.004	0.20	-0.125
Fin Length	0.00	1.25	0.500	0.63	0.998	1.25	0.125
Inner Tube Diameter	1.75	6.00	0.500	3.88	0.002	1.76	-0.125
Fin Thickness	0.063	0.125	0.500	0.094	0.844	0.115	0
Net Annual Cost			$1,079,520		$337,348		

Test name: NominalTfg2c							
	Range		**Starting Value**		**Optimal Value**		**Si**
	Min	**Max**	**Normalized**	**Actual**	**Normalized**	**Actual**	
Gas-side Surface Area						167,415	
Tube Length						11.9	
Gas Velocity	7.5	80.0	0.584	49.9	0.585	49.9	-0.5
Air Velocity	7.5	50.0	0.001	7.5	0.001	7.5	0.5
Fin Pitch	0.20	1.00	0.000	0.20	0.000	0.20	0.5
Fin Length	0.00	1.25	1.000	1.25	1.000	1.25	-0.5
Inner Tube Diameter	1.75	6.00	0.000	1.75	0.000	1.75	0.5
Fin Thickness	0.063	0.125	0.749	0.109	0.749	0.109	-1
Net Annual Cost			$320,388		$320,317		

Test name: NominalTfg2d							
	Range		**Starting Value**		**Optimal Value**		**Si**
	Min	**Max**	**Normalized**	**Actual**	**Normalized**	**Actual**	
Gas-side Surface Area						165,867	
Tube Length						11.9	
Gas Velocity	7.5	80.0	0.584	49.9	0.591	50.4	0.125
Air Velocity	7.5	50.0	0.001	7.5	0.006	7.7	0.125
Fin Pitch	0.20	1.00	0.000	0.20	0.000	0.20	0.125
Fin Length	0.00	1.25	1.000	1.25	1.000	1.25	-0.125
Inner Tube Diameter	1.75	6.00	0.000	1.75	0.000	1.75	0.125
Fin Thickness	0.063	0.125	0.749	0.109	0.778	0.111	0.125
Net Annual Cost			$320,388		$320,045		

Test name: NominalTfg2d	
Flue Gas Flow rate [lbm/hr]	6,000,000
Vapor Flow rate [lbm/hr]	403,720
Cooling Air Flow rate [lbm/hr]	56,361,486
Flue Gas Velocity [ft/sec]	46.1
Cooling Air Velocity [ft/sec]	7.9
Inlet Flue Gas Temperature [F]	150
Inlet Cooling Air Temperature [F]	75
Exit Flue Gas Temperature [F]	106.2
Exit Cooling Air Temperature [F]	94.3
Tube Inner Diameter [inch]	1.75
Tube Thickness [inch]	0.2
Fin Length [inches]	1.25
Fin Pitch [inches]	0.2
Fin Thickness [inches]	0.111
Number of Tube Rows	2
Transverse Tube Spacing [inches]	4.65
Longitudinal Tube Spacing [inches]	4.65
Number of Tubes	30000
Tube Length [ft]	11.9
Gas-side Surface Area [ft2]	165,867
Air-side Surface Area [ft2]	8,630,426
Field Erected Capital Cost	$5,403,208
Annualized Capital Cost	$433,567
Annualized Operating Cost	$122,386
Estimated Annual Savings in Water Costs @ $1.50 per 1000 gallon	$235,909
Net Annualized Cost [20 yrs @ 5%]	$320,045
Gas-Side Fan Power [kW]	233
Air-Side Fan Power [kW]	72
Sensible Heat Transfer [BTU/hr]	66,786,347
Latent Heat Transfer [BTU/hr]	195,477,668
Condensation Rate [lbm/hr]	187,416
Condensation Efficiency	46%
Inlet//Exit Moisture Concentration [F]	11/6.2

Appendix B.4.3 – Inlet Flue Gas Temperature: 175°F

The following tables are the 4 optimization simulations performed with an inlet flue gas temperature of 175°F, and the details of the ACC's design for the best of the four optimizations.

Test name: NominalTfg3a							
	Range		**Starting Value**		**Optimal Value**		**Si**
	Min	**Max**	**Normalized**	**Actual**	**Normalized**	**Actual**	
Gas-side Surface Area						168,608	
Tube Length						12.5	
Gas Velocity	7.5	80.0	0.500	43.8	0.648	54.4	0.125
Air Velocity	7.5	50.0	0.500	28.8	0.010	7.9	-0.4
Fin Pitch	0.20	1.00	0.500	0.60	0.002	0.20	-0.4
Fin Length	0.00	1.25	0.500	0.63	0.985	1.23	0.4
Inner Tube Diameter	1.75	6.00	0.500	3.88	0.000	1.75	-0.4
Fin Thickness	0.063	0.125	0.500	0.094	0.999	0.125	0.4
Net Annual Cost			$1,161,755		$344,372		

Test name: NominalTfg3b							
	Range		**Starting Value**		**Optimal Value**		**Si**
	Min	**Max**	**Normalized**	**Actual**	**Normalized**	**Actual**	
Gas-side Surface Area						172,491	
Tube Length						12.3	
Gas Velocity	7.5	80.0	0.500	43.8	0.614	52.0	0.125
Air Velocity	7.5	50.0	0.500	28.8	0.013	8.1	-0.125
Fin Pitch	0.20	1.00	0.500	0.60	0.004	0.20	-0.125
Fin Length	0.00	1.25	0.500	0.63	1.000	1.25	0.125
Inner Tube Diameter	1.75	6.00	0.500	3.88	0.000	1.75	-0.125
Fin Thickness	0.063	0.125	0.500	0.094	0.850	0.116	0.125
Net Annual Cost			$1,161,755		$343,635		

Test name: NominalTfg3c							
	Range		**Starting Value**		**Optimal Value**		**Si**
	Min	**Max**	**Normalized**	**Actual**	**Normalized**	**Actual**	
Gas-side Surface Area						175,747	
Tube Length						12.2	
Gas Velocity	7.5	80.0	0.584	49.9	0.596	50.7	-0.5
Air Velocity	7.5	50.0	0.001	7.5	0.003	7.6	0.5
Fin Pitch	0.20	1.00	0.000	0.20	0.000	0.20	0.5
Fin Length	0.00	1.25	1.000	1.25	0.998	1.25	-0.5
Inner Tube Diameter	1.75	6.00	0.000	1.75	0.000	1.75	0.5
Fin Thickness	0.063	0.125	0.749	0.109	0.781	0.111	-0.5
Net Annual Cost			$344,546		$342,666		

Test name: NominalTfg3d							
	Range		**Starting Value**		**Optimal Value**		**Si**
	Min	**Max**	**Normalized**	**Actual**	**Normalized**	**Actual**	
Gas-side Surface Area						176,657	
Tube Length						12.2	
Gas Velocity	7.5	80.0	0.584	49.9	0.592	50.4	0.125
Air Velocity	7.5	50.0	0.001	7.5	0.000	7.5	0.125
Fin Pitch	0.20	1.00	0.000	0.20	0.000	0.20	0.125
Fin Length	0.00	1.25	1.000	1.25	1.000	1.25	-0.125
Inner Tube Diameter	1.75	6.00	0.000	1.75	0.000	1.75	0.125
Fin Thickness	0.063	0.125	0.749	0.109	0.759	0.110	0.125
Net Annual Cost			$344,546		$342,908		

Test name: NominalTfg3c	
Flue Gas Flow rate [lbm/hr]	6,000,000
Vapor Flow rate [lbm/hr]	403,720
Cooling Air Flow rate [lbm/hr]	58,683,398
Flue Gas Velocity [ft/sec]	45.6
Cooling Air Velocity [ft/sec]	7.8
Inlet Flue Gas Temperature [F]	175
Inlet Cooling Air Temperature [F]	75
Exit Flue Gas Temperature [F]	113.7
Exit Cooling Air Temperature [F]	95.4
Tube Inner Diameter [inch]	1.75
Tube Thickness [inch]	0.2
Fin Length [inches]	1.25
Fin Pitch [inches]	0.2
Fin Thickness [inches]	0.111
Number of Tube Rows	2
Transverse Tube Spacing [inches]	4.65
Longitudinal Tube Spacing [inches]	4.65
Number of Tubes	31000
Tube Length [ft]	12.2
Gas-side Surface Area [ft2]	175,747
Air-side Surface Area [ft2]	9,140,335
Field Erected Capital Cost	$5,659,168
Annualized Capital Cost	$454,106
Annualized Operating Cost	$122,996
Estimated Annual Savings in Water Costs @ $1.50 per 1000 gallon	$234,436
Net Annualized Cost [20 yrs @ 5%]	$342,666
Gas-Side Fan Power [kW]	228
Air-Side Fan Power [kW]	75
Sensible Heat Transfer [BTU/hr]	93,944,326
Latent Heat Transfer [BTU/hr]	194,206,831
Condensation Rate [lbm/hr]	186,246
Condensation Efficiency	46%
Inlet/Exit Moisture Concentration [% wet-basis]	11/6.2

Appendix B.4.4 – Inlet Flue Gas Temperature: 200°F

The following tables are the 4 optimization simulations performed with an inlet flue gas temperature of 200°F, and the details of the ACC's design for the best of the four optimizations.

Test name: NominalTfg4a							
	Range		**Starting Value**		**Optimal Value**		**Si**
	Min	**Max**	**Normalized**	**Actual**	**Normalized**	**Actual**	
Gas-side Surface Area						179,157	
Tube Length						13.4	
Gas Velocity	7.5	80.0	0.500	43.8	0.644	54.2	0.125
Air Velocity	7.5	50.0	0.500	28.8	0.023	8.5	-0.4
Fin Pitch	0.20	1.00	0.500	0.60	0.000	0.20	-0.4
Fin Length	0.00	1.25	0.500	0.63	1.000	1.25	0.4
Inner Tube Diameter	1.75	6.00	0.500	3.88	0.020	1.83	-0.4
Fin Thickness	0.063	0.125	0.500	0.094	0.988	0.124	0.4
Net Annual Cost			$1,246,022		$368,726		

Test name: NominalTfg4b							
	Range		**Starting Value**		**Optimal Value**		**Si**
	Min	**Max**	**Normalized**	**Actual**	**Normalized**	**Actual**	
Gas-side Surface Area						177,019	
Tube Length						12.7	
Gas Velocity	7.5	80.0	0.500	43.8	0.649	54.5	0.125
Air Velocity	7.5	50.0	0.500	28.8	0.012	8.0	-0.125
Fin Pitch	0.20	1.00	0.500	0.60	0.000	0.20	-0.125
Fin Length	0.00	1.25	0.500	0.63	1.000	1.25	0.125
Inner Tube Diameter	1.75	6.00	0.500	3.88	0.001	1.75	-0.125
Fin Thickness	0.063	0.125	0.500	0.094	0.929	0.121	0.125
Net Annual Cost			$1,246,022		$364,298		

Test name: NominalTfg4c							
	Range		**Starting Value**		**Optimal Value**		**Si**
	Min	**Max**	**Normalized**	**Actual**	**Normalized**	**Actual**	
Gas-side Surface Area						186,510	
Tube Length						12.4	
Gas Velocity	7.5	80.0	0.584	49.9	0.594	50.6	-0.5
Air Velocity	7.5	50.0	0.001	7.5	0.002	7.6	0.5
Fin Pitch	0.20	1.00	0.000	0.20	0.000	0.20	0.5
Fin Length	0.00	1.25	1.000	1.25	1.000	1.25	-0.5
Inner Tube Diameter	1.75	6.00	0.000	1.75	0.000	1.75	0.5
Fin Thickness	0.063	0.125	0.749	0.109	0.771	0.111	-0.5
Net Annual Cost			$367,341		$365,370		

Test name: NominalTfg4d							
	Range		**Starting Value**		**Optimal Value**		**Si**
	Min	**Max**	**Normalized**	**Actual**	**Normalized**	**Actual**	
Gas-side Surface Area						187,092	
Tube Length						12.4	
Gas Velocity	7.5	80.0	0.584	49.9	0.592	50.4	0.125
Air Velocity	7.5	50.0	0.001	7.5	0.001	7.5	0.125
Fin Pitch	0.20	1.00	0.000	0.20	0.000	0.20	0.125
Fin Length	0.00	1.25	1.000	1.25	1.000	1.25	-0.125
Inner Tube Diameter	1.75	6.00	0.000	1.75	0.000	1.75	0.125
Fin Thickness	0.063	0.125	0.749	0.109	0.756	0.110	0.125
Net Annual Cost			$367,340		$365,680		

Test name: NominalTfg4b	
Flue Gas Flow rate [lbm/hr]	6,000,000
Vapor Flow rate [lbm/hr]	403,720
Cooling Air Flow rate [lbm/hr]	60,140,506
Flue Gas Velocity [ft/sec]	48.3
Cooling Air Velocity [ft/sec]	8.2
Inlet Flue Gas Temperature [F]	200
Inlet Cooling Air Temperature [F]	75
Exit Flue Gas Temperature [F]	121
Exit Cooling Air Temperature [F]	96.7
Tube Inner Diameter [inch]	1.75
Tube Thickness [inch]	0.2
Fin Length [inches]	1.25
Fin Pitch [inches]	0.2
Fin Thickness [inches]	0.121
Number of Tube Rows	2
Transverse Tube Spacing [inches]	4.65
Longitudinal Tube Spacing [inches]	4.65
Number of Tubes	30000
Tube Length [ft]	12.7
Gas-side Surface Area [ft2]	177,019
Air-side Surface Area [ft2]	9,257,933
Field Erected Capital Cost	$5,691,934
Annualized Capital Cost	$456,735
Annualized Operating Cost	$140,205
Estimated Annual Savings in Water Costs @ $1.50 per 1000 gallon	$232,642
Net Annualized Cost [20 yrs @ 5%]	$364,298
Gas-Side Fan Power [kW]	255
Air-Side Fan Power [kW]	77
Sensible Heat Transfer [BTU/hr]	121,610,715
Latent Heat Transfer [BTU/hr]	192,668,389
Condensation Rate [lbm/hr]	184,821
Condensation Efficiency	46%
Inlet/Exit Moisture Concentration [% wet-basis]	11/6.3

Appendix B.4.5 – Inlet Flue Gas Temperature: 225°F

The following tables are the 4 optimization simulations performed with an inlet flue gas temperature of 225°F, and the details of the ACC's design for the best of the four optimizations.

Test name: NominalTfg225a							
	Range		**Starting Value**		**Optimal Value**		**Si**
	Min	**Max**	**Normalized**	**Actual**	**Normalized**	**Actual**	
Surface Area						179,157	
Tube Length						13.4	
Gas Velocity	7.5	80.0	0.500	43.8	0.639	53.8	0.125
Air Velocity	7.5	50.0	0.500	28.8	0.027	8.6	-0.4
Fin Pitch	0.20	1.00	0.500	0.60	0.002	0.20	-0.4
Fin Length	0.00	1.25	0.500	0.63	0.965	1.21	0.4
Inner Tube Diameter	1.75	6.00	0.500	3.88	0.000	1.75	-0.4
Fin Thickness	0.063	0.125	0.500	0.094	1.000	0.125	0.4
Net Annual Cost			$1,331,823		$389,146		

Test name: NominalTfg225b							
	Range		**Starting Value**		**Optimal Value**		**Si**
	Min	**Max**	**Normalized**	**Actual**	**Normalized**	**Actual**	
Surface Area						177,019	
Tube Length						12.7	
Gas Velocity	7.5	80.0	0.500	43.8	0.686	57.2	0.125
Air Velocity	7.5	50.0	0.500	28.8	0.029	8.7	-0.125
Fin Pitch	0.20	1.00	0.500	0.60	0.002	0.20	-0.125
Fin Length	0.00	1.25	0.500	0.63	1.000	1.25	0.125
Inner Tube Diameter	1.75	6.00	0.500	3.88	0.000	1.75	-0.125
Fin Thickness	0.063	0.125	0.500	0.094	0.919	0.120	0.125
Net Annual Cost			$1,331,823		$388,761		

Test name: NominalTfg4c							
	Range		**Starting Value**		**Optimal Value**		**Si**
	Min	**Max**	**Normalized**	**Actual**	**Normalized**	**Actual**	
Surface Area						186,510	
Tube Length						12.4	
Gas Velocity	7.5	80.0	0.584	49.9	0.585	49.9	-0.5
Air Velocity	7.5	50.0	0.001	7.5	0.001	7.5	0.5
Fin Pitch	0.20	1.00	0.000	0.20	0.000	0.20	0.5
Fin Length	0.00	1.25	1.000	1.25	1.000	1.25	-0.5
Inner Tube Diameter	1.75	6.00	0.000	1.75	0.000	1.75	0.5
Fin Thickness	0.063	0.125	0.749	0.109	0.748	0.109	-0.5
Net Annual Cost			$388,645		$388,486		

Test name: NominalTfg4d							
	Range		**Starting Value**		**Optimal Value**		**Si**
	Min	**Max**	**Normalized**	**Actual**	**Normalized**	**Actual**	
Surface Area						196,499	
Tube Length						12.6	
Gas Velocity	7.5	80.0	0.584	49.9	0.592	50.4	0.125
Air Velocity	7.5	50.0	0.001	7.5	0.009	7.9	0.125
Fin Pitch	0.20	1.00	0.000	0.20	0.000	0.20	0.125
Fin Length	0.00	1.25	1.000	1.25	0.998	1.25	-0.125
Inner Tube Diameter	1.75	6.00	0.000	1.75	0.002	1.76	0.125
Fin Thickness	0.063	0.125	0.749	0.109	0.788	0.112	0.125
Net Annual Cost			$388,645		$388,339		

Test name: OptimalTfg_225d	
Flue Gas Flow rate [lbm/hr]	6,000,000
Vapor Flow rate [lbm/hr]	403,720
Cooling Air Flow rate [lbm/hr]	67,243,928
Flue Gas Velocity [ft/sec]	44.0
Cooling Air Velocity [ft/sec]	8.0
Inlet Flue Gas Temperature [F]	225
Inlet Cooling Air Temperature [F]	75
Exit Flue Gas Temperature [F]	123.8
Exit Cooling Air Temperature [F]	96.5
Tube Inner Diameter [inch]	1.76
Tube Thickness [inch]	0.2
Fin Length [inches]	1.25
Fin Pitch [inches]	0.2
Fin Thickness [inches]	0.112
Number of Tube Rows	2
Transverse Tube Spacing [inches]	4.65
Longitudinal Tube Spacing [inches]	4.65
Number of Tubes	34000
Tube Length [ft]	12.6
Gas-side Surface Area [ft2]	196,499
Air-side Surface Area [ft2]	10,183,960
Field Erected Capital Cost	$6,187,726
Annualized Capital Cost	$496,519
Annualized Operating Cost	$125,168
Estimated Annual Savings in Water Costs @ $1.50 per 1000 gallon	$233,348
Net Annualized Cost [20 yrs @ 5%]	$388,339
Gas-Side Fan Power [kW]	281
Air-Side Fan Power [kW]	89
Sensible Heat Transfer [BTU/hr]	149,564,528
Latent Heat Transfer [BTU/hr]	193,267,297
Condensation Rate [lbm/hr]	185,381
Condensation Efficiency	46%
Inlet/Exit Moisture Concentration [% wet-basis]	11/6.1

Appendix B.5 – Details of the Optimization Simulations for the Cases that Included a Wet FGD System

Appendix B.5 tabulate the optimization results and initial simplexes for the simulations discussed in Section 5.4.1, which discussed the effects of increasing the condensation efficiency.

Each table represents one optimization simulation. The variables optimized are listed in the table and the range of each variable is given in the second and third columns. The columns labeled "Starting Value" list the variables used as the initial guess, which was one vertex of the initial simplex. The column labeled "Si" is the parameter assigned to each variable which built the remaining vertexes of the simplex using the Tilted Initial Simplex Method described in Walters [42]. The columns labeled "Optimal Value" list the values of the optimal heat exchanger design. Under the headings "Starting Value" and "Optimal Value", there are "Normalized" and "Actual" values. These correspond to the dimensionless and absolute values of the variables, respectively. Recall from Section 2.4, the variables were normalized during the optimization to remove the units from the optimization equations.

Appendix B.5.1 – Inlet Flue Gas Temperature of 128°F and 25 Percent Condensation Efficiency in the ACC

The following tables list the values of the variables included in the optimization simulations for the cases when there was an FGD system. The last table in the section lists the details for the best of the four optimizations.

Test name: Nominal128_25a							
	Range		**Starting Value**		**Optimal Value**		**Si**
	Min	**Max**	**Normalized**	**Actual**	**Normalized**	**Actual**	
Surface Area						45,162	
Tube Length						3.1	
Gas Velocity	7.5	80.0	0.500	43.8	0.530	45.9	0.125
Air Velocity	7.5	50.0	0.500	28.8	0.089	11.3	-0.4
Fin Pitch	0.20	1.00	0.500	0.60	0.000	0.20	-0.4
Fin Length	0.00	1.25	0.500	0.63	1.000	1.25	0.4
Inner Tube Diameter	1.75	6.00	0.500	3.88	0.000	1.75	-0.4
Fin Thickness	0.063	0.125	0.500	0.094	1.000	0.125	0.4
Net Annual Cost			$298,225		$71,986		

Test name: Nominal128_25b							
	Range		Starting Value		Optimal Value		Si
	Min	Max	Normalized	Actual	Normalized	Actual	
Surface Area						56,223	
Tube Length						8.2	
Gas Velocity	7.5	80.0	0.500	43.8	0.551	47.5	0.125
Air Velocity	7.5	50.0	0.500	28.8	0.202	16.1	-0.125
Fin Pitch	0.20	1.00	0.500	0.60	0.000	0.20	-0.125
Fin Length	0.00	1.25	0.500	0.63	0.998	1.25	0.125
Inner Tube Diameter	1.75	6.00	0.500	3.88	0.448	3.65	-0.125
Fin Thickness	0.063	0.125	0.500	0.094	0.503	0.094	0.125
Net Annual Cost			$298,225		$109,290		

Test name: Nominal128_25c							
	Range		Starting Value		Optimal Value		Si
	Min	Max	Normalized	Actual	Normalized	Actual	
Surface Area						50,224	
Tube Length						3	
Gas Velocity	7.5	80.0	0.584	49.9	0.453	40.3	-0.5
Air Velocity	7.5	50.0	0.001	7.5	0.045	9.4	0.5
Fin Pitch	0.20	1.00	0.000	0.20	0.000	0.20	0.5
Fin Length	0.00	1.25	1.000	1.25	1.000	1.25	-0.5
Inner Tube Diameter	1.75	6.00	0.000	1.75	0.000	1.75	0.5
Fin Thickness	0.063	0.125	0.749	0.109	0.619	0.101	-0.5
Net Annual Cost			$81,148		$68,050		

Test name: Nominal128_25d							
	Range		Starting Value		Optimal Value		Si
	Min	Max	Normalized	Actual	Normalized	Actual	
Surface Area						50,087	
Tube Length						3	
Gas Velocity	7.5	80.0	0.584	49.9	0.454	40.4	0.125
Air Velocity	7.5	50.0	0.001	7.5	0.038	9.1	0.125
Fin Pitch	0.20	1.00	0.000	0.20	0.000	0.20	0.125
Fin Length	0.00	1.25	1.000	1.25	1.000	1.25	-0.125
Inner Tube Diameter	1.75	6.00	0.000	1.75	0.000	1.75	0.125
Fin Thickness	0.063	0.125	0.749	0.109	0.586	0.099	0.125
Net Annual Cost			$81,148		$67,892		

Test name: Nominal128_25d	
Flue Gas Flow Rate [lbm/hr]	6,000,000
Vapor Flow Rate [lbm/hr]	532,881
Cooling Air Flow Rate [lbm/hr]	20,884,768
Flue Gas Velocity [ft/sec]	39.0
Cooling Air Velocity [ft/sec]	9.4
Inlet Flue Gas Temperature [F]	128
Inlet Cooling Air Temperature [F]	75
Exit Flue Gas Temperature [F]	116.5
Exit Cooling Air Temperature [F]	95.1
Tube Inner Diameter [inch]	1.75
Tube Thickness [inch]	0.2
Fin Length [inches]	1.25
Fin Pitch [inches]	0.2
Fin Thickness [inches]	0.099
Number of Tube Rows	2
Transverse Tube Spacing [inches]	4.65
Longitudinal Tube Spacing [inches]	4.65
Number of Tubes	37000
Tube Length [ft]	3
Gas-side Surface Area [ft2]	50,087
Air-side Surface Area [ft2]	2,597,166
Field Erected Capital Cost	$2,073,117
Annualized Capital Cost	$166,352
Annualized Operating Cost	$53,097
Estimated Annual Savings in Water Costs @ $1.50 per 1000 gallon	$53,097
Net Annualized Cost [20 yrs @ 5%]	$67,892
Gas-Side Fan Power [kW]	84
Air-Side Fan Power [kW]	27
Sensible Heat Transfer [BTU/hr]	15,932,526
Latent Heat Transfer [BTU/hr]	125,116,670
Condensation Rate [lbm/hr]	120,403
Condensation Efficiency	23%
Inlet/Exit Moisture Concentration [% wet-basis]	14.4/11.5

Appendix B.5.2 – Inlet Flue Gas Temperature of 128°F and 40 Percent Condensation Efficiency in the ACC

The following tables list the values of the variables included in the optimization simulations for the cases when there was an FGD system. The last table in the section lists the details for the best of the four optimizations.

Test name: Nominal128_40a							
	Range		**Starting Value**		**Optimal Value**		**Si**
	Min	**Max**	**Normalized**	**Actual**	**Normalized**	**Actual**	
Surface Area						90,523	
Tube Length						7.5	
Gas Velocity	7.5	80.0	0.500	43.8	0.596	50.7	0.125
Air Velocity	7.5	50.0	0.500	28.8	0.608	33.3	-0.4
Fin Pitch	0.20	1.00	0.500	0.60	0.000	0.20	-0.4
Fin Length	0.00	1.25	0.500	0.63	0.994	1.24	0.4
Inner Tube Diameter	1.75	6.00	0.500	3.88	0.044	1.94	-0.4
Fin Thickness	0.063	0.125	0.500	0.094	1.000	0.125	0.4
Net Annual Cost			$570,133		$123,197		

Test name: Nominal128_40b							
	Range		**Starting Value**		**Optimal Value**		**Si**
	Min	**Max**	**Normalized**	**Actual**	**Normalized**	**Actual**	
Surface Area						88,167	
Tube Length						7.4	
Gas Velocity	7.5	80.0	0.500	43.8	0.677	56.6	0.125
Air Velocity	7.5	50.0	0.500	28.8	0.106	12.0	-0.125
Fin Pitch	0.20	1.00	0.500	0.60	0.000	0.20	-0.125
Fin Length	0.00	1.25	0.500	0.63	0.724	0.90	0.125
Inner Tube Diameter	1.75	6.00	0.500	3.88	0.000	1.75	-0.125
Fin Thickness	0.063	0.125	0.500	0.094	0.781	0.111	0.125
Net Annual Cost			$570,133		$143,057		

Test name: Nominal128_40c							
	Range		**Starting Value**		**Optimal Value**		**Si**
	Min	**Max**	**Normalized**	**Actual**	**Normalized**	**Actual**	
Surface Area						91,882	
Tube Length						6.6	
Gas Velocity	7.5	80.0	0.584	49.9	0.572	48.9	-0.5
Air Velocity	7.5	50.0	0.001	7.5	0.015	8.1	0.5
Fin Pitch	0.20	1.00	0.000	0.20	0.001	0.20	0.5
Fin Length	0.00	1.25	1.000	1.25	1.000	1.25	-0.5
Inner Tube Diameter	1.75	6.00	0.000	1.75	0.000	1.75	0.5
Fin Thickness	0.063	0.125	0.749	0.109	0.834	0.115	-0.5
Net Annual Cost			$119,228		$116,372		

Test name: Nominal128_40d							
	Range		**Starting Value**		**Optimal Value**		**Si**
	Min	**Max**	**Normalized**	**Actual**	**Normalized**	**Actual**	
Surface Area						94,705	
Tube Length						6.3	
Gas Velocity	7.5	80.0	0.584	49.9	0.523	45.4	0.125
Air Velocity	7.5	50.0	0.001	7.5	0.029	8.7	0.125
Fin Pitch	0.20	1.00	0.000	0.20	0.000	0.20	0.125
Fin Length	0.00	1.25	1.000	1.25	1.000	1.25	-0.125
Inner Tube Diameter	1.75	6.00	0.000	1.75	0.000	1.75	0.125
Fin Thickness	0.063	0.125	0.749	0.109	0.784	0.111	0.125
Net Annual Cost			$119,228		$113,574		

Test name: Nominal128_40d	
Flue Gas Flow Rate [lbm/hr]	6,000,000
Vapor Flow Rate [lbm/hr]	532,881
Cooling Air Flow Rate [lbm/hr]	36,241,187
Flue Gas Velocity [ft/sec]	43.0
Cooling Air Velocity [ft/sec]	9.0
Inlet Flue Gas Temperature [F]	128
Inlet Cooling Air Temperature [F]	75
Exit Flue Gas Temperature [F]	108.6
Exit Cooling Air Temperature [F]	93.9
Tube Inner Diameter [inch]	1.75
Tube Thickness [inch]	0.2
Fin Length [inches]	1.25
Fin Pitch [inches]	0.2
Fin Thickness [inches]	0.111
Number of Tube Rows	2
Transverse Tube Spacing [inches]	4.65
Longitudinal Tube Spacing [inches]	4.65
Number of Tubes	33000
Tube Length [ft]	6.3
Gas-side Surface Area [ft2]	94,705
Air-side Surface Area [ft2]	4,930,719
Field Erected Capital Cost	$3,450,974
Annualized Capital Cost	$276,915
Annualized Operating Cost	$82,873
Estimated Annual Savings in Water Costs @ $1.50 per 1000 gallon	$246,215
Net Annualized Cost [20 yrs @ 5%]	$113,574
Gas-Side Fan Power [kW]	143
Air-Side Fan Power [kW]	37
Sensible Heat Transfer [BTU/hr]	26,941,208
Latent Heat Transfer [BTU/hr]	203,435,198
Condensation Rate [lbm/hr]	195,603
Condensation Efficiency	37%
Inlet/Exit Moisture Concentration [% wet-basis]	14.4/9.6

Appendix B.5.3 – Inlet Flue Gas Temperature of 128°F and 50% Condensation Efficiency in the ACC

The following tables list the values of the variables included in the optimization simulations for the cases when there was an FGD system. The last table in the section lists the details for the best of the four optimizations.

Test name: Nominal128_saturated							
	Range		**Starting Value**		**Optimal Value**		**Si**
	Min	**Max**	**Normalized**	**Actual**	**Normalized**	**Actual**	
Surface Area						127,494	
Tube Length						9.9	
Gas Velocity	7.5	80.0	0.500	43.8	0.613	52.0	0.125
Air Velocity	7.5	50.0	0.500	28.8	0.040	9.2	-0.4
Fin Pitch	0.20	1.00	0.500	0.60	0.000	0.20	-0.4
Fin Length	0.00	1.25	0.500	0.63	1.000	1.25	0.4
Inner Tube Diameter	1.75	6.00	0.500	3.88	0.006	1.78	-0.4
Fin Thickness	0.063	0.125	0.500	0.094	0.908	0.119	0.4
Net Annual Cost			$778,637		$164,734		

Test name: Nominal128_saturated_b							
	Range		**Starting Value**		**Optimal Value**		**Si**
	Min	**Max**	**Normalized**	**Actual**	**Normalized**	**Actual**	
Surface Area						133,000	
Tube Length						9.9	
Gas Velocity	7.5	80.0	0.500	43.8	0.583	49.8	0.125
Air Velocity	7.5	50.0	0.500	28.8	0.017	8.2	-0.125
Fin Pitch	0.20	1.00	0.500	0.60	0.006	0.20	-0.125
Fin Length	0.00	1.25	0.500	0.63	1.000	1.25	0.125
Inner Tube Diameter	1.75	6.00	0.500	3.88	0.004	1.77	-0.125
Fin Thickness	0.063	0.125	0.500	0.094	0.923	0.120	0.125
Net Annual Cost			$778,637		$164,593		

Test name: Nominal128_saturated_c							
	Range		**Starting Value**		**Optimal Value**		**Si**
	Min	**Max**	**Normalized**	**Actual**	**Normalized**	**Actual**	
Surface Area						134,048	
Tube Length						9.8	
Gas Velocity	7.5	80.0	0.584	49.9	0.578	49.4	-0.5
Air Velocity	7.5	50.0	0.001	7.5	0.003	7.6	0.5
Fin Pitch	0.20	1.00	0.000	0.20	0.001	0.20	0.5
Fin Length	0.00	1.25	1.000	1.25	1.000	1.25	-0.5
Inner Tube Diameter	1.75	6.00	0.000	1.75	0.000	1.75	0.5
Fin Thickness	0.063	0.125	0.749	0.109	0.759	0.110	-0.5
Net Annual Cost			$164,159		$163,543		

Test name: Nominal128_saturated_d							
	Range		**Starting Value**		**Optimal Value**		**Si**
	Min	**Max**	**Normalized**	**Actual**	**Normalized**	**Actual**	
Surface Area						130,636	
Tube Length						9.8	
Gas Velocity	7.5	80.0	0.584	49.9	0.596	50.7	0.125
Air Velocity	7.5	50.0	0.001	7.5	0.017	8.2	0.125
Fin Pitch	0.20	1.00	0.000	0.20	0.000	0.20	0.125
Fin Length	0.00	1.25	1.000	1.25	0.998	1.25	-0.125
Inner Tube Diameter	1.75	6.00	0.000	1.75	0.000	1.75	0.125
Fin Thickness	0.063	0.125	0.749	0.109	0.831	0.114	0.125
Net Annual Cost			$164,160		$162,861		

Test name: Nominal128_saturated_d	
Flue Gas Flow Rate [lbm/hr]	6,000,000
Vapor Flow Rate [lbm/hr]	532,881
Cooling Air Flow Rate [lbm/hr]	46,479,753
Flue Gas Velocity [ft/sec]	47.3
Cooling Air Velocity [ft/sec]	8.4
Inlet Flue Gas Temperature [F]	128
Inlet Cooling Air Temperature [F]	75
Exit Flue Gas Temperature [F]	105.4
Exit Cooling Air Temperature [F]	101
Tube Inner Diameter [inch]	1.75
Tube Thickness [inch]	0.2
Fin Length [inches]	1.25
Fin Pitch [inches]	0.2
Fin Thickness [inches]	0.114
Number of Tube Rows	2
Transverse Tube Spacing [inches]	4.65
Longitudinal Tube Spacing [inches]	4.65
Number of Tubes	29000
Tube Length [ft]	9.8
Gas-side Surface Area [ft2]	130,636
Air-side Surface Area [ft2]	6,800,863
Field Erected Capital Cost	$4,463,680
Annualized Capital Cost	$358,177
Annualized Operating Cost	$114,525
Estimated Annual Savings in Water Costs @ $1.50 per 1000 gallon	$309,840
Net Annualized Cost [20 yrs @ 5%]	$162,862
Gas-Side Fan Power [kW]	220
Air-Side Fan Power [kW]	60
Sensible Heat Transfer [BTU/hr]	34,739,873
Latent Heat Transfer [BTU/hr]	256,059,554
Condensation Rate [lbm/hr]	246,150
Condensation Efficiency	46%
Inlet/Exit Moisture Concentration [% wet-basis]	14.4/8.3

Appendix B.5.4 – Inlet Flue Gas Temperature of 128°F and 60% Condensation Efficiency in the ACC

The following tables list the values of the variables included in the optimization simulations for the cases when there was an FGD system. The last table in the section lists the details for the best of the four optimizations.

Test name: Nominal128_saturated_60a							
	Range		**Starting Value**		**Optimal Value**		**Si**
	Min	**Max**	**Normalized**	**Actual**	**Normalized**	**Actual**	
Surface Area						193,783	
Tube Length						14.2	
Gas Velocity	7.5	80.0	0.500	43.8	0.579	49.5	0.125
Air Velocity	7.5	50.0	0.500	28.8	0.000	7.5	-0.4
Fin Pitch	0.20	1.00	0.500	0.60	0.000	0.20	-0.4
Fin Length	0.00	1.25	0.500	0.63	0.999	1.25	0.4
Inner Tube Diameter	1.75	6.00	0.500	3.88	0.002	1.76	-0.4
Fin Thickness	0.063	0.125	0.500	0.094	0.801	0.113	0.4
Net Annual Cost			$1,058,680		$241,259		

Test name: Nominal128_saturated_60b							
	Range		**Starting Value**		**Optimal Value**		**Si**
	Min	**Max**	**Normalized**	**Actual**	**Normalized**	**Actual**	
Surface Area						178,832	
Tube Length						15.9	
Gas Velocity	7.5	80.0	0.500	43.8	0.712	59.1	0.125
Air Velocity	7.5	50.0	0.500	28.8	0.025	8.6	-0.125
Fin Pitch	0.20	1.00	0.500	0.60	0.000	0.20	-0.125
Fin Length	0.00	1.25	0.500	0.63	0.902	1.13	0.125
Inner Tube Diameter	1.75	6.00	0.500	3.88	0.009	1.79	-0.125
Fin Thickness	0.063	0.125	0.500	0.094	0.346	0.084	0.125
Net Annual Cost			$1,058,680		$264,253		

Test name: Nominal128_saturated_60c							
	Range		**Starting Value**		**Optimal Value**		**Si**
	Min	**Max**	**Normalized**	**Actual**	**Normalized**	**Actual**	
Surface Area						190,362	
Tube Length						14.1	
Gas Velocity	7.5	80.0	0.584	49.9	0.591	50.3	-0.5
Air Velocity	7.5	50.0	0.001	7.5	0.003	7.6	0.5
Fin Pitch	0.20	1.00	0.000	0.20	0.000	0.20	0.5
Fin Length	0.00	1.25	1.000	1.25	1.000	1.25	-0.5
Inner Tube Diameter	1.75	6.00	0.000	1.75	0.000	1.75	0.5
Fin Thickness	0.063	0.125	0.749	0.109	0.760	0.110	-0.5
Net Annual Cost			$241,873		$240,946		

Test name: Nominal128_saturated_60d							
	Range		Starting Value		Optimal Value		Si
	Min	Max	Normalized	Actual	Normalized	Actual	
Surface Area						190,136	
Tube Length						14.2	
Gas Velocity	7.5	80.0	0.584	49.9	0.592	50.4	0.125
Air Velocity	7.5	50.0	0.001	7.5	0.003	7.6	0.125
Fin Pitch	0.20	1.00	0.000	0.20	0.000	0.20	0.125
Fin Length	0.00	1.25	1.000	1.25	1.000	1.25	-0.125
Inner Tube Diameter	1.75	6.00	0.000	1.75	0.000	1.75	0.125
Fin Thickness	0.063	0.125	0.749	0.109	0.757	0.110	0.125
Net Annual Cost			$241,873		$240,746		

Test name: Nominal128_saturated_60d	
Flue Gas Flow Rate [lbm/hr]	6,000,000
Vapor Flow Rate [lbm/hr]	532,881
Cooling Air Flow Rate [lbm/hr]	63,700,259
Flue Gas Velocity [ft/sec]	46.2
Cooling Air Velocity [ft/sec]	7.8
Inlet Flue Gas Temperature [F]	128
Inlet Cooling Air Temperature [F]	75
Exit Flue Gas Temperature [F]	98.8
Exit Cooling Air Temperature [F]	98.3
Tube Inner Diameter [inch]	1.75
Tube Thickness [inch]	0.2
Fin Length [inches]	1.25
Fin Pitch [inches]	0.2
Fin Thickness [inches]	0.11
Number of Tube Rows	2
Transverse Tube Spacing [inches]	4.65
Longitudinal Tube Spacing [inches]	4.65
Number of Tubes	29000
Tube Length [ft]	14.2
Gas-side Surface Area [ft2]	190,136
Air-side Surface Area [ft2]	9,899,044
Field Erected Capital Cost	$6,026,921
Annualized Capital Cost	$483,616
Annualized Operating Cost	$135,538
Estimated Annual Savings in Water Costs @ $1.50 per 1000 gallon	$378,408
Net Annualized Cost [20 yrs @ 5%]	$240,746
Gas-Side Fan Power [kW]	262
Air-Side Fan Power [kW]	82
Sensible Heat Transfer [BTU/hr]	44,181,735
Latent Heat Transfer [BTU/hr]	312,946,275
Condensation Rate [lbm/hr]	300,623
Condensation Efficiency	56%
Inlet/Exit Moisture Concentration [% wet-basis]	14.4/6.9

Appendix B.5.5 – Inlet Flue Gas Temperature of 128°F and 70% Condensation Efficiency in the ACC

The following tables list the values of the variables included in the optimization simulations for the cases when there was an FGD system. The last table in the section lists the details for the best of the four optimizations.

Test name: Nominal128_saturated_69a							
	Range		**Starting Value**		**Optimal Value**		**Si**
	Min	**Max**	**Normalized**	**Actual**	**Normalized**	**Actual**	
Surface Area						263,812	
Tube Length						20.3	
Gas Velocity	7.5	80.0	0.500	43.8	0.617	52.2	0.125
Air Velocity	7.5	50.0	0.500	28.8	0.019	8.3	-0.4
Fin Pitch	0.20	1.00	0.500	0.60	0.000	0.20	-0.4
Fin Length	0.00	1.25	0.500	0.63	0.987	1.23	0.4
Inner Tube Diameter	1.75	6.00	0.500	3.88	0.000	1.75	-0.4
Fin Thickness	0.063	0.125	0.500	0.094	0.829	0.114	0.4
Net Annual Cost			$1,464,009		$405,546		

Test name: Nominal128_saturated_69b							
	Range		**Starting Value**		**Optimal Value**		**Si**
	Min	**Max**	**Normalized**	**Actual**	**Normalized**	**Actual**	
Surface Area						263,271	
Tube Length						22.3	
Gas Velocity	7.5	80.0	0.500	43.8	0.689	57.4	0.125
Air Velocity	7.5	50.0	0.500	28.8	0.000	7.5	-0.125
Fin Pitch	0.20	1.00	0.500	0.60	0.047	0.24	-0.125
Fin Length	0.00	1.25	0.500	0.63	0.999	1.25	0.125
Inner Tube Diameter	1.75	6.00	0.500	3.88	0.000	1.75	-0.125
Fin Thickness	0.063	0.125	0.500	0.094	0.870	0.117	0.125
Net Annual Cost			$1,464,009		$446,627		

Test name: Nominal128_saturated_69c							
	Range		**Starting Value**		**Optimal Value**		**Si**
	Min	**Max**	**Normalized**	**Actual**	**Normalized**	**Actual**	
Surface Area						272,946	
Tube Length						20.2	
Gas Velocity	7.5	80.0	0.584	49.9	0.588	50.1	-0.5
Air Velocity	7.5	50.0	0.001	7.5	0.001	7.6	0.5
Fin Pitch	0.20	1.00	0.000	0.20	0.000	0.20	0.5
Fin Length	0.00	1.25	1.000	1.25	1.000	1.25	-0.5
Inner Tube Diameter	1.75	6.00	0.000	1.75	0.000	1.75	0.5
Fin Thickness	0.063	0.125	0.749	0.109	0.749	0.109	-0.5
Net Annual Cost			$405,740		$404,209		

Test name: Nominal128_saturated_69d							
	Range		**Starting Value**		**Optimal Value**		**Si**
	Min	**Max**	**Normalized**	**Actual**	**Normalized**	**Actual**	
Surface Area						271,240	
Tube Length						20.2	
Gas Velocity	7.5	80.0	0.584	49.9	0.593	50.5	0.125
Air Velocity	7.5	50.0	0.001	7.5	0.005	7.7	0.125
Fin Pitch	0.20	1.00	0.000	0.20	0.000	0.20	0.125
Fin Length	0.00	1.25	1.000	1.25	1.000	1.25	-0.125
Inner Tube Diameter	1.75	6.00	0.000	1.75	0.000	1.75	0.125
Fin Thickness	0.063	0.125	0.749	0.109	0.758	0.110	0.125
Net Annual Cost			$405,740		$404,031		

Test name: Nominal128_saturated_69d	
Flue Gas Flow Rate [lbm/hr]	6,000,000
Vapor Flow Rate [lbm/hr]	532,881
Cooling Air Flow Rate [lbm/hr]	92,016,091
Flue Gas Velocity [ft/sec]	45.3
Cooling Air Velocity [ft/sec]	7.8
Inlet Flue Gas Temperature [F]	128
Inlet Cooling Air Temperature [F]	75
Exit Flue Gas Temperature [F]	91.3
Exit Cooling Air Temperature [F]	94.1
Tube Inner Diameter [inch]	1.75
Tube Thickness [inch]	0.2
Fin Length [inches]	1.25
Fin Pitch [inches]	0.2
Fin Thickness [inches]	0.11
Number of Tube Rows	2
Transverse Tube Spacing [inches]	4.65
Longitudinal Tube Spacing [inches]	4.65
Number of Tubes	29000
Tube Length [ft]	20.2
Gas-side Surface Area [ft2]	271,240
Air-side Surface Area [ft2]	14,125,836
Field Erected Capital Cost	$8,428,241
Annualized Capital Cost	$676,304
Annualized Operating Cost	$172,380
Estimated Annual Savings in Water Costs @ $1.50 per 1000 gallon	$444,653
Net Annualized Cost [20 yrs @ 5%]	$404,031
Gas-Side Fan Power [kW]	324
Air-Side Fan Power [kW]	118
Sensible Heat Transfer [BTU/hr]	54,633,017
Latent Heat Transfer [BTU/hr]	368,071,326
Condensation Rate [lbm/hr]	353,251
Condensation Efficiency	66%
Inlet/Exit Moisture Concentration [% wet-basis]	14.4/5.4

Appendix B.5.6 - Inlet Flue Gas Temperature of 128°F and 75% Condensation Efficiency in the ACC

The following tables list the values of the variables included in the optimization simulations for the cases when there was an FGD system. The last table in the section lists the details for the best of the four optimizations.

Test name: Nominal128_saturated_75a							
	Range		**Starting Value**		**Optimal Value**		**Si**
	Min	**Max**	**Normalized**	**Actual**	**Normalized**	**Actual**	
Surface Area						354,471	
Tube Length						27.9	
Gas Velocity	7.5	80.0	0.500	43.8	0.631	53.2	0.125
Air Velocity	7.5	50.0	0.500	28.8	0.015	8.1	-0.4
Fin Pitch	0.20	1.00	0.500	0.60	0.000	0.20	-0.4
Fin Length	0.00	1.25	0.500	0.63	1.000	1.25	0.4
Inner Tube Diameter	1.75	6.00	0.500	3.88	0.000	1.75	-0.4
Fin Thickness	0.063	0.125	0.500	0.094	0.882	0.118	0.4
Net Annual Cost			$1,944,311		$647,151		

Test name: Nominal128_saturated_75b							
	Range		**Starting Value**		**Optimal Value**		**Si**
	Min	**Max**	**Normalized**	**Actual**	**Normalized**	**Actual**	
Surface Area						343,261	
Tube Length						31.3	
Gas Velocity	7.5	80.0	0.500	43.8	0.748	61.7	0.125
Air Velocity	7.5	50.0	0.500	28.8	0.000	7.5	-0.125
Fin Pitch	0.20	1.00	0.500	0.60	0.049	0.24	-0.125
Fin Length	0.00	1.25	0.500	0.63	0.997	1.25	0.125
Inner Tube Diameter	1.75	6.00	0.500	3.88	0.000	1.75	-0.125
Fin Thickness	0.063	0.125	0.500	0.094	0.890	0.118	0.125
Net Annual Cost			$1,944,311		$697,310		

Test name: Nominal128_saturated_75c							
	Range		**Starting Value**		**Optimal Value**		**Si**
	Min	**Max**	**Normalized**	**Actual**	**Normalized**	**Actual**	
Surface Area						361,542	
Tube Length						27.5	
Gas Velocity	7.5	80.0	0.584	49.9	0.607	51.5	-0.5
Air Velocity	7.5	50.0	0.001	7.5	0.018	8.3	0.5
Fin Pitch	0.20	1.00	0.000	0.20	0.003	0.20	0.5
Fin Length	0.00	1.25	1.000	1.25	0.995	1.24	-0.5
Inner Tube Diameter	1.75	6.00	0.000	1.75	0.000	1.75	0.5
Fin Thickness	0.063	0.125	0.749	0.109	1.000	0.125	-0.5
Net Annual Cost			$651,923		$649,366		

Test name: Nominal128_saturated_75d							
	Range		**Starting Value**		**Optimal Value**		**Si**
	Min	**Max**	**Normalized**	**Actual**	**Normalized**	**Actual**	
Surface Area						372,247	
Tube Length						27.4	
Gas Velocity	7.5	80.0	0.584	49.8	0.585	49.9	0.125
Air Velocity	7.5	50.0	0.001	7.5	0.001	7.6	0.125
Fin Pitch	0.20	1.00	0.000	0.20	0.000	0.20	0.125
Fin Length	0.00	1.25	1.000	1.25	1.000	1.25	-0.125
Inner Tube Diameter	1.75	6.00	0.000	1.75	0.000	1.75	0.125
Fin Thickness	0.063	0.125	0.749	0.109	0.750	0.109	0.125
Net Annual Cost			$651,923		$651,486		

Test name: Nominal128_saturated_75a	
Flue Gas Flow Rate [lbm/hr]	6,000,000
Vapor Flow Rate [lbm/hr]	532,881
Cooling Air Flow Rate [lbm/hr]	123,503,334
Flue Gas Velocity [ft/sec]	46.8
Cooling Air Velocity [ft/sec]	8.3
Inlet Flue Gas Temperature [F]	128
Inlet Cooling Air Temperature [F]	75
Exit Flue Gas Temperature [F]	85.3
Exit Cooling Air Temperature [F]	90.8
Tube Inner Diameter [inch]	1.75
Tube Thickness [inch]	0.2
Fin Length [inches]	1.25
Fin Pitch [inches]	0.2
Fin Thickness [inches]	0.118
Number of Tube Rows	2
Transverse Tube Spacing [inches]	4.65
Longitudinal Tube Spacing [inches]	4.65
Number of Tubes	28000
Tube Length [ft]	27.9
Gas-side Surface Area [ft2]	354,471
Air-side Surface Area [ft2]	18,517,992
Field Erected Capital Cost	$11,230,508
Annualized Capital Cost	$901,165
Annualized Operating Cost	$237,003
Estimated Annual Savings in Water Costs @ $1.50 per 1000 gallon	$491,020
Net Annualized Cost [20 yrs @ 5%]	$647,148
Gas-Side Fan Power [kW]	440
Air-Side Fan Power [kW]	158
Sensible Heat Transfer [BTU/hr]	62,959,491
Latent Heat Transfer [BTU/hr]	406,686,130
Condensation Rate [lbm/hr]	390,086
Condensation Efficiency	73%
Inlet/Exit Moisture Concentration [% wet-basis]	14.4/4.3

Appendix B.5.7 – Inlet Flue Gas Temperature of 128°F and 25% Condensation Efficiency in the ACC

The following tables list the values of the variables included in the optimization simulations for the cases when there was an FGD system. The last table in the section lists the details for the best of the four optimizations.

Test name: 60_25a							
	Range		Starting Value		Optimal Value		Si
	Min	Max	Normalized	Actual	Normalized	Actual	
Surface Area						38,655	
Tube Length						2.6	
Gas Velocity	7.5	80.0	0.500	43.8	0.531	46.0	0.125
Air Velocity	7.5	50.0	0.500	28.8	0.107	12.0	-0.4
Fin Pitch	0.20	1.00	0.500	0.60	0.000	0.20	-0.4
Fin Length	0.00	1.25	0.500	0.63	0.908	1.14	0.4
Inner Tube Diameter	1.75	6.00	0.500	3.88	0.000	1.75	-0.4
Fin Thickness	0.063	0.125	0.500	0.094	1.000	0.125	0.4
Net Annual Cost			$211,756		$44,487		

Test name: 60_25b							
	Range		Starting Value		Optimal Value		Si
	Min	Max	Normalized	Actual	Normalized	Actual	
Surface Area						44,303	
Tube Length						2.5	
Gas Velocity	7.5	80.0	0.500	43.8	0.419	37.8	0.125
Air Velocity	7.5	50.0	0.500	28.8	0.068	10.4	-0.125
Fin Pitch	0.20	1.00	0.500	0.60	0.000	0.20	-0.125
Fin Length	0.00	1.25	0.500	0.63	0.911	1.14	0.125
Inner Tube Diameter	1.75	6.00	0.500	3.88	0.002	1.76	-0.125
Fin Thickness	0.063	0.125	0.500	0.094	0.172	0.073	0.125
Net Annual Cost			$211,756		$40,612		

Test name: 60_25c							
	Range		Starting Value		Optimal Value		Si
	Min	Max	Normalized	Actual	Normalized	Actual	
Surface Area						42,867	
Tube Length						2.5	
Gas Velocity	7.5	80.0	0.584	49.9	0.437	39.2	-0.5
Air Velocity	7.5	50.0	0.001	7.5	0.027	8.7	0.5
Fin Pitch	0.20	1.00	0.000	0.20	0.000	0.20	0.5
Fin Length	0.00	1.25	1.000	1.25	0.996	1.24	-0.5
Inner Tube Diameter	1.75	6.00	0.000	1.75	0.000	1.75	0.5
Fin Thickness	0.063	0.125	0.749	0.109	0.557	0.097	-0.5
Net Annual Cost			$49,777		$37,593		

Test name: 60_25d							
	Range		**Starting Value**		**Optimal Value**		**Si**
	Min	**Max**	**Normalized**	**Actual**	**Normalized**	**Actual**	
Surface Area						43,232	
Tube Length						2.5	
Gas Velocity	7.5	80.0	0.584	49.9	0.433	38.9	0.125
Air Velocity	7.5	50.0	0.001	7.5	0.037	9.1	0.125
Fin Pitch	0.20	1.00	0.000	0.20	0.000	0.20	0.125
Fin Length	0.00	1.25	1.000	1.25	0.998	1.25	-0.125
Inner Tube Diameter	1.75	6.00	0.000	1.75	0.000	1.75	0.125
Fin Thickness	0.063	0.125	0.749	0.109	0.792	0.112	0.125
Net Annual Cost			$49,777		$37,596		

Test name: 60_saturated_25c	
Flue Gas Flow Rate [lbm/hr]	6,000,000
Vapor Flow Rate [lbm/hr]	532,881
Cooling Air Flow Rate [lbm/hr]	17,456,910
Flue Gas Velocity [ft/sec]	37.8
Cooling Air Velocity [ft/sec]	9.0
Inlet Flue Gas Temperature [F]	128
Inlet Cooling Air Temperature [F]	60
Exit Flue Gas Temperature [F]	116.7
Exit Cooling Air Temperature [F]	94.9
Tube Inner Diameter [inch]	1.75
Tube Thickness [inch]	0.2
Fin Length [inches]	1.25
Fin Pitch [inches]	0.2
Fin Thickness [inches]	0.09734
Number of Tube Rows	2
Transverse Tube Spacing [inches]	4.65
Longitudinal Tube Spacing [inches]	4.65
Number of Tubes	37,000
Tube Length [ft]	2.5
Gas-side Surface Area [ft2]	42,867
Air-side Surface Area [ft2]	2,208,438
Field Erected Capital Cost	$1,830,375
Annualized Capital Cost	$146,874
Annualized Operating Cost	$45,572
Estimated Annual Savings in Water Costs @ $1.50 per 1000 gallon	$154,853
Net Annualized Cost [20 yrs @ 5%]	$37,593
Gas-Side Fan Power [kW]	86
Air-Side Fan Power [kW]	27
Sensible Heat Transfer [BTU/hr]	18,157,076
Latent Heat Transfer [BTU/hr]	128,483,817
Condensation Rate [lbm/hr]	123,022
Condensation Efficiency	23%
Inlet/Exit Moisture Concentration [% wet-basis]	14.4/11.5

Appendix B.5.8 - Inlet Flue Gas Temperature of 128°F and 40% Condensation Efficiency in the ACC

The following tables list the values of the variables included in the optimization simulations for the cases when there was an FGD system. The last table in the section lists the details for the best of the four optimizations.

Test name: 60_40a							
	Range		**Starting Value**		**Optimal Value**		**Si**
	Min	**Max**	**Normalized**	**Actual**	**Normalized**	**Actual**	
Surface Area						78,318	
Tube Length						6.3	
Gas Velocity	7.5	80.0	0.500	43.8	0.549	47.3	0.125
Air Velocity	7.5	50.0	0.500	28.8	0.063	10.2	-0.4
Fin Pitch	0.20	1.00	0.500	0.60	0.000	0.20	-0.4
Fin Length	0.00	1.25	0.500	0.63	1.000	1.25	0.4
Inner Tube Diameter	1.75	6.00	0.500	3.88	0.063	2.02	-0.4
Fin Thickness	0.063	0.125	0.500	0.094	0.659	0.104	0.4
Net Annual Cost			$381,563		$69,243		

Test name: 60_40b							
	Range		**Starting Value**		**Optimal Value**		**Si**
	Min	**Max**	**Normalized**	**Actual**	**Normalized**	**Actual**	
Surface Area						74,749	
Tube Length						5.3	
Gas Velocity	7.5	80.0	0.500	43.8	0.563	48.3	0.125
Air Velocity	7.5	50.0	0.500	28.8	0.046	9.5	-0.125
Fin Pitch	0.20	1.00	0.500	0.60	0.000	0.20	-0.125
Fin Length	0.00	1.25	0.500	0.63	0.953	1.19	0.125
Inner Tube Diameter	1.75	6.00	0.500	3.88	0.001	1.75	-0.125
Fin Thickness	0.063	0.125	0.500	0.094	0.947	0.122	0.125
Net Annual Cost			$381,563		$62,556		

Test name: 60_40c							
	Range		**Starting Value**		**Optimal Value**		**Si**
	Min	**Max**	**Normalized**	**Actual**	**Normalized**	**Actual**	
Surface Area						80,128	
Tube Length						5.3	
Gas Velocity	7.5	80.0	0.584	49.9	0.518	45.0	-0.5
Air Velocity	7.5	50.0	0.001	7.5	0.007	7.8	0.5
Fin Pitch	0.20	1.00	0.000	0.20	0.000	0.20	0.5
Fin Length	0.00	1.25	1.000	1.25	0.984	1.23	-0.5
Inner Tube Diameter	1.75	6.00	0.000	1.75	0.004	1.77	0.5
Fin Thickness	0.063	0.125	0.749	0.109	0.582	0.099	-0.5
Net Annual Cost			$64,517		$61,559		

Test name: 60_40d							
	Range		**Starting Value**		**Optimal Value**		**Si**
	Min	**Max**	**Normalized**	**Actual**	**Normalized**	**Actual**	
Surface Area						77,000	
Tube Length						5.3	
Gas Velocity	7.5	80.0	0.584	49.9	0.534	46.2	0.125
Air Velocity	7.5	50.0	0.001	7.5	0.020	8.4	0.125
Fin Pitch	0.20	1.00	0.000	0.20	0.000	0.20	0.125
Fin Length	0.00	1.25	1.000	1.25	1.000	1.25	-0.125
Inner Tube Diameter	1.75	6.00	0.000	1.75	0.000	1.75	0.125
Fin Thickness	0.063	0.125	0.749	0.109	0.768	0.111	0.125
Net Annual Cost			$64,517		$60,075		

Test name: 60_saturated_40d	
Flue Gas Flow Rate [lbm/hr]	6,000,000
Vapor Flow Rate [lbm/hr]	532,881
Cooling Air Flow Rate [lbm/hr]	29,058,730
Flue Gas Velocity [ft/sec]	43.6
Cooling Air Velocity [ft/sec]	8.6
Inlet Flue Gas Temperature [F]	128
Inlet Cooling Air Temperature [F]	60
Exit Flue Gas Temperature [F]	108.6
Exit Cooling Air Temperature [F]	93.9
Tube Inner Diameter [inch]	1.75
Tube Thickness [inch]	0.2
Fin Length [inches]	1.25
Fin Pitch [inches]	0.2
Fin Thickness [inches]	0.111
Number of Tube Rows	2
Transverse Tube Spacing [inches]	4.65
Longitudinal Tube Spacing [inches]	4.65
Number of Tubes	32000
Tube Length [ft]	5.3
Gas-side Surface Area [ft2]	77,000
Air-side Surface Area [ft2]	4,011,053
Field Erected Capital Cost	$2,924,394
Annualized Capital Cost	$234,661
Annualized Operating Cost	$74,301
Estimated Annual Savings in Water Costs @ $1.50 per 1000 gallon	$248,887
Net Annualized Cost [20 yrs @ 5%]	$60,075
Gas-Side Fan Power [kW]	143
Air-Side Fan Power [kW]	37
Sensible Heat Transfer [BTU/hr]	30,279,631
Latent Heat Transfer [BTU/hr]	206,681,937
Condensation Rate [lbm/hr]	197,726
Condensation Efficiency	37%
Inlet/Exit Moisture Concentration [% wet-basis]	14.4/9.6

Appendix B.5.9 – Inlet Flue Gas Temperature of 128°F and 50% Condensation Efficiency in the ACC

The following tables list the values of the variables included in the optimization simulations for the cases when there was an FGD system. The last table in the section lists the details for the best of the four optimizations.

Test name: 60_saturated							
	Range		Starting Value		Optimal Value		Si
	Min	Max	Normalized	Actual	Normalized	Actual	
Surface Area						107,671	
Tube Length						7.9	
Gas Velocity	7.5	80.0	0.500	43.8	0.580	49.6	0.125
Air Velocity	7.5	50.0	0.500	28.8	0.009	7.9	-0.4
Fin Pitch	0.20	1.00	0.500	0.60	0.000	0.20	-0.4
Fin Length	0.00	1.25	0.500	0.63	1.000	1.25	0.4
Inner Tube Diameter	1.75	6.00	0.500	3.88	0.000	1.75	-0.4
Fin Thickness	0.063	0.125	0.500	0.094	0.801	0.113	0.4
Net Annual Cost			$549,740		$87,231		

Test name: 60_saturated_b							
	Range		Starting Value		Optimal Value		Si
	Min	Max	Normalized	Actual	Normalized	Actual	
Surface Area						98,011	
Tube Length						8.1	
Gas Velocity	7.5	80.0	0.500	43.8	0.668	56.0	0.125
Air Velocity	7.5	50.0	0.500	28.8	0.077	10.8	-0.125
Fin Pitch	0.20	1.00	0.500	0.60	0.000	0.20	-0.125
Fin Length	0.00	1.25	0.500	0.63	0.906	1.13	0.125
Inner Tube Diameter	1.75	6.00	0.500	3.88	0.000	1.75	-0.125
Fin Thickness	0.063	0.125	0.500	0.094	1.000	0.125	0.125
Net Annual Cost			$549,740		$97,627		

Test name: 60_saturated_c							
	Range		Starting Value		Optimal Value		Si
	Min	Max	Normalized	Actual	Normalized	Actual	
Surface Area						107,059	
Tube Length						7.9	
Gas Velocity	7.5	80.0	0.584	49.9	0.584	49.8	-0.5
Air Velocity	7.5	50.0	0.001	7.5	0.001	7.5	0.5
Fin Pitch	0.20	1.00	0.000	0.20	0.000	0.20	0.5
Fin Length	0.00	1.25	1.000	1.25	1.000	1.25	-0.5
Inner Tube Diameter	1.75	6.00	0.000	1.75	0.000	1.75	0.5
Fin Thickness	0.063	0.125	0.749	0.109	0.749	0.109	-0.5
Net Annual Cost			$87,379		$87,380		

Test name: 60_saturated_d							
	Range		**Starting Value**		**Optimal Value**		**Si**
	Min	**Max**	**Normalized**	**Actual**	**Normalized**	**Actual**	
Surface Area						107,895	
Tube Length						7.9	
Gas Velocity	7.5	80.0	0.584	49.9	0.578	49.4	0.125
Air Velocity	7.5	50.0	0.001	7.5	0.009	7.9	0.125
Fin Pitch	0.20	1.00	0.000	0.20	0.000	0.20	0.125
Fin Length	0.00	1.25	1.000	1.25	1.000	1.25	-0.125
Inner Tube Diameter	1.75	6.00	0.000	1.75	0.001	1.75	0.125
Fin Thickness	0.063	0.125	0.749	0.109	0.781	0.111	0.125
Net Annual Cost			$87,380		$86,600		

Test name: 60_saturated_50d	
Flue Gas Flow Rate [lbm/hr]	6,000,000
Vapor Flow Rate [lbm/hr]	532,881
Cooling Air Flow Rate [lbm/hr]	38,351,833
Flue Gas Velocity [ft/sec]	46.0
Cooling Air Velocity [ft/sec]	8.2
Inlet Flue Gas Temperature [F]	128
Inlet Cooling Air Temperature [F]	60
Exit Flue Gas Temperature [F]	102.3
Exit Cooling Air Temperature [F]	92.7
Tube Inner Diameter [inch]	1.75
Tube Thickness [inch]	0.2
Fin Length [inches]	1.25
Fin Pitch [inches]	0.2
Fin Thickness [inches]	0.111
Number of Tube Rows	2
Transverse Tube Spacing [inches]	4.65
Longitudinal Tube Spacing [inches]	4.65
Number of Tubes	30000
Tube Length [ft]	7.9
Gas-side Surface Area [ft2]	107,895
Air-side Surface Area [ft2]	5,616,079
Field Erected Capital Cost	$3,830,396
Annualized Capital Cost	$307,361
Annualized Operating Cost	$95,399
Estimated Annual Savings in Water Costs @ $1.50 per 1000 gallon	$315,439
Net Annual Cost	$95,400
Gas-Side Fan Power [kW]	188
Air-Side Fan Power [kW]	49
Sensible Heat Transfer [BTU/hr]	39,429,414
Latent Heat Transfer [BTU/hr]	262,061,802
Condensation Rate [lbm/hr]	250,598
Condensation Efficiency	47%
Inlet/Exit Moisture Concentration [% wet-basis]	14.4/8.2

Appendix B.5.10 - Inlet Flue Gas Temperature of 128°F and 60% Condensation Efficiency in the ACC

The following tables list the values of the variables included in the optimization simulations for the cases when there was an FGD system. The last table in the section lists the details for the best of the four optimizations.

Test name: 60_saturated_60a							
	Range		**Starting Value**		**Optimal Value**		**Si**
	Min	**Max**	**Normalized**	**Actual**	**Normalized**	**Actual**	
Surface Area						148,238	
Tube Length						11	
Gas Velocity	7.5	80.0	0.500	43.8	0.591	50.3	0.125
Air Velocity	7.5	50.0	0.500	28.8	0.002	7.6	-0.4
Fin Pitch	0.20	1.00	0.500	0.60	0.000	0.20	-0.4
Fin Length	0.00	1.25	0.500	0.63	1.000	1.25	0.4
Inner Tube Diameter	1.75	6.00	0.500	3.88	0.000	1.75	-0.4
Fin Thickness	0.063	0.125	0.500	0.094	0.907	0.119	0.4
Net Annual Cost			$731,121		$129,745		

Test name: 60_saturated_60b							
	Range		**Starting Value**		**Optimal Value**		**Si**
	Min	**Max**	**Normalized**	**Actual**	**Normalized**	**Actual**	
Surface Area						150,407	
Tube Length						16	
Gas Velocity	7.5	80.0	0.500	43.8	0.649	54.5	0.125
Air Velocity	7.5	50.0	0.500	28.8	0.072	10.5	-0.125
Fin Pitch	0.20	1.00	0.500	0.60	0.000	0.20	-0.125
Fin Length	0.00	1.25	0.500	0.63	1.000	1.25	0.125
Inner Tube Diameter	1.75	6.00	0.500	3.88	0.133	2.32	-0.125
Fin Thickness	0.063	0.125	0.500	0.094	0.791	0.112	0.125
Net Annual Cost			$731,121		$159,952		

Test name: 60_saturated_60c							
	Range		**Starting Value**		**Optimal Value**		**Si**
	Min	**Max**	**Normalized**	**Actual**	**Normalized**	**Actual**	
Surface Area						149,420	
Tube Length						11	
Gas Velocity	7.5	80.0	0.584	49.9	0.585	49.9	-0.5
Air Velocity	7.5	50.0	0.001	7.5	0.000	7.5	0.5
Fin Pitch	0.20	1.00	0.000	0.20	0.000	0.20	0.5
Fin Length	0.00	1.25	1.000	1.25	0.998	1.25	-0.5
Inner Tube Diameter	1.75	6.00	0.000	1.75	0.000	1.75	0.5
Fin Thickness	0.063	0.125	0.749	0.109	0.747	0.109	-0.5
Net Annual Cost			$130,375		$130,199		

Test name: 60_saturated_60d							
	Range		**Starting Value**		**Optimal Value**		**Si**
	Min	**Max**	**Normalized**	**Actual**	**Normalized**	**Actual**	
Surface Area						147,681	
Tube Length						11	
Gas Velocity	7.5	80.0	0.584	49.9	0.593	50.5	0.125
Air Velocity	7.5	50.0	0.001	7.5	0.007	7.8	0.125
Fin Pitch	0.20	1.00	0.000	0.20	0.000	0.20	0.125
Fin Length	0.00	1.25	1.000	1.25	1.000	1.25	-0.125
Inner Tube Diameter	1.75	6.00	0.000	1.75	0.000	1.75	0.125
Fin Thickness	0.063	0.125	0.749	0.109	0.784	0.112	0.125
Net Annual Cost			$130,375		$130,005		

Test name: 60_saturated_60a	
Flue Gas Flow Rate [lbm/hr]	6,000,000
Vapor Flow Rate [lbm/hr]	532,881
Cooling Air Flow Rate [lbm/hr]	49,252,766
Flue Gas Velocity [ft/sec]	46.0
Cooling Air Velocity [ft/sec]	7.8
Inlet Flue Gas Temperature [F]	128
Inlet Cooling Air Temperature [F]	60
Exit Flue Gas Temperature [F]	95.5
Exit Cooling Air Temperature [F]	90.8
Tube Inner Diameter [inch]	1.75
Tube Thickness [inch]	0.2
Fin Pitch [inches]	0.2
Fin Thickness [inches]	0.119
Number of Tube Rows	2
Transverse Tube Spacing [inches]	4.65
Longitudinal Tube Spacing [inches]	4.65
Number of Tubes	29000
Tube Length [ft]	11
Gas-side Surface Area [ft2]	148,238
Air-side Surface Area [ft2]	7,749,020
Field Erected Capital Cost	$4,938,680
Annualized Capital Cost	$396,292
Annualized Operating Cost	$113,375
Estimated Annual Savings in Water Costs @ $1.50 per 1000 gallon	$379,922
Net Annualized Cost [20 yrs @ 5%]	$129,745
Gas-Side Fan Power [kW]	225
Air-Side Fan Power [kW]	63
Sensible Heat Transfer [BTU/hr]	49,215,407
Latent Heat Transfer [BTU/hr]	315,866,487
Condensation Rate [lbm/hr]	301,826
Condensation Efficiency	57%
Inlet/Exit Moisture Concentration [% wet-basis]	14.4/6.8

Appendix B.5.11 - Inlet Flue Gas Temperature of 128°F and 70% Condensation Efficiency in the ACC

The following tables list the values of the variables included in the optimization simulations for the cases when there was an FGD system. The last table in the section lists the details for the best of the four optimizations.

Test name: 60_saturated_69a							
	Range		**Starting Value**		**Optimal Value**		**Si**
	Min	**Max**	**Normalized**	**Actual**	**Normalized**	**Actual**	
Surface Area						194,333	
Tube Length						15.2	
Gas Velocity	7.5	80.0	0.500	43.8	0.629	53.1	0.125
Air Velocity	7.5	50.0	0.500	28.8	0.010	7.9	-0.4
Fin Pitch	0.20	1.00	0.500	0.60	0.000	0.20	-0.4
Fin Length	0.00	1.25	0.500	0.63	1.000	1.25	0.4
Inner Tube Diameter	1.75	6.00	0.500	3.88	0.000	1.75	-0.4
Fin Thickness	0.063	0.125	0.500	0.094	0.847	0.115	0.4
Net Annual Cost			$967,725		$198,949		

Test name: 60_saturated_69b							
	Range		**Starting Value**		**Optimal Value**		**Si**
	Min	**Max**	**Normalized**	**Actual**	**Normalized**	**Actual**	
Surface Area						198,034	
Tube Length						16.2	
Gas Velocity	7.5	80.0	0.500	43.8	0.661	55.4	0.125
Air Velocity	7.5	50.0	0.500	28.8	0.000	7.5	-0.125
Fin Pitch	0.20	1.00	0.500	0.60	0.057	0.25	-0.125
Fin Length	0.00	1.25	0.500	0.63	1.000	1.25	0.125
Inner Tube Diameter	1.75	6.00	0.500	3.88	0.000	1.75	-0.125
Fin Thickness	0.063	0.125	0.500	0.094	0.862	0.116	0.125
Net Annual Cost			$967,725		$217,732		

Test name: 60_saturated_69c							
	Range		**Starting Value**		**Optimal Value**		**Si**
	Min	**Max**	**Normalized**	**Actual**	**Normalized**	**Actual**	
Surface Area						203,659	
Tube Length						15	
Gas Velocity	7.5	80.0	0.584	49.9	0.586	50.0	-0.5
Air Velocity	7.5	50.0	0.001	7.5	0.000	7.5	0.5
Fin Pitch	0.20	1.00	0.000	0.20	0.000	0.20	0.5
Fin Length	0.00	1.25	1.000	1.25	0.990	1.24	-0.5
Inner Tube Diameter	1.75	6.00	0.000	1.75	0.000	1.75	0.5
Fin Thickness	0.063	0.125	0.749	0.109	0.723	0.108	-0.5
Net Annual Cost			$201,288		$200,605		

Test name: 60_saturated_69d							
	Range		**Starting Value**		**Optimal Value**		**Si**
	Min	**Max**	**Normalized**	**Actual**	**Normalized**	**Actual**	
Surface Area						197,648	
Tube Length						15.1	
Gas Velocity	7.5	80.0	0.584	49.9	0.610	51.7	0.125
Air Velocity	7.5	50.0	0.001	7.5	0.011	8.0	0.125
Fin Pitch	0.20	1.00	0.000	0.20	0.000	0.20	0.125
Fin Length	0.00	1.25	1.000	1.25	1.000	1.25	-0.125
Inner Tube Diameter	1.75	6.00	0.000	1.75	0.000	1.75	0.125
Fin Thickness	0.063	0.125	0.749	0.109	0.795	0.112	0.125
Net Annual Cost			$201,288		$199,949		

Test name: 60_saturated_69a	
Flue Gas Flow Rate [lbm/hr]	6,000,000
Vapor Flow Rate [lbm/hr]	532,881
Cooling Air Flow Rate [lbm/hr]	68,582,018
Flue Gas Velocity [ft/sec]	47.6
Cooling Air Velocity [ft/sec]	8.2
Inlet Flue Gas Temperature [F]	128
Inlet Cooling Air Temperature [F]	60
Exit Flue Gas Temperature [F]	87.6
Exit Cooling Air Temperature [F]	86.1
Tube Inner Diameter [inch]	1.75
Tube Thickness [inch]	0.2
Fin Length [inches]	1.25
Fin Pitch [inches]	0.2
Fin Thickness [inches]	0.115
Number of Tube Rows	2
Transverse Tube Spacing [inches]	4.65
Longitudinal Tube Spacing [inches]	4.65
Number of Tubes	28000
Tube Length [ft]	15.2
Gas-side Surface Area [ft2]	194,333
Air-side Surface Area [ft2]	10,143,477
Field Erected Capital Cost	$6,133,105
Annualized Capital Cost	$492,136
Annualized Operating Cost	$151,263
Estimated Annual Savings in Water Costs @ $1.50 per 1000 gallon	$444,450
Net Annualized Cost [20 yrs @ 5%]	$198,949
Gas-Side Fan Power [kW]	296
Air-Side Fan Power [kW]	88
Sensible Heat Transfer [BTU/hr]	60,261,723
Latent Heat Transfer [BTU/hr]	369,883,698
Condensation Rate [lbm/hr]	353,090
Condensation Efficiency	66%
Inlet/Exit Moisture Concentration [% wet-basis]	14.4/5.4

Appendix B.5.12 – Inlet Flue Gas Temperature of 128°F and 75% Condensation Efficiency in the ACC

The following tables list the values of the variables included in the optimization simulations for the cases when there was an FGD system. The last table in the section lists the details for the best of the four optimizations.

Test name: 60_saturated_75a							
	Range		**Starting Value**		**Optimal Value**		**Si**
	Min	**Max**	**Normalized**	**Actual**	**Normalized**	**Actual**	
Surface Area						239,351	
Tube Length						19.5	
Gas Velocity	7.5	80.0	0.500	43.8	0.657	55.1	0.125
Air Velocity	7.5	50.0	0.500	28.8	0.014	8.1	-0.4
Fin Pitch	0.20	1.00	0.500	0.60	0.000	0.20	-0.4
Fin Length	0.00	1.25	0.500	0.63	0.965	1.21	0.4
Inner Tube Diameter	1.75	6.00	0.500	3.88	0.001	1.75	-0.4
Fin Thickness	0.063	0.125	0.500	0.094	1.000	0.125	0.4
Net Annual Cost			$1,197,668		$302,149		

Test name: 60_saturated_75b							
	Range		**Starting Value**		**Optimal Value**		**Si**
	Min	**Max**	**Normalized**	**Actual**	**Normalized**	**Actual**	
Surface Area						250,727	
Tube Length						20.1	
Gas Velocity	7.5	80.0	0.500	43.8	0.644	54.2	0.125
Air Velocity	7.5	50.0	0.500	28.8	0.000	7.5	-0.125
Fin Pitch	0.20	1.00	0.500	0.60	0.054	0.24	-0.125
Fin Length	0.00	1.25	0.500	0.63	1.000	1.25	0.125
Inner Tube Diameter	1.75	6.00	0.500	3.88	0.000	1.75	-0.125
Fin Thickness	0.063	0.125	0.500	0.094	0.871	0.117	0.125
Net Annual Cost			$1,197,668		$324,796		

Test name: 60_saturated_75c							
	Range		**Starting Value**		**Optimal Value**		**Si**
	Min	**Max**	**Normalized**	**Actual**	**Normalized**	**Actual**	
Surface Area						251,996	
Tube Length						19	
Gas Velocity	7.5	80.0	0.584	49.9	0.600	51.0	-0.5
Air Velocity	7.5	50.0	0.001	7.5	0.001	7.5	0.5
Fin Pitch	0.20	1.00	0.000	0.20	0.000	0.20	0.5
Fin Length	0.00	1.25	1.000	1.25	0.998	1.25	-0.5
Inner Tube Diameter	1.75	6.00	0.000	1.75	0.000	1.75	0.5
Fin Thickness	0.063	0.125	0.749	0.109	0.743	0.109	-0.5
Net Annual Cost			$301,487		$300,223		

Test name: 60_saturated_75d							
	Range		**Starting Value**		**Optimal Value**		**Si**
	Min	**Max**	**Normalized**	**Actual**	**Normalized**	**Actual**	
Surface Area						253,486	
Tube Length						18.9	
Gas Velocity	7.5	80.0	0.584	49.8	0.593	50.5	0.125
Air Velocity	7.5	50.0	0.001	7.5	0.001	7.5	0.125
Fin Pitch	0.20	1.00	0.000	0.20	0.000	0.20	0.125
Fin Length	0.00	1.25	1.000	1.25	1.000	1.25	-0.125
Inner Tube Diameter	1.75	6.00	0.000	1.75	0.000	1.75	0.125
Fin Thickness	0.063	0.125	0.749	0.109	0.749	0.109	0.125
Net Annual Cost			$301,487		$300,524		

Test name: 60_saturated_75c	
Flue Gas Flow Rate [lbm/hr]	6,000,000
Vapor Flow Rate [lbm/hr]	532,881
Cooling Air Flow Rate [lbm/hr]	85,963,979
Flue Gas Velocity [ft/sec]	45.0
Cooling Air Velocity [ft/sec]	7.7
Inlet Flue Gas Temperature [F]	128
Inlet Cooling Air Temperature [F]	60
Exit Flue Gas Temperature [F]	81.6
Exit Cooling Air Temperature [F]	83
Tube Inner Diameter [inch]	1.75
Tube Thickness [inch]	0.2
Fin Length [inches]	1.25
Fin Pitch [inches]	0.2
Fin Thickness [inches]	0.109
Number of Tube Rows	2
Transverse Tube Spacing [inches]	4.65
Longitudinal Tube Spacing [inches]	4.65
Number of Tubes	29000
Tube Length [ft]	19
Gas-side Surface Area [ft2]	251,996
Air-side Surface Area [ft2]	13,084,190
Field Erected Capital Cost	$7,829,443
Annualized Capital Cost	$628,255
Annualized Operating Cost	$160,120
Estimated Annual Savings in Water Costs @ $1.50 per 1000 gallon	$488,152
Net Annualized Cost [20 yrs @ 5%]	$300,223
Gas-Side Fan Power [kW]	309
Air-Side Fan Power [kW]	88
Sensible Heat Transfer [BTU/hr]	68,535,549
Latent Heat Transfer [BTU/hr]	406,516,098
Condensation Rate [lbm/hr]	387,808
Condensation Efficiency	73%
Inlet/Exit Moisture Concentration [% wet-basis]	14.4/4.4

Appendix B.6 - Details of the Optimization Simulations for the Cases in which the ACC was used to Pre-Heat Combustion Air.

Appendix B.6 tabulates the optimization results and initial simplexes for the simulations discussed in Section 6.2, which discussed the effects of using the ACC to pre-heat combustion air. In these designs, there was also a wet flue gas desulphurization system. The inlet flue gas temperatures studied were 128^{o}F and 135^{o}F. In both cases, the flue gas was saturated with water vapor.

Each table in this section of the appendix represents one optimization simulation. The variables optimized are listed in the table and the range of each variable is given in the second and third columns. The columns labeled "Starting Value" list the variables used as the initial guess, which was one vertex of the initial simplex. The column labeled "Si" is the parameter assigned to each variable which built the remaining vertexes of the simplex using the Tilted Initial Simplex Method described in Walters [42]. The columns labeled "Optimal Value" list the values of the optimal heat exchanger design. Under the headings "Starting Value" and "Optimal Value", there are "Normalized" and "Actual" values. These correspond to the dimensionless and absolute values of the variables, respectively. Recall from Section 2.4, the variables were normalized during the optimization to remove the units from the optimization equations.

Appendix B.6.1 – Increasing the Combustion Air Temperature from 80 to 125 ^{o}F when the Inlet Flue Gas Temperature is 128^{o}F.

The following tables list the values of the variables included in the optimization simulations for the cases when the combustion air temperature was increased from 80^{o}F to 125^{o}F that entered the ACC at 128^{o}F and saturated. The last table in the section lists the details for the best of the four optimizations.

optimalAPH_125a							
	Range		Starting Value		Optimal Value		Si
	Min	Max	Normalized	Actual	Normalized	Actual	
Surface Area						75,094	
Tube Length						30	
Delta T Combustion Air						45	
Gas Velocity	7.5	80.0	0.500	43.8	0.651	54.7	0.4
Air Velocity	7.5	50.0	0.500	28.8	0.128	12.9	-0.4
Fin Pitch	0.20	1.00	0.500	0.60	0.002	0.20	-0.4
Fin Length	0.00	1.25	0.500	0.63	1.000	1.25	0.4
Inner Tube Diameter	1.75	6.00	0.500	3.88	0.220	2.68	-0.4
Fin Thickness	0.063	0.125	0.500	0.094	0.659	0.104	0.4
Net Annual Cost			$802,986		$274,394		

optimalAPH_125b							
	Range		Starting Value		Optimal Value		Si
	Min	Max	Normalized	Actual	Normalized	Actual	
Surface Area						93,156	
Tube Length						30	
Delta T Combustion Air						45	
Gas Velocity	7.5	80.0	0.500	43.8	0.442	39.5	0.125
Air Velocity	7.5	50.0	0.500	28.8	0.135	13.2	-0.125
Fin Pitch	0.20	1.00	0.500	0.60	0.000	0.20	0.125
Fin Length	0.00	1.25	0.500	0.63	0.793	0.99	-0.125
Inner Tube Diameter	1.75	6.00	0.500	3.88	0.723	4.82	-0.125
Fin Thickness	0.063	0.125	0.500	0.094	0.233	0.077	0.125
Net Annual Cost			$802,986		$304,486		

optimalAPH_125c							
	Range		Starting Value		Optimal Value		Si
	Min	Max	Normalized	Actual	Normalized	Actual	
Surface Area						81,300	
Tube Length						30	
Delta T Combustion Air						45	
Gas Velocity	7.5	80.0	0.584	49.8	0.684	57.1	0.125
Air Velocity	7.5	50.0	0.001	7.5	0.024	8.5	0.125
Fin Pitch	0.20	1.00	0.000	0.20	0.017	0.21	0.125
Fin Length	0.00	1.25	1.000	1.25	0.999	1.25	-0.125
Inner Tube Diameter	1.75	6.00	0.000	1.75	0.044	1.94	0.125
Fin Thickness	0.063	0.125	0.749	0.109	0.724	0.108	0.125
Net Annual Cost			$295,265		$281,120		

optimalAPH_125d							
	Range		Starting Value		Optimal Value		Si
	Min	Max	Normalized	Actual	Normalized	Actual	
Surface Area						80,955	
Tube Length						30	
Delta T Combustion Air						45	
Gas Velocity	7.5	80.0	0.584	49.8	0.580	49.5	-0.4
Air Velocity	7.5	50.0	0.001	7.5	0.019	8.3	0.4
Fin Pitch	0.20	1.00	0.000	0.20	0.000	0.20	0.4
Fin Length	0.00	1.25	1.000	1.25	1.000	1.25	-0.4
Inner Tube Diameter	1.75	6.00	0.000	1.75	0.136	2.33	0.4
Fin Thickness	0.063	0.125	0.749	0.109	0.801	0.113	-0.4
Net Annual Cost			$295,266		$267,933		

optimalAPH_125d	
Flue Gas Flow Rate [lbm / hr]	1,545,807
Vapor Flow Rate [lbm / hr]	139,751
Cooling Air Flow Rate [lbm / hr]	5,300,000
Flue Gas Velocity [ft/sec]	47.2
Cooling Air Velocity [ft/sec]	8.7
Inlet Flue Gas Temperature [^{o}F]	128
Exit Flue Gas Temperature [^{o}F]	113
Inlet Cooling Air Temperature [^{o}F]	80
Exit Cooling Air Temperature [^{o}F[	125
Inlet Moisture Concentration [% wet basis]	14.4
Exit Moisture Concentration [% wet basis]	9.8
Tube Inner Diameter [inches]	2.33
Tube Thickness [inches]	0.2
Fin Length [inches]	1.25
Fin Pitch [inches]	0.2
Fin Thickness [inches]	0.113
Number of Tube Rows in the direction of the Air Flow	5
Transverse Tube Spacing [inches]	5.23
Longitudinal Tube Spacing [inches]	5.23
Number of Tubes	4425
Tube Length [ft]	30
Gas-Side Surface Area [ft^2]	80,955
Air-Side Surface Area [ft^2]	1,873,582
Air-Side Fan Power [kW]	10.8
Additional Gas-Side Fan Power [kW]	89
Field Erected Capital Cost	$3,500,531
Annualized Capital Cost	$280,892
Annualized Operating Cost	$49,372
Estimated Annual Savings in Water Costs @ $1.50 per 1000 gallon	$62,331
Estimated Annual Fuel Savings @ $50 per ton	$234,000
Net Annualized Cost [20 yrs @ 5%]	$33,933
Sensible Heat Transfer [BTU/hr]	6,177,588
Latent Heat Transfer [BTU/hr]	51,127,139
Condensation Rate [lbm / hr]	49,518
Condensation Efficiency of Processed Glue Gas	35%
Condensation Efficiency of Total Flue Gas	9.6%

Appendix B.6.2 – Increasing the Combustion Air Temperature from 80 to 132°F when the Inlet Flue Gas Temperature is 135°F.

The following tables list the values of the variables included in the optimization simulations for the cases when the combustion air temperature was increased from 80°F to 132°F with a flue gas that entered the ACC at 135°F and saturated. The last table in the section lists the details for the best of the four optimizations.

optimalAPH_135a							
	Range		**Starting Value**		**Optimized Value**		**Si**
	Min	**Max**	**Normalized**	**Actual**	**Normalized**	**Actual**	
Surface Area						58,023	
Tube Length						30	
Delta T Combustion Air						51.9	
Gas Velocity	7.5	80.0	0.500	43.8	0.652	54.8	0.4
Air Velocity	7.5	50.0	0.500	28.8	0.113	12.3	-0.4
Fin Pitch	0.20	1.00	0.500	0.60	0.000	0.20	-0.4
Fin Length	0.00	1.25	0.500	0.63	0.996	1.24	0.4
Inner Tube Diameter	1.75	6.00	0.500	3.88	0.421	3.54	-0.4
Fin Thickness	0.063	0.125	0.500	0.094	0.999	0.125	0.4
Net Annual Cost			$797,070		$201,447		

optimalAPH_135b							
	Range		**Starting Value**		**Optimized Value**		**Si**
	Min	**Max**	**Normalized**	**Actual**	**Normalized**	**Actual**	
Surface Area						87,619	
Tube Length						30	
Delta T Combustion Air						51.9	
Gas Velocity	7.5	80.0	0.500	43.8	0.374	34.6	0.125
Air Velocity	7.5	50.0	0.500	28.8	0.068	10.4	-0.125
Fin Pitch	0.20	1.00	0.500	0.60	0.000	0.20	0.125
Fin Length	0.00	1.25	0.500	0.63	0.680	0.85	-0.125
Inner Tube Diameter	1.75	6.00	0.500	3.88	0.447	3.65	-0.125
Fin Thickness	0.063	0.125	0.500	0.094	0.803	0.113	0.125
Net Annual Cost			$797,070		$253,890		

optimalAPH_135c							
	Range		**Starting Value**		**Optimized Value**		**Si**
	Min	**Max**	**Normalized**	**Actual**	**Normalized**	**Actual**	
Surface Area						69,923	
Tube Length						30	
Delta T Combustion Air						51.9	
Gas Velocity	7.5	80.0	0.584	49.8	0.712	59.1	0.125
Air Velocity	7.5	50.0	0.068	10.4	0.092	11.4	0.125
Fin Pitch	0.20	1.00	0.000	0.20	0.001	0.20	0.125
Fin Length	0.00	1.25	1.000	1.25	0.956	1.20	-0.125
Inner Tube Diameter	1.75	6.00	0.000	1.75	0.043	1.93	0.125
Fin Thickness	0.063	0.125	0.749	0.109	0.780	0.111	0.125
Net Annual Cost			$270,018		$246,519		

optimalAPH_135d							
	Range		**Starting Value**		**Optimized Value**		**Si**
	Min	**Max**	**Normalized**	**Actual**	**Normalized**	**Actual**	
Surface Area						81,012	
Tube Length						30	
Delta T Combustion Air						51.9	
Gas Velocity	7.5	80.0	0.584	49.8	0.558	48.0	-0.4
Air Velocity	7.5	50.0	0.001	7.5	0.013	8.0	0.4
Fin Pitch	0.20	1.00	0.000	0.20	0.000	0.20	0.4
Fin Length	0.00	1.25	1.000	1.25	1.000	1.25	-0.4
Inner Tube Diameter	1.75	6.00	0.000	1.75	0.051	1.96	0.4
Fin Thickness	0.063	0.125	0.749	0.109	0.743	0.109	-0.4
Net Annual Cost			$281,983		$250,573		

optimalAPH_135a	
Flue Gas Flow Rate [lbm/hr]	1,823,864
Vapor Flow Rate [lbm/hr]	201,994
Cooling Air Flow Rate [lbm/hr]	5,300,000
Flue Gas Velocity [ft/sec]	52.7
Cooling Air Velocity [ft/sec]	12.9
Inlet Flue Gas Temperature [^{o}F]	135
Exit Flue Gas Temperature [^{o}F]	123
Inlet Cooling Air Temperature [F]	80
Exit Cooling Air Temperature [^{o}F]	132
Inlet Moisture Concentration [% wet basis]	17.4
Exit Moisture Concentration [% wet basis]	13.0
Tube Inner Diameter [inch]	3.54
Tube Thickness [inch]	0.2
Fin Length [inches]	1.25
Fin Pitch [inches]	0.2
Fin Thickness [inches]	0.125
Number of Tube Rows in the direction of the Air Flow	3
Transverse Tube Spacing [inches]	6.43
Longitudinal Tube Spacing [inches]	6.43
Number of Tubes	2088
Tube Length [ft]	30
Gas-side Surface Area [ft^2]	58,023
Air-side Surface Area [ft^2]	1,149,016
Air-Side Fan Power [kW]	16.3
Gas-Side Fan Power [kW]	90.4
Field Erected Capital Cost	$2,681,759
Annualized Capital Cost	$215,191
Annualized Operating Cost	$60,003
Estimated Annual Savings in Water Costs @ $1.50 per 1000 gallon	$73,747
Estimated Annual Savings in Fuel @ $50 per ton	$270,000
Net Annualized Cost [20 yrs @ 5%]	-$32,553
Sensible Heat Transfer [BTU/hr]	5,892,501
Latent Heat Transfer [BTU/hr]	60,299,506
Condensation Rate [lbm/hr]	58,587
Condensation Efficiency of Processed Flue Gas	29%
Condensation Efficiency of Total Flue Gas	9.3%

Appendix C – Calculation of Fuel Consumption Rate for a 600 MW Power Plant. (Used in Section 6.3)

This Appendix describes how the fuel flow rate used in Section 6.3 was calculated. Equation C.1 is net unit heat rate.

$$Net\ Unit\ Heat\ Rate = \frac{HR_{TC}}{\eta_B}\left(\frac{P_g}{P_g - P_{SS}}\right) \tag{C.1}$$

where P_g is the gross power generated by the plant, P_{ss} is the station servicve power. The difference between P_g and P_{ss} is the net power sent to the grid (see Equation (C.2)). For a 600 MW power plant, P_{net} is 600 MW.

$$P_{net} = P_g - P_{ss} \tag{C.2}$$

In Equation C.1, η_B is the boiler efficiency, and HR_{TC} is the turbine cycle heat rate. Another way to calculate net unit heat rate is with Equation C.3.

$$Net\ Unit\ Heat\ Rate = \frac{\dot{m}_{coal} * HHV_{fuel}}{P_g - P_{ss}} \tag{C.3}$$

where $\dot{m}_{coal}$ is the flow rate of coal into the boiler, and HHV_{fuel} is the higher heating value of the coal, and P_g and P_{ss} are gross power generated and station service power.

Equations C.1 and C.3 were used to determine the fuel flow rate for a 600 MW power plant using assumed values for boiler efficiency, turbine cycle heat rate, higher heating value of coal, and flue gas flow rate. See values listed in Table C.1.

Table C.1 – Assumed values used in the calculation of the fuel flow rate for a 600 MW power plant.

Net Power Generated P_{net}	600 MW
Boiler Efficiency η_B	88 %
Turbine Cycle Heat Rate HR_{TC}	7650 BTU/kW-hr
Higher Heating Value of Coal HHV_{fuel}	12,000 BTU/lbm
Flue Gas Flow Rate	$6*10^6$ lbm/hr
P_{ss}/P_g	0.06

Using the values in Table C.1, the performance characteristics of the power plant are:

- Net Unit Heat Rate: 9215 BTU/kW-hr
- Fuel Flow Rate of Coal: 460,000 lbm/hr

Vita

Michael Kessen was born March 22, 1984 in Milwaukee, Wisconsin to Robert and Diane Kessen. He attended Milwaukee School of Engineering from 2002 to 2006 and received a Bachelor's of Science in Mechanical Engineering. Michael attended graduate school at Lehigh University and received a Master's of Science in Mechanical Engineering in 2009 and a Doctor of Philosophy in Mechanical Engineering in 2012. While at Lehigh Michael was a Rossin Doctoral Fellow from 2010 to 2011. In the summer of 2011 he was an Adjunct Professor at Lehigh University and taught Fluid Mechanics. After completing graduate studies, Michael moved to work as a powertrain cooling engineer at General Motors Technical Center in Warren, Michigan.